



National Library of Canada

Bibliothèque nationale du Canada

0-315-03607-9

Canadian Theses Division / Division des thèses canadiennes

Ottawa, Canada K1A 0N4

51502

PERMISSION TO MICROFILM — AUTORISATION DE MICROFILMER

Please print or type — Écrire en lettres moulées ou dactylographier

Full Name of Author — Nom complet de l'auteur

DONALD RALPH HULL

Date of Birth — Date de naissance

August 19, 1942

Country of Birth — Lieu de naissance

United States

Permanent Address — Résidence fixe

245 PETER'S SPRING ROAD
CONCORD, MASSACHUSETTS
01742 USA.

Title of Thesis — Titre de la thèse

The Development and Characterization of an
Electrothermal Vaporization Sample Introduction
System for the Inductively Coupled Plasma

University — Université

UNIVERSITY OF ALBERTA

Degree for which thesis was presented — Grade pour lequel cette thèse fut présentée

Ph.D

Year this degree conferred — Année d'obtention de ce grade

SPRING 1981

Name of Supervisor — Nom du directeur de thèse

DR. G. HERLICK

Permission is hereby granted to the NATIONAL LIBRARY OF CANADA to microfilm this thesis and to lend or sell copies of the film.

L'autorisation est, par la présente, accordée à la BIBLIOTHÈQUE NATIONALE DU CANADA de microfilmer cette thèse et de prêter ou de vendre des exemplaires du film.

The author reserves other publication rights, and neither the thesis nor extensive extracts from it may be printed or otherwise reproduced without the author's written permission.

L'auteur se réserve les autres droits de publication; ni la thèse ni de longs extraits de celle-ci ne doivent être imprimés ou autrement reproduits sans l'autorisation écrite de l'auteur.

Date

December 1/81

Signature

Donald Hull



National Library of Canada
Collections Development Branch

Canadian Theses on
Microfiche Service

Bibliothèque nationale du Canada
Direction du développement des collections

Service des thèses canadiennes
sur microfiche

NOTICE

The quality of this microfiche is heavily dependent upon the quality of the original thesis submitted for microfilming. Every effort has been made to ensure the highest quality of reproduction possible.

If pages are missing, contact the university which sent the degree.

Some pages may have indistinct print especially if the original pages were typed with a poor typewriter ribbon or if the university sent us a poor photocopy.

Previously copyrighted materials (journal articles, published tests, etc.) are not filmed.

Reproduction in full or in part of this film is governed by the Canadian Copyright Act, R.S.C. 1970, c. C-30. Please read the authorization forms which accompany this thesis.

**THIS DISSERTATION
HAS BEEN MICROFILMED
EXACTLY AS RECEIVED**

AVIS

La qualité de cette microfiche dépend grandement de la qualité de la thèse soumise au microfilmage. Nous avons tout fait pour assurer une qualité supérieure de reproduction.

S'il manque des pages, veuillez communiquer avec l'université qui a conféré le grade.

La qualité d'impression de certaines pages peut laisser à désirer, surtout si les pages originales ont été dactylographiées à l'aide d'un ruban usé ou si l'université nous a fait parvenir une photocopie de mauvaise qualité.

Les documents qui font déjà l'objet d'un droit d'auteur (articles de revue, examens publiés, etc.) ne sont pas microfilmés.

La reproduction, même partielle, de ce microfilm est soumise à la Loi canadienne sur le droit d'auteur, SRC 1970, c. C-30. Veuillez prendre connaissance des formules d'autorisation qui accompagnent cette thèse.

**LA THÈSE A ÉTÉ
MICROFILMÉE TELLE QUE
NOUS L'AVONS REÇUE**

THE UNIVERSITY OF ALBERTA

THE DEVELOPMENT AND CHARACTERIZATION OF AN
ELECTROTHERMAL VAPORIZATION SAMPLE INTRODUCTION
SYSTEM FOR THE INDUCTIVELY COUPLED PLASMA

by



DONALD R. HULL

A THESIS

SUBMITTED TO THE FACULTY OF GRADUATE STUDIES AND RESEARCH
IN PARTIAL FULFILMENT OF THE REQUIREMENTS FOR THE DEGREE
OF DOCTOR OF PHILOSOPHY

DEPARTMENT CHEMISTRY

EDMONTON, ALBERTA

SPRING, 1981

THE UNIVERSITY OF ALBERTA

RELEASE FORM

NAME OF AUTHOR Donald R. Hull
.....
TITLE OF THESIS The Development and Characterization of an
.....
Electrothermal Vaporization Sample Intro-
.....
duction System for the Inductively Coupled
.....
Plasma
.....
DEGREE FOR WHICH THIS THESIS WAS PRESENTED Ph.D.
.....
YEAR THIS DEGREE GRANTED 1981
.....

Permission is hereby granted to THE UNIVERSITY OF ALBERTA LIBRARY to reproduce single copies of this thesis and to lend or sell such copies for private, scholarly or scientific research purposes only.

The author reserves other publication rights, and neither the thesis nor extensive extracts from it may be printed or otherwise reproduced without the author's written permission.

(Signed) *D. M. A.*

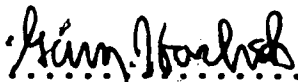
PERMANENT ADDRESS:

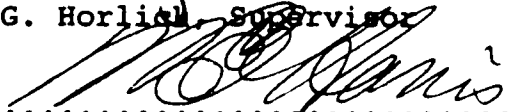
248 Peters Spring Road
.....
- Concord, Mass 01742
.....


DATED .. *April 15* 1981

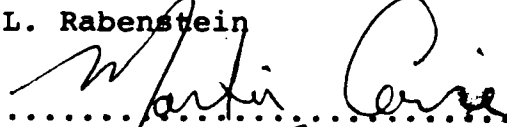
THE UNIVERSITY OF ALBERTA
FACULTY OF GRADUATE STUDIES AND RESEARCH

The undersigned certify that they have read, and recommend to the Faculty of Graduate Studies and Research for acceptance, a thesis entitled THE DEVELOPMENT AND CHARACTERIZATION OF AN ELECTROTHERMAL VAPORIZATION SAMPLE INTRODUCTION SYSTEM FOR THE INDUCTIVELY COUPLED PLASMA submitted by DONALD R. HULL in partial fulfilment of the requirements for the degree of Doctor of Philosophy in Analytical Chemistry.


.....
G. Horlich, Supervisor


.....
W.E. Harris


.....
D.L. Rabenstein


.....
M. Cowie


.....
H.E. Bell


.....
S.R. Koirtyohang, External Examiner

Date January 26, 1981

Dedication

The author wishes to dedicate this work to those who most made it possible, his parents.

My Father:

He taught me that a man must continue on,
even when he stumbles and falls.

My Mother:

She showed me that the necessary courage
is there if you only reach deep enough
inside.

No son has ever received greater gifts or more love.

ABSTRACT

The analytical aspects of the use of a graphite cup electrothermal atomizer in combination with inductively coupled argon plasma-optical emission spectrometers has been investigated as a means of analyzing small volume samples in solution and for the direct analysis of solid samples.

Preliminary investigations using single element solutions and a single channel detector system have illustrated the temporal behavior and analytical capabilities of electrothermal atomization-inductively coupled argon plasma-optical emission spectroscopy. The temporal studies have shown that changes of emission background are present during atomization and that the analyte emission profile changes with increasing analyte amount. The analytical studies have shown that a linear dynamic range of three to four orders of magnitude is possible.

A study of the effect of a NaCl matrix on the emission of Pb has shown that changes take place in the vertical emission profile and in the background emission levels. Use of a matching reference blank and proper choice of slit height and position have been shown to allow correct analysis of lead at a NaCl concentration greater than that of sea water.

Spex G-Standards and National Bureau of Standards-Standard Reference Materials have been used to test the

direct analysis of solids. These studies show that matrix effects are present but that direct solids analysis is possible.

Acknowledgements

Professor G. Horlick has exerted a major influence on the author's professional life during the course of this work. He helped develop the problem, offered invaluable suggestions and help in the experimental work, provided excellent experimental facilities and a stimulating environment in which the research could be conducted.

The experimental apparatus used in this work was constructed in the Department of Chemistry Glass and Machine Shops and I would like to thank all who work in those shops for their excellent work. Mr. J. Toonev of the Glass Shop and Mr. H. Hofmann of the Machine shop deserve special recognition for their help.

For financial aid in the form of teaching assistantships and a research assistantship, the author gratefully acknowledges the Department of Chemistry, University of Alberta.

The author thanks Miss A. Wiseman for an excellent job in typing this thesis and all my committee members for help in proof reading.

Finally the author wishes to thank his children, Kerry and Christopher, for their continuing love and understanding during this time.

TABLE OF CONTENTS

CHAPTER	PAGE
I. Introduction	1
II. Instrumentation: Description and Modifications	17
A. The Graphite Furnace	17
1. Modifications of the Graphite Cup	23
2. Modification of the Varian Model 63 Carbon Cup Atomizer Control/Power Supply	31
B. Inductively Coupled Argon Plasma	36
C. Monochromator	38
D. Detector-Readout Systems	38
1. Monochromator-Photomultiplier Readout System	42
2. Computer Coupled Photodiode Array Readout Systems	47
III. Characterization of EA-ICAP-OES Emission Behavior for Single Elements in Solution	49
A. Temporal Behavior of EA-ICAP-OES System	49
B. Analytical Results for Single Elements in Solution	62
IV. Effect of NaCl Matrix on Pb(II) EA-ICAP-OES Analysis	103
A. Effect of NaCl Matrix on Pb(II) Emission Temporal Behavior and Emission Intensity	104
B. Matrix Effects on Pb(II) Spatial Emission Profiles	110

TABLE OF CONTENTS

CHAPTER	PAGE
V. Direct Solids Analysis by EA-ICAP-OES Using a Computer Coupled Photodiode Array Direct Reading Spectrometer	117
A. Analysis of Spex G-Standard Mixture	119
B. Analysis of NBS Standard Reference Materials	130

Summary	151
Bibliography	155
Appendix A	160
Appendix B	173
Appendix C	179
Appendix D	189
Appendix E	195
Appendix F	207
Appendix G	212
Appendix H	218

LIST OF FIGURES

<u>Figure</u>	<u>Description</u>	<u>Page</u>
1	Spectrochemical measurement block diagram.	1
2	Induction-coupled plasma torch for crystal growth.	7
3	(a) Powder injection assembly. (b) Swirl cup chamber. (c) Fluidized-bed chamber.	9
4	Block diagram of computer coupled photo-multiplier spectrometer.	18
5	Block diagram of computer coupled photodiode array spectrometer.	19
6	Varian Model 63 Carbon Rod Furnace.	20
7	Vaporization cell for graphite cup EA-ICAP-OES.	22
8	Modification of Varian graphite cup for use in EA-ICAP-OES.	24
9	Applied voltage vs time for step mode of operation of the Varian Model 63 Carbon Rod Atomizer.	26
10	Timer Block - Varian Model 63 Carbon Rod Atomizer Controller/Power Supply.	33
11	Timer Board Assembly - Varian Model 63 Carbon Rod Atomizer Controller/Power Supply.	34
12	(a) External circuitry and Model 63 modification for synchronizing atomization and photodiode array spectrometer system data acquisition. (b) Timing diagram.	35
13	ICAP torch.	37
14	Current-to-voltage convertor for use with PMT detector in EA-ICAP-OES spectrometer system.	45

<u>Figure</u>	<u>Description</u>	<u>Page</u>
15	Pulse characterization times for a graphite furnace.	51
16	EA-ICAP-OES temporal profile for Pb(II) emission at 220.353 nm from 100 ng of Pb. Recorded with computer system.	54
17	EA-ICAP-OES temporal profile for Pb(II) emission at 220.353 nm from 100 ng of Pb. Recorded with a Heath Strip Chart Recorder, Model # EU-20B	57
18	EA-ICAP-OES temporal profile for Pb(II) emission at 220.353 nm from 10 ng of Pb. Recorded with computer system.	58
19	EA-ICAP-OES temporal profile for Pb(II) emission at 220.353 nm from Pb blank. Recorded with computer system.	60
20	EA-ICAP-OES temporal profile for Mg(II) emission at 279.553 nm from 1000 ng Mg. Recorded with computer system.	61
21	EA-ICAP-OES temporal profile for Zn(I) emission at 213.856 nm from 20 ng Zn. Recorded with computer system.	63
22	Temporal profile, 2 ng Zn(I) - 213.856 nm.	65
23	Temporal profile, 5 ng Zn(I) - 213.856 nm.	66
24	Temporal profile, 20 ng Zn(I) - 213.856 nm.	67
25	Temporal profile, 50 ng Zn(I) - 213.856 nm.	68
26	Temporal profile, 200 ng Zn(I) - 213.856 nm.	69
27	Temporal profile, 500 ng Zn(I) - 213.856 nm.	70
28	Temporal profile, 2000 ng Zn(I) - 213.856 nm.	71
29	Temporal profile, 5000 ng Zn(I) - 213.856 nm.	72

<u>Figure</u>	<u>Description</u>	<u>Page</u>
30	Linear calibration plot for Mg(I) - 285.213 nm, E_p data.	76
31	Log-log calibration plot for Mg(I) - 285.213 nm, E_p data.	77
32	Linear calibration plot for Mg(I) - 285.213 nm, $\int E_t dt$ data.	78
33	Log-log calibration plot for Mg(I) - 285.213 nm, $\int E_t dt$ data.	79
34	Log-log calibration plot for Pb(I) - 405.783 nm.	92
35	Log-log calibration plot for Pb(II) - 220.353 nm.	93
36	Log-log calibration plot for Mg(II) - 279.553 nm.	94
37	Log-log calibration plot for Ag(I) - 328.068 nm.	95
38	Log-log calibration plot for Cu(I) - 324.754 nm.	96
39.	Log-log calibration plot for Cd(I) - 228.802 nm.	97
40.	Log-log calibration plot for Cd(II) - 214.438 nm.	98
41	Log-log calibration plot for Zn(I) - 213.856 nm.	99
42	Log-log calibration plot for Pb(I) - 405.783 nm, Meinhard nebulizer.	100
43	Log-log calibration plot for Pb(II) - 220.353 nm, Meinhard nebulizer.	101
44	Temporal profile, blank Pb(II) - 220.353 nm.	106
45.	Temporal profile, blank containing 200,000 ng Na^+ as NaCl, Pb(II) - 220.353 nm.	107
46	Temporal profile, 100 ng Pb(II) - 220.353 nm.	108

<u>Figure</u>	<u>Description</u>	<u>Page</u>
47	Temporal profile, 100 ng Pb(II) - 220.353 nm. Matrix of 200,000 ng of Na ⁺ as NaCl.	109
48	Effect of Sodium on Pb(II) - 220.353 nm emission.	112
49	Vertical emission profile, Na/Pb = 0.	114
50	Vertical emission profile, Na/Pb = 20.	115
51	Time study of 5.2 mg of Spex G3 Standard containing 49 elements at 0.001% level and 0.1% In.	123
52	Spectrum taken between 1.2 and 1.6 second from Spex G3 Standard time study, Figure 51.	124
53.	Log-log calibration plot for Spex G-Standards, (Cd(I) - 228.802 nm)/sample weight.	125
54	Log-log calibration plot for Spex G-Standards, (Cd(I) - 228.802 nm)/(In(II) - 230.606 nm).	126
55	Log-log calibration plot for Spex G-Standards, (Zn(I) - 213.856 nm)/sample weight.	127
56	Log-log calibration plot for Spex G-Standards (Zn(I) - 213.856 nm)/(In(II) - 230.606 nm).	128
57	Spectrum from 300 ng each of Mn and Zn.	132
58	Spectrum from 2000 ng of Fe.	133
59	Spectrum from 10,000 ng of Si.	134
60	Spectrum from 2.6 mg of 50:50 mixture of NBS-SRM Coal #1632 and graphite (0.2% In).	136
61	Spectrum from 2.6 mg of 50:50 mixture of NBS-SRM Coal #1635 and graphite (0.2% In).	137
62	Spectrum from 2.5 mg. of 50:50 mixture of NBS-SRM Coal Fly Ash #1633 and graphite (0.2% In).	138

<u>Figure</u>	<u>Description</u>	<u>Page</u>
63	Spectrum from 2.8 mg of 50:50 mixture of NBS-SRM Spinach #1570 and graphite (0.2% In).	139
64	Spectrum from 2.1 mg of 50:50 mixture of NBS-SRM Orchard Leaves #1571 and graphite (0.2% In).	140
65	Spectrum from 2.3 mg of 50:50 mixture of NBS-SRM Tomato Leaves #1573 and graphite (0.2% In).	141
66	Spectrum from 2.4 mg of 50:50 mixture of NBS-SRM Pine Needles #1575 and graphite (0.2% In).	142
67	Calibration plot - Mn(II) emission/sample weight vs concentration of Mn in NBS-SRM.	147
68	Calibration plot - Mn(II) emission/In(I) emission vs concentration of Mn in NBS-SRM.	148
69	Calibration plot - Zn(I) emission/sample weight vs concentration of Zn in NBS-SRM.	149
70	Calibration plot - Zn(I) emission/In(I) emission vs concentration of Zn in NBS-SRM.	150

LIST OF TABLES

<u>Table</u>	<u>Description</u>	<u>Page</u>
I	Rough overall assessment of the main analytical capabilities of various "established" spectroscopic methods and ICP-AES.	5
II	ICAP specifications and operating conditions.	39
III	Specifications for Monochromator Unit, Model EU-700-70.	40
IV	Calibration data for current-to-voltage convertor.	44
V	Emission peak characteristics for Zn(I) - 213.85 nm.	74
VI	Calibration data for Mg(I) - 285.213 nm.	75
VII	EA-ICAP-OES analytical data.	81
VIII	Calibration data for Pb(I) - 405.783 nm.	82
IX	Calibration data for Pb(II) - 220.353 nm.	83
X	Calibration data for Mg(II) - 279.553 nm.	84
XI	Calibration data for Ag(I) - 328.068 nm.	85
XII	Calibration data for Cd(I) - 324.754 nm.	86
XIII	Calibration data for Cd(I) - 282.802 nm.	87
XIV	Calibration data for Cd(II) - 214.438 nm.	88
XV	Calibration data for Zn(I) - 213.856 nm.	89
XVI	Calibration data for Pb(I) - 405.783 nm, Meinhard nebulizer.	90
XVII	Calibration data for Pb(II) - 220.353 nm, Meinhard nebulizer.	91
XVIII	Effect of sodium on Pb(II) - 220.353 nm emission.	111
XIX	Calibration data for Cd(I) - 228.802 nm in Spex G-Standards.	121

<u>Table</u>	<u>Description</u>	<u>Page</u>
XX	Calibration data for Zn(I) - 213.856 nm in Spex G-Standards.	122
XXI	Concentration of Mn and Zn in NBS-SRM's.	143
XXII	Calibration data for Mn(II) - 257.610 nm emission in NBS-SRM's.	145
XXIII	Calibration data for Zn(I) - 213.856 nm emission in NBS-SRM's.	146

CHAPTER I

Introduction

Optical emission spectroscopy (OES) utilizing an inductively coupled argon plasma (ICAP) source is the direct descendent of Bunsen and Kirchhoff's discovery that the spectra of flames colored by metallic salts were characteristic of the metals. In inductively coupled argon plasma-optical emission spectroscopy (ICAP-OES) the ICAP replaces the flame as an energy source capable of transforming a sample from a solid, liquid, or gas into atomic vapor and then exciting these atoms to a higher electronic energy state from which photon emission can take place. This photon emission process can be thought of as encoding information about the sample in terms of frequency, intensity, time, and space. Decoding and recovery of this information about the sample is generally accomplished by means of a spectrometer. A general diagram of this process is shown in Figure 1 (1).

Research in the use of an ICAP (then called an induction-coupled plasma torch) as an optical emission source was independently performed by Greenfield (2) and Fassel (3) in the early 1960's and the first commercial instrument was introduced in 1974 (4). In the six short years since, ICAP-OES sales have captured an important

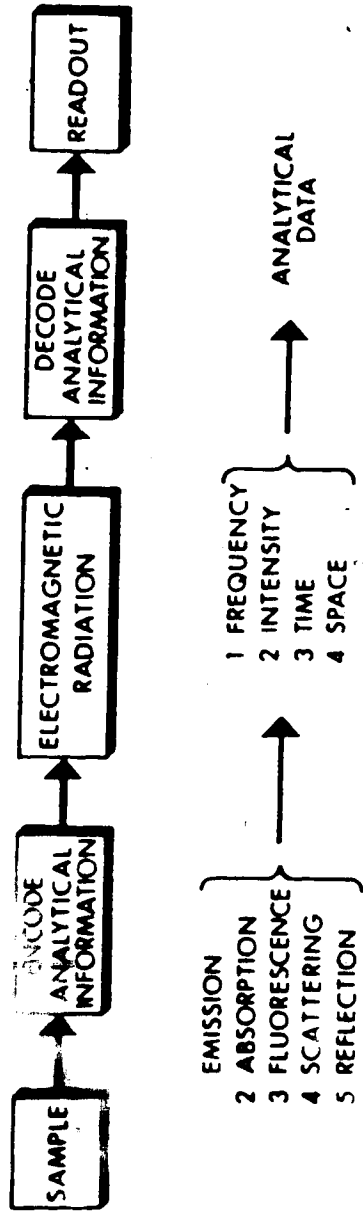


Figure 1. Spectrochemical measurement block diagram.

share of the OES instrument market because of several important characteristics of the ICAP source. The high temperature, chemical inertness and optical thinness of this source result in low detection limits, high sensitivities, linear responses of four to five orders of magnitude with respect to concentration, and low interference effects. ICAP-OES with the various commercial instruments can be used to simultaneously analyze qualitatively and quantitatively for 25 to 35 metal and metalloid elements in 30 or more samples per hour.

A major limit on ICAP-OES has been the almost exclusive use of pneumatic nebulization to introduce samples into the plasma. This sample introduction method requires that samples either be liquid or be converted to a solution and that several mL of sample be available. The use of samples in solution has several advantages such as the following, which are taken from an article by Boumans (5):

- a) Many samples are given as liquids, e.g. biological fluids, surface and effluent waters, oils, soil extracts, samples in wet chemical laboratories.
- b) Dissolution of solids prior to analysis circumvents interferences due to the solid structure; consequently accurate results can be attained with relatively simple reference samples (standards).
- c) Bulk analysis of inhomogeneous samples is feasible."

While most samples can be converted into a liquid form this is often a difficult and time-consuming process and

analytical errors often enter the analysis at this step.

These problems are again summarized well by Boumans (5):

- 1) the dissolution of a solid sample may be time-consuming and difficult;
- 2) there is a risk of contamination;
- 3) there is a risk of losses of volatile elements;
- 4) the dissolution of a solid entails a dilution, and this may lead to poor detection limits unless high efficiency of sample introduction and excitation compensate for this."

Boumans' summary of the performance of ICAP-OES and other established methods is shown in Table I from Reference 5. This comparison shows that ICAP-OES has the multi-element capability lacking in flame atomic emission and absorption (AES/AAS) or furnace atomic absorption (furnace AAS) and better precision and/or accuracy than furnace AAS, Arc AES, or liquid analysis with the spark-rotrode combination. X-Ray fluorescence spectrometry (XRFS) is an excellent technique except that without preconcentration its detection limits for liquid samples are approximately three orders of magnitude greater than those of ICAP-OES. The major weakness of ICAP-OES is then in the area of solid sample analysis. Another weakness of ICAP-OES, which has received very little attention, is the requirement that liquid samples have a volume of at least several milliliters. This is a requirement of the means used to introduce the sample into the plasma, the pneumatic nebulizer. Whether the nebulizer used is of a cross-flow or concentric construction type their liquid uptake rate is

Table I
 Rough Overall Assessment of the Main Analytical Capabilities of Various
 "Established" Spectroscopic Methods and ICP-AES

Capability for	Direct solid analysis	Direct liquid analysis	Multi-element analysis	Trace Analysis	Precise Analysis	Accurate Analysis
Flame AES/AAS	-	+	-	+	+	+
Furnace AAS	-')	+	-	+	+	(+)
Arc AES	+	-	+	+	-	-
Spark AES (metals)	+	-	+	(+)	+	+
Spark AES (rotrode)	-	+	+	(+)	+	+
XRFS	+	+	+	-")	+	+
ICP-AES	-')	+	+	+	+	+

Key: + good - poor (+) reasonable (-) unsatisfactory

Notes: ') + with solid sampling technique
 ") + with preconcentration technique

generally between 2 and 5 mL per minute. Since flush out, signal stabilization, and analysis times generally total 1 to 2 minutes it is easy to see why a sample volume of several milliliters is required.

The ICAP was first developed by Reed (6) for use in growing refractory crystals. Figure 2 shows Reed's modified induction-coupled plasma torch. Reed's torch was the precursor of present analytical torches and consisted of three concentric quartz tubes with three independent gas flows. The plasma was formed and centered within the torch by the gas flowing through the outer and intermediate tubes. The powdered refractory material flowed through the central tube in a high velocity stream of gas. This stream was able to punch through the center of the plasma where it was efficiently heated. Reed's intent was to raise the temperature of the powdered refractory material only to the melting point so that it could resolidify and thus allow boules of these refractory materials to be grown. One area needing improvement noted by Reed was that when small particle sizes were used these small particles tended to vaporize and this caused a "considerable increase in radiation". This statement is the start of ICAP-OES.

Since this first application of the ICAP was with a solid material it might be supposed that strong development in this area would continue, however the majority of work has been with liquid sample techniques. The first report

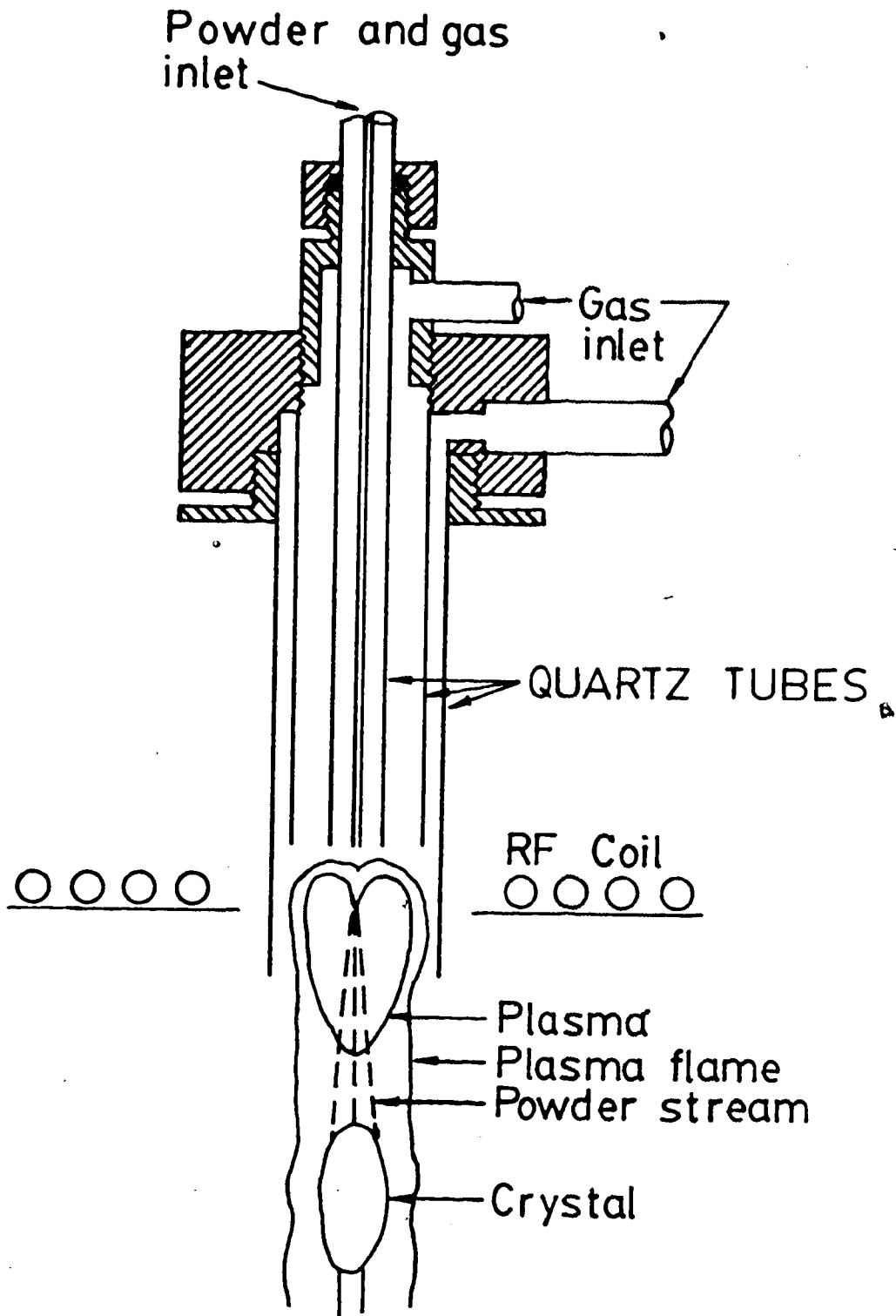


Figure 2. Induction-coupled plasma torch for crystal growth.

of solids analysis by ICAP-OES was in 1967 by Hoare and Mostyn (7). The system of Hoare and Mostyn was used for the analysis of powdered samples and is shown in Figure 3a. The sample was contained in a cup and a combination of mechanical agitation and swirling by a stream of argon gas caused the powder to become suspended in the argon stream for transport to the torch. Hoare and Mostyn reported no difficulty in transporting or smoothly exciting powders of widely different densities with this system, however they found that "the preparative history of the standards is of major importance and should be as near as possible identical to that of the samples". They also reported that it was necessary to use very small particle sizes (#300 mesh screen) and low injection rates since larger particles pass through the plasma virtually unchanged.

Aerosol injection of powders has also been reported by Dickinson (8) and by Dagnall, Smith, and West (9). The sample introduction systems used by Dagnall, et al. are shown in Figure 3b and 3c. The first of these is a swirl cup system similar to that used by Hoare and Mostyn (7). The second system utilized a fluidised bed design and according to the authors was found to work better than the swirl cup arrangement. Mechanical agitation of both systems was found to help smooth delivery of the powder to the plasma. The authors tested sample matrices and rejected several because of particle sticking, high emission

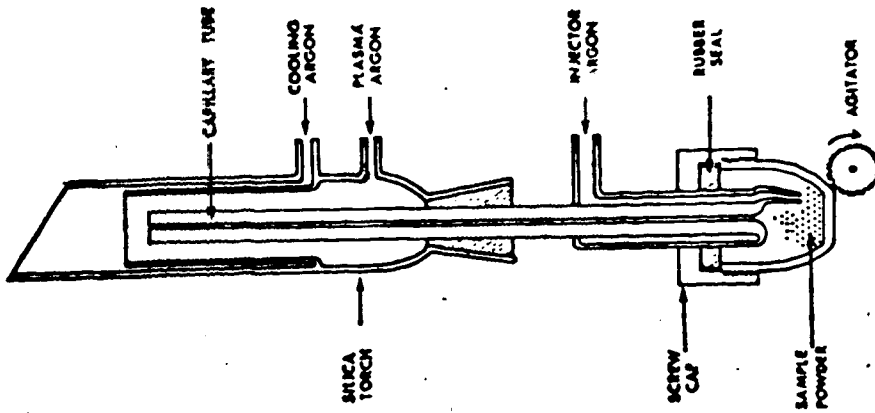
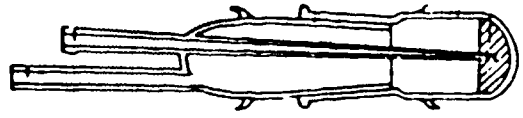


Figure 3 (a). Powder injection assembly.



(b). Swirl cup chamber.



(c). Fluidized-bed chamber.

background, or a high contamination level. With a MgO matrix, they were able to analyze for added Be and B but found that the powder feed rate decayed exponentially, therefore readings had to be taken after a selected delay time. The calibration curves for Be or B are linear over only about two orders of magnitude compared to the normal three or four orders of magnitude range common to ICAP-OES.

In general the following seem to apply to direct aerosol injection of powders into a plasma:

- a) Sample history and matrix are critical.
- b) The sample particles must be non-sticking, less than about 10 μm in diameter, and have a small size range.
- c) Sample sizes of several grams are required.
- d) Emission may vary with time, thereby complicating the measurement.

Pneumatic nebulization of powdered samples suspended in liquid as a slurry has been reported by Chapman and Gordon (10) and Dahlquist (11) has reported vaporization of a slurry from a graphite yarn electrothermal vaporizer, however very little information is available about these procedures. Fassel and Dickinson (12) have reported that low-melting alloys can be analyzed by using ultrasonic nebulization of the molten material but this technique is obviously limited in applicability.

Conductive metals or briquetted materials have been analyzed by a combination of producing an aerosol by

sampling the material with a spark or an arc and then exciting this aerosol to produce emission with an ICAP. The use of a remote d.c. arc sampling device was first reported by Dahlquist, Knoll, and Hoyt (13) in 1975. This device, in the form of a small remote sampler known as a Direct Solids Nebulizer (DSN), is now commercially available from Applied Research Laboratories, Sunland, California. The DSN has been applied to the analysis of a large variety of metals ranging from aluminum to steels. The DSN-ICAP combination has been reported as giving excellent detection limits, linear calibration curves of two to three orders of magnitude, minimum matrix effects, and excellent precision. In contrast direct emission analysis by a.c. spark or d.c. arc suffers from large matrix effects, limited linear working ranges, poorer spark detection limits, and poorer arc precision. The use of an a.c. spark has been investigated by Human, Scott, Oakes, and West (14), Norris and Watters, Jr. (15), Brech (16), and Beaty, Crawford, and Wahlers (17). The SSEA, or Separate Sampling and Excitation Analysis, discussed by Brech and Beaty, et al. is based on the work of Norris and Watters and makes use of a controlled waveform spark source for improved sampling. While this system is not commercially available it appears to have similar characteristics to the DSN system. The major limit on these systems is that they

obviously require electrically conductive samples.

The combination of laser vaporization and separate a.c. spark excitation for OES is a well known method for microprobe analysis and for the analysis of nonconducting materials. Laser vaporization with separate ICAP excitation for OES has also been applied to the analysis of airborne particulates collected on a filter by Abercrombie (18) and for powders and metals by Salin, Carr, and Horlick (19), Carr and Horlick (20), and Carr (21). Abercrombie considered the results to be only semiquantitative and used the technique as a screening method. Carr and co-workers results are more complete and show excellent detection limits, fair precision, and reasonable analytical ranges but severe matrix effects were noted. The expense of a high power laser for vaporization must also be considered as a drawback to this technique.

As mentioned earlier the use of a nebulizer for analysis of liquid samples by ICAP-OES generally requires a sample volume of several milliliters. In many cases, such as with biological samples, this can be a severe restriction. Often dilution of the sample cannot be used since this might reduce the element of interest to below an acceptable analytical concentration. In order to analyze 50 to 100 μL size biological samples Baddiel and Skerten (22) utilized a flow injection system connected to

an ICAP nebulizer. Greenfield and Smith (23) and Kniseley, Fassel, and Butler (24) found that as little as 25 μL of biological fluids could be analyzed by connecting a μL pipette to the nebulizer liquid intake. A short pulse of analyte aerosol was thus produced by each of these means and carried to the ICAP torch in the normal manner. The detection limits obtained with these pulsed emission systems would be expected to be considerably higher than those obtained with integration of a steady emission level obtained by normal nebulization techniques. The poor aerosol production by nebulizers (nominally 2-10%) also means that the sample was inefficiently used.

In the field of atomic absorption spectroscopy electrothermal atomization has become an important technique since it efficiently uses small liquid samples and produces very low detection limits. Electrothermal vaporization techniques have been applied to ICAP-OES for liquids analysis by several researchers. Dahlquist, Knoll, and Hoyt (13) have reported using a graphite yarn electrothermal vaporizer for simultaneous multielement analysis of urine for Hg, As, and Pb with a 25 μL sample. Detection limits comparable to or better than those obtained with a nebulizer were reported for 28 elements and the linear analytical range was given as greater than two orders of magnitude. A tantalum strip electrothermal vaporizer was reported by Nixon, Fassel, and Kniseley (25). Good precision

and very low detection limits were obtained with a sample size of about 100 μ L. Recently Gunn, Millard, and Kirkbright (26), Kirkbright and Snook (27), and Millard, Shan, and Kirkbright (28) have reported in a series of papers their work with a graphite rod electrothermal vaporization device for ICAP-OES. This work has concentrated on the analysis of small liquid samples utilizing carrier distillation to lower the detection limits of several elements.

The reported uses of electrothermal vaporization have been limited to liquid samples, however one thermal vaporization technique has been reported for both liquid and solid samples. Salin and Horlick (29,30) have published preliminary results for a direct sample insertion device (DSID) in which the sample is placed in a d.c. arc cup electrode with a boiler cup and this combination directly inserted into the ICAP. Their early data indicates that detection limits and precision comparable to those of d.c. arc can be obtained for liquid samples and that the analysis of powdered samples is possible.

In consideration of some of the previous work above it was decided to investigate the possibility of developing a sample handling device which could be used for the analysis of both small volume liquid samples and solid samples. Requirements for this device were:

1. μ L size liquid sample handling capabilities.
2. Solid sample handling capabilities.
3. Single or multielement analysis capabilities.
4. Reasonable analytical ease and speed.
5. Useful detection limits and sensitivity.
6. Useful accuracy and precision.
7. Low matrix effects.

In order to achieve the above goals it was decided to use an AAS graphite carbon cup electrothermal atomization device for sample vaporization and to transport the vaporized sample in a flowing argon stream to the ICAP for OES analysis. The major reasons for this decision were:

1. Carbon cup electrothermal atomizers are able to rapidly reach temperatures capable of vaporizing most elements.
2. The carbon cup electrothermal atomizer is relatively compact and thus could be enclosed in a small flow through cell to keep vapor volume at a minimum and thus detection limits low.
3. Liquid samples can be easily injected into the cup with a syringe allowing rapid and easy analysis of liquid samples.
4. The cup can be easily changed allowing solid materials to be added to the cups and sample weights determined externally.
5. Matrix effects are common in furnace AAS but separate

excitation with the ICAP was expected to reduce this.

6. A large body of literature was available on carbon cup or tube electrothermal vaporization.

CHAPTER II

Instrumentation: Description and Modifications

A generalized block diagram of a spectrochemical measurement system was given in Figure 1. In this chapter a more detailed description of the spectrochemical measurement system used for this experimental work will be presented. Two types of systems were used for decoding the analytical information, a monochromator-photomultiplier detector system and a photodiode array based direct reader system. Each of these systems are shown in detailed block diagrams in Figures 4 and 5 and are described in Section D of this chapter. The readout system is based on the use of a minicomputer for data storage and manipulation and is very similar for both detection systems and will also be described in Section D.

A. The Graphite Furnace

The graphite furnace used throughout this experimental work was developed from a commercially available Varian Model-63 Carbon Rod Atomizer (31). The Carbon Rod Atomizer as it is normally used for atomic absorption spectrometry is shown in Figure 6 from Reference 31. With the Model-63 unit either a tube furnace or a cup furnace may be used. The furnace is held between two graphite rod electrodes which are in turn held by water cooled chromium plated

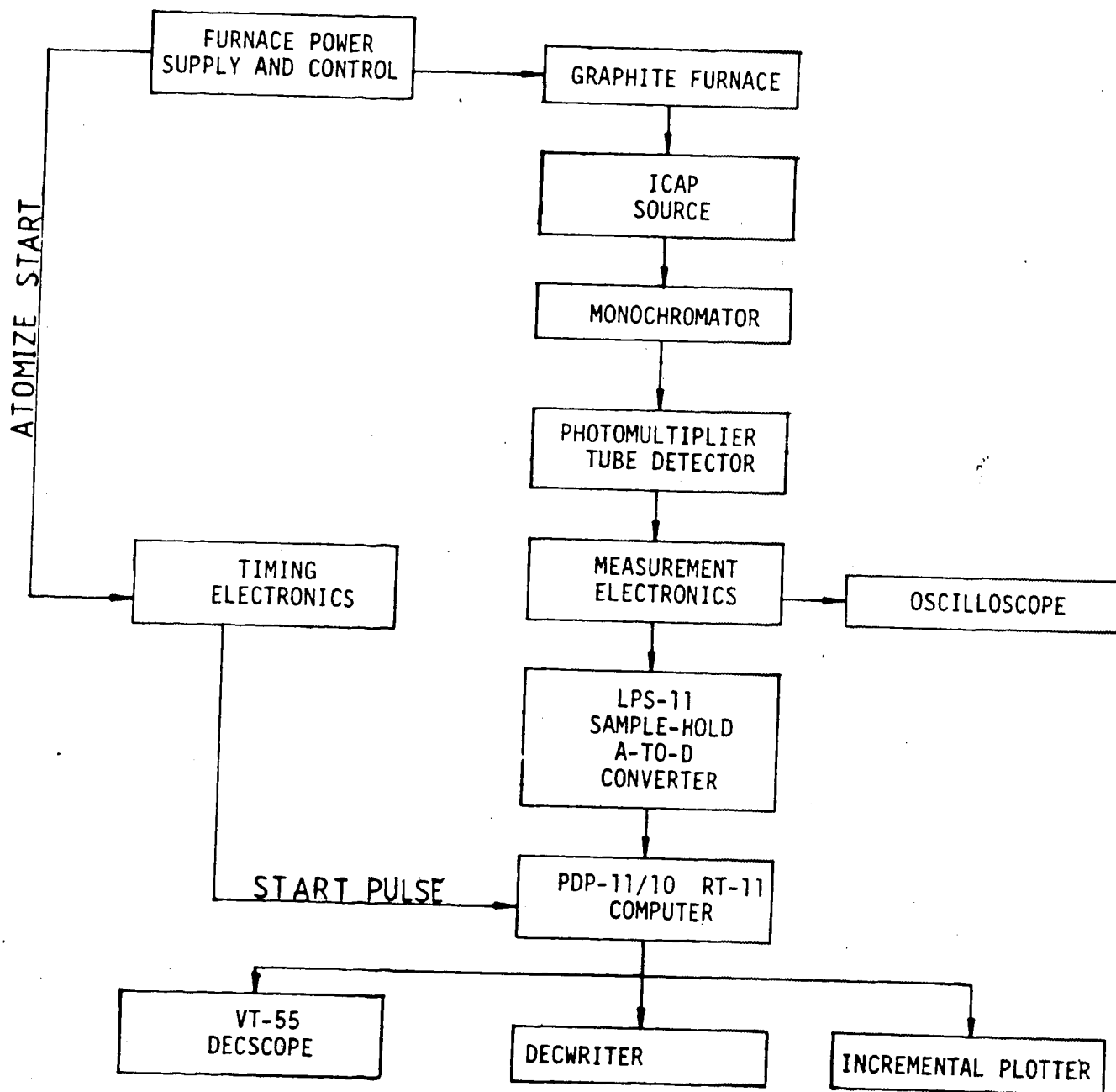


Figure 4. Block diagram of computer coupled photomultiplier spectrometer.

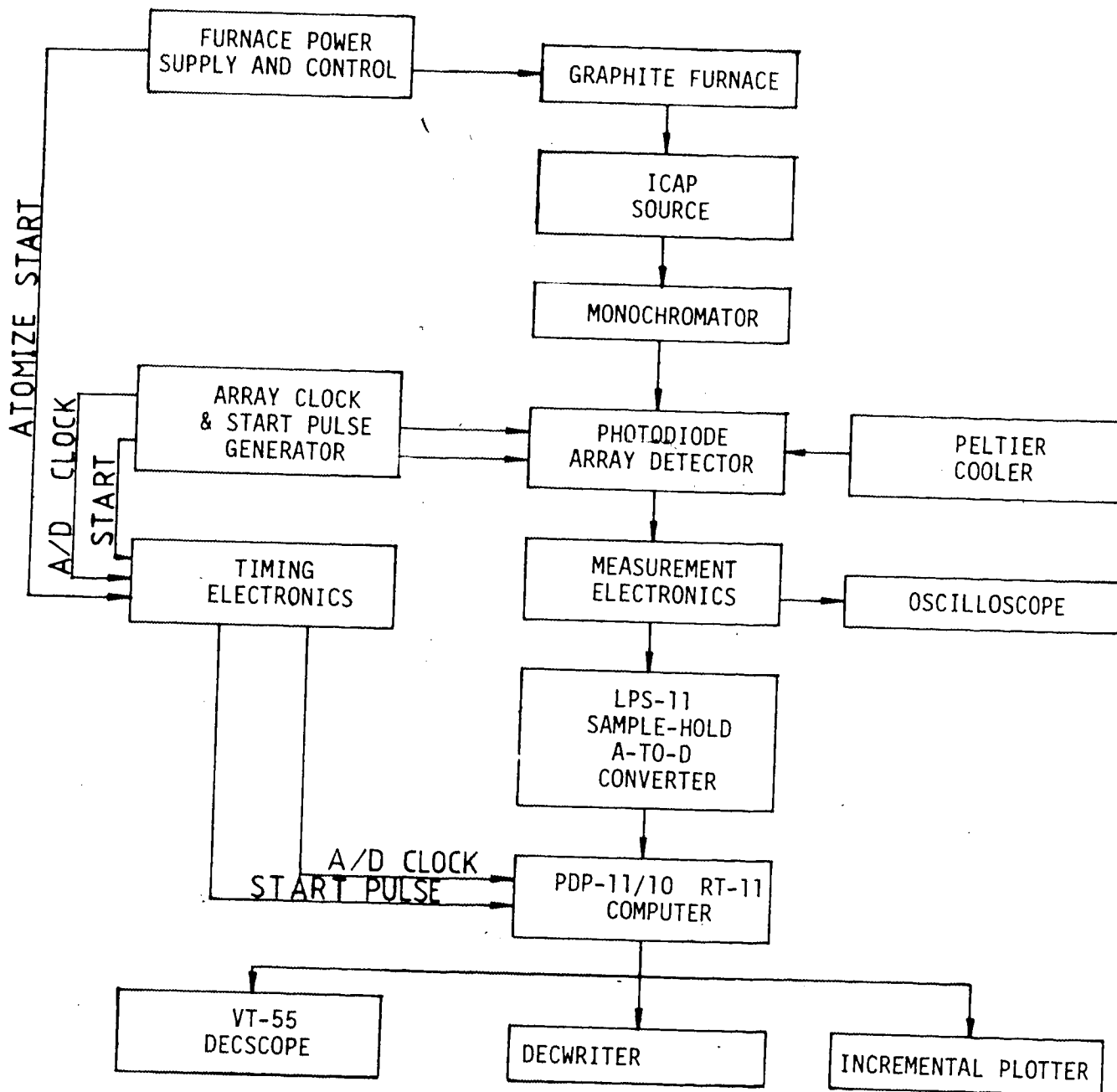


Figure 5. Block diagram of computer coupled photodiode array spectrometer.

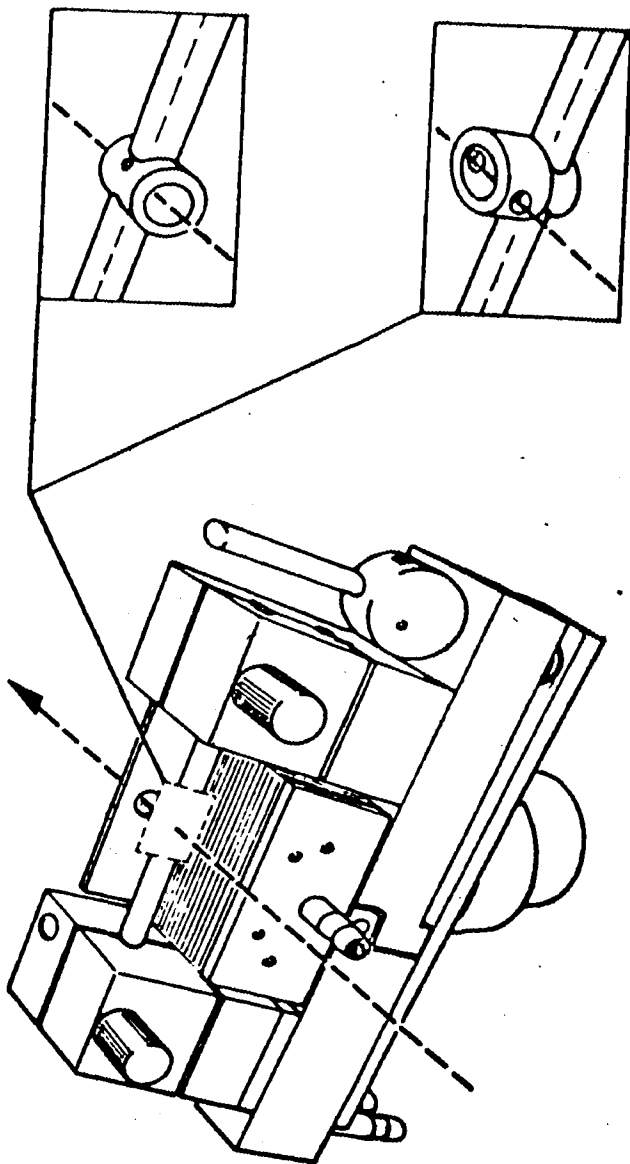


Figure 6. Varian Model 63 Carbon Rod Furnace.

steel clamps. Electrical contact with the electrodes-furnace assembly is also provided by these clamps. For this work the carbon cup shown in the lower right of Figure 6 was used although the carbon cup was modified.

The Model-63 Carbon Rod Furnace was enclosed in a quartz cell which was attached to the bottom of the ICAP torch by a 10 inch long Pyrex tube. The quartz vaporization cell, shown in Figure 7, is in two parts and is constructed from a quartz 35/20 ball-and-socket joint. The two piece construction allows easy access for sample or sample cup changing. The ball-and-socket joint construction also allows flexibility in joining the two halves of the cell after opening and for thermal expansion. Argon flowing through the cell sweeps the analyte vapor from the furnace, out the top of the vaporization cell, and into the plasma.

The vaporization cell is approximately 1 inch in diameter and 4 inches in height with a volume of about 50 mL. Emission intensity is dependent upon the concentration of the analyte in the argon gas introduced into the plasma therefore it is important to keep the vaporization cell volume small. The electrode rods pass through the walls of the lower half of the vaporization cell. O-rings form a seal between the vaporization cell and the steel clamps of the Model-63 Carbon Rod Furnace assembly. These o-rings are made by punching a 3/16 inch diameter hole through a

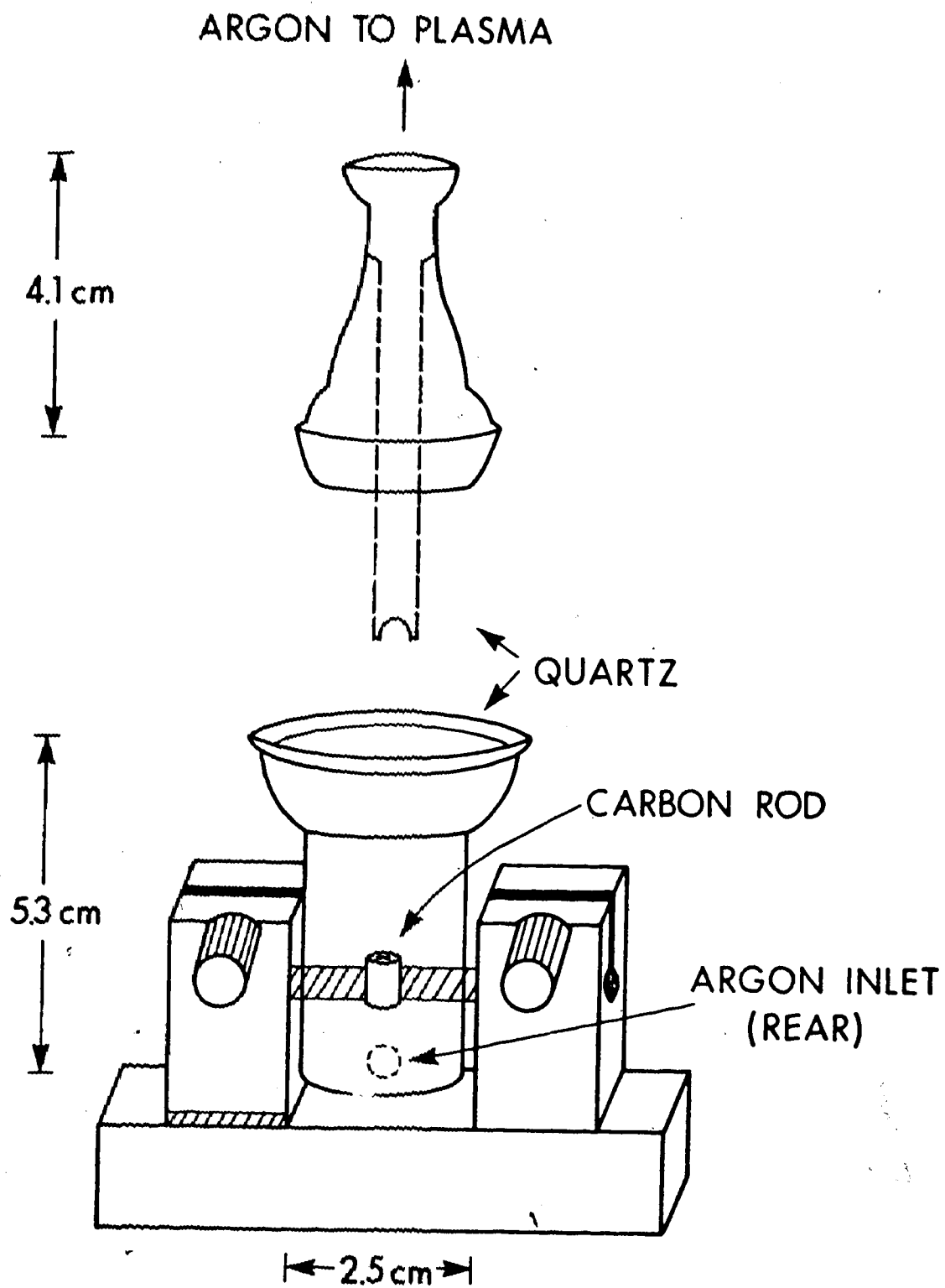


Figure 7. Vaporization cell for graphite cup EA-ICAP-OES.

high temperature gas chromatograph septum. O-rings made from Varian No. 69-000179-01 septums have proven to be useful for between 50 and 100 atomization cycles. The argon gas inlet for the vaporization cell is located at the lower rear of the bottom half of the cell.

The top of the upper half of the vaporization cell is a 12/5 socket to allow connection to the ICAP torch by means of the intermediate Pyrex tube mentioned earlier. Although not shown in Figure II-2 an injection port was added to this part of the vaporization cell to facilitate the introduction of liquid samples.

The 10 inch intermediate tube which connects the vaporization cell to the ICAP torch is constructed of 0.5 mm internal diameter Pyrex tubing. The lower end of the tube is a 12/5 ball to mate with the vaporization cell while the upper end is a 12/5 socket which mates with the torch. About 1 1/4 inches from the lower end is a 3-way stopcock which allows the cell to be flushed to the atmosphere or connected straight through to the plasma torch.

1. Modifications of the Graphite Cup

A detailed drawing of the graphite cup is shown in Figure 8 to illustrate the first major modification. The normal carbon cup is designed as a two part cup. Electrical resistance heating takes place in the lower portion of the

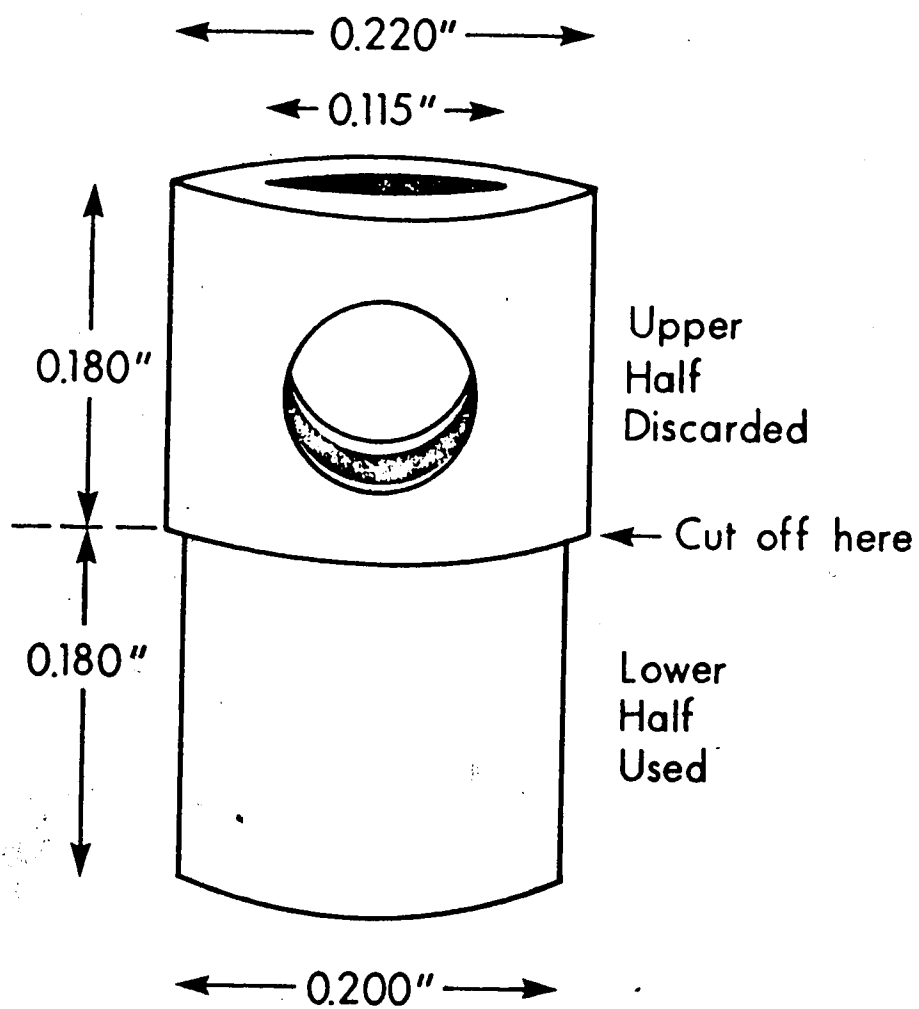


Figure 8. Modification of Varian graphite cup for use in EA-ICAP-OES.

cup. This heating is controlled by varying the electrical voltage applied to the unit. With the Model 63 this heating control is in three separate stages for sample drying, ashing, and atomizing.

The first two stages can range from 0 to 60 seconds long with the applied voltage changing instantly at the start of each stage and remaining constant in that stage. The atomization stage can be either a step heating or a ramp heating one. The step heating mode is like the drying and ashing ones except that it is limited to about 10 seconds or less. In the ramp heating mode the applied voltage increases linearly as a function of time until a pre-selected maximum is reached and heating ceases. The slope for the voltage increase, and thus the heating rate, is variable over a wide range. Shown in Figure 9 (31) is a diagram of applied voltage vs time for the step mode of operation. Typically a temperature of 90-110°C is used for drying, 500-900°C for ashing and during the atomization stage temperatures in excess of 2500°C may be used to allow atomization of virtually all elements.

The upper portion of the cup is the atomic absorption cell. The atomic vapor produced in the lower portion of the cell during atomization diffuses upward into the atomic absorption spectrometer optical beam, which passes through the apertures in the upper half of the cup, and then out

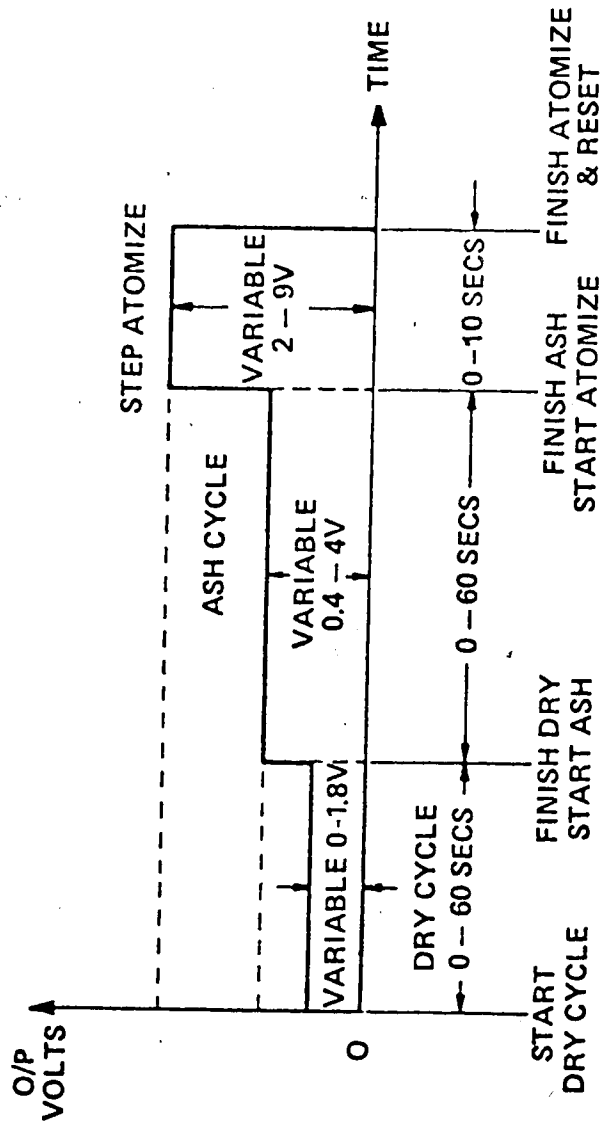


Figure 9. Applied voltage vs time for step mode of operation of the Varian Model 63 Carbon Rod Atomizer.

of the cup. For atomic absorption spectrometry it is desirable to keep the vapor inside the absorption cell for a fairly long time to simplify the absorption measurement and to obtain the greatest absorption possible. A long vapor retention time is achieved by making the cup quite deep with respect to its width (2.4:1).

One of the difficulties that can be encountered with this type of furnace is caused by the fact that while the lower portion of the cup is heated electrically the upper portion is only heated by conduction. The result is that the temperature of the upper portion lags behind that of the lower portion. When the bottom of the cup passes through the vaporization temperature for the element of interest it will vaporize and then condensation-revaporization can occur in the upper portion of the cup. This process is accentuated when ramp atomization is used since the slower heating allows a longer time for the condensation-revaporization process to occur. When this process does occur analyte vapor production is not a smooth, continuous process but proceeds as an irregular and prolonged process and the maximum analyte vapor concentration is depressed.

The carbon cup atomizer was used in this experimental work only as a sample vaporization device and a low retention time for the sample vapor was desired. In order to reduce the retention time most of the upper half of the

atomization cup was cut off and discarded. The small amount of the upper portion left formed a small lip around the top of the cup which aided in the vertical positioning of the cup between the graphite electrodes. The remaining cup was approximately 0.1 inch deep and had a volume of approximately 2×10^{-2} inches³ or 30 L. This modification resulted in four desirable changes.

1. The sample vapor retention time was reduced.
2. Condensation-revaporization in the upper part of the cup was eliminated.
3. The mass of the cup was reduced, therefore the heating rate was increased.
4. A higher temperature was obtained at any given power setting than with the larger normal cup.

The second modification was to change the nature of the carbon cup itself. Normally graphite is a layered structure with an inner atomic distance of 1.415 Å within the layer and a separation of 3.35 Å between the layers (32). It is possible for many molecules or atoms to penetrate this loose, layered structure at high temperatures.

Sturgeon and Chakrabarti (33) have determined that the rate of loss of Mo and V atomic vapor from an uncoated atomic absorbance graphite tube furnace was increased by 21% and 12%, respectively, over that obtained with pyrolytic-graphite-coated tubes. The pyrolytic-graphite coating

porosity, defined as the percentage of volume of the pores in relation to the total volume, is effectively zero, as compared to 17% for regular high-purity graphite (34). This reduction in porosity is brought about by the elimination of the layered structure of regular graphite. The use of pyrolytic-graphite-coated furnaces has become quite common since the reduction of loss through the furnace walls increases sensitivity. The pyrolytic-graphite-coating is also mechanically stronger and has a higher sublimation point than regular graphite therefore furnace life is extended. The Varian No. 56-1000159-00 carbon cup furnaces used in this experimental work were pyrolytic-graphite-coated.

Many elements are also known to react with carbon to form a variety of types of compounds. For atomic absorption spectroscopy the reduction of several metal oxides to the free metal by carbon is extremely beneficial, however some elements can react to form non-volatile refractory carbides. This loss of volatile analyte can be reduced by the use of pyrolytic-graphite-coated furnaces or by first converting the furnace carbon into a nonreactive form. This change is easily accomplished by treating the furnace with a suitable carbide-forming compound such as lanthanum, zirconium, silicon (35), or tantalum (36) prior to use. These stable carbide coatings can reduce carbide formation by other

elements in two ways. The first is by reducing the porosity in a manner similar to pyrolytic-graphite-coating and the second is by preventing contact between carbon of the furnace with the sample.

The treatment of the carbon cup furnaces used in this work with a TaF_5 solution in the manner given in Reference 36 was used. The carbon cups were placed in a TaF_5 solution contained in a plastic dish in a vacuum desiccator. The desiccator was evacuated for about one minute and then allowed to refill with air. After a second evacuation the cups, filled with TaF_5 solution, were placed in an oven at $110^\circ C$ for several hours. Immediately prior to use the furnace was assembled and three or four firings at high temperature completed the reaction between the Ta and the carbon of the furnaces. These firings also served to clean any contamination out of the furnaces. The experimental results indicated that there was some increase in the sensitivity of several elements but there was a loss in the mechanical strength of the furnace. This loss of strength was not important when liquid samples were analyzed and the cups were satisfactory for 50 to 100 atomization cycles. Deterioration was mainly caused by arcing between the electrode rods and the furnace cup. This arcing was present in untreated cups but was worse with the Ta treated cups, perhaps due to a change in electrical conductivity or to a

small change in dimensions causing gaps between the electrode rods and the cup. With solid samples the cups must be removed and replaced with each sample and the Ta treated cups were found to deteriorate much more rapidly than the untreated ones. Because of the design of the furnace used, this arcing problem could not be overcome and the use of Ta treated cups was discontinued with solid samples.

2. Modification of the Varian Model 63 Carbon Cup Atomizer Control/Power Supply

The controller/power supply of the Varian Model 63 Carbon Rod Atomizer normally controls all operation of the carbon rod furnace. This unit contains all necessary electronics for controlling the temperature and timing of the three sequential steps used - Dry, Ash, and Atomize (refer to Figure 9). In order to properly acquire data it was necessary to synchronize data acquisition and the atomization step. The "Trigger" pulse available from the controller/power supply was used for this purpose with the PMT data acquisition system. Additional external circuitry was necessary with the photodiode array spectrometer systems to accurately synchronize the start of the atomization step with the start of an integration cycle of the photodiode array.

Timing in the Model 63 is by means of a series of three

ramp generator-comparator blocks. A simplified diagram of a TIMER BLOCK is shown in Figure 10 (31).

When an INPUT TRIGGER pulse is received the HOLD CIRCUIT opens the RESET SWITCH and closes the switch connecting the +15 V supply to the RAMP GENERATOR input circuit causing its output to ramp negative at a constant rate. When the negative ramp exceeds the magnitude of the TIME input voltage, set by a front panel voltage divider, the COMPARATOR output switches from -15 V to +15 V. This pulse is differentiated and the negative pulse is clipped off to produce a positive OUTPUT PULSE. This pulse is fed backward to the RESET of the HOLD CIRCUIT and forward as the INPUT TRIGGER of the next TIMER BLOCK. At the completion of the Ash step the OUTPUT PULSE is also used as the external TRIGGER pulse.

A complete diagram of the TIMER BOARD ASSEMBLY is shown in Figure 11 (31) and a complete description of the circuit operation can be found in Reference 3. In order to connect the external circuitry necessary to synchronize the photodiode array spectrometer systems it was necessary to modify the connection between the ASH TIMER BLOCK and the RAMP/STEP switch. The area modified is enclosed in the heavy dashed line in Figure 11. The modification, external circuit, and timing diagram are shown in Figure 12.

When switch S1 is in the INTERNAL position the Varian

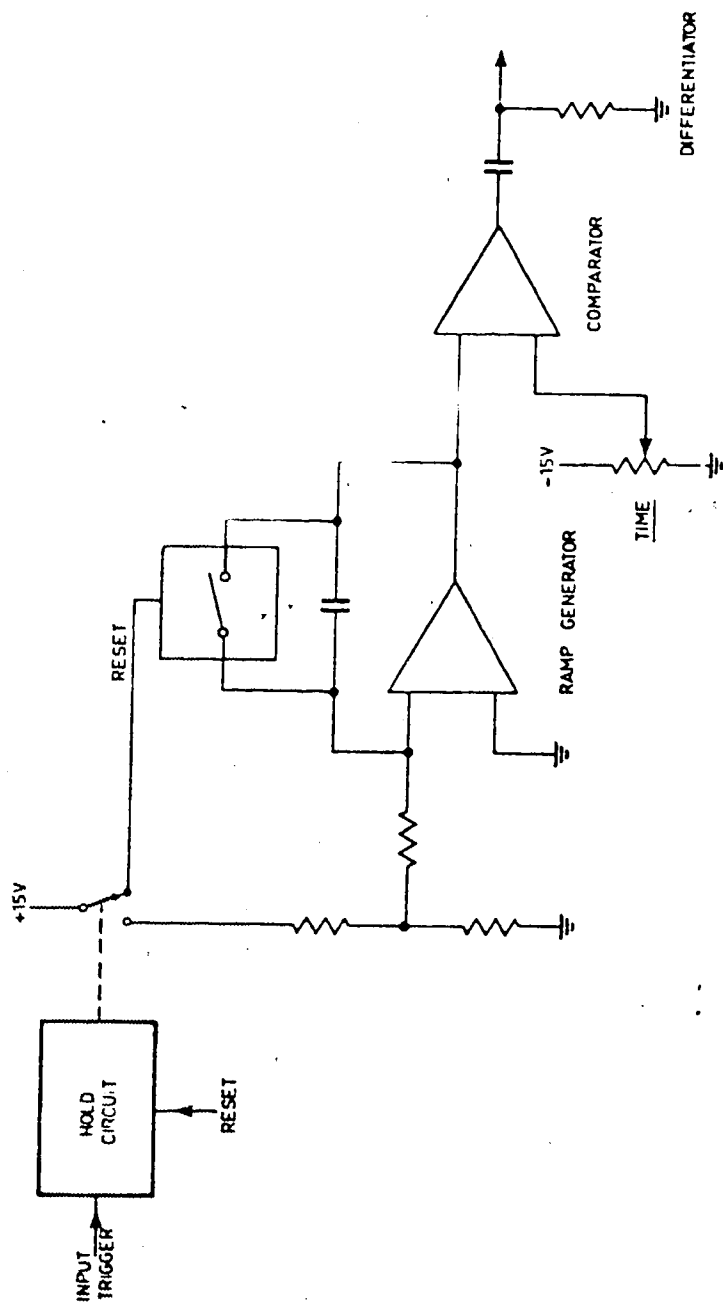


Figure 10. Timer Block - Varian Model 63 Carbon Rod Atomizer Controller/Power Supply.

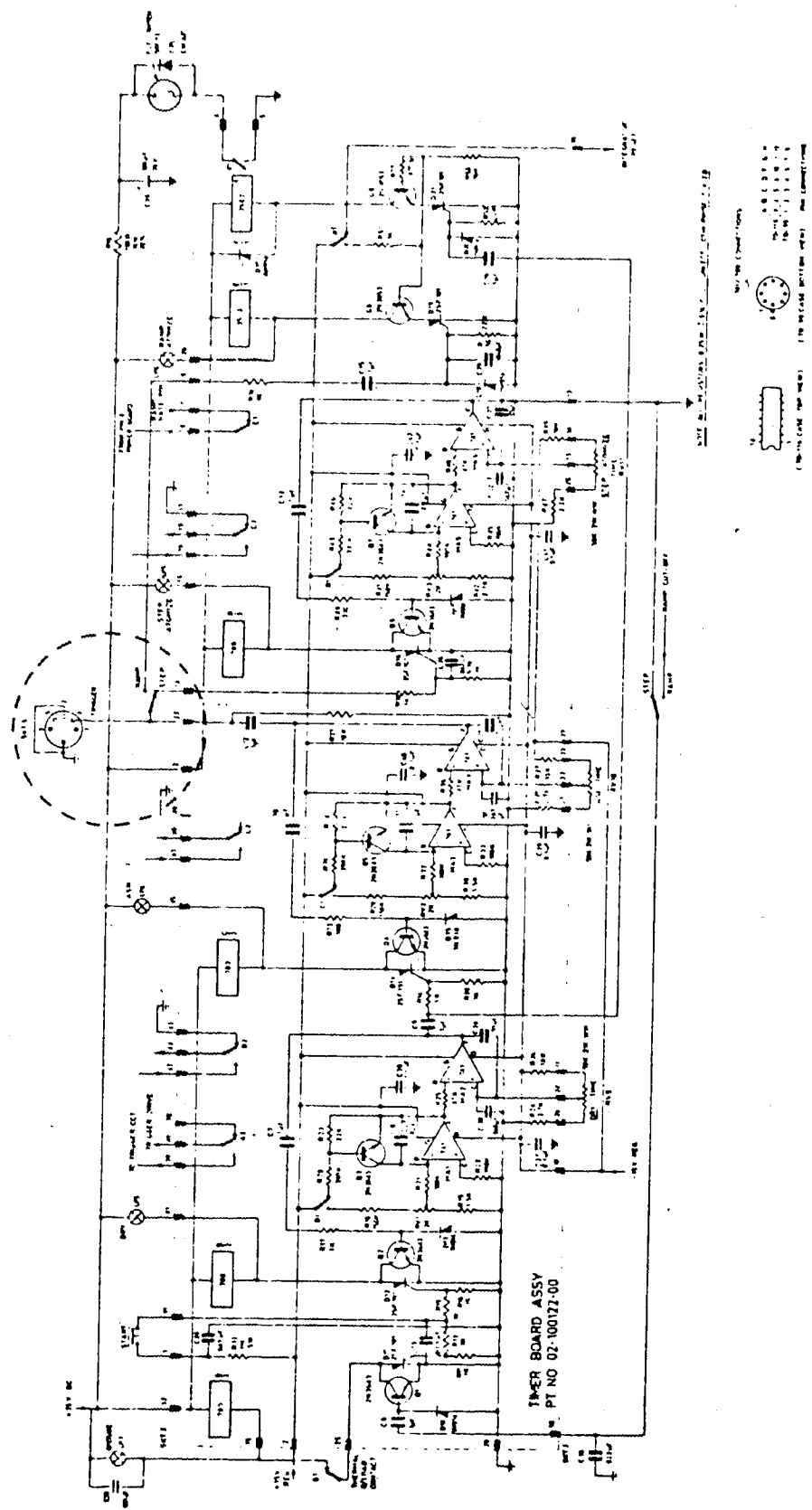


Figure 11. Timer Board Assembly - Varian Model 63 Carbon Rod Atomizer Controller/Power Supply. Circled area shows portion modified as shown in Figure 12.

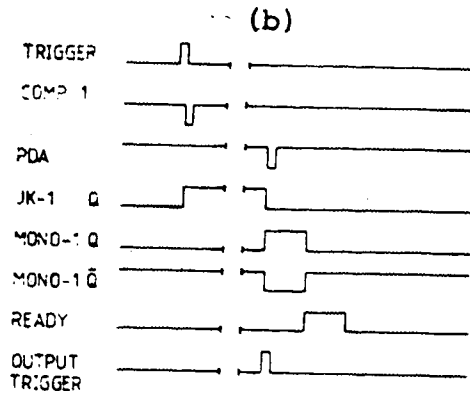
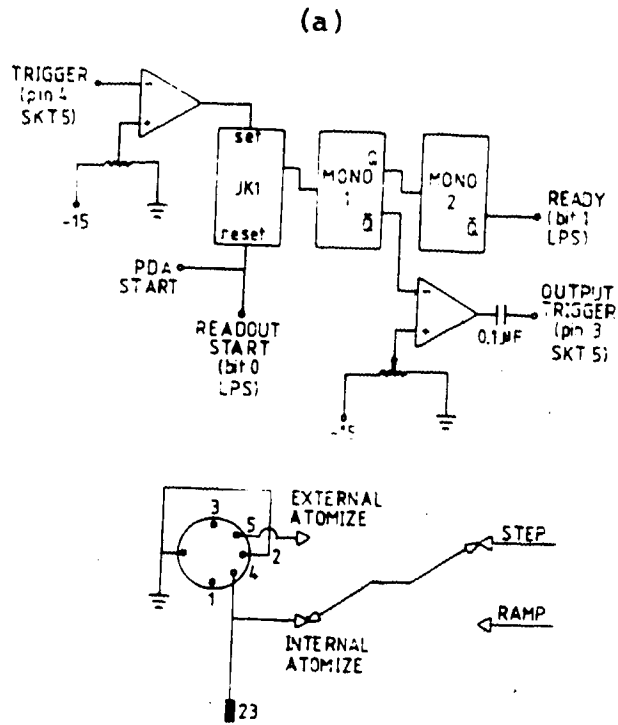


Figure 12. (a) External circuitry and Model 63 modification for synchronizing atomization and photo-diode array spectrometer system data acquisition.

(b) Timing diagram.

63 power supply operates in the normal manner. When switch S1 is in the EXTERNAL position an externally generated INPUT TRIGGER is connected to the ATOMIZER TIMER BLOCK. The model 63 TRIGGER pulse from SKT5 causes JK1 to be "set" and then the next photodiode array READOUT START signal "results" JK1. These operations produce a positive pulse at the Q output of JK1, the negative edge of which triggers MONO stable 1. When MONO stable 1 is triggered the \bar{Q} output changes from -5 V to 0 V for 1 msecond, causing the output of COMPArator 2 to momentarily change from -15 V to +15 V. This generates a pulse which is returned to the RAMP/STEP switch via pin 5 of SKT5 and starts the atomization step. At the end of the pulse from MONO stable 1 the \bar{Q} output of MONO stable 2 changes to 0 V for 1 msecond. This momentary ground signal is transmitted to the LPS11 parallel input and serves as the data acquisition READY flag. Succeeding photodiode array READOUT START signals trigger acquisition of photodiode array data.

B. Inductively Coupled Argon Plasma

The ICAP used for this work was a 5 KW ICAP manufactured by Plasma-Therm Inc. (Kreston, N.J.). The ICAP torch used is shown in Figure 13. The torch supplied by Plasma-Therm has a constricted outlet for the central, or sample tube. This central tube was replaced with a 1.5 mm internal diameter

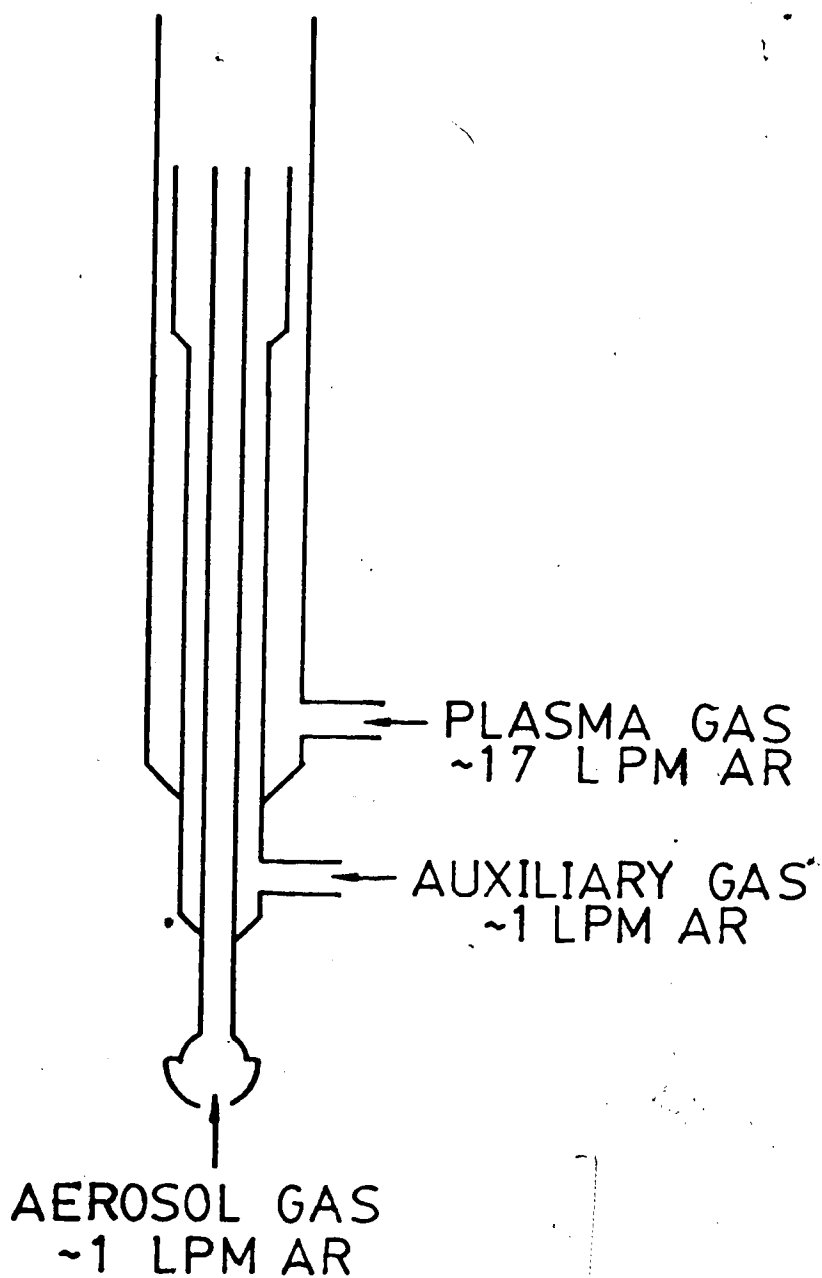


Figure 13. ICAP torch.

straight bore tube to provide a more laminar flow of sample gas through the torch and thereby reduce the chance of sample particles adhering to the walls of this tube. This type of torch proved to be easy to construct and operate and the operating characteristics were very constant from torch to torch. Table II lists the ICAP specifications and operating conditions.

C. Monochromator

The monochromator system used was the Heath Scanning Monochromator Model EU-700-70 with accompanying electronic Control Unit Model EU-700-51. This Heath monochromator is a single-pass Czerny-Turner design with folding mirrors to provide entrance and exit beams on a common optic axis. Selected specifications are given in Table III from Reference 37.

The plasma was imaged on the entrance slit of the monochromator by a 100 mm focal length quartz lens. With the PMT data acquisition image magnification was -0.5. With the computer-coupled photodiode array spectrometer systems an image magnification of -0.5 was used for spectral studies and of -0.25 for spatial emission studies.

D. Detector-Readout Systems

The detector-readout systems used are of two basic

Table II
ICAP Specifications and Operating Conditions

Plasma:	ICP 5000 (Plasma-Therm)
R.F. Generator:	Type HFS 5000D (Plasma-Therm)
Frequency:	27.12 MHz
Power Available:	5.0 Kw
Power Used:	1.5 Kw
Plasma Argon Flow:	17.0 Lpm
Auxiliary Argon Flow:	~1.2 Lpm
Sample Argon Flow:	0.8 - 1.0 Lpm
Observation Height:	Centered at 15-17 mm above load coil

Table III

Specifications for Monochromator Unit Model EU-700-70

Type of Mount:	Single-pass Czerny-Turner mounting with folding mirrors to provide entrance and exit beams on a common optic axis.
Aperture Ratio:	f/6.8 at 2000 angstroms.
Focal Length:	350 millimeters.
Resolving Power:	Better than 1 angstrom; Line-profile half-width less than 0.5 angstrom, with 3 mm slit height.
Stray Light:	0.1% or less within $\pm 1-1/2$ bandwidths of a given line.
Reciprocal Dispersion:	Approximately 20 angstroms per mm at exit slit with 1180 lines per mm grating, depending on wavelength.
Grating:	Precision plane grating replica; 48 mm x 48 mm ruled area. Standard grating of 1180 lines per mm, blaze wavelength 2500 angstroms.
Slit Width:	Continuously variable between 5 and 2000 micrometers.
Slit Height:	12 mm maximum.

types--photomultiplier tube (P.M.T.) and photodiode array (P.D.A.) based systems. The P.M.T. has a venerable history as a single channel detector for O.E.S. The reasons for the almost universal use of the P.M.T. detector are mainly its low dark current, its high sensitivity, and a linear response range of up to 6 orders of magnitude.

Multichannel detection in O.E.S. has traditionally been done with a wavelength scanning single channel detector, a photographic plate multichannel detector, or a series of single channel detectors as in a direct reader. Alternatives to these systems which have been proposed for multichannel detectors are television camera tubes (38,39) and photodiode arrays (40,41,42,43). These electronic multichannel detectors have the advantage of providing for a real time readout of spectra. A response range of several orders of magnitude can be easily obtained by using integration times varying from 100 msec. to 52.4 seconds for each cycle of the array readout and by time averaging the information from a number of readout cycles. The individual cycles can also be used for time studies of O.E.S. signals which vary with time (44).

Following either the P.M.T. or the P.D.A. detector systems used in this work was a digital data acquisition-readout system. The basic components of these systems were amplifiers to condition the signals, an analog-to-digital

converter, a computer for data storage and manipulation, a printer and an incremental plotter. These systems will be discussed in greater detail in the following sections.

1. Monochromator-Photomultiplier Readout System

The P.M.T. was chosen as the detector for single element analysis in this experimental work because of the characteristics mentioned earlier. The long linear response range is particularly significant since it matches the similar linear response range of the ICAP.

The P.M.T. used was a 1P28 which was operated at 600.0 V. This P.M.T. was powered by and enclosed in a Heath Photomultiplier Module EU-701-30 which is a companion module to the Heath Monochromator Module EU-700-70. The spectral range covered with this P.M.T. is from about 185 nm to 650 nm. No work was attempted at wavelengths below 200 nm since light absorbance by O_2 begins to become significant in this range and because there were no emission lines pertinent to this work below this wavelength.

Conversion of the P.M.T. current signal into a voltage signal and amplification/filtering of this signal was performed by two systems in this work. In the early work a current-to-voltage converter constructed from a Burr-Brown, Tucson, Arizona, 3308/12C operational amplifier which was used with a Tektronix Inc. (Beaverton, Oregon), AM 502

Differential Amplifier to provide further amplification and filtering. In the latter part of the work a Keithly Instruments, Inc. (Cleveland, Ohio) Model 427 Current Amplifier was used. The Keithly amplifier proved easier to use but no significant differences in performance were noted between the two systems.

The circuit diagram for the current-to-voltage convertor is shown in Figure 14. The i/v convertor has an RC time constant of 0.01 second which allows the rapid changes in emission intensity from electrothermally vaporized analytes to be accurately followed. The i/v convertor was constructed to allow operation in two amplifier ranges. The first has an output voltage of 10 V for an input current of -10^{-6} amps and the second has an output voltage of 10 V for an input current of -10^{-5} amps. Photomultiplier response is generally only linear up to about 10^{-6} amps therefore only the first amplifier range was used for analytical work and when the current exceeded 10^{-6} A a neutral density filter, OD1, was interposed between the ICAP and the Monochromator to reduce the P.M.T. current to less than 10^{-6} amps. Table IV lists the calibration data for this i/v convertor.

The Tektronix AM 502 Differential Amplifier used with the i/v convertor served mainly to provide final filtering if necessary, further amplification, and a d.c. offset to

Table IV

Calibration Data for Current-to-Voltage Convertor

$$i = V_{in}/R_{in} = V_{in}/1.000 \times 10^6 \Omega$$

V_{in}	i (μA)	V_o (10^{-6} Range)	V_o (10^{-5} Range)
1.0001	1.0001	10.16	1.002
0.5000	0.5000	5.07	0.501
0.7501	0.7501	7.62	0.751
0.2500	0.2500	2.54	0.250
0.1000	0.1000	1.015	0.100
0.0750	0.0750	0.762	0.0754
0.0500	0.0500	0.508	0.0502
0.0251	0.0251	0.255	0.0253
0.0100	0.0100	0.1029	0.0102
0.0075	0.0075	0.0768	0.0076
0.0050	0.0050	0.0521	0.0052
0.0024	0.0024	0.0252	0.0026
0.0011	0.0011	0.0118	0.0013

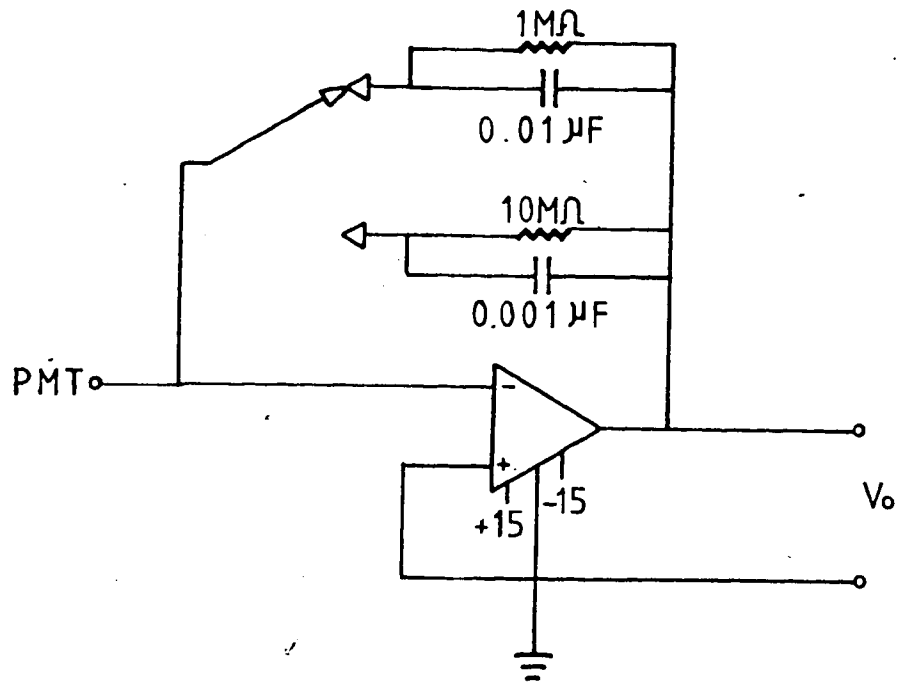


Figure 14. Current-to-voltage convertor for use with PMT detector in EA-ICAP-OES spectrometer system.

±5 V before analog-to-digital conversion which was performed at 100 Hz.

Digital data conversion was performed by a Digital Equipment Corporation (DEC) Laboratory Peripheral System Model LPS11 (45,46). This data acquisition unit contains all the electronic components for connection to external analog, digital, and timing signals and interfaces directly to a DEC PDP-11/10 sixteen bit minicomputer. The LPS unit contains a 12-bit analog-to-digital convertor giving a resolution of 1:4096 and can perform conversion under program control at up to 20,000 Hz (50 μ sec/conversion). A total of two or three digital inputs and one analog input were used during data acquisition. The LPS11 internal clock provided the A/D conversion clock.

The DEC PDP-11/10 minicomputer was operated under the RT11-026 disk-based operating system with 16 K words of core memory available. Programming was in Fortran and Macro 01C assembly language. Mass storage was available by means of a single 2.5 megabyte DEC RK-05J cartridge disk drive. Alphanumeric and graphic display was available with a DEC VT-55 video terminal. Hard copy output was available from the internal printer of the VT-55, a Decwriter II, or a Zeta Research Corporation, Lafayette, California, 100/1200 Series Incremental Plotter (45,47). A description of software including a description and documented printouts is contained in Appendices A and B.

2. Computer Coupled Photodiode Array Readout Systems

The computer coupled photodiode array readout systems used in this work have been developed in this laboratory over the last eight years. A number of articles have been written about these systems by Horlick et al. but of particular interest are References 48 and 49 which are general review articles concerning the characteristics of these systems for spectrochemical measurements.

The first system used was the computer coupled photodiode array direct reading spectrometer shown in Figure 5. In this system an array, consisting of 1024 photodiodes 0.001 inch wide by 0.017 inch tall, is placed horizontally in the exit focal plane of a Heath Monochromator Model EU-700-70. The dispersion of this monochromator varies slightly with wavelength but is approximately 20 \AA per mm and therefore the 1.024 inch photodiode array gives a spectral window of slightly more than 50 nm (500 \AA). The computer-based data acquisition system operates at up to 20 KHz and the photodiode array is generally clocked at this rate. Integration times of an array cooled to about -20°C can vary from 0.1024 to 52.4287 seconds between readout cycles of the photodiode array and individual readout cycles can be stored under computer control or can be time averaged and background subtracted.

The second photodiode array based system uses a photo-

diode array mounted vertically in the exit focal plane of a Heath Monochromator, Model EU-700-70. In this system an array of 256 elements 0.001 inch wide by 0.001 inch tall is used for direct readout of the vertical spatial emission intensity of a source (50,51). When clocked at 20 KHz integration cycle times between 0.0128 and 52.4280 seconds are possible when the photodiode array is cooled to about -20°C . Time averaging of readout cycles and background subtraction are also available under computer control.

The remainder of the data acquisition system and readout system are similar to that described in Section D1 with the Tektronix AM 502 Differential Amplifier being used to amplify and filter the photodiode array signals prior to analog-to-digital conversion. With the photodiode array systems A/D conversion clocking was provided by the photodiode array electronics. Software descriptions and documented printouts are contained in Appendices C, D, E, and F.

CHAPTER III

Characterization of EA-ICAP-OES Emission Behavior for Single Elements in Solution

The discussions in Chapters I and II introduced the concepts involved in EA-ICAP-OES, and descriptions of the systems used for data acquisition were provided. In this chapter the experiments using the PMT data acquisition system will be discussed.

Reference to Figure 1 will show that the emission information may be encoded in up to four ways--frequency, intensity, time, and space. With a single channel data acquisition system frequency decoding was performed entirely by the monochromator. Extensive spatial information is very difficult to decode for transient signals with a PMT-based data system as only one area at a time can be observed. It will be seen in Chapter IV that spatially resolved spectral measurements can be easily accomplished with a photodiode array mounted vertically in the exit focal plane of a monochromator. The PMT-based system is used best in decoding the emission signal to recover the time and intensity data.

A. Temporal Behavior of EA-ICAP-OES System

From the very beginning of this work it was apparent that the EA-ICAP-OES process would show a temporal behavior

because of the use of an atomic absorption graphite furnace atomization system for sample vaporization. Sturgeon and Chakrabarti (33) give an excellent review and discussion of the temporal behavior of the carbon furnace atomizer process. The absorption pulse characteristic times is shown in Figure 15 (Reference 33, p. 40) for a graphite furnace. This same figure can also be used to describe the emission pulse characteristics of the EA-ICAP-OES process and to point out the similarities and differences between the two analytical methods.

At the beginning of the AAS atomization cycle a large current is passed through the furnace causing rapid heating. A curve representing furnace temperature vs time for such a case is shown in Figure 15. As the furnace temperature exceeds the analyte vaporization temperature the concentration of analyte atoms in the absorption cell starts to rise. At some point the absorbance signal will rise above the background level. This is the appearance time ($\tau_{\text{appearance}}$) which is measured from the start of the atomization cycle. There are a number of factors which may affect this appearance time such as:

1. Furnace heating rate.
2. Element being investigated.
3. Mass of analyte (and matrix if present)
4. Chemical form of element.

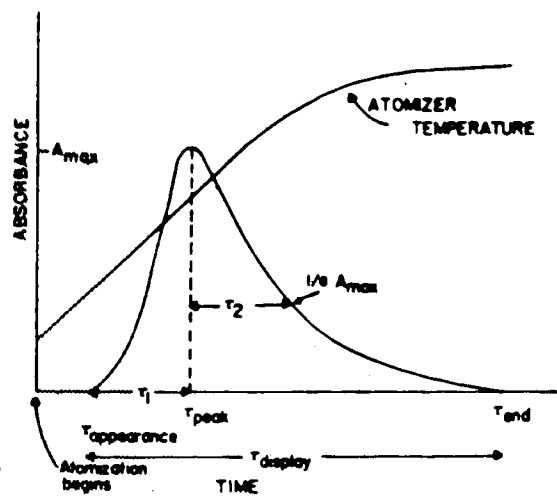


Figure 15. Pulse characterization times for a graphite furnace.

If there are no complicating competing processes, such as chemical reaction with the carbon of the furnace, and if heating continues long enough then atomization will continue until all of the analyte has been vaporized. Under normal conditions this is a rapid process and the result is that the concentration of analyte in the absorption cell rapidly increases to a maximum at the end of the analyte atomization. The time of maximum absorbance (τ_{peak}) is the sum of appearance time ($\tau_{\text{appearance}}$) and atomization time (τ_1).

Diffusion of the analyte out of the absorbance cell will cause the absorbance signal to fall after the τ_{peak} is reached. The residence time (τ_2) is the mean length of time spent by an atom within the absorbance cell and is the time necessary for the absorbance signal to fall to a value of $1/e A_{\text{max}}$. As the analyte continues to diffuse from the absorbance cell the absorbance will finally reach the background level again at τ_{end} .

The emission signal for the EA-ICAP-OES system used is very similar in appearance to the absorbance signal described above but the processes involved are different in detail. The vaporization cell replaces the absorbance cell and as the analyte is rapidly vaporized its concentration rapidly raises in the cell. As before, the maximum concentration is reached at the end of the vaporization and then

decreases. With the EA-ICAP-OES the reduction of vapor concentration within the vaporization cell is caused by the flushing of the vapor out the top of the cell to the plasma by the argon entering the bottom of the cell. $\tau_{\text{appearance}}$, τ_{peak} , τ_1 , τ_2 , and τ_{end} may then be determined, if desired, from the emission peaks in a manner analogous to their determination with graphite furnace AAS. With EA-ICAP-OES all times will be delayed about 0.5-0.6 seconds since the vapor must travel through the connecting tube and torch a distance of about 16 inches, before emission can occur. Figure 16 is an example of the emission intensity obtained for 100 ng of lead using the EA-ICAP-OES system developed for this experimental work.

This experimental work was primarily an investigation into the use of a graphite furnace based system for analytical EA-ICAP-OES therefore vaporization conditions were adjusted to give as little variation in temporal behavior as possible in the emission signals of the various elements. The conditions which met this criteria were primarily the use of a standard and reproducible torch design, a fixed value of sample argon flow rate, and the highest possible furnace heating rate attainable with the equipment used. When these conditions were met the temporal behavior varied only a small amount from element to element, with the quantity present, and with the matrix. Typical values were:

PB142-100NG

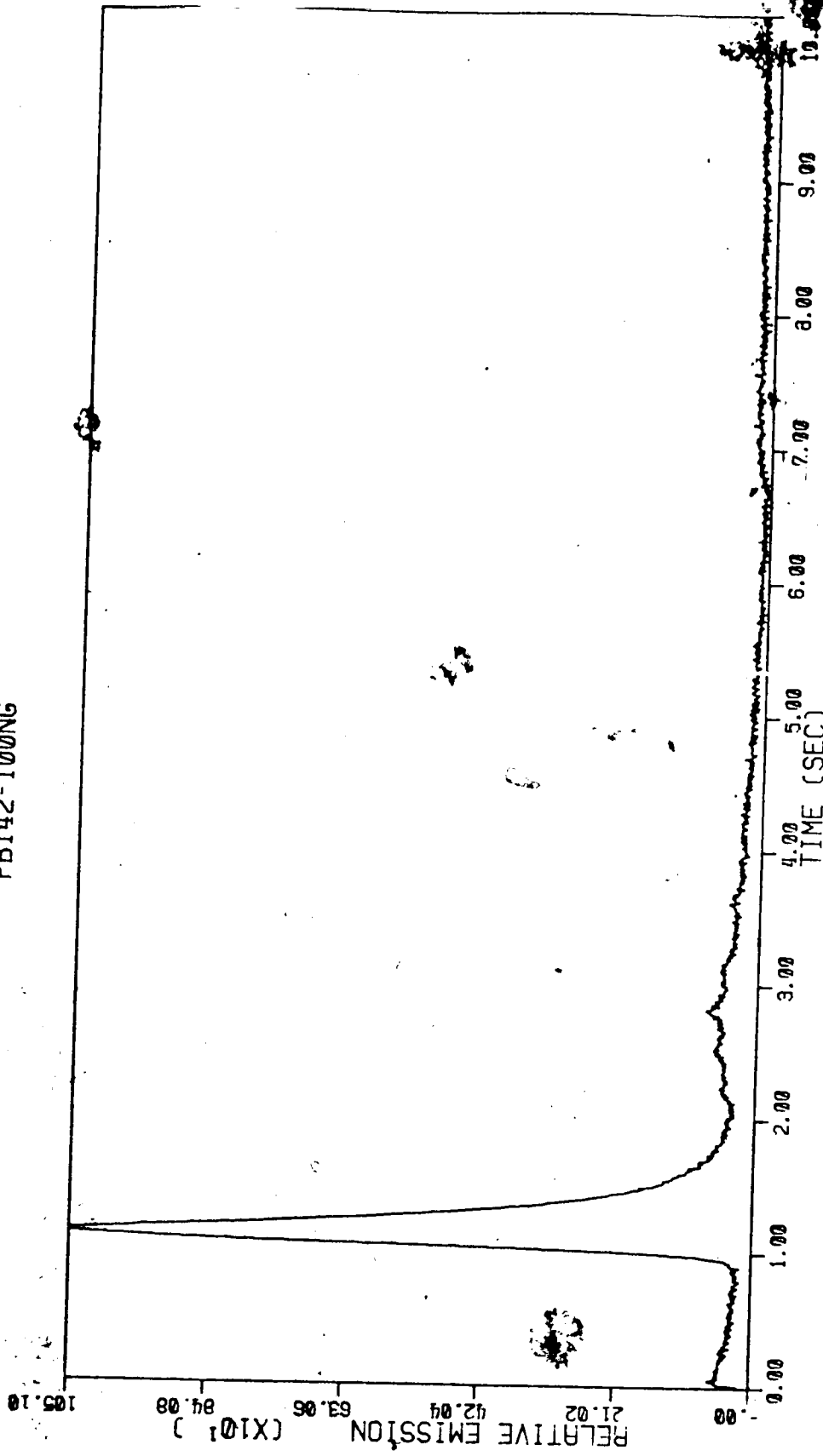


Figure 16. EA-ICAP-OES temporal profile for Pb(II) emission at 220.353 nm from 100 ng of Pb. Recorded with computer system.

$\tau_{\text{appearance}}$	- 0.6-0.8 seconds
τ_{peak}	- 0.9-1.2 seconds
τ_{end}	- 2.0-3.5 seconds

τ_2 values were not determined for the EA-ICAP-OES system.

The distribution of sample vapor was investigated by visually observing the spread of NH_4Cl vapor as it was vaporized from the furnace. The distribution was very unhomogeneous with the greatest concentration at the top of the cell and with almost no vapor being seen below the sample cup. This distribution was easily understood since there was approximately 0.8 Lpm of argon entering the bottom of the cell for the purpose of sweeping the analyte vapor out the top of the cell. Contributing to the unhomogeneous distribution was also the fact that the sample was vaporized from a cup which opens upwards, therefore the vapor was expelled in an upward direction. The fact that any vapor was seen below the vaporization cup was undoubtedly due to turbulent flow of argon in the cell.

When a pulse signal, such as found in graphite furnace AAS or in EA-ICAP-OES is to be analyzed, then care must be exercised in the design of the detection readout system. In many cases a chart recorder has been used to record the transient signal being obtained from the analytical system. Most early graphite furnace AAS systems used this readout system. The EA-ICAP-OES system of Nixon, Fassel and

Kniseley (25) and of Kirkbright et al. (26, 27, 28) also used chart recorders as readout systems. Chart recorders have a fairly long response time compared to the time behavior of either a graphite furnace AAS system or a EA-ICAP-OES, therefore a great deal of distortion in the recorded signal could be expected. Sturgeon and Chakrabarti (33) discuss this problem thoroughly in connection with graphite furnace AAS and show clearly how increasing the time constant of the recording system reduces the peak height obtained while increasing τ_{end} . This distortion of the signal is accompanied by a loss of fine detail.

Figure 17 is a recording of the emission from 10 μL of 10 ppm Pb (100 ng) as recorded by a Heath Laboratory Strip Chart Recorder Model EU-20B. The response time of this recorder is 1 second full scale (0.1 sec/inch). If this recording is compared with Figure 16, which was recorded with the equipment described in Chapter II having a RC time constant of 0.01 second, the signal distortion is readily apparent. The strip chart recording has a peak height of 0.19×10^{-8} amps, including pen overshoot, as compared with a value of 2×10^{-8} amps from the detector-readout system developed for this experimental work.

Several features are clearly visible in Figure 18, a recording for 10 ng of Pb, that were less easily seen in Figure 16 which was recorded at a lower amplification level.

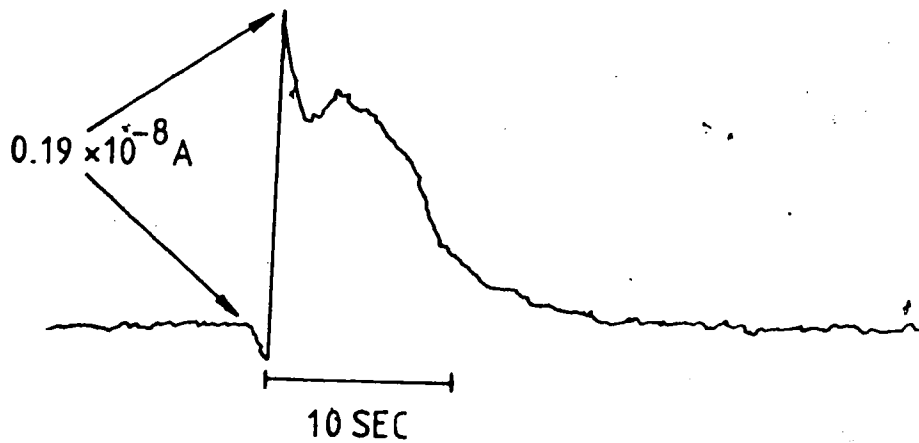


Figure 17. EA-ICAP-OES temporal profile for Pb(II) emission at 220.353 nm from 100 ng of Pb. Recorded with a Heath Strip Chart Recorder, Model # EU-20B.

PB149-10NG

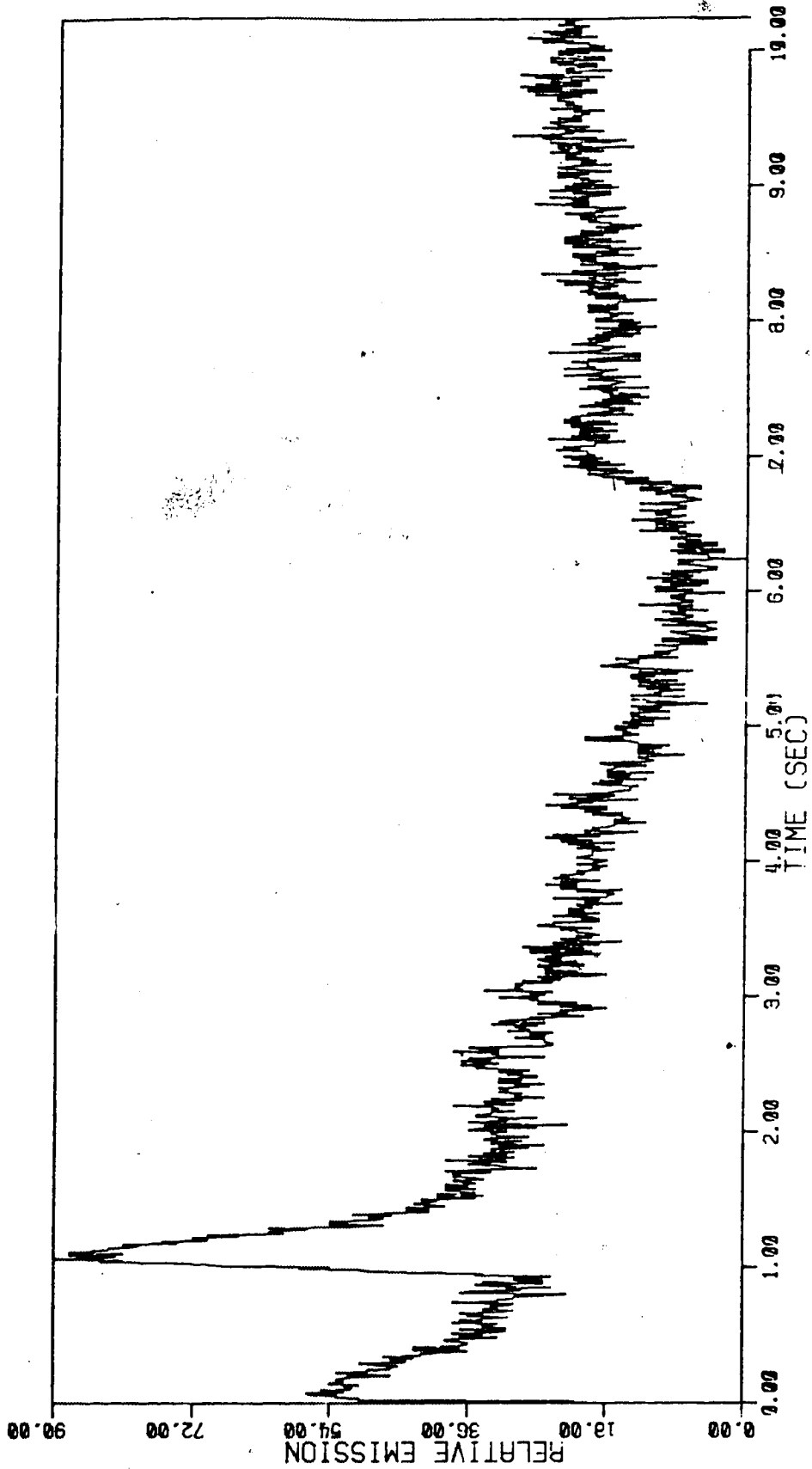


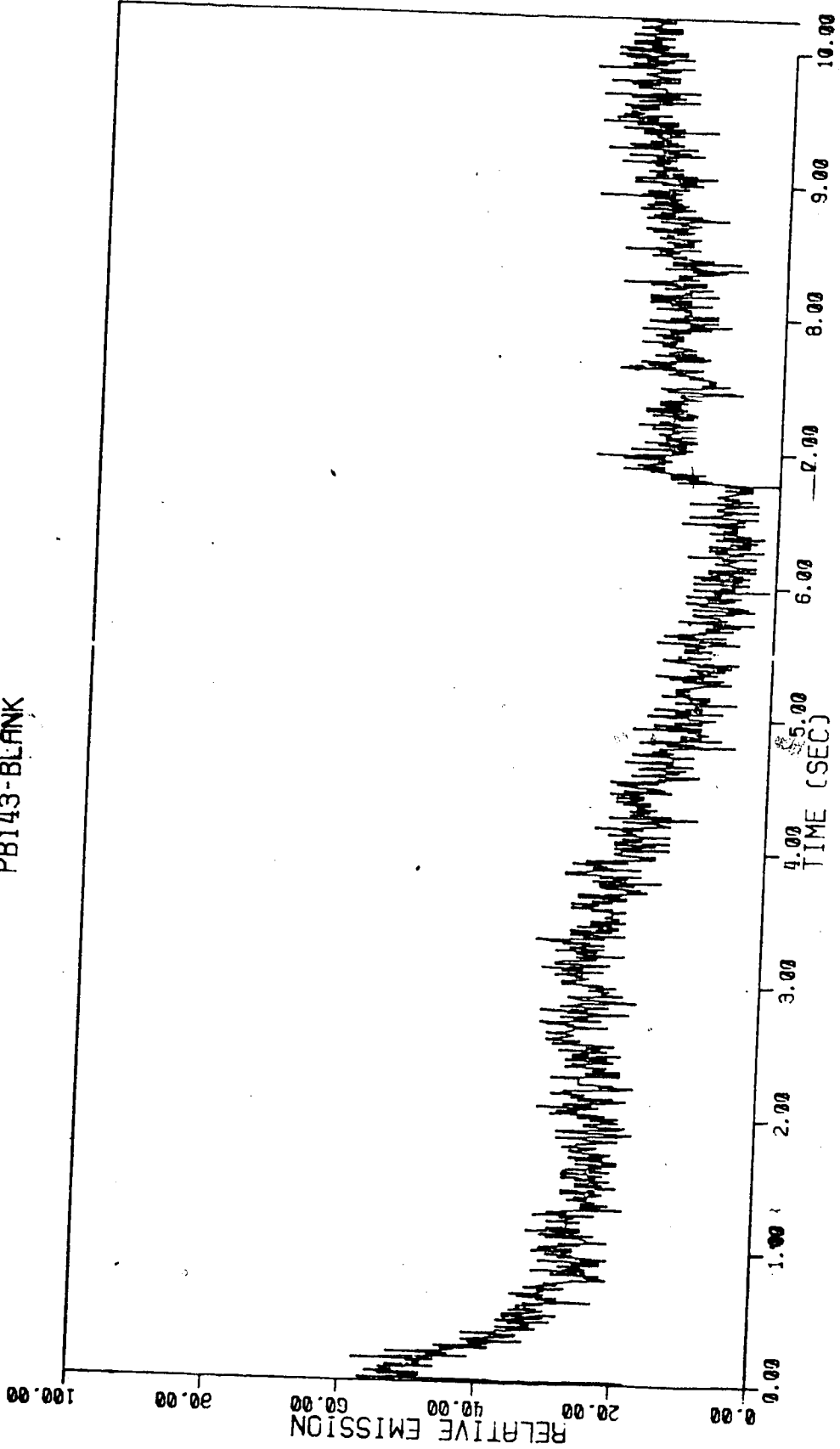
Figure 18. EA-ICAP-OES temporal profile for Pb(II) emission at 220.353 nm from 10 ng of Pb. Recorded with computer system.

In addition to the lead emission peak several rapid changes in the background level are seen prior to the emission peak and another change in background level is seen at between 6 and 7 seconds. These changes in background level are more clearly shown in Figure 19 which is a recording of background emission during atomization of a blank (1 μ L of distilled water). The rapid changes in background emission level during the first second of the atomization cycle are apparently caused by rapid changes in sample argon flow rate. These changes are caused by the rapid heating of argon in the vaporization cell causing a pressure increase and thus an increase in the flow rate of the argon leaving the cell. Similar plasma background emission level changes can be seen in the temporal profiles published by Nixon and Fassel (25) and by Kirkbright et al. (26,27,28). The rapid increase in emission level between 6 and 7 seconds is caused by the cooling of the argon in the vaporization cell at the completion of the atomization cycle.

The fast response of the system used in this experimental work has proven very valuable in another area. In Figure 20 the emission signal recorded is obviously not as expected. In this case the electrode rods were found to be making poor contact with the graphite cup furnace with the result that heating and atomization did not proceed smoothly. The sharp emission spikes at about 1.25 and 1.5 seconds in

Figure 19. EA-ICAP-OES temporal profile for Pb(II) emission at 220.353 nm from Pb blank.
Recorded with computer system.

PB143-BLANK



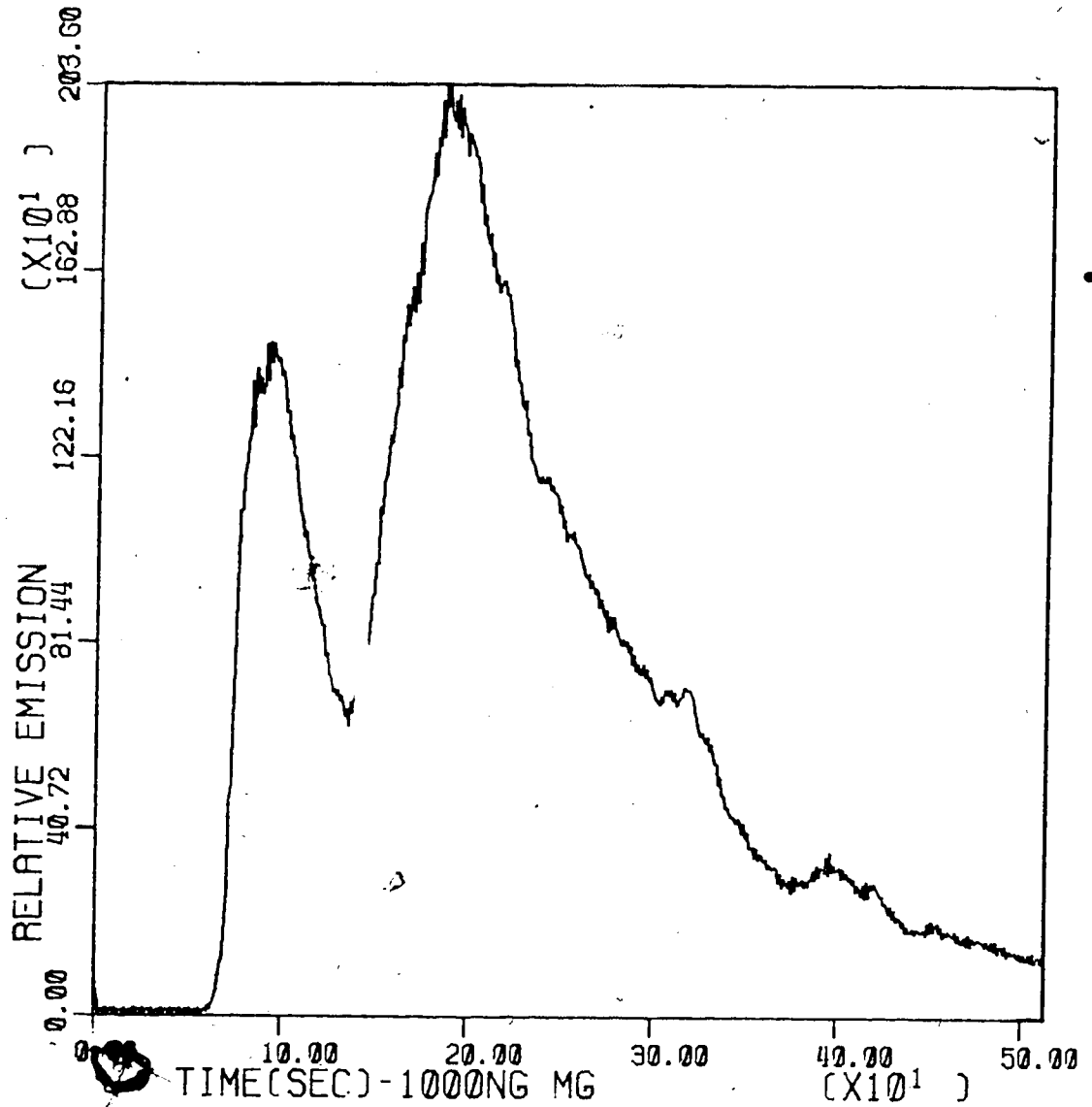


Figure 20. EA-ICAP-OES temporal profile for Mg(II) emission at 279.553 nm from 1000 ng Mg. Recorded with computer system.

Figure 21 are caused by particles containing Zn breaking loose from the vaporization cell. These spikes generally occur only after the system has been used for long periods of time without cleaning or after samples containing very high levels of analyte have been run and are eliminated by cleaning of the vaporization cell and connecting tube. The detail available in the emission recordings proved to be very valuable in system fault detection and maintenance.

B. Analytical Results for Single Elements in Solution

The emission pulses obtained with the electrothermal vaporization system developed for this work were shown in the previous section to have many similar features with those obtained by graphite furnace AAS. Because of these similarities it was at first assumed that, as with graphite furnace AAS, either the peak height value, E_p , or the background corrected integrated peak area, $\int E_t dt$, could be used to characterize the peak.

Early work disclosed several facts which led to the rejection of analytical measurements based on peak signal values. The first problem encountered was the fact that the emission signal is not exclusively due to analyte emission. The signal is the sum of the analyte emission and the changes caused in background plasma emission by the sample argon flow fluctuations during sample vaporization.

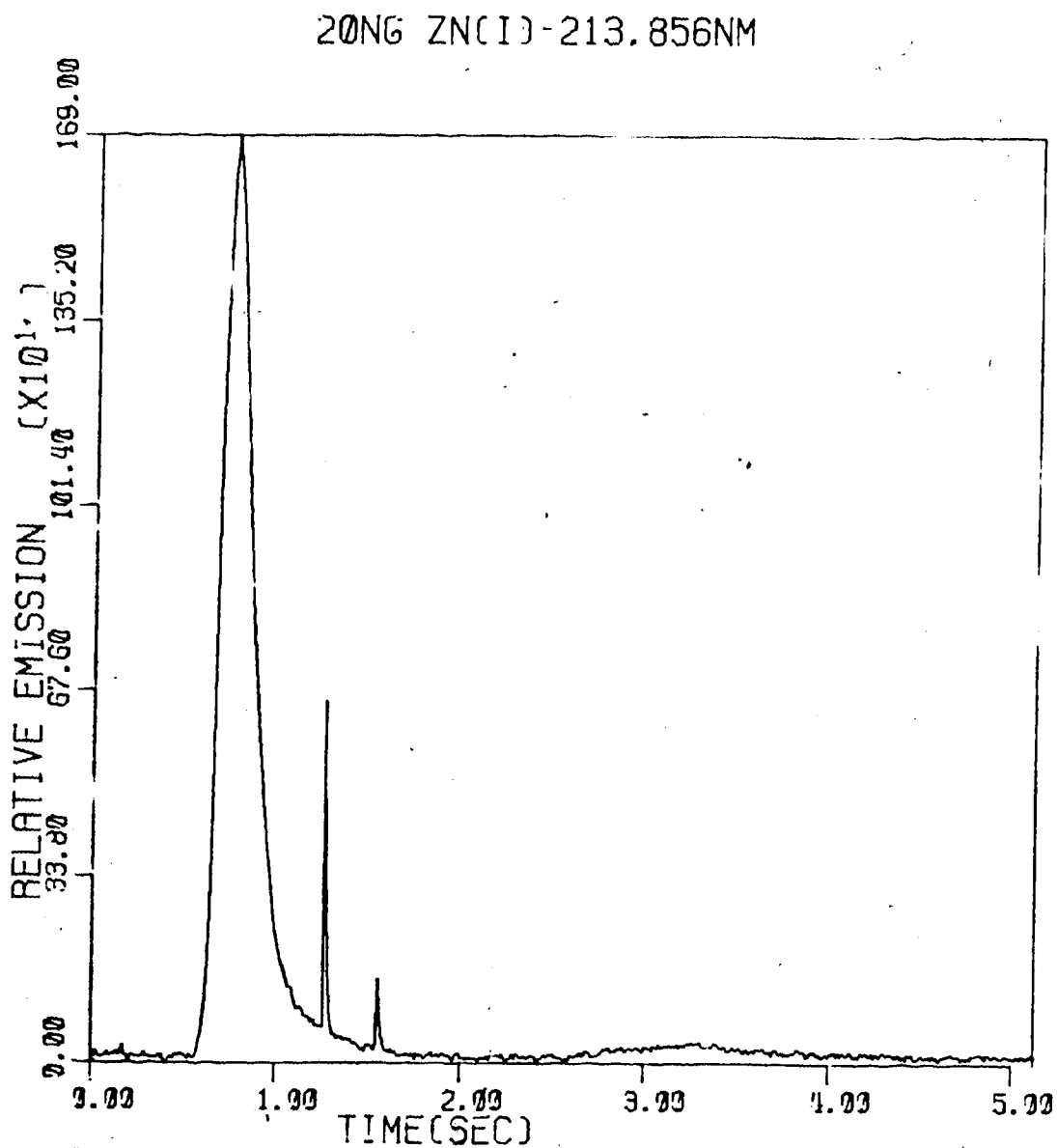


Figure 21. EA-ICAP-OES temporal profile for Zn(I) emission at 213.856 nm from 20 mg Zn. Recorded with computer system.

These plasma background emission changes were shown in Figure 19 and discussed in the previous section. Small changes in vaporization conditions were found to cause fairly large changes in the minimum found just before analyte emission starts to rise quickly and to a lesser extent in the background emission levels in general.

Background and analyte emission plots are shown in Figure 22 through Figure 29. Digital filtering of the data was performed prior to plotting to smooth the appearance of the plots. The background becomes too small with respect to analyte emission in Figure 26 through Figure 29 to be clear, but can be easily seen in Figure 22 through Figure 25. These backgrounds, which were collected immediately before the analyte data and under the same conditions, show the variations just mentioned. These changes are probably due to changes in the sample argon flow rate caused by fluctuations in the furnace heating rate. These background emission level changes from vaporization to vaporization made it impossible to assign a single point or area in an analyte emission plot as a background level for E_p measurement.

Integrated background values were found to be fairly consistent therefore an average value could be subtracted from the integrated emission area values to obtain analyte only integrated emission area for analytical uses.

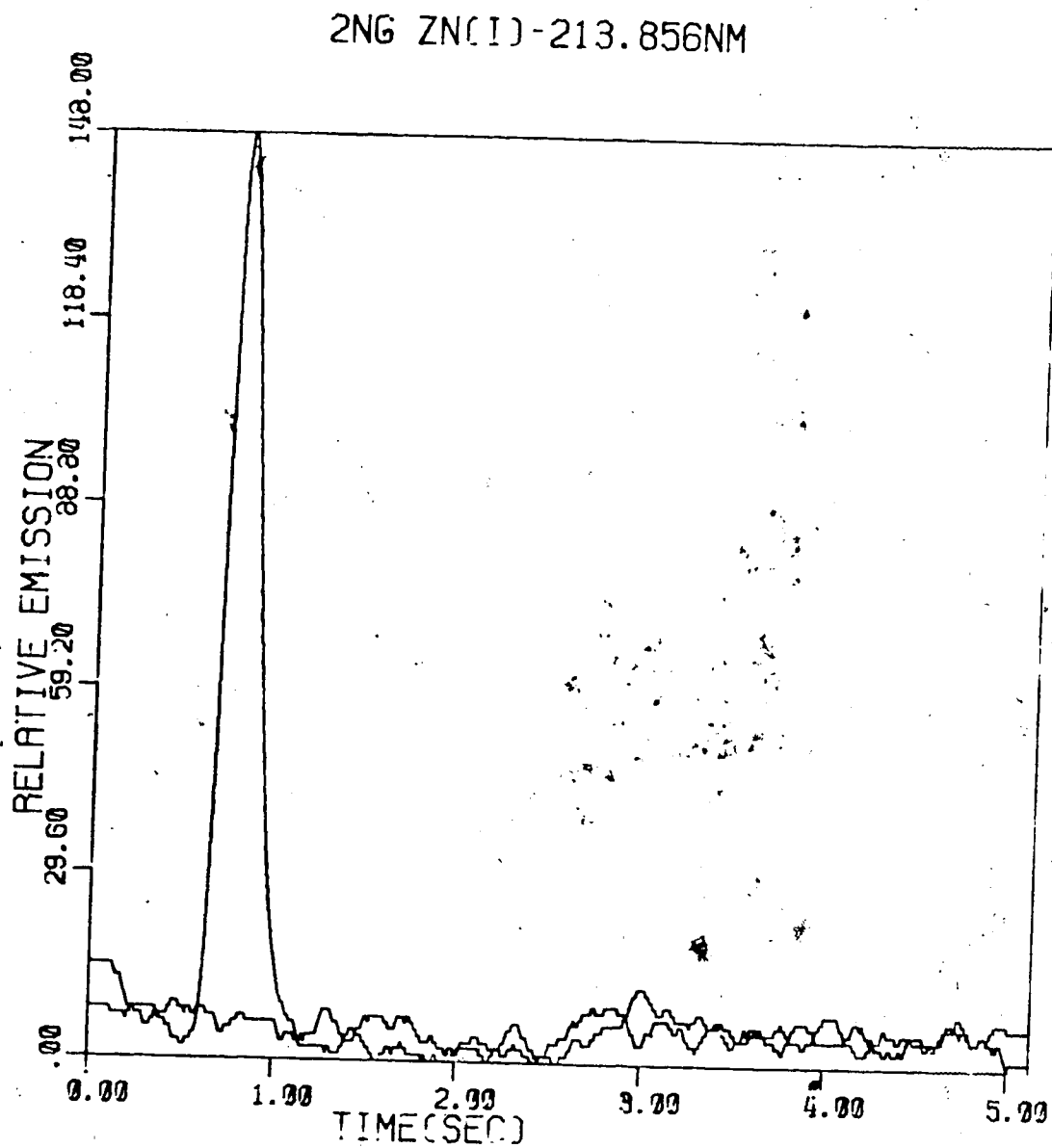


Figure 22. Temporal profile, 2 ng Zn(I) - 213.856 nm.

5NG ZN(I)-213.856NM

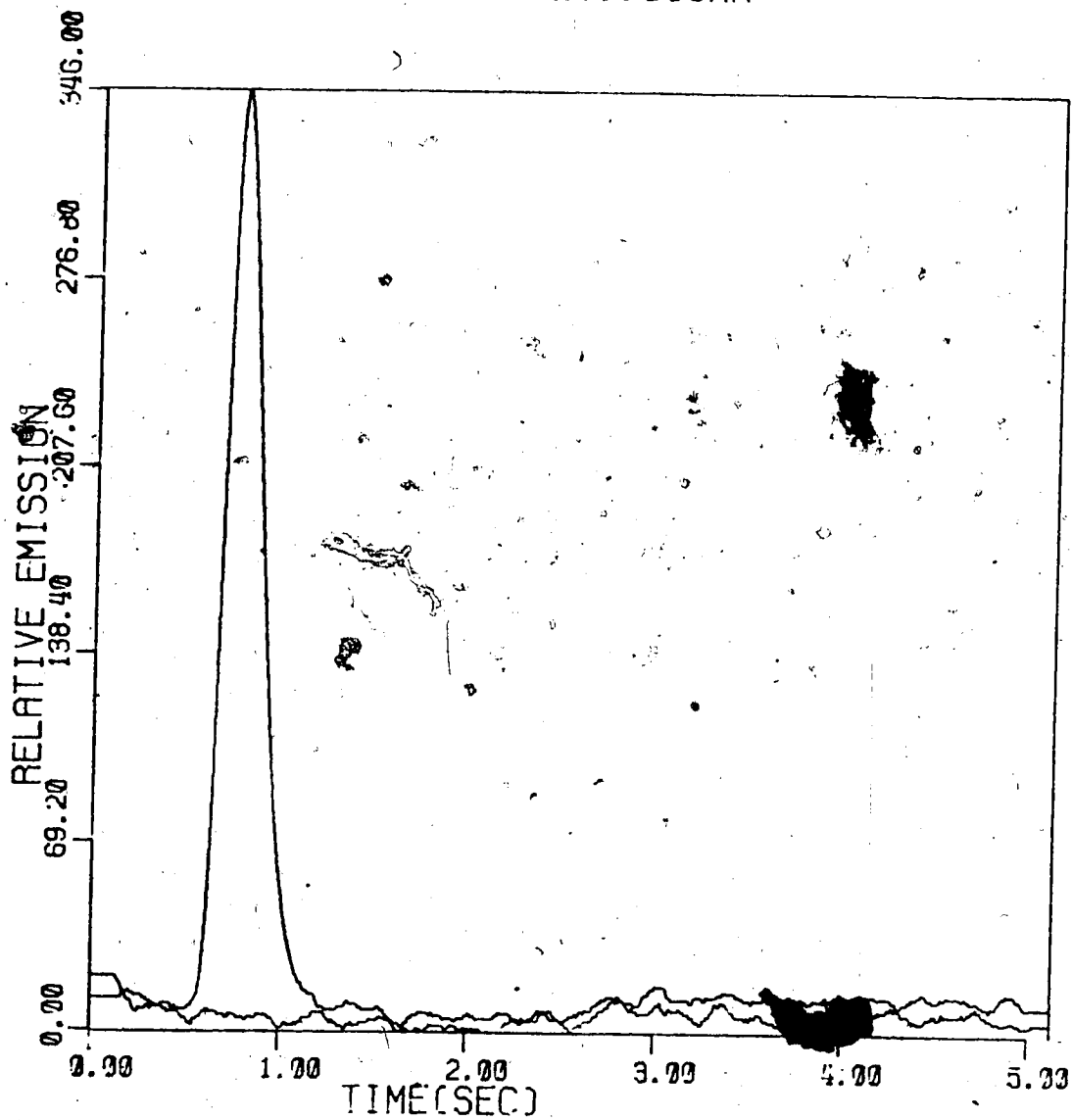


Figure 23. Temporal profile, 5 ng Zn(I) - 213.856 nm.

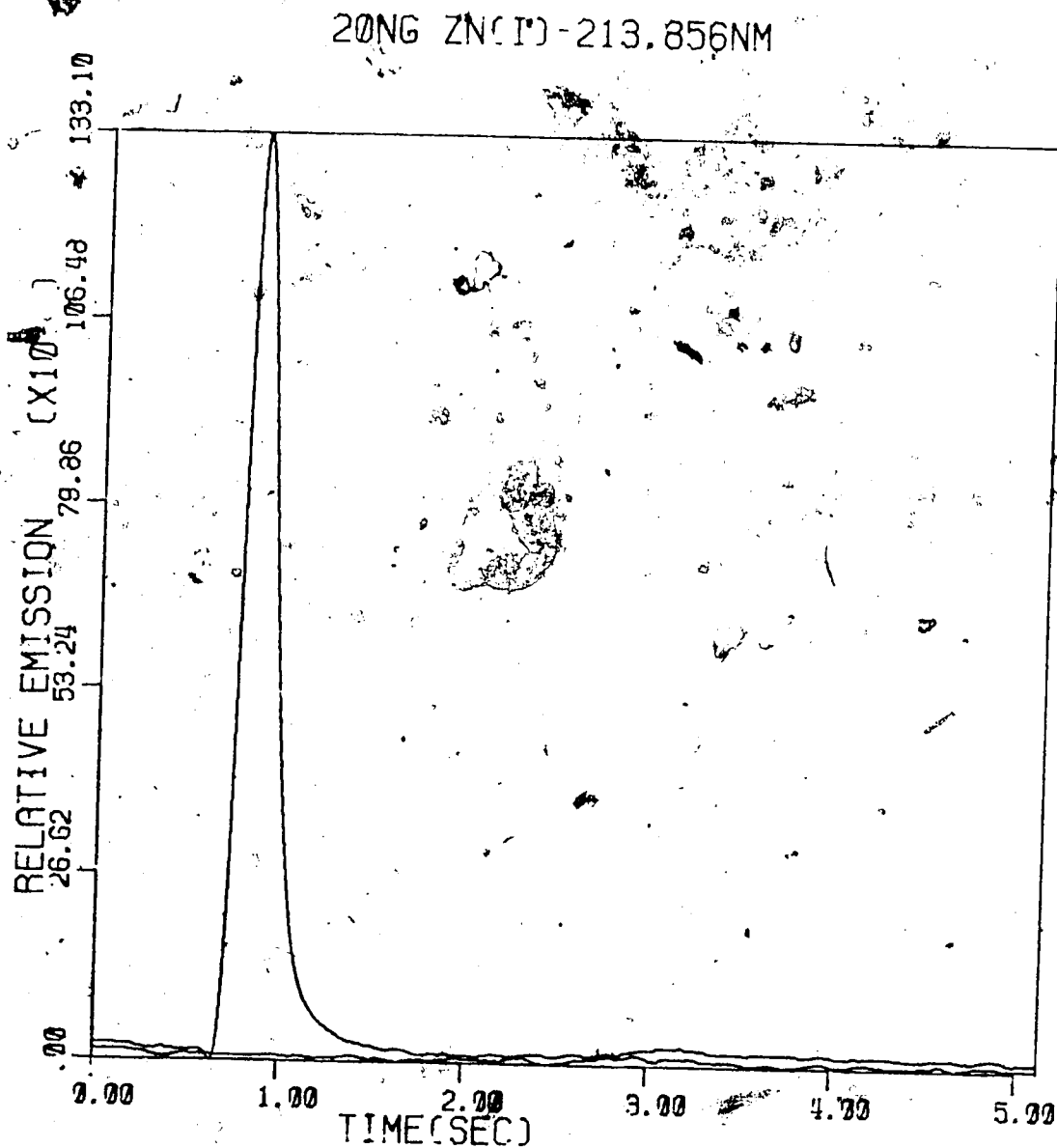


Figure 24. Tempora. profile, 20 ng Zn(I) - 213.856 nm.

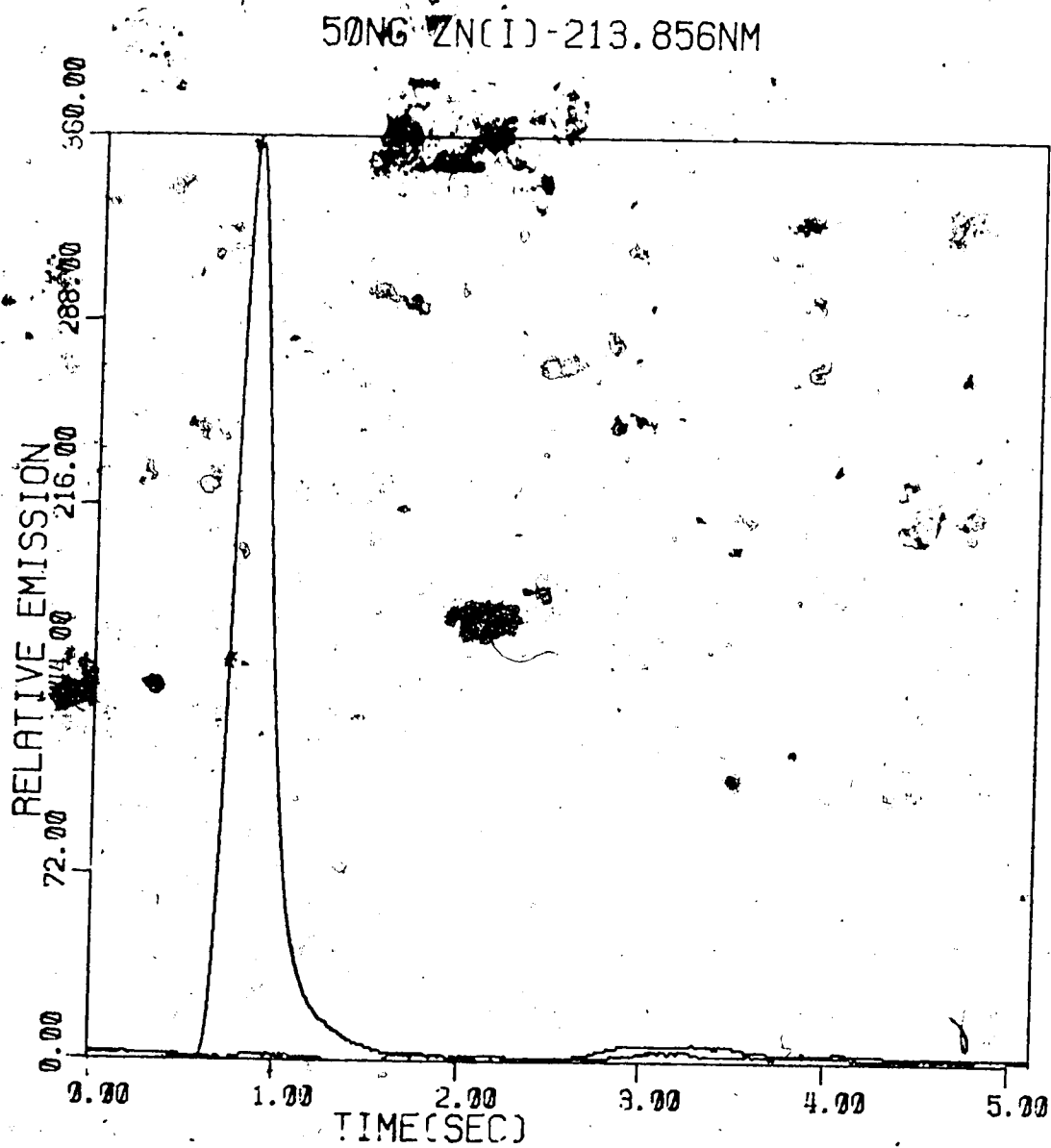


Figure 25. Temporal profile, 50 ng Zn(I) - 213.856 nm.

200NG ZN(I)-213.856N

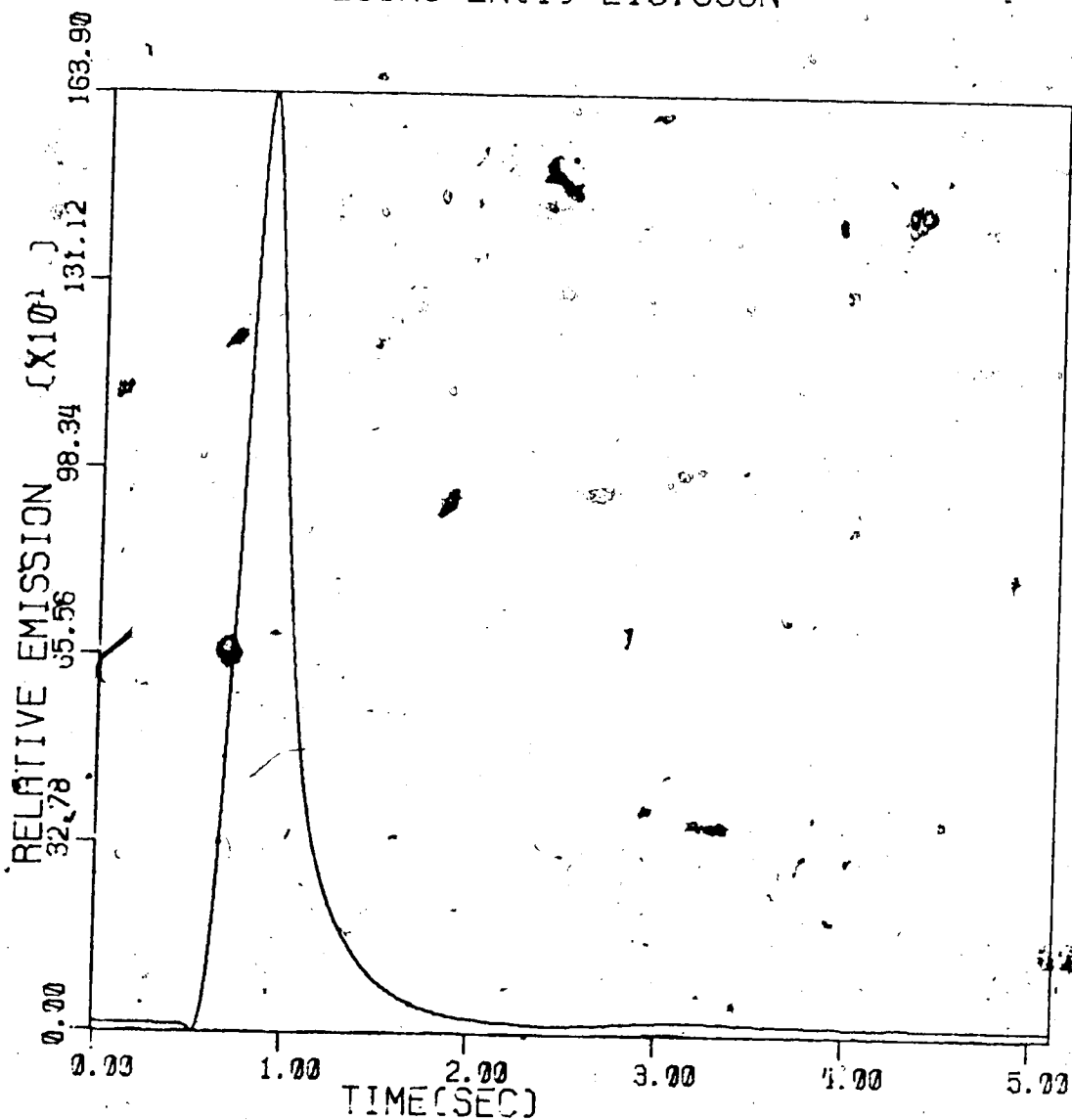


Figure 26. Temporal profile, 200 ng Zn(I) - 213.856 nm.

500NG ZN(I)-213.856N

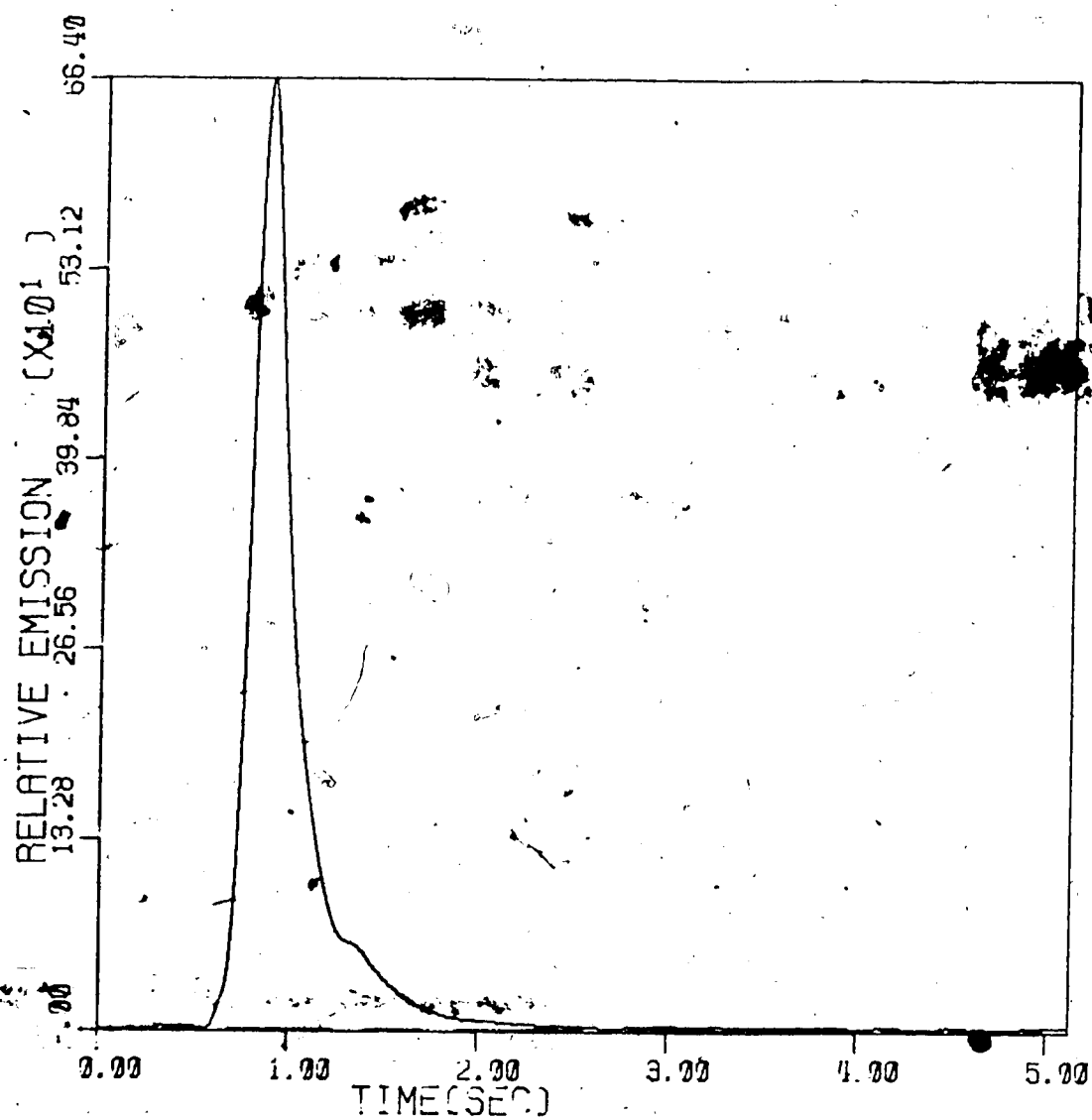


Figure 27. Temporal profile, 500 ng Zn(I) - 213.856 nm.

2.000NG ZN(I)-213.85

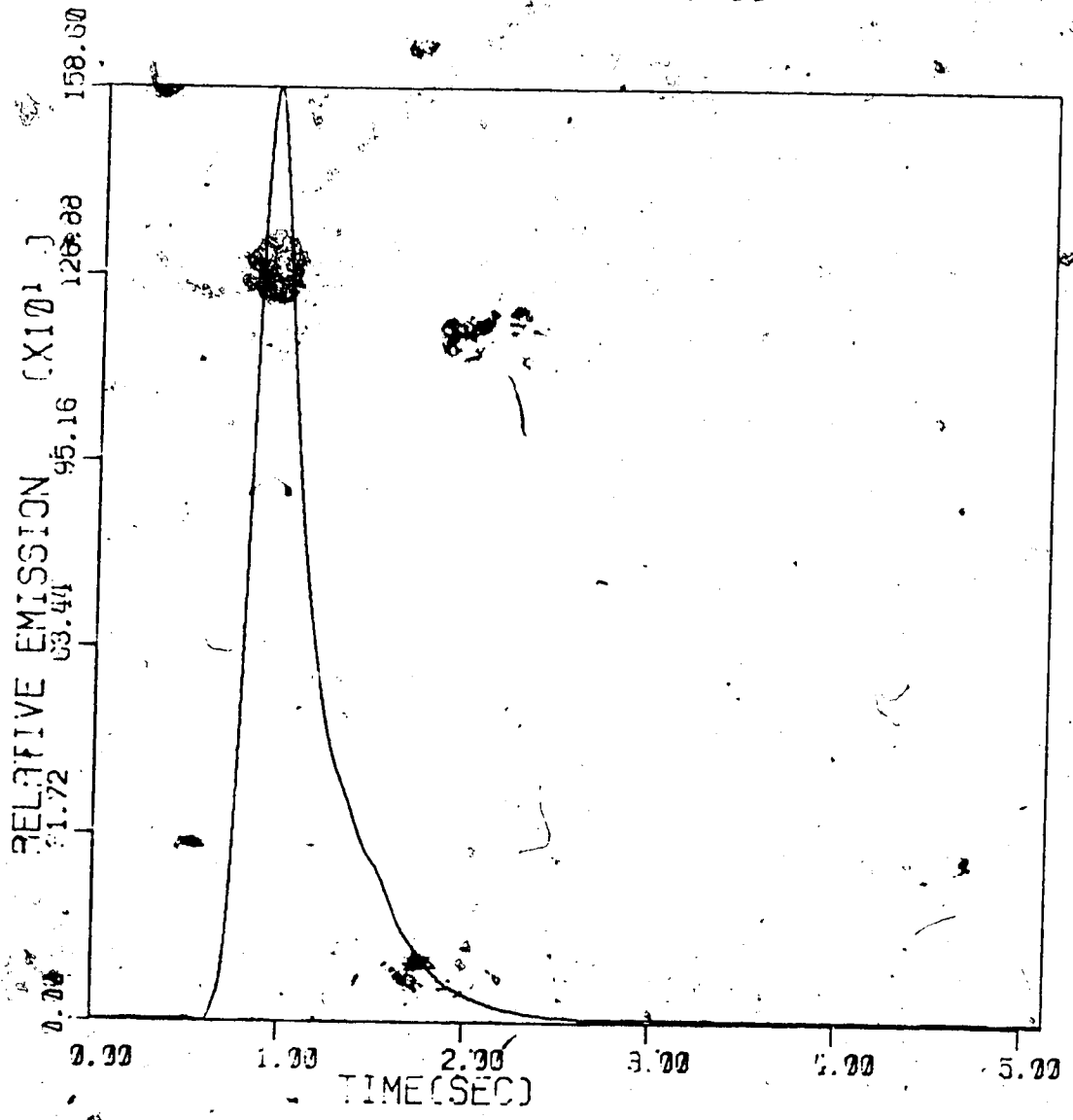


Figure 28. Temporal profile, 2000 ng Zn(I) λ 213.856 nm.

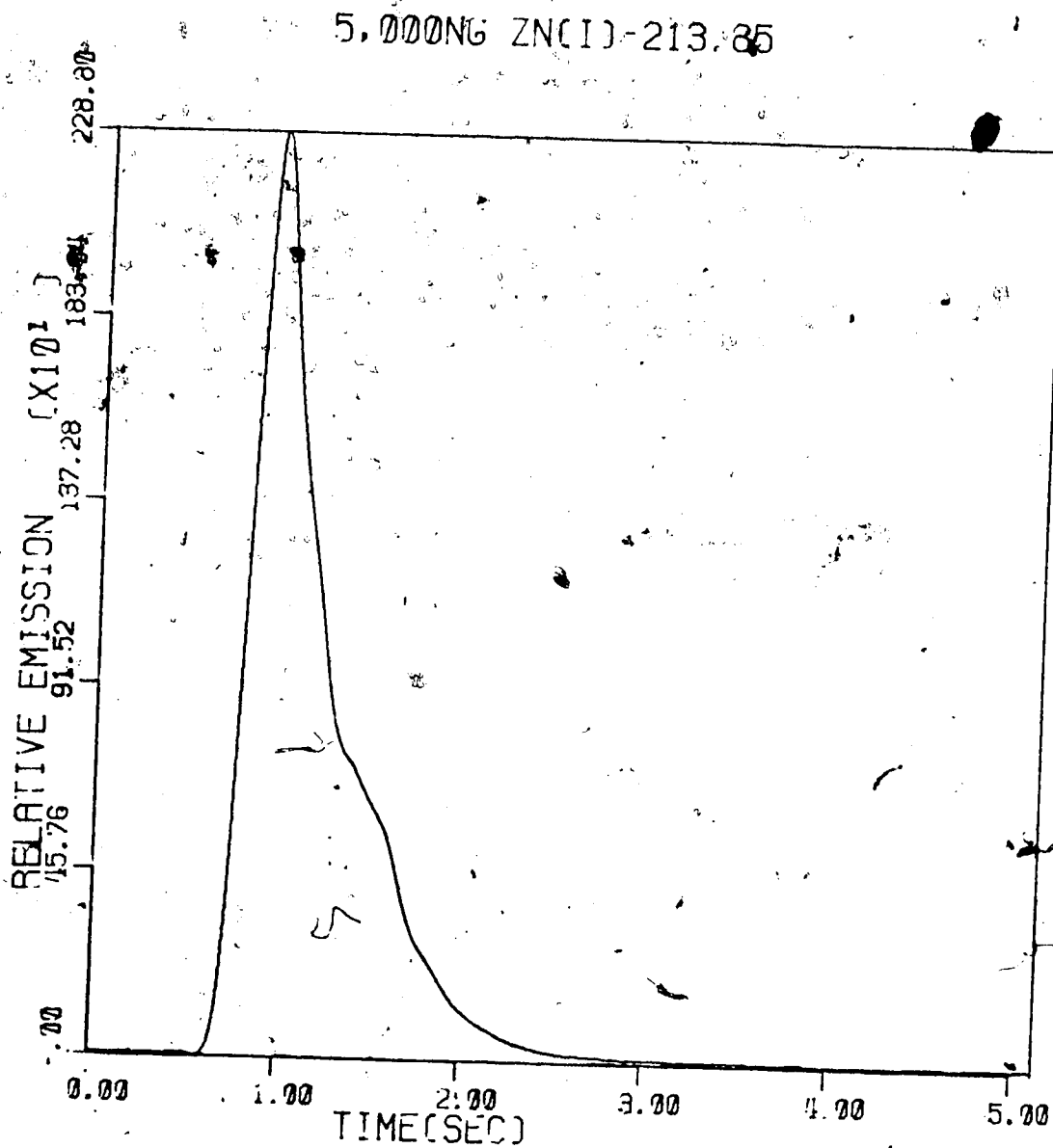


Figure 29. Temporal profile, 5000 ng Zn(I) 213.856 nm.

The second problem encountered is one common to graphite furnace AAS, that of changing temporal behavior with increasing sample size or matrix. An example of one of the changes possible is seen in the series of emission peak recordings shown in Figures 22-29.

The same vaporization conditions were used throughout, thus all of these peaks should superimpose, however as the quantity of analyte increases τ_{peak} and τ_{end} increase and the shape of the emission curve becomes irregular at the highest quantities. Values of τ_{peak} and approximate τ_{end} values are given in Table V. Even though these peak shapes change with amount of analyte, the integrated emission area should increase linearly with quantity.

A test of the use of peak height and integrated emission area for characterization of the analyte emission peaks was performed with magnesium. The Mg(I) emission line at 285.213 nm was used and the concentration range of 1 to 1000 ng was covered. The amplifiers were set to give a full scale signal for 10^{-7} amps up to 50 ng of Mg and then a full scale signal for up to 10^{-6} amps up to 1000 ng. The results are shown in Table VI and in Figure 30 through Figure 33. As is shown by the data and figures, calibration plots can be prepared with either peak height or background corrected emission area values, but the relative standard deviation (RSD) values are substantially less with the background corrected integrated peak area values.

Table V

Emission Peak Characteristics for Zn(I) - 213.85 nm

<u>Quantity</u> <u>(ng)</u>	<u>τ_{peak}</u> <u>(seconds)</u>	<u>τ_{end}</u> <u>(seconds)</u>
2	0.78	1.17
5	0.78	1.27
20	0.86	1.60
50	0.86	1.64
200	0.88	2.30
500	0.88	2.31
2000	0.94	2.65
5000	0.95	3.14

Table VI
Calibration Data for Mg(I) - 285.213 nm

Amount Mg (ng)	\bar{E}_p^*	RSD %	$\int E_t dt^*$	RSD %
1	57	7.0	7,311	4.6
2	101	12.6	12,010	7.5
5	346	17.5	27,698	6.0
10	496	22.5	46,294	3.7
20	828	11.9	86,729	5.8
50	2,154	15.1	231,149	4.0
100	4,953	9.7	418,640	4.5
200	7,647	7.1	778,950	2.5
500	13,883	10.7	1,848,150	5.4
1000	27,697	3.2	3,562,130	1.2
0 (10V=10 ⁻⁷ amps)	-	-	65,605	4.2
0 (10V=10 ⁻⁶ amps)	-	-	1,238,160	(0.7)

\bar{E}_p :

Slope = 0.89

R = 1.0

$\int E_t dt$

Slope = 0.91

R = 1.0

* The average \bar{E}_p or $\int E_t dt$ values are shown in their entirety for clarity, however it should be realized that based on the % RSD values these values are only accurate to 3 significant figures.

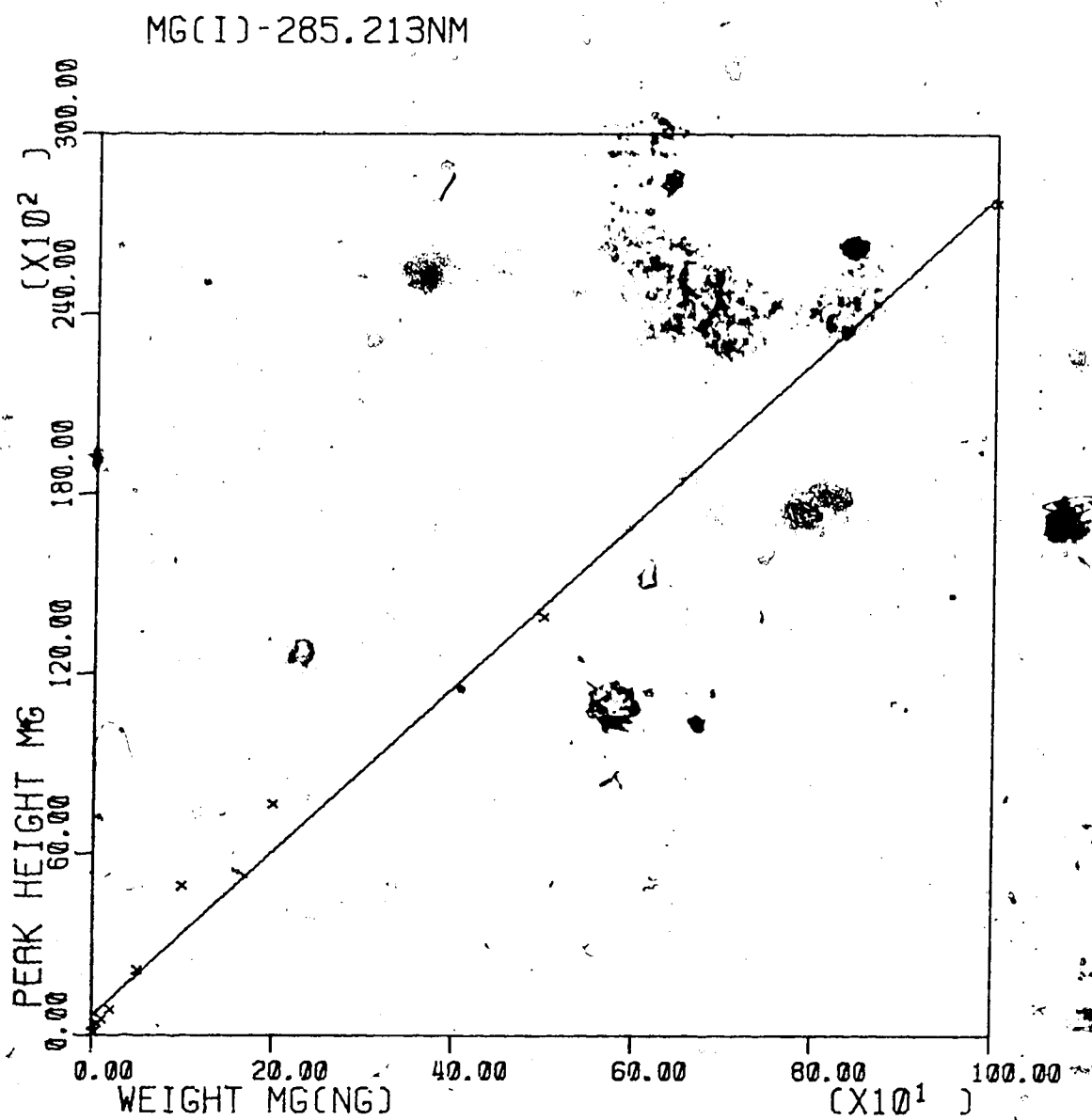


Figure 30. Linear calibration plot for Mg(I) - 285.213 nm, E_p data.

Mg(I)-285.213NM

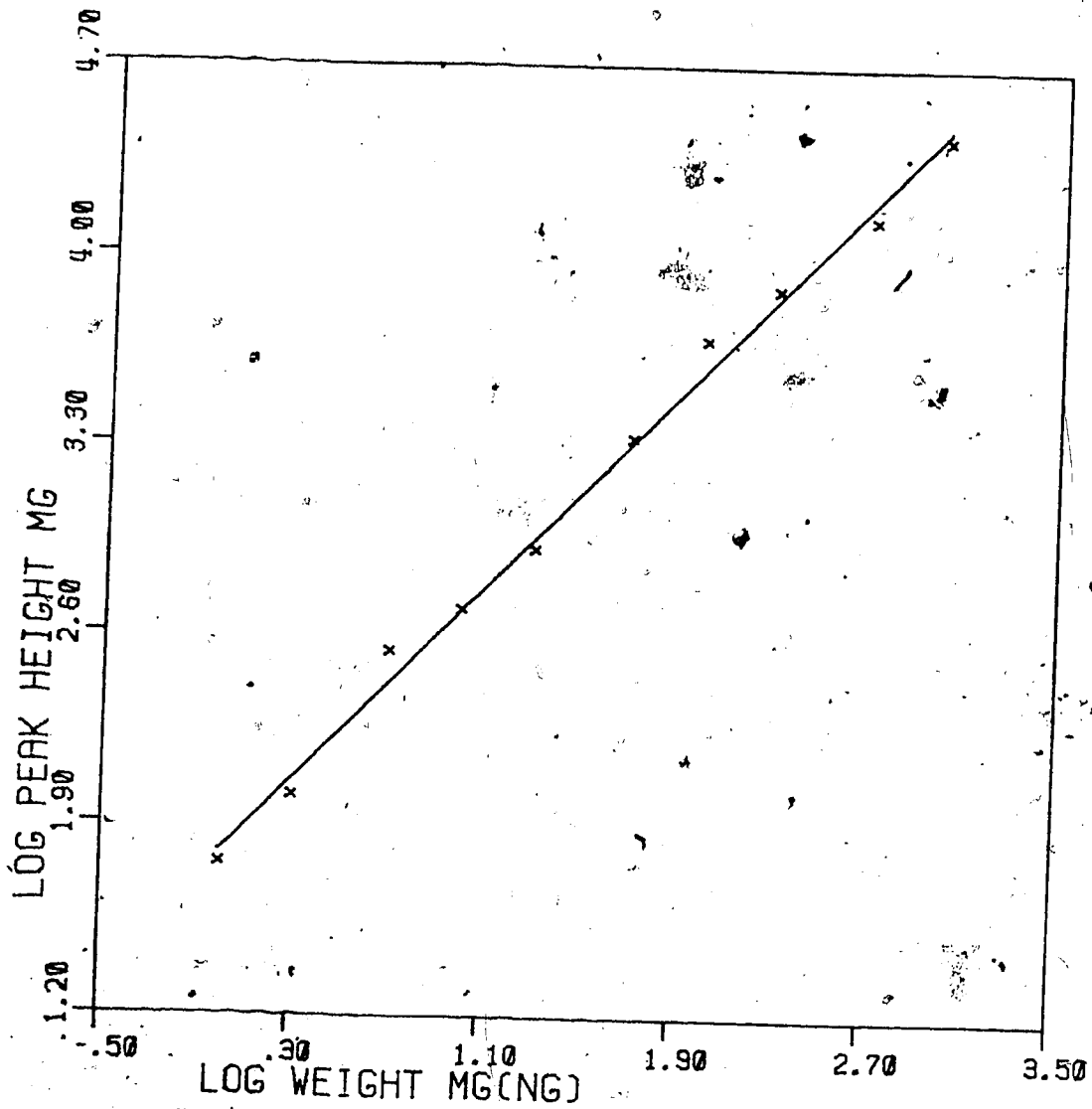


Figure 31. Log-log calibration plot for Mg(I) - 285.213 nm, E_p data.

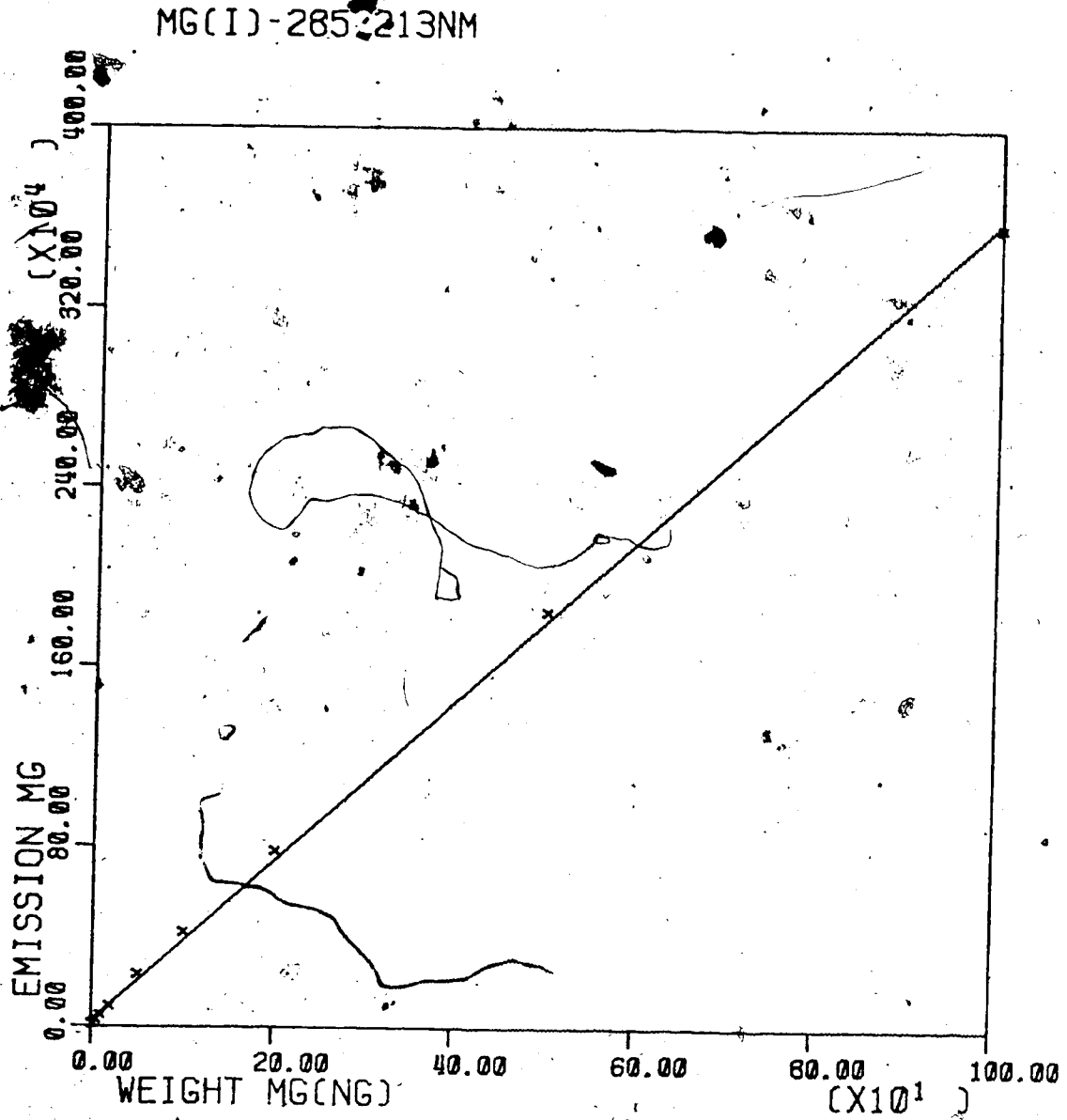


Figure 32. Linear calibration plot for Mg(I) - 285.213 nm, $\int E_t dt$ data.

Mg(I)-285.213NM

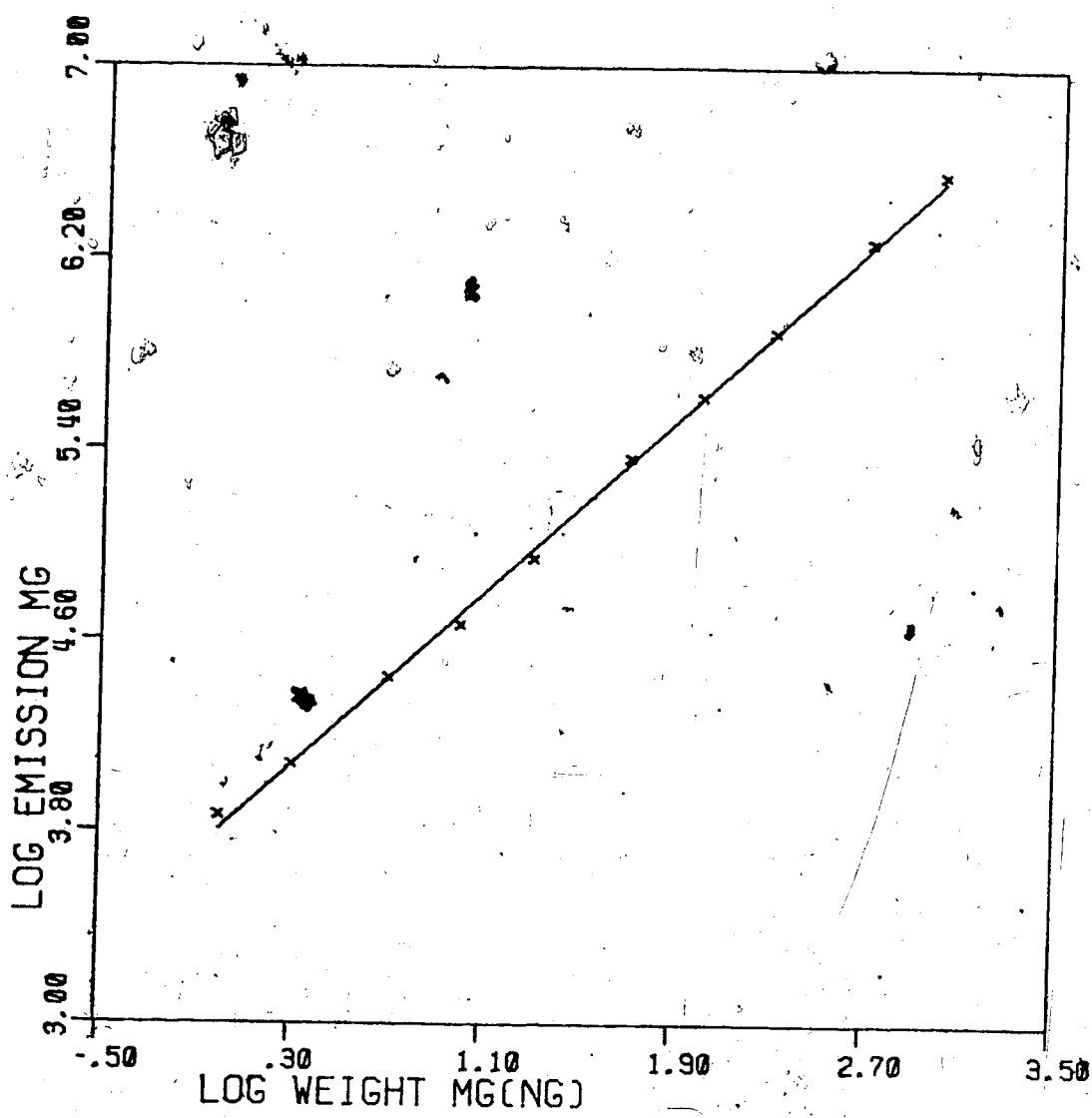


Figure 33. Log-log calibration plot for Mg(I) - 285.213 nm, E_t data.

All subsequent analytical data were obtained by integration of the computer data system recorded emission peaks. Table VII is a compilation of the analytical data for a number of elements tested. Table VIII through Table XVI are the calibration data for each element tested while Figure 34 through Figure 41 are the log-log calibration plots for that data.

In order to compare the sensitivity of this EA system with the normal nebulizer-based system calibration data was collected for both the 405.783 nm Pb(I) and the 220.353 nm Pb(II) emission lines while using a commercial Meinhard concentric glass nebulizer. The experimental arrangement of plasma, monochromator, and PMT detector remained the same as with the graphite furnace system but the Laboratory Data Acquisition System developed in our laboratory by M. Blades (52) was used for data acquisition. This Data Acquisition System is a microprocessor-controlled integrating DVM based on the use of a voltage-to-frequency convertor and counters. Full details of this Laboratory Data Acquisition System are given in the above reference. The results are summarized in Table VII and full data and calibration plots are given in Table XVI and Table XVII and Figures 42 and 43. When measured at about 100 times the detection limits the RSD of both nebulizer and EA systems are about equal. The detection limits are also about

Table VII

EA-ICAP-OES Analytical Data

<u>Analytical Line (nm)</u>	<u>Range (ng)</u>	<u>Detection Limit (ng)</u>
Pb(I) 405.783	10^1-10^4	53
Pb(II) 220.353	10^1-10^4	9
Mg(I) 285.213	10^0-10^3	1.2
Mg(II) 279.553	10^0-10^3	0.1
Ag(I) 328.068	10^0-10^3	0.1
Cu(I) 324.754	$10^{-1}-10^2$	0.06
Cd(I) 228.802	10^0-10^4	1.4
Cd(II) 214.438	10^0-10^4	1.0
Zn(I) 213.856	10^0-10^4	0.8

Meinhard Nebulizer

Pb(I) 405.783	10^0-10^3	3.6 ppm
Pb(II) 220.353	10^0-10^3	1.0 ppm

Table VIII
Calibration Data Pb(I) - 405.783 nm

<u>Weight Pb</u> <u>ng</u>	<u>$\bar{J}E_t$</u>	<u>RSD</u> <u>%</u>
50	7,807	80.3
100	30,056	21.8
200	61,974	16.2
500	115,621	19.7
1000	270,360	8.8
2000	541,627	19.5
5000	1,392,077	7.2
10,000	2,804,412	3.4

Slope = 1.1

R = 1.0

Table IX
Calibration Data Pb(II) - 220.353 nm

<u>Weight Pb</u> <u>ng</u>	<u>$\bar{J}E_t dt$</u>	<u>RSD</u> <u>%</u>
10	2,357	27.2
20	5,182	16.6
50	14,916	3.5
100	29,302	2.1
200	70,160	6.4
500	182,635	10.6
1000	358,830	2.6
2000	774,870	4.8
5000	1,696,250	5.1
10,000	4,029,133	4.6

Slope = 1.1

R = 1.0

Table X
Calibration Data Mg(II) - 279.553 nm

<u>Weight Mg</u> <u>ng</u>	<u>$\bar{I}E_t dt$</u>	<u>RSD</u> <u>%</u>
1	4,958	15.7
2	10,358	3.7
5	28,578	2.6
10	42,372	8.2
20	73,228	1.1
50	200,654	12.0
100	472,733	2.0
200	820,927	2.3
500	1,791,657	2.5
1000	2,813,737	3.9

Slope = 0.93

R = 1.0

Table XI
Calibration Data Ag(I)' - 328.068 nm

<u>Weight Ag</u> <u>ng</u>	<u>\bar{E}_t</u>	<u>RSD</u> <u>%</u>
1	2,137	22.3
2	3,043	3.1
5	11,289	6.2
10	20,249	1.2
20	56,643	4.2
50	128,700	11.1
100	271,758	7.5
200	542,116	13.2
500	1,366,645	6.5
1000	3,016,789	-

Slope = 1.1

R = 1.0

Table XII
Calibration Data Cu(I) - 324.754 nm

<u>Weight Cu</u> <u>ng</u>	<u>\bar{E}_t</u>	<u>RSD</u> <u>%</u>
0.1	3,660	59.1
0.3	10,061	36.6
0.5	13,543	12.7
1	57,483	14.1
3	76,605	6.2
5	146,582	8.8
10	488,370	15.8
30	884,835	1.3
50	2,083,550	3.9
100	5,269,633	6.9

Slope = 1.6

R = 1.0

Table XIII
 Calibration Data Cd(I) - 228.802 nm

<u>Weight Cd</u> <u>ng</u>	<u>$\bar{J}E_t dt$</u>	<u>RSD</u> <u>%</u>
1	483	24.2
3	3,390	33.4
10	13,316	18.3
30	69,050	5.7
100	415,967	5.0
300	3,564,925	3.4
1000	17,022,000	6.7
3000	39,943,000	6.3
10,000	115,312,250	5.7

Slope = 1.4

R = 1.0

Table XIV
Calibration Data Cd(II) - 214.399 nm

<u>Weight Cd</u> <u>ng</u>	<u>$\int E_t dt$</u>	<u>RSD</u> <u>%</u>
1	839	622
3	11,952	39.4
10	60,260	14.3
100	2,216,100	8.2
1000	33,252,000	3.5
3000	75,508,333	4.7
10,000	213,180,000	7.0

Slope = 1.3

R = 1.0

Table XV

Calibration Data Zn(I) - 213.856 nm

<u>Weight Zn</u> <u>ng</u>	<u>$\bar{f}E_t dt$</u>	<u>RSD</u> <u>%</u>
1	926	23.8
2	3,160	28.1
5	9,412	20.2
10	22,899	22.4
20	30,546	15.6
50	101,034	9.2
100	286,799	7.7
200	597,191	7.0
500	1,971,730	6.8
1000	4,361,705	5.2
2000	5,745,205	3.1
5000	11,718,955	2.3
10,000	16,440,230	1.8

Slope = 1.1

R = 1.0

Table XVI
Calibration Data Pb(I) - 405.783 nm - Meinhard Nebulizer

<u>Conc. Pb</u> <u>ppm</u>	<u>$\int E_t dt$</u>	<u>RSD</u> <u>%</u>
1	236	1061
10	12,220	22.8
100	75,732	4.9
1000	715,782	2.1

Slope = 1.1

R = 1.0

Table XVII
Calibration Data Pb(II) - 220.55 nm - Meinhard Nebulizer

<u>Conc. Pb</u> <u>ppm</u>	<u>$\bar{I}_{E,t}$</u>	<u>RSD</u> <u>%</u>
1	3,538	49.8
10	35,800	16.0
100	318,892	4.3
1000	3,284,320	4.0

Slope = 1.0

R = 1.0

Pb(I)-405.783NM

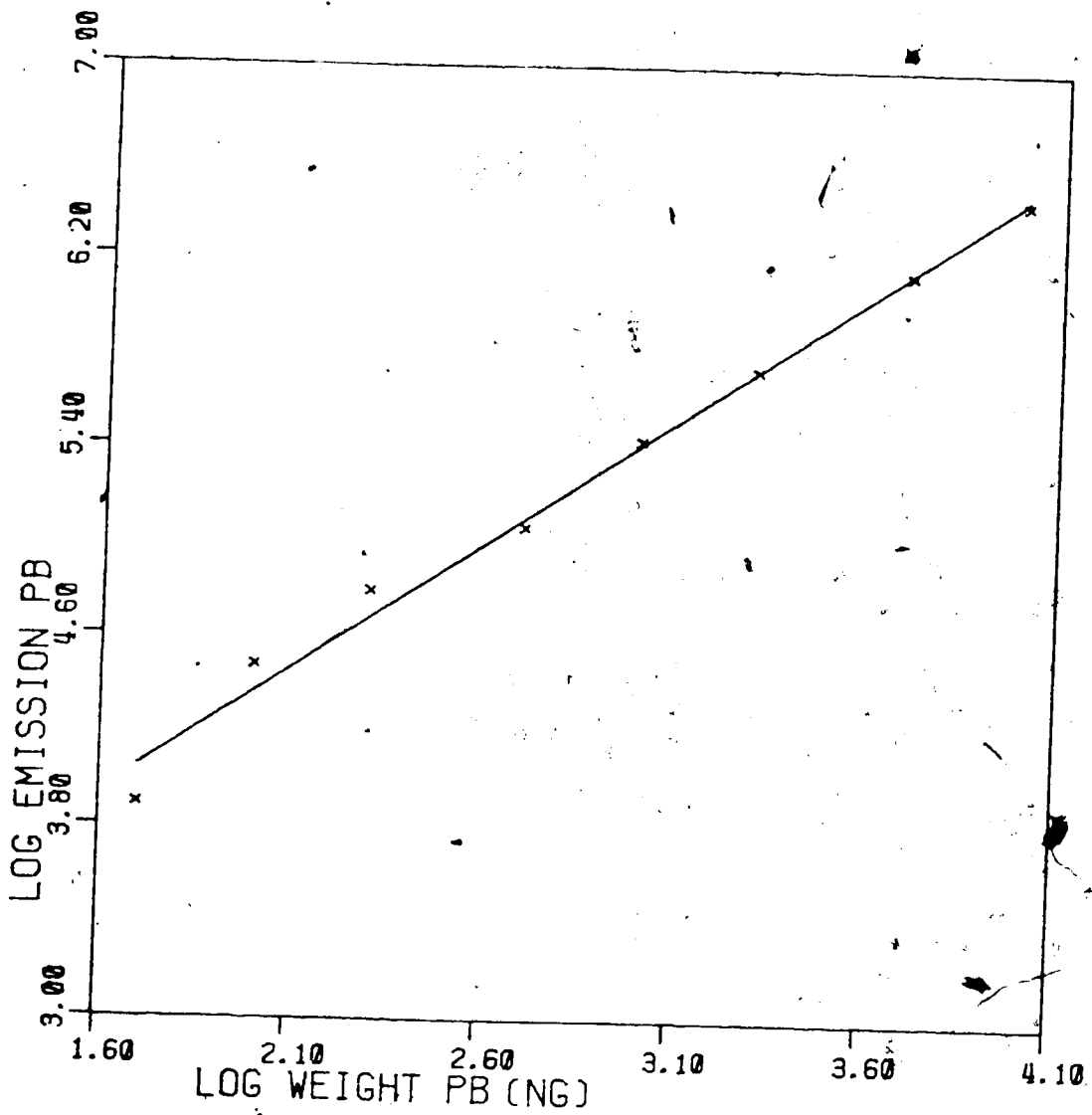


Figure 34. Log-log calibration plot for Pb(I) - 405.783 nm.

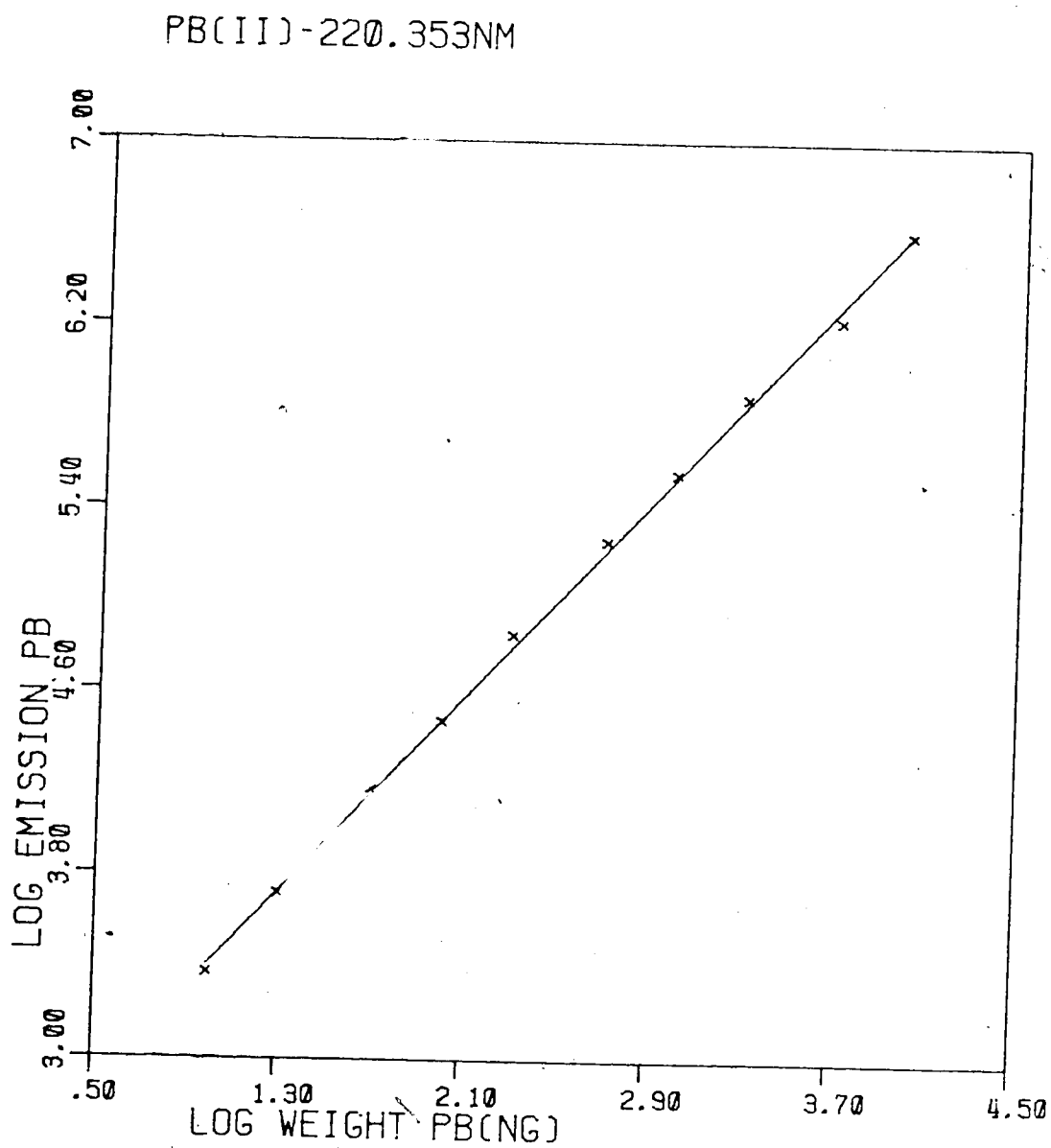


Figure 35. Log-log calibration plot for Pb(II) - 220.353 nm.

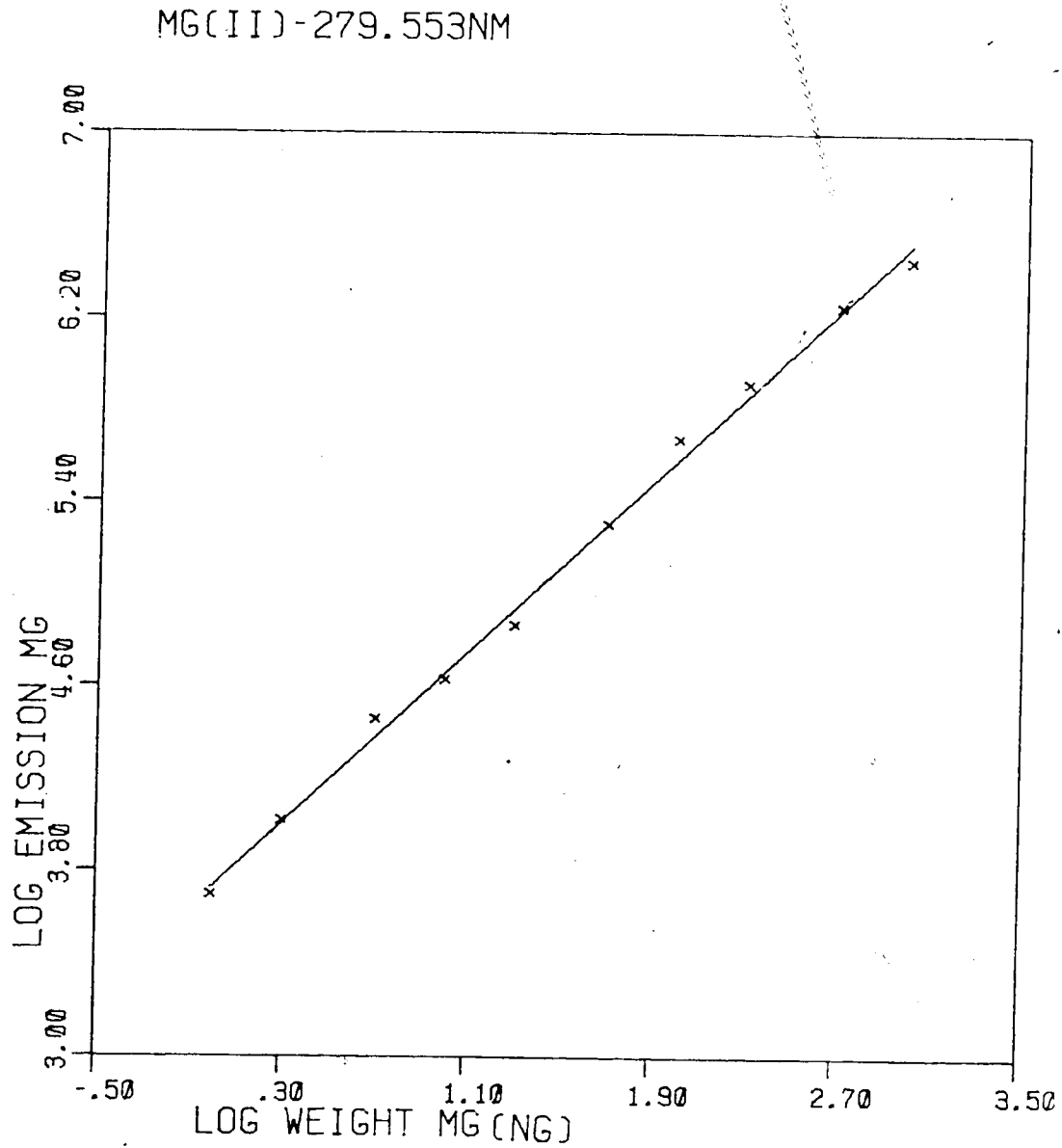


Figure 36. Log-log calibration plot for Mg(II) - 279.553 nm.

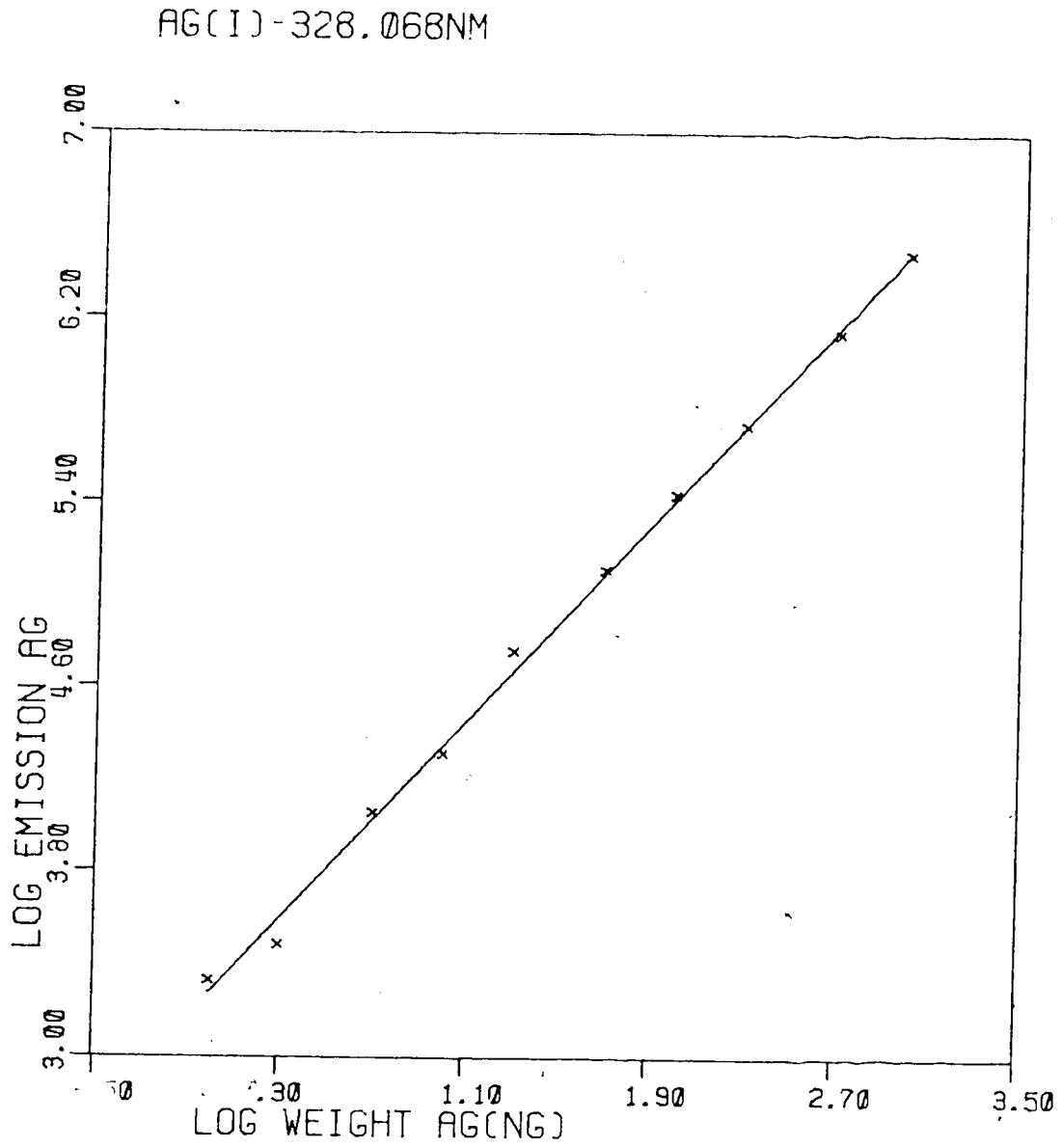


Figure 37. Log-log calibration plot for Ag(I) - 328.068 nm.

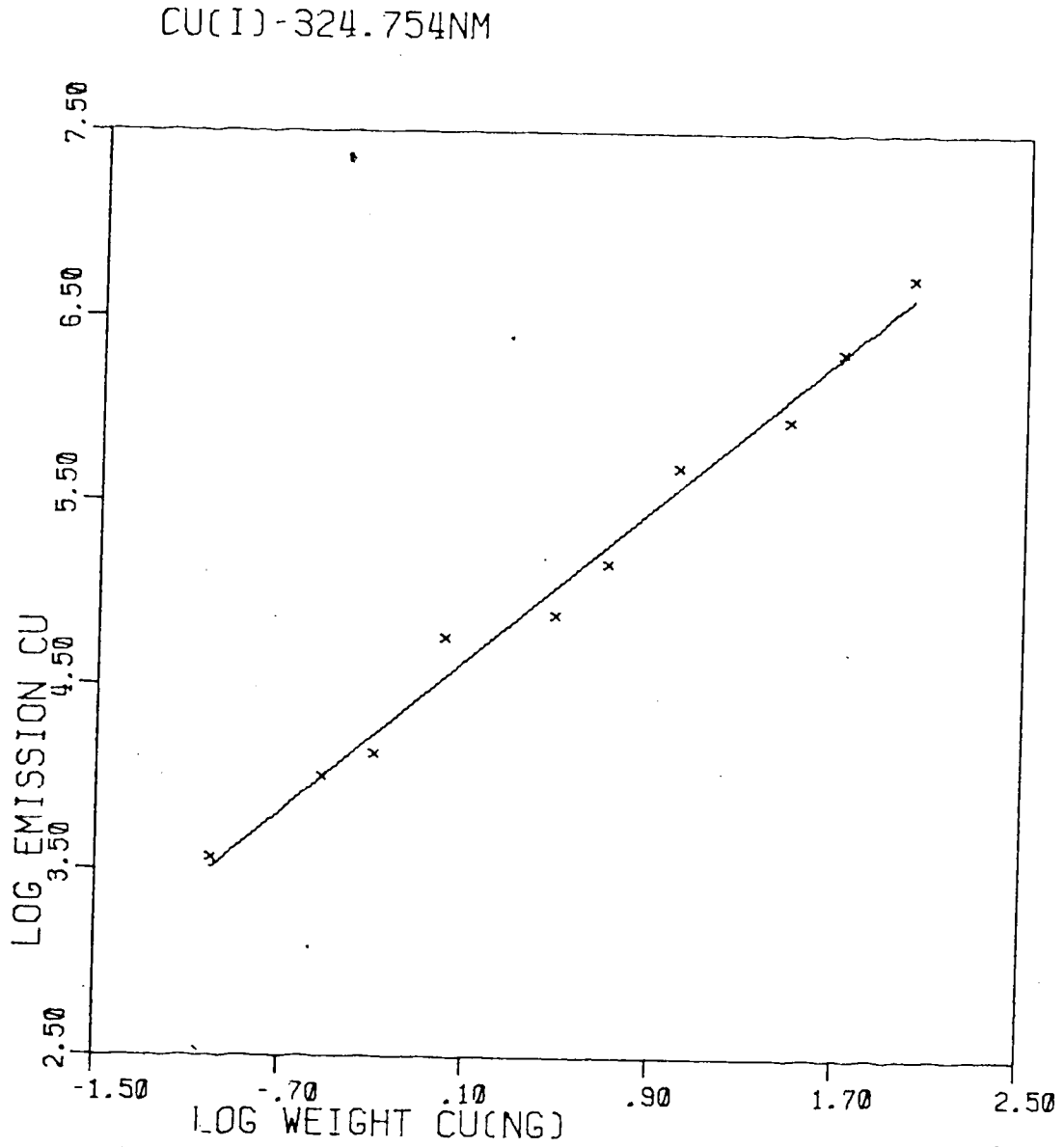


Figure 38. Log-log calibration plot for Cu(I) - 324.754 nm.

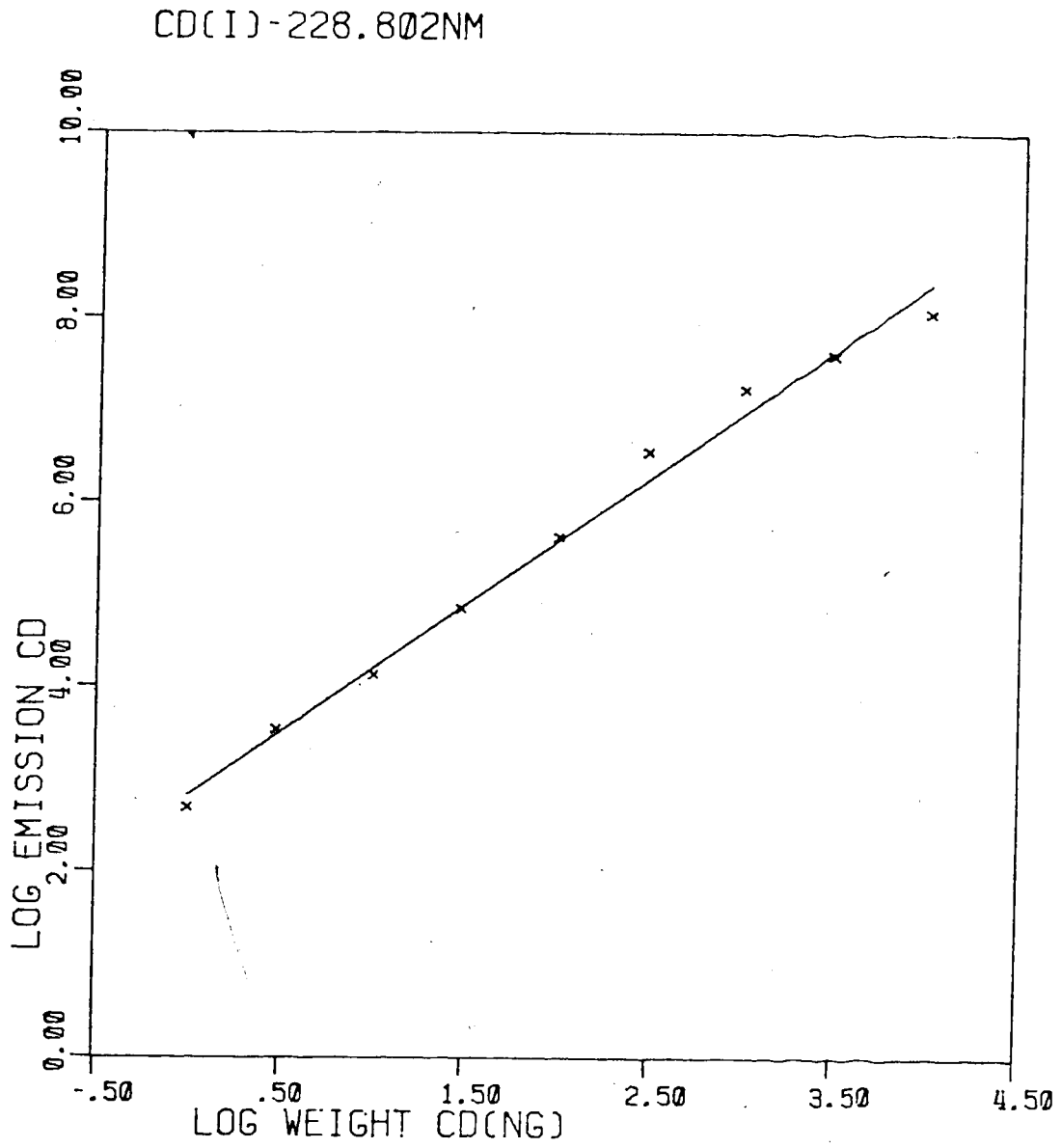


Figure 39. Log-log calibration plot for Cd(I) - 228.802 nm.

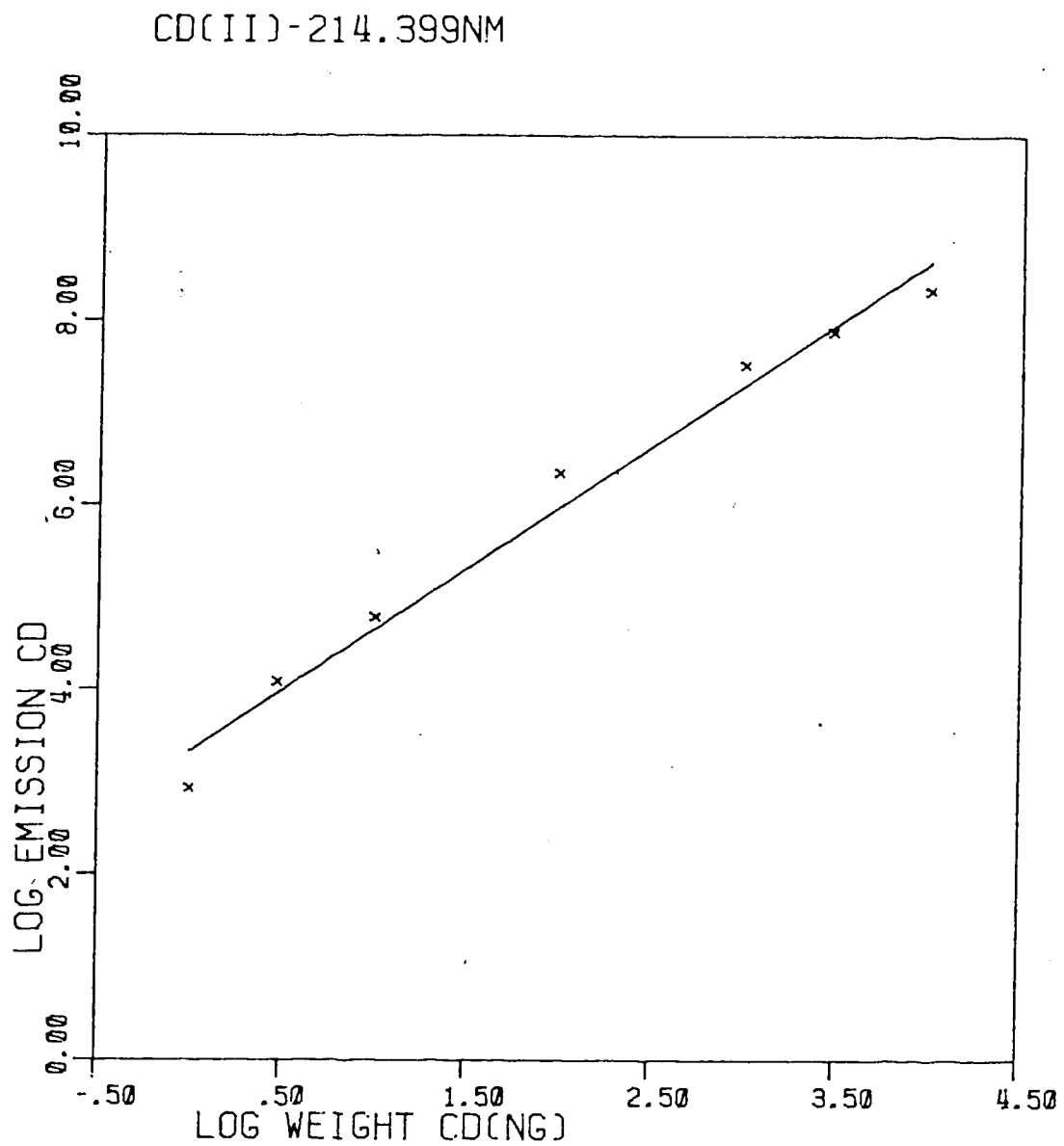


Figure 40. Log-log calibration plot for Cd(II) - 214.438 nm.

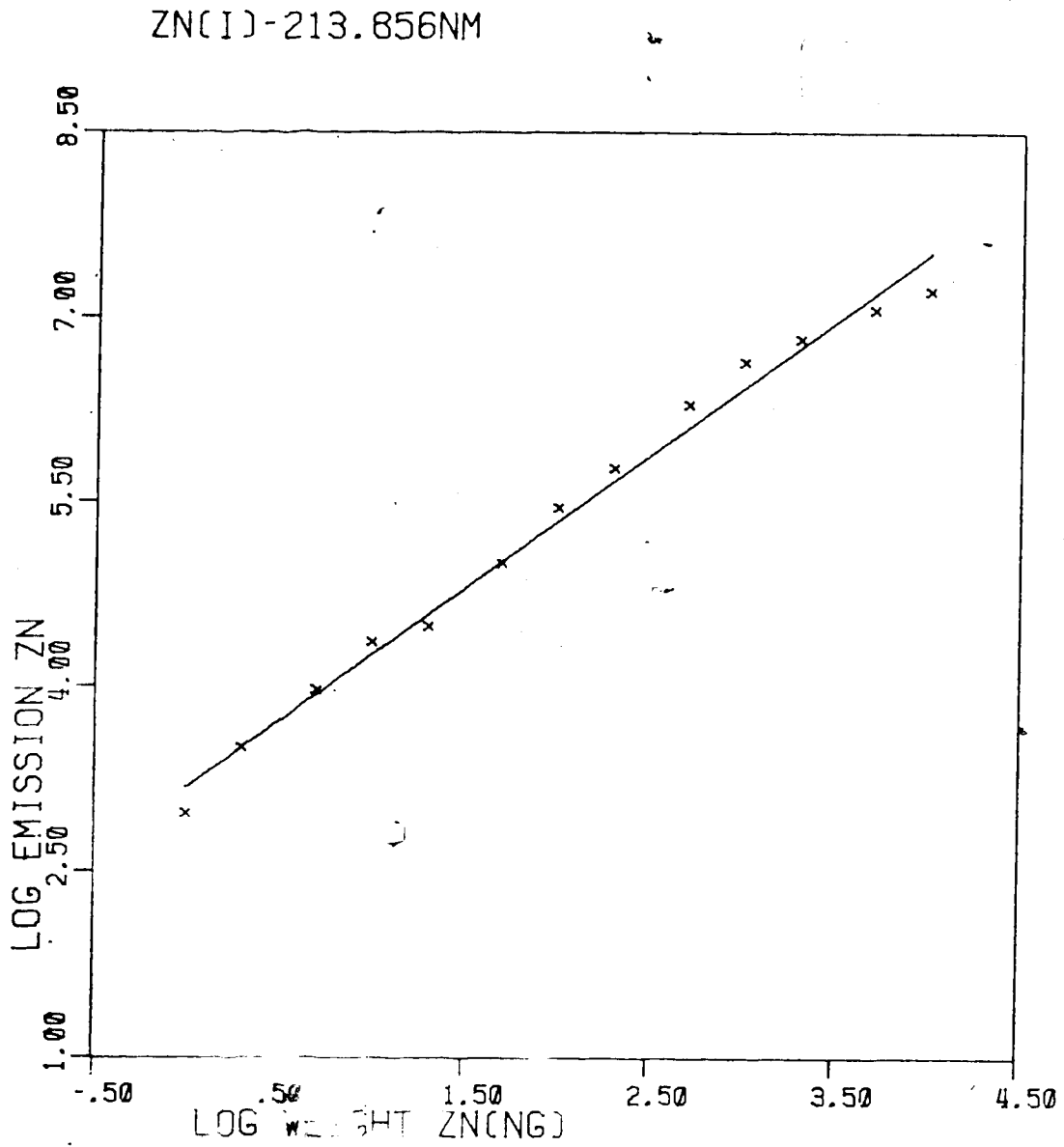


Figure 41. Log-log calibration plot for Zn(I) - 213.856 nm.

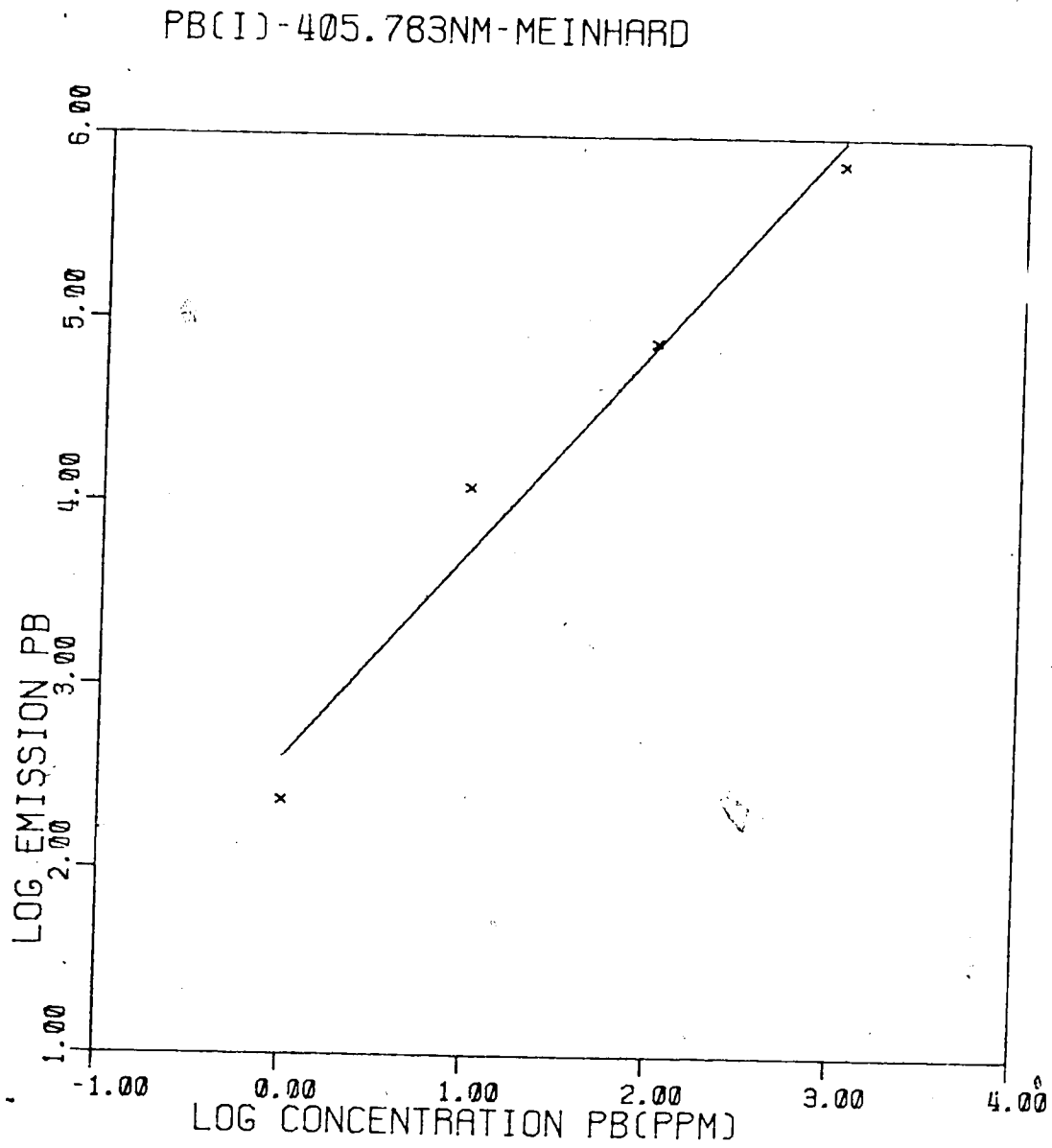


Figure 42. Log-log calibration plot for Pb(I) - 405.783 nm, Meinhard nebulizer.

PB(II)-220.353NM-MEINHARD

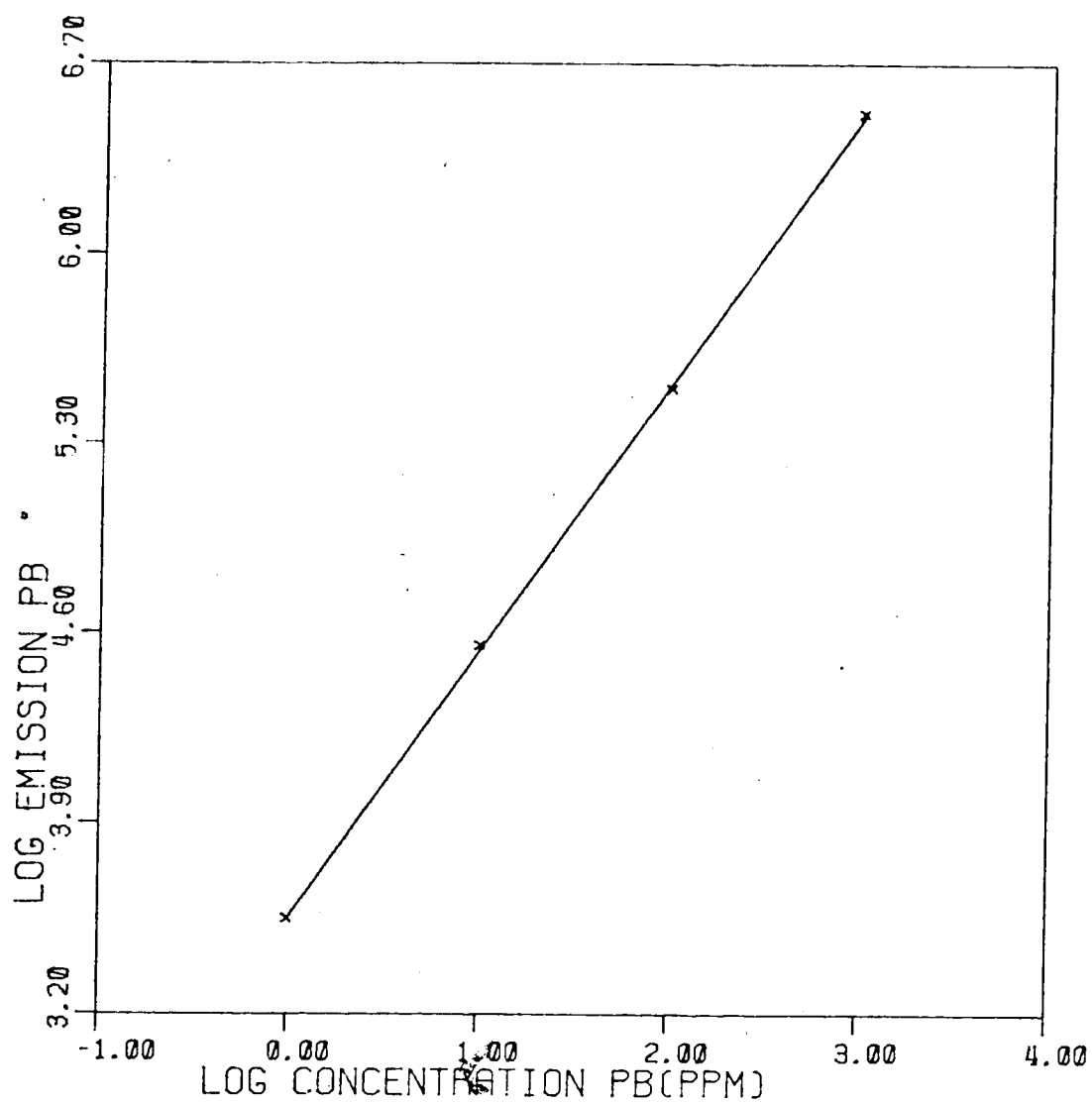


Figure 43. Log-log calibration plot for Pb(II) - 220.353 nm, Meinhard nebulizer.

equal. The detection limit is defined as the concentration (or quantity) of analyte which gives a signal equal to twice the standard deviation in the background signal. A simple calculation will show that, for instance, the 1.0 ppm solution which can just be detected with the Pb(II) emission line and the nebulizer can just be detected when the graphite furnace EA system is used with a 10 μ L sample since $10 \mu\text{L} \times 1.0 \text{ ppm} = 10 \text{ ng}$. Similar results are also obtained with the Pb(I) emission line. It is possible to extend the "concentration" detection limit for the graphite furnace EA system to a lower level by repeatedly adding 10 to 20 μ L samples with drying between additions. This technique is commonly used in graphite furnace AA and has been found to work well.

CHAPTER IV

Effect of NaCl Matrix on Pb(II) EA-ICAP-OES Analysis

Perhaps one of the most widely analyzed materials by graphite furnace AAS is lead. Unfortunately this analysis suffers from severe matrix effects. The most common matrix which causes trouble is NaCl which is found in sea water, blood plasma, and urine. This matrix material causes loss of lead as molecular lead chloride, reducing the amount of lead produced as an atomic vapor. The NaCl also causes both molecular absorption and light scattering from recondensed NaCl particles which interfere in the light absorption measurement. These interference problems have been investigated by a large number of workers and several techniques have been developed to reduce these interferences. The use of background absorption correction helps but chemical modification techniques have also been shown to be very helpful. The most common chemical modification techniques are the use of added HNO_3 (53,54), NH_4NO_3 (55, 56), or $\text{La}(\text{NO}_3)_3$ (57,58). The use of a constant temperature Woodriff AAS furnace has also been suggested as a means of overcoming the interference effect of NaCl or other salts on Pb determination (59).

Matrix interference effects in ICAP-OES have generally been found to be quite small when compared to the inter-

ferences found in flame emission or in either flame or non-flame atomic absorption spectrometry. A short review of the matrix interferences in ICAP-OES is given in Reference 5 and it is pointed out that when ICAP operating conditions are properly chosen these interferences can be reduced to negligible proportions.

The results presented in Chapter III have shown that with EA-ICAP-OES large amounts of analyte have caused changes in the vaporization behavior, but good analytical results could still be obtained by using a signal integration technique. The determination of Pb in a NaCl matrix was chosen as a test of the effect of matrix interference on EA-ICAP OES. This system was chosen because it was felt that EA-ICAP-OES might offer an alternative solution to determination of Pb by AAS.

This study of NaCl matrix interferences on Pb emission can be separated into three parts. The first is a study of Pb(II) emission and plasma background emission temporal changes, second is a study of background corrected Pb emission intensity changes, and the third is a study of changes in spatial emission intensity. The first two studies will be discussed in this section and the spatial study in the next.

A. Effect of NaCl Matrix on Pb(II) Emission Temporal Behavior and Emission Intensity

The study of changes in temporal behavior can be summed up in four plots of emission intensity vs time. Figure 44 is a normal blank plasma background while Figure 45 is the plasma background when 200,000 ng of sodium as NaCl are vaporized as a blank. The NaCl blank shows a significant rise in the plasma background emission level, especially after the first two seconds while a distilled water blank shows a decrease in plasma background emission after the first two seconds. This change in plasma background emission is large enough to cause an increase in the Pb emission intensity value at high NaCl levels unless a blank of approximately equal NaCl concentration is used.

Figure 46 is a plot of emission intensity vs time for a 10 μ L sample of 10 ppm solution (100 ng Pb) in distilled water. The peak shape is normal in that it shows a quick rise to a maximum and a smooth decay to a level background level. Figure 47 is also an emission vs time plot for 100 ng of Pb, but with 200,000 ng of sodium as NaCl also present. The peak height is obviously depressed, the decay is no longer smooth, and emission is extended over a slightly longer time. The temporal changes caused by the large amount of matrix material appears to be similar to those caused by a large amount of analyte. One possible explanation of these temporal effects is that the larger mass of material requires a longer time to vaporize, thus

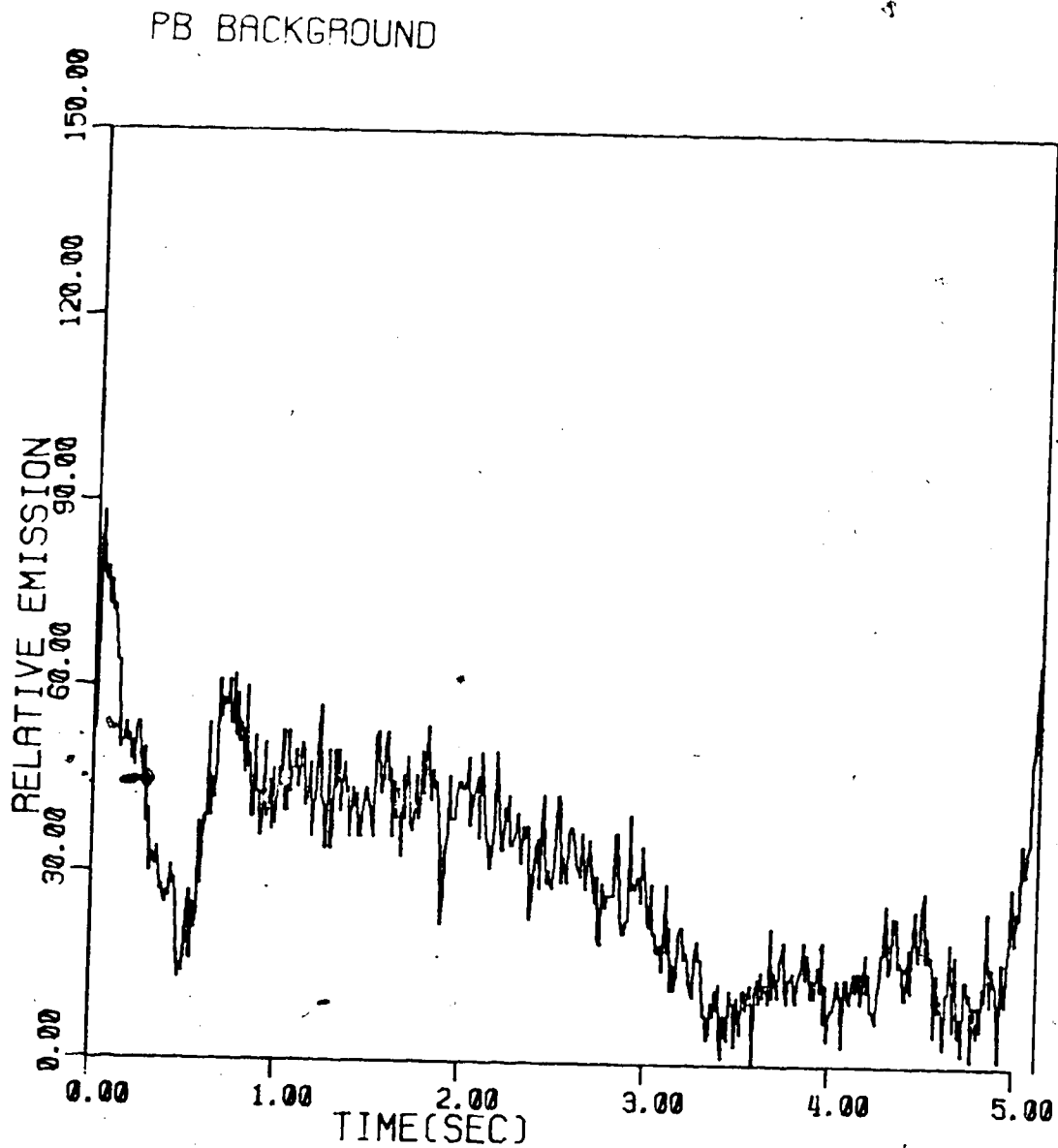


Figure 44. Temporal profile, blank Pb(II) - 220.353 nm.

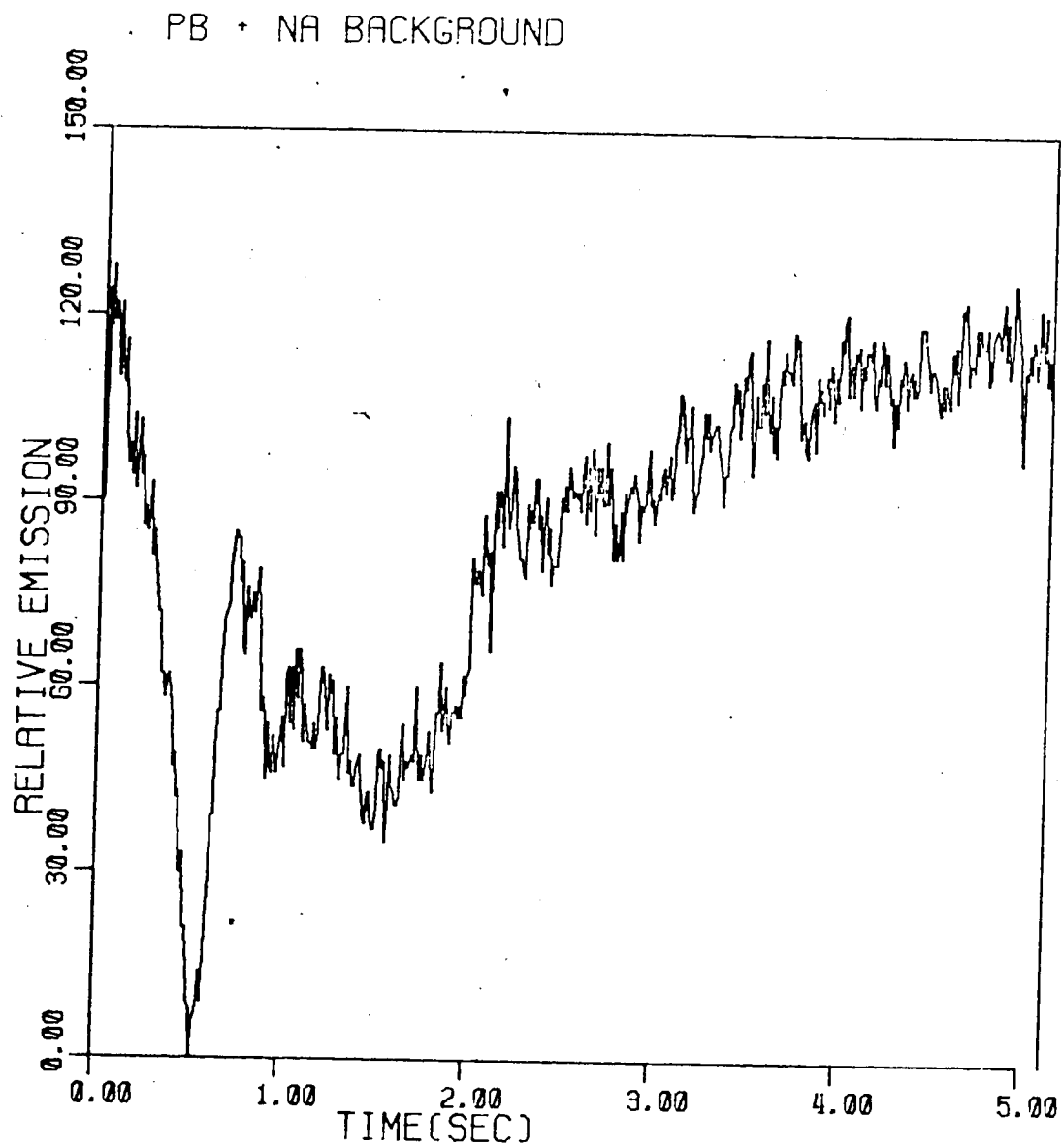


Figure 45. Temporal profile, blank containing 200,000 ng Na⁺ as NaCl, Pb(II) - 220.353 nm.

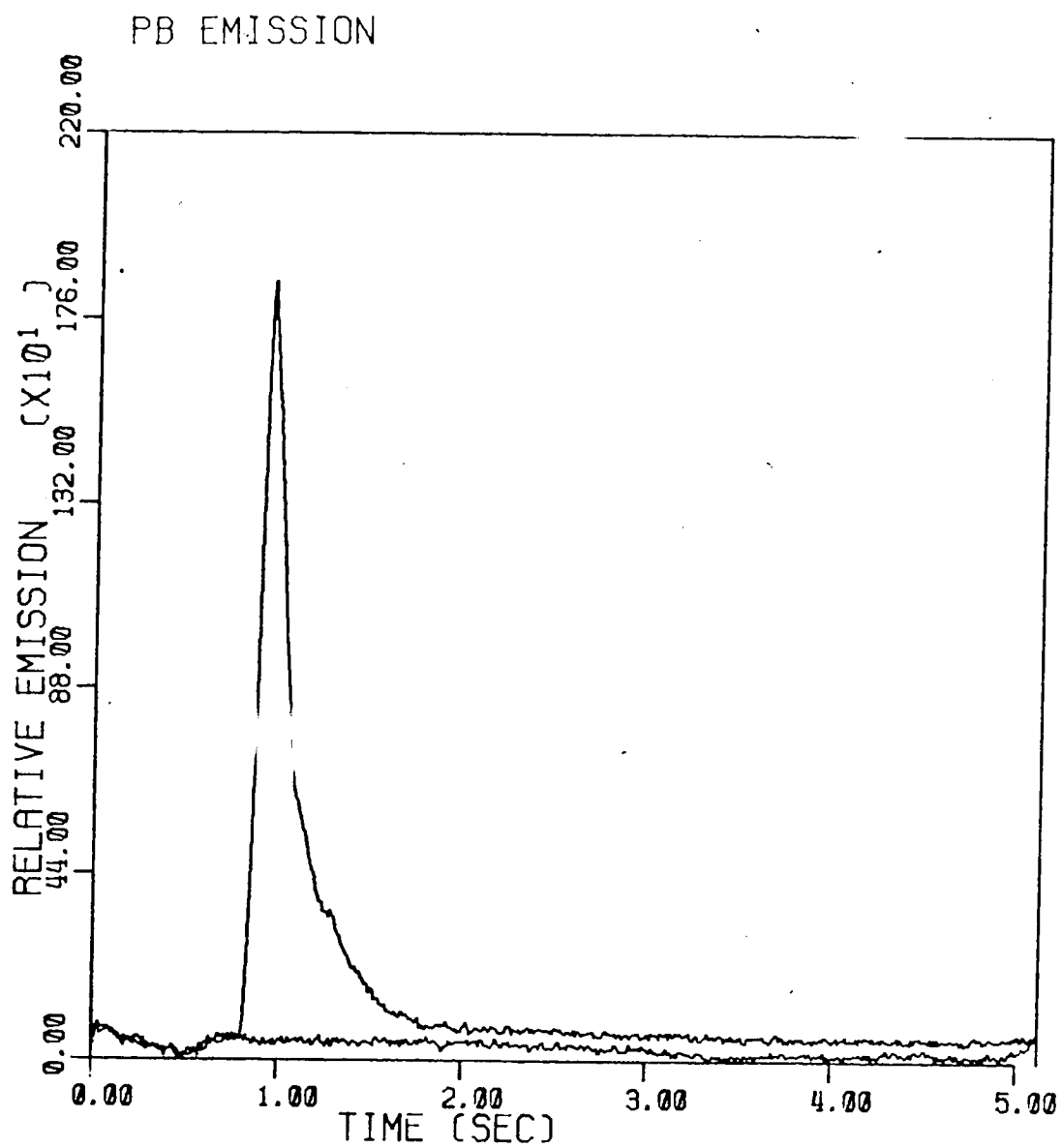


Figure 46. Temporal profile, 100 ng Pb(II) - 220.353 nm.

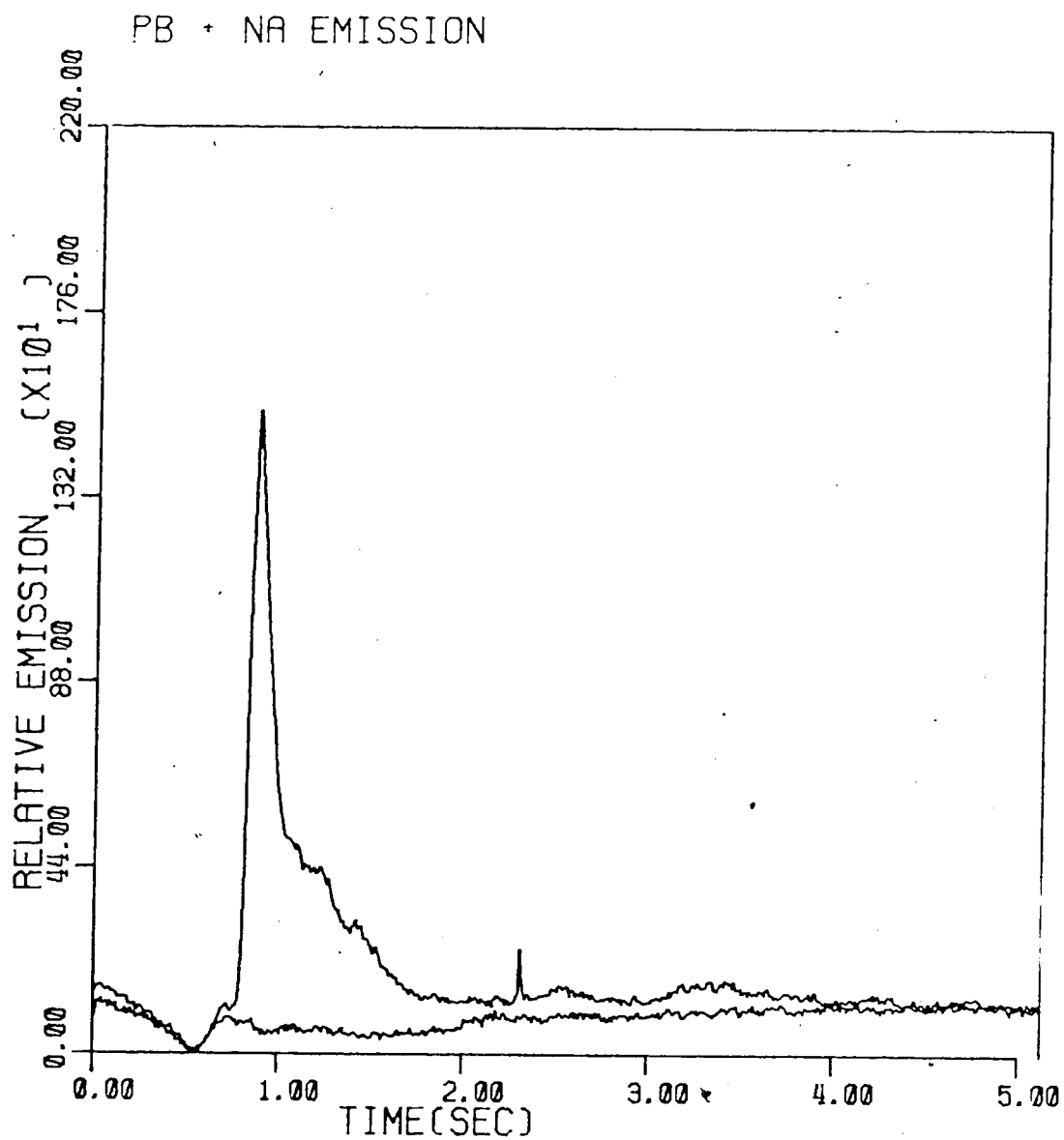


Figure 47. Temporal profile, 100 ng Pb(II) - 220.353 nm.
Matrix of 200,000 ng of Na⁺ as NaCl.

reducing the peak emission and extending the time of emission.

Table XVIII gives the Pb emission intensity data for a series of solutions containing zero to 20,000 ppm of added sodium as NaCl which is greater than the concentration of NaCl in sea water. The data given is background corrected, where the background is for a blank solution containing the same concentration of NaCl as the Pb solution. The sample size was 10 μ L, therefore the Pb quantity was 100 ng and the sodium quantity ranged from 0 to 200,000 ng (0.2 mg). The results are shown graphically in Figure 48. Although the plot shows a slight rise in Pb emission intensity with increasing NaCl concentration this increase is not significant. This increase in intensity is probably due to instrumental drift during the four hours required for this experiment.

B. Matrix Effects on Pb(II) Spatial Emission Profiles

In Chapter II the use of a photodiode array mounted vertically in the focal plane of the monochromator was introduced as a tool for measuring vertical spatial emission intensity profiles. References 50 and 51 are examples of how this technique has been used. Data given in Reference 59 for Ca(II) emission at 393.3 nm and Cr(II) emission at 283.5 nm show that as the ratio of an easily ionized matrix material to analyte increases the emission

Table XVIII
Effect of Sodium on Pb(II) - 220.353 nm Emission
All Samples 100 ng Pb

<u>Wt. Na as NaCl</u> <u>ng</u>	<u>$\bar{I}E_t$</u>	<u>RSD</u> <u>%</u>
0	43,992	3.4
2	46,110	13.1
20	38,729	13.1
200	43,754	4.3
2,000	43,653	4.7
20,000	48,629	5.0
200,000	46,820	25.9

EFFECT OF NA-PB(II)-220.353NM

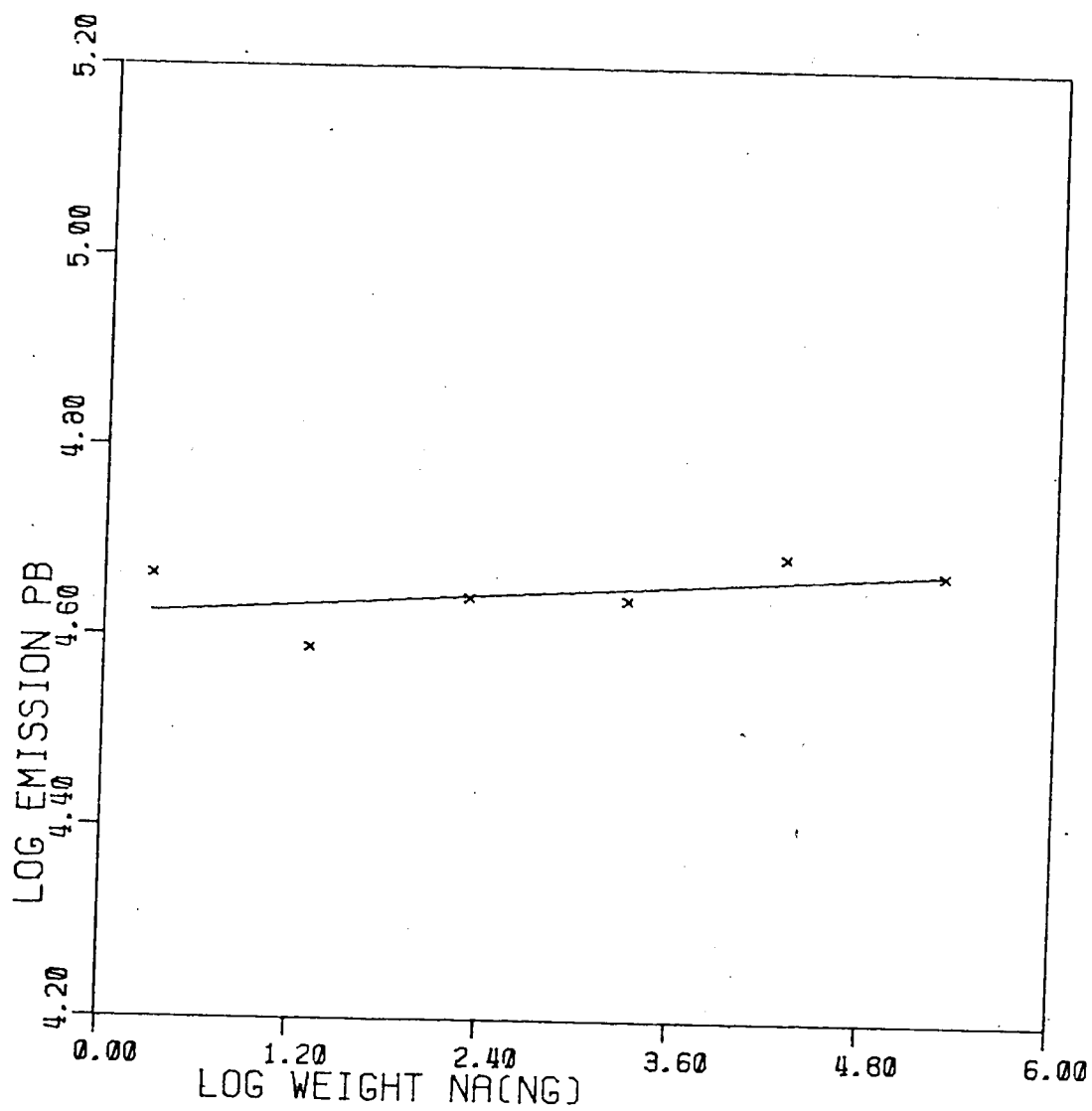


Figure 48. Effect of Sodium ion Pb(II) - 220.353 nm emission.

profile of the analyte shifts lower in the plasma. In order to check for this type of behavior 5 μ L samples of 1000 ppm Pb in distilled water were vaporized both with and without 5 or 10 μ L additions of 20,000 ppm sodium as NaCl. The vertical spatial emission profiles obtained for the Pb(II) emission line at 220.353 nm for ratios of Na/Pb = 0 and Na/Pb = 20 are given in Figure 49 and 50. The results obtained are consistent with the results shown for Ca(II) and Cr(II) in Reference 51 in that the emission shows an increase at lower heights above the coil and a decrease in emission at higher heights. The point of maximum emission has also shifted from 14.7 mm above the load coil to 12.2 mm. This spatial shift would be expected to increase as the ratio of matrix material to analyte increases, therefore, the choice of slit height and the height of observation can be very important. As an example, if the slit height were chosen to be small, for instance 1 mm or 2 mm, and centered at about 15 mm above the load coil then a large excess of matrix could cause the measured signal to decrease. On the other hand if the slit was centered at 12 mm above the load coil the emission intensity could increase under the same conditions. In the measurement described in section B a slit height of 12 mm centered at about 17 above the coil and an image magnification of -0.5 meant that the height observed was from about 5 mm to 30 mm above the load coil.

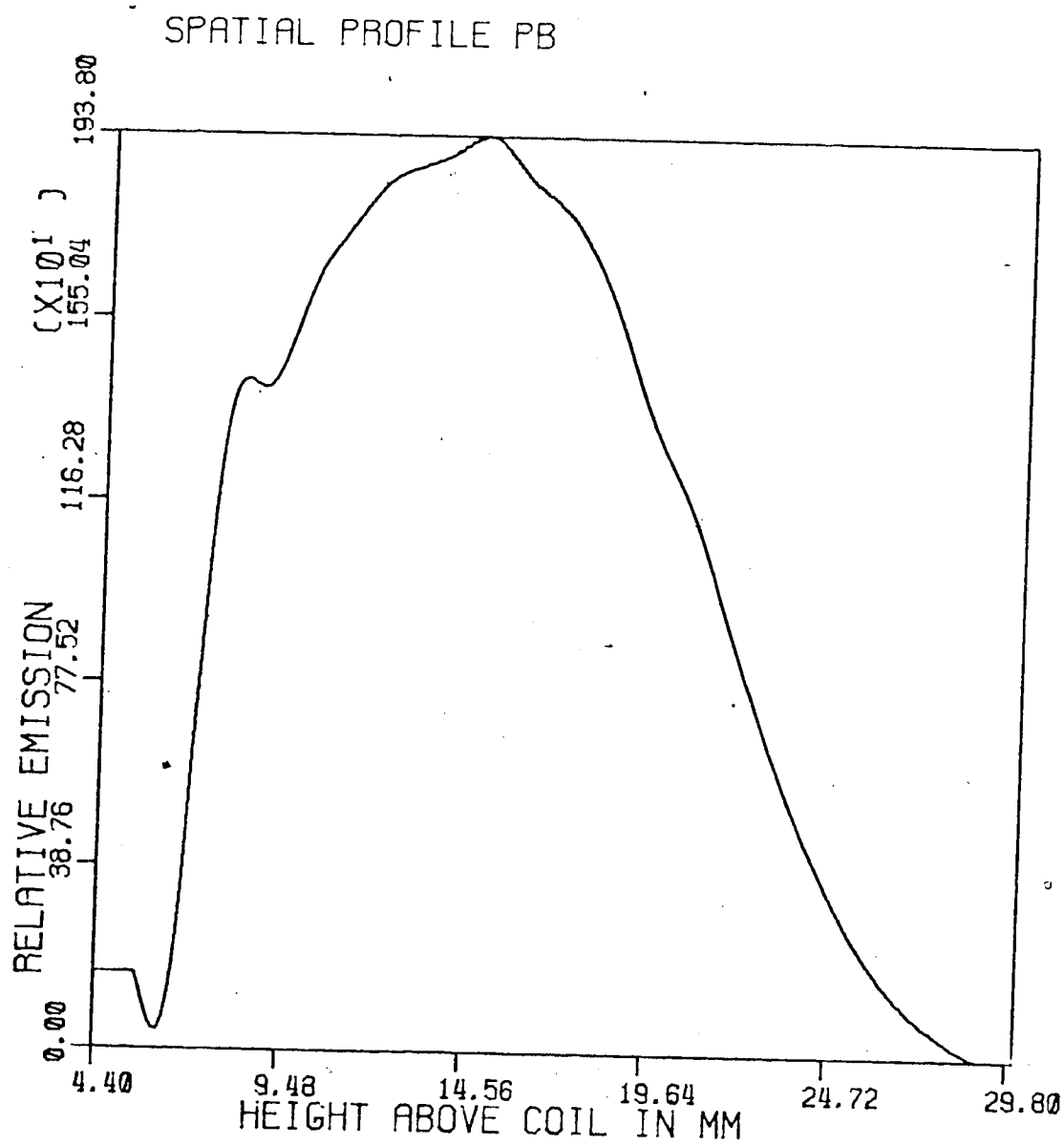


Figure 49. Vertical emission profile, Na/Pb = 0.

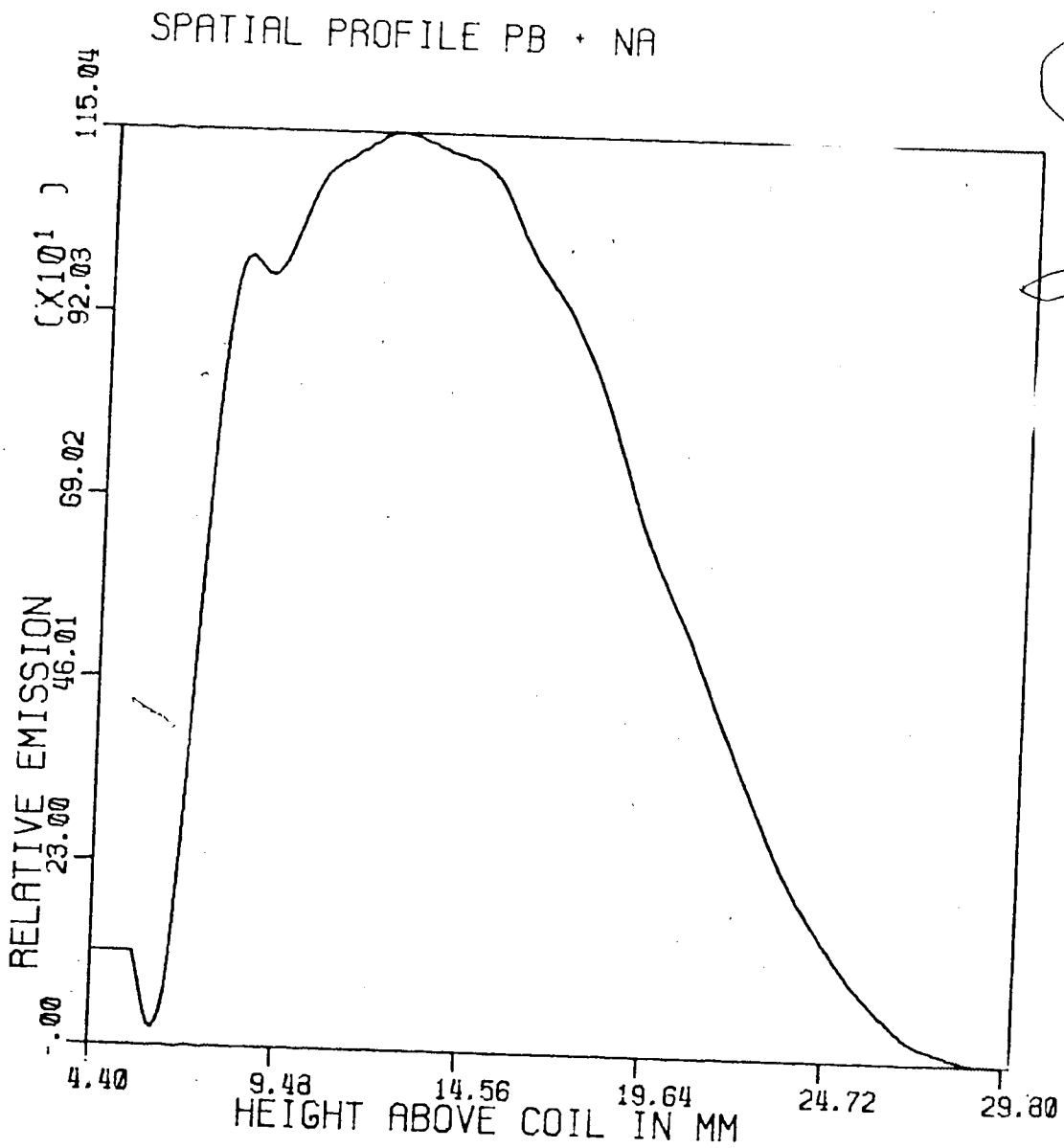


Figure 50. Vertical emission profile, Na/Pb = 20.

With these conditions spatial shifts would be expected to cause little change in measured emission intensity as observed in the work reported in section A.

CHAPTER V

Direct Solids Analysis by EA-ICAP-OES Using a Computer Coupled Photodiode Array Direct Reading Spectrometer

One of the main objectives of this experimental work was to test the graphite furnace EA-ICAP-PES technique as a direct solids analysis technique. Direct solids analysis is in many ways the most difficult type of analysis to perform. The matrix is frequently complex and the elements being analyzed for are generally only present in small amounts, frequently at the ppm level. Volatilization behavior can vary because of inhomogeneous particle sizes if powders are analyzed and in almost all cases there is an inhomogeneous distribution of analyte. This last problem is particularly difficult or impossible to overcome and can be a limiting factor in direct solids analysis when sample size reaches the level of about 2 mg or less. In the review entitled "Direct Analysis of Solids by Atomic-absorption Spectrophotometry", Langmyhr (60) summarizes this problem:

"Brittle inorganic materials are usually analyzed in the form of powders. The errors introduced by the sampling of powders for trace analysis vary considerably with the distribution pattern of the analyte."

and

"In the sampling and treatment of solid materials of human, animal and plant origin, the diversity of the samples and the widely differing properties of the

analytes make it difficult to give any general procedure. The amount of material available is often small and the elements to be determined may be inhomogeneously distributed, and consequently sampling errors may occur."

The fact that d.c. arc analysis and graphite furnace AAS analysis are widely used for the direct analysis of solids clearly demonstrates that the above problems can be overcome to an acceptable degree. It must be noted, however, that in direct solids analysis a much higher RSD is generally acceptable than in the analysis of solutions by such techniques as flame AAS.

One technique which has been successfully used in d.c. arc analysis to minimize or eliminate the problems encountered in direct solids analysis is the use of an internal standard. In this technique a known amount of a material not normally present is added to the sample and the analysis is based on the ratio of the analyte emission intensity to that of the internal standard. This technique assumes that the internal standard and the sample will behave in a similar manner during sample volatilization, excitation, and emission, therefore the choice of internal standard can be very important.

The use of an internal standard requires the simultaneous measurement of the analyte and internal standard emission and thus requires multielement analysis capability. It was felt that the use of an internal standard might be

helpful in this experimental work therefore it was decided to use the photodiode array direct reading spectrograph developed in this laboratory over the last 8 years. This instrument also has the advantages of allowing quick checking for spectral interference by other elements present in the sample matrix and allows the measurement of the plasma background emission at a wavelength adjacent to that of the analyte. This was felt to be a very useful feature in view of the fact that the background emission was found to vary with the matrix as shown in the previous chapter.

A. Analysis of Spex G-Standard Mixture

The Spex G-Standards manufactured by Spex Industries, Meluchen, N.J., are commonly used as standards for d.c. arc emission spectroscopy. These standards consist of a graphite matrix containing a known amount (0.0001% to 0.1%) of 49 elements and 0.1% of In as the internal standard. These standards were chosen as model solids for a test of EA-ICAP-OES direct solids analysis.

Analyte emission temporal behavior has been shown earlier to be affected by the matrix therefore it is obvious that a time study of emission with direct solids analysis would be necessary. The PDA direct reading spectrometer has been shown to be useful for such studies (44) with d.c. arc emission and while the temporal resolution is much less than

with the PMT system it was felt that it would be adequate for this purpose. The results are seen in Figure 51. The PDA integration time was set to approximately 0.4 seconds and each scan is stored and then plotted separately. The wavelength region covered is from about 250 nm at diode number 0 to about 195 nm at diode number 1024. Some of the emission lines shown are identified in Figure 52. Examination of Figure 51 will show, for instance, that Cd and Zn, present at the 0.001% level, show emission between 1.2 and 2.8 seconds with their maximum emission occurring in the integration period between 1.2 and 1.6 seconds. The internal standard In which is present at 0.1% shows emission starting at 1.2 seconds, reaching a maximum at 2.0 seconds, and is still showing emission at 2.8 seconds, the last scan plotted. The results of this time study are that the emission of Cd and Zn show similar, but not identical, behavior to that of the internal standard, and that the PDA signals must be time-averaged for about 3 seconds to include all the emission due to Cd, Zn, or In. The calibration data and curves for Cd(I) and Zn(I) in the G-Standards are shown in Tables XIX and XX and Figures 53 through 56 where concentration of Cd and Zn are plotted vs. the ratio of the analyte emission to the sample weight and to the internal standard emission. Acceptable calibration plots can be prepared from either of these types of data but in all

Table XIX

Calibration Data for Cd(I) - 228.802 nm
in Spex G-Standards

Amount Cd %	$\bar{J}_{E_t} dt(Cd)/Spl.Wt.$	RSD %	$\bar{J}_{E_t} dt(Cd)/\bar{J}_{E_t} dt(In)$	RSD %
0.00033	56.5	19.6	0.0182	23.8
0.001	1,004.5	14.8	0.288	11.5
0.010	23,440.1	36.4	4.273	/ 31.3

$\bar{J}_{E_t} dt(Cd)/Spl.Wt.:$

Slope = 1.7

R = 1.0

$\bar{J}_{E_t} dt(cd)/\bar{J}_{E_t} dt(In):$

Slope = 1.5

R = 1.0

Table XX
 Calibration Data for Zn(I) - 213.856 nm
 in Spex G-Standards

Amount Zn %	$\bar{I}_{E_t} dt(Zn)/Spl.Wt.$	RSD %	$\bar{I}_{E_t} dt(Zn)/\bar{I}_{E_t} dt(In)$	RSD %
0.00033	237.2	11	0.0756	6.5
0.001	897.8	11	0.258	12.9
0.01	24,324.5	26	4.439	1.0

$\bar{I}_{E_t} dt(Zn)/Spl.Wt.:$

Slope = 1.4

R = 1.0

$\bar{I}_{E_t} dt(Zn)/\bar{I}_{E_t} dt(In):$

Slope = 1.2

R = 1.0

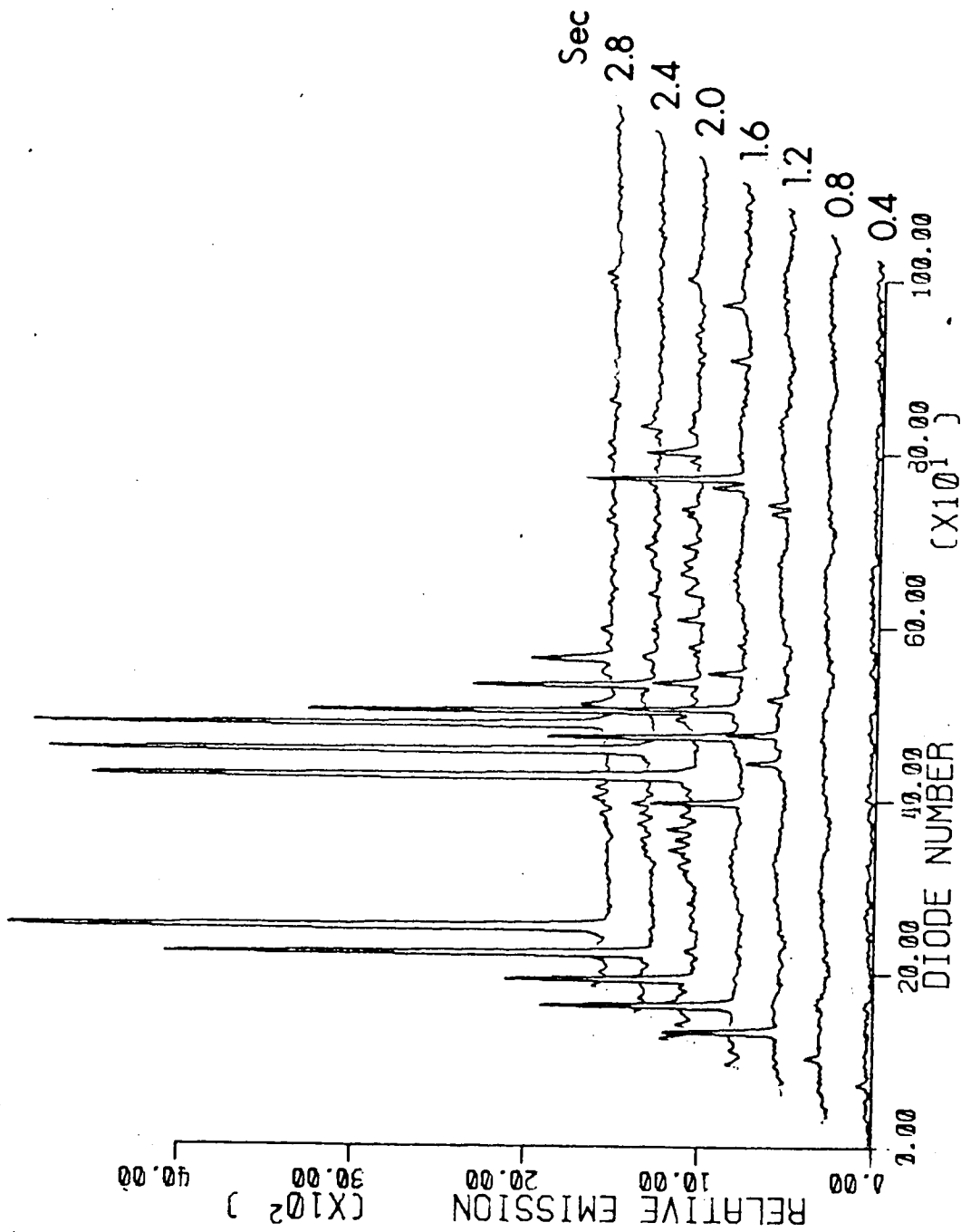


Figure 51. Time study of 5.2 mg of Spex G3 Standard Containing 49 elements at 0.001% level and 0.1% In.

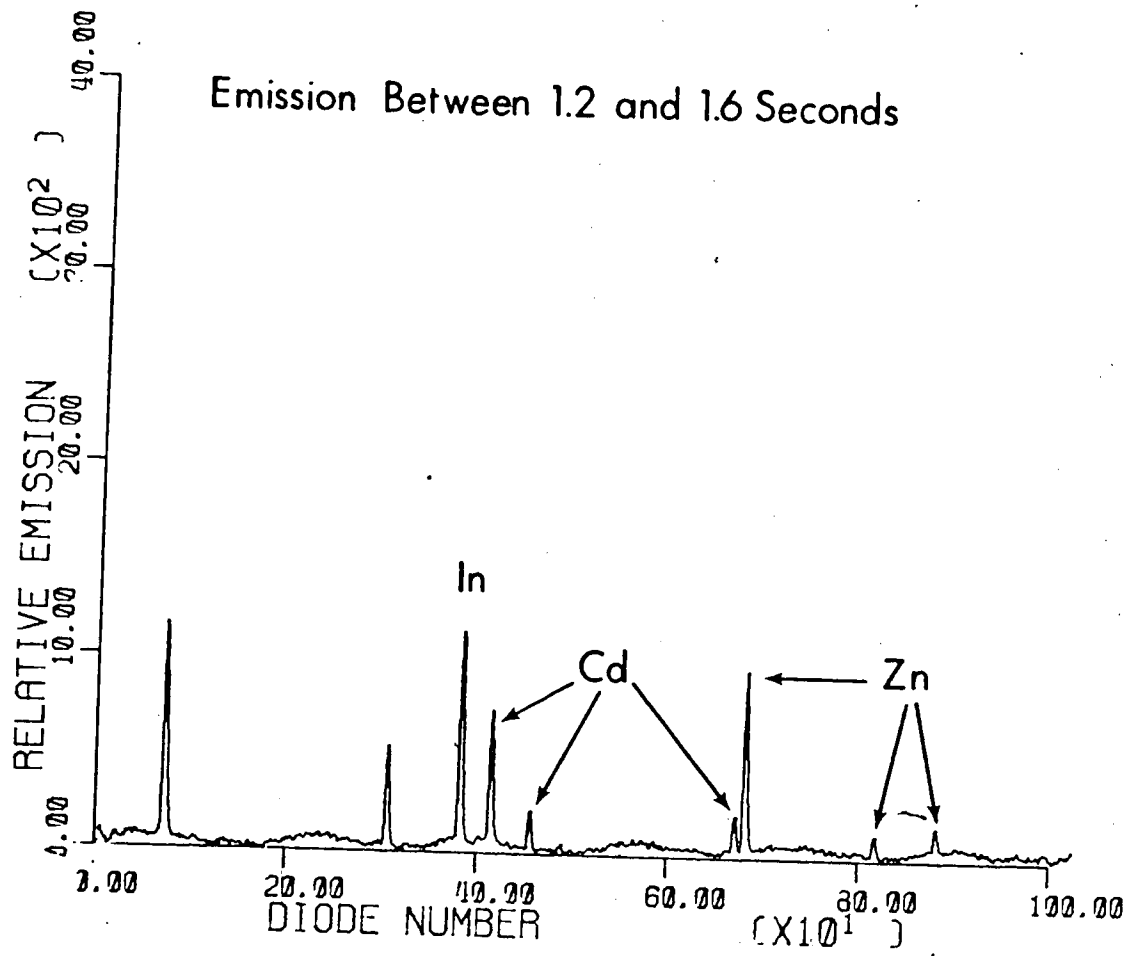


Figure 52. Spectrum taken between 1.2 and 1.6 second from Spex G3 Standard time study, Figure 51.

SPEX STANDARDS CD(I)-228.802NM

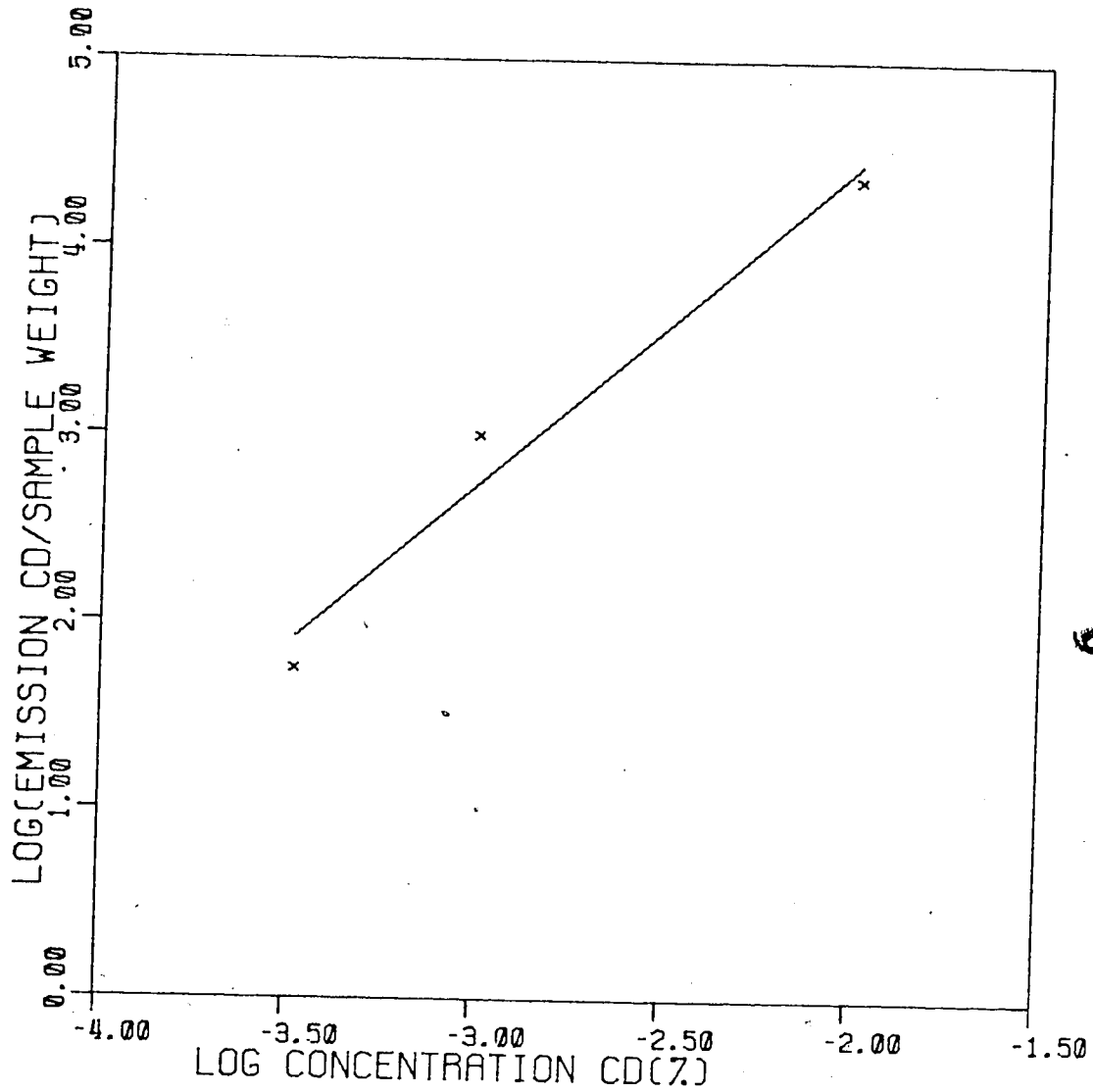


Figure 53. Log-log calibration plot for Spex G-Standards Cd(I) - 228.802 nm/sample weight.

SPEX G STANDARDS Cd(I) - 228.802 nm

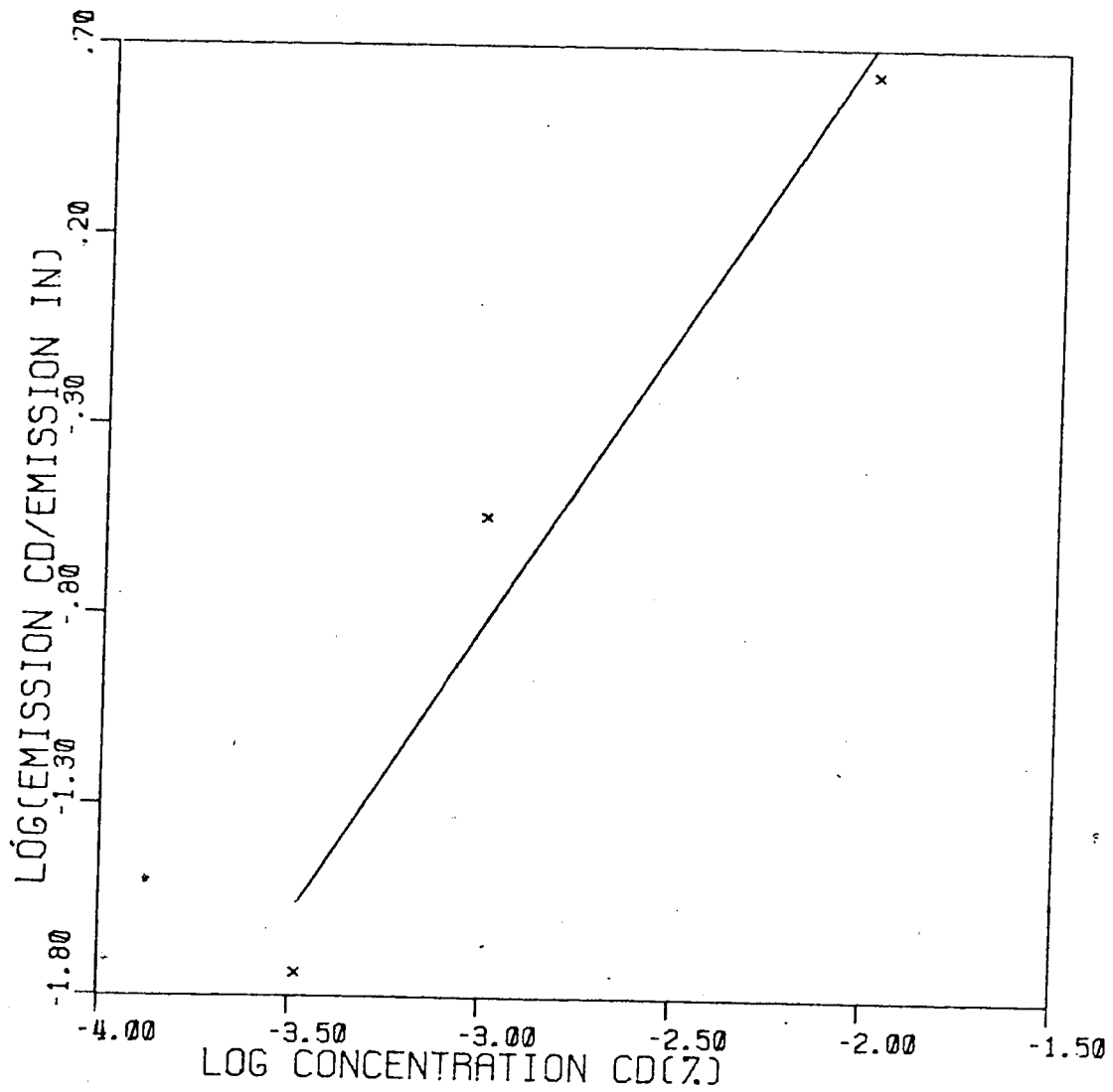


Figure 54. Log-log calibration plot for Spex G-Standards (Cd(I) - 228.802 nm)/(In(II) - 230.606 nm).

SPEX G STANDARDS ZN(I)-213.856NM

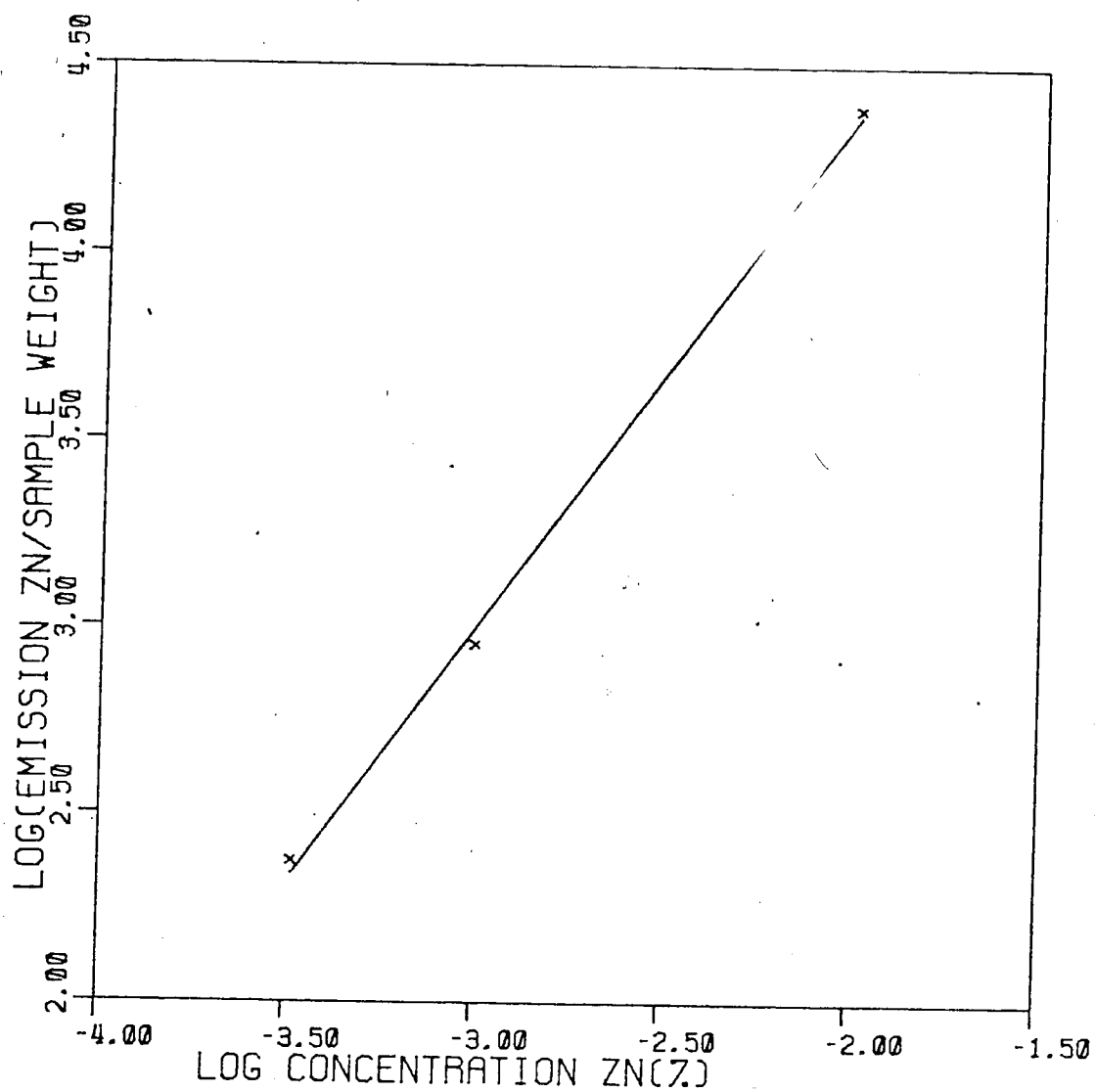


Figure 55. Log-log calibration plot for Spex G-Standards Zn(I) - 213.856 nj/sample weight.

SPEX G STANDARDS ZN(I)-213.856NM

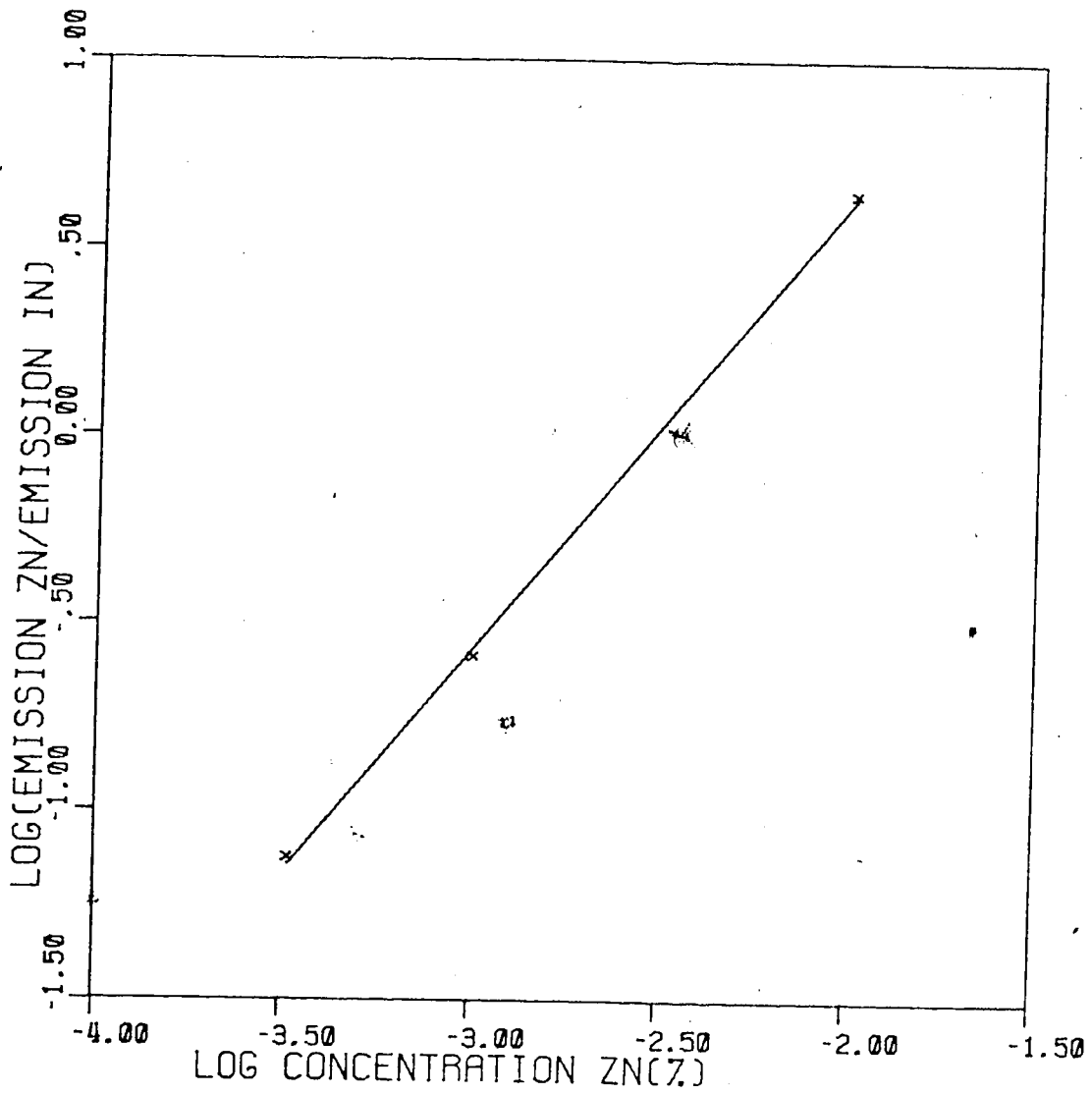


Figure 56. Log-log calibration plot for Spex G-Standards (Zn(I) - 213.856 nm)/(In(II) - 230.606 nm).

cases the slopes of the log-log plots indicate that a matrix effect is present. The slopes of the log-log plots of the ratio of Mn emission to that of In, the internal standard plots, are closer to 1 therefore these show the least matrix effect. The RSD values for the Cd(I) and Zn(I) emission lines vs. weight of sample or the internal standard In(II) emission are quite similar. This indicates that with these Spex G-Standards the major cause of analytical error was variations in the sample vaporization, and was not due sampling errors.

The linear range covered with these curves is only from 0.00033% (3.3 ppm) to 0.01% (100 ppm). The use of an OD 1 filter would have allowed extension to higher analyte concentration but this was felt to be unnecessary since this was only a preliminary test of the system. Extension of the analytical curve to a lower concentration was not found to be possible with this PDA based direct reading spectrometer system since the integration time was limited to about 0.4 seconds by the need to keep the In emission from saturating the array. At longer integration times the Cd(I) and Zn(I) emission could be detected but the saturation of the In(I) emission line meant that its emission could not be accurately recorded.

B. Analysis of NBS Standard Reference Materials

Several U.S. National Bureau of Standards-Standard Reference Materials (NBS-SRM) were used to test how well direct solids analysis of "real" materials could be performed with EA-ICAP-OES. These materials were four botanicals, two coal samples, and one coal fly ash sample representing a wide range of sample matrices.

The NBS-SRM's were prepared for analysis by grinding in a vibrating ball mill a mixture of 100 mg of the SRM and 100 mg of spectroscopic grade graphite containing 0.2% In. The spectroscopic grade graphite containing 0.2% In was prepared by grinding together 48.4 mg of finely powdered In_2O_3 and 10 g of the spectroscopic grade graphite powder. The grinding containers and balls were plastic to keep contamination of the sample as low as possible during this process and all materials were ground together for at least 10 minutes to ensure that mixing was as thorough as possible.

It must be noted at this point that the amount of In_2O_3 dispersed in the graphite is quite small and there exists a large chance for non-homogeneous distribution. The amount of SRM used is also quite small and sampling of the SRM may also be non-homogeneous. These problems are emphasized by the fact that only 2 to 3 mg of the mixture were vaporized during these experiments. As will be seen, the results indicate that there is indeed a problem with non-homogeneous

distribution.

Because of the complexity of the matrices, another problem was encountered in analyzing these "real" solid samples, that of spectral interference. The resolution available with the PDA based direct reading spectrometer places the lower limit on the resolution obtainable. In order to maximize the resolution the monochromator entrance slit was set to about 8 μm and all electronic filtering of the PDA signals was eliminated. Under these conditions a strong emission peak forms an image about 14 diodes FWHM which means that emission lines 0.67 nm apart could be baseline resolved.

Figure 57 is a plot showing the emission spectrum produced by 300 ng each of manganese and zinc. The samples were in the form of single element solutions and 3 μL each of their 100 ppm solutions were used with the EA-ICAP-OES system. The Mn(II) emission peaks are at 260.569 nm, 259.373 nm, and 257.610 nm and the Zn(I) and Zn(II) emission peaks are at 213.856 nm and 206.191 nm respectively. The 257.610 nm Mn(II) line and the 213.856 nm Zn(I) line were chosen for the analytical lines because they are strongest and had the least spectral interference from overlapping emission lines.

Figure 58 is the spectrum for 2000 ng of Fe while Figure 59 is for 10,000 ng of Si. These materials are present in

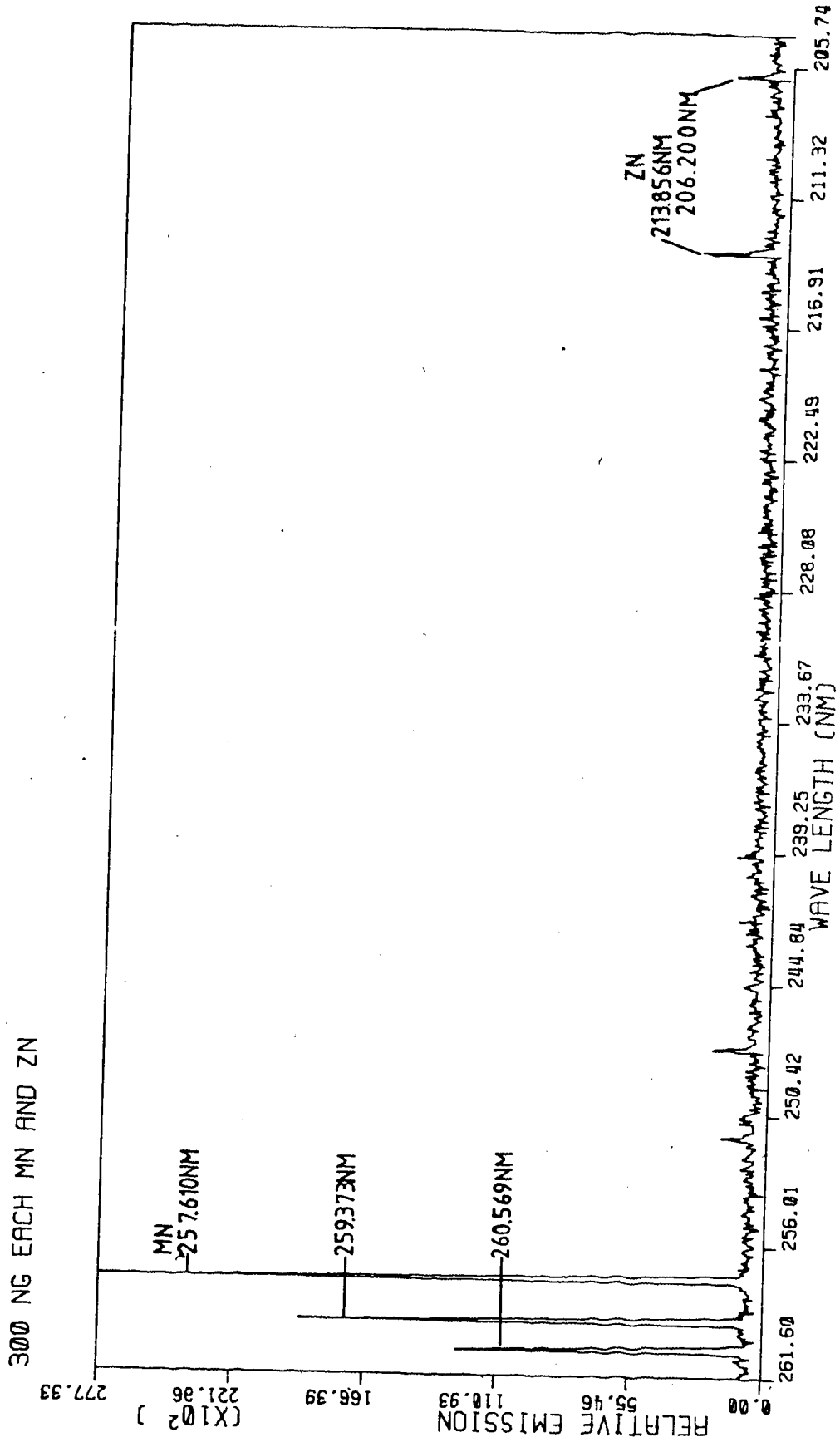


Figure 57. Spectrum from 300 ng each of Mn and Zn.

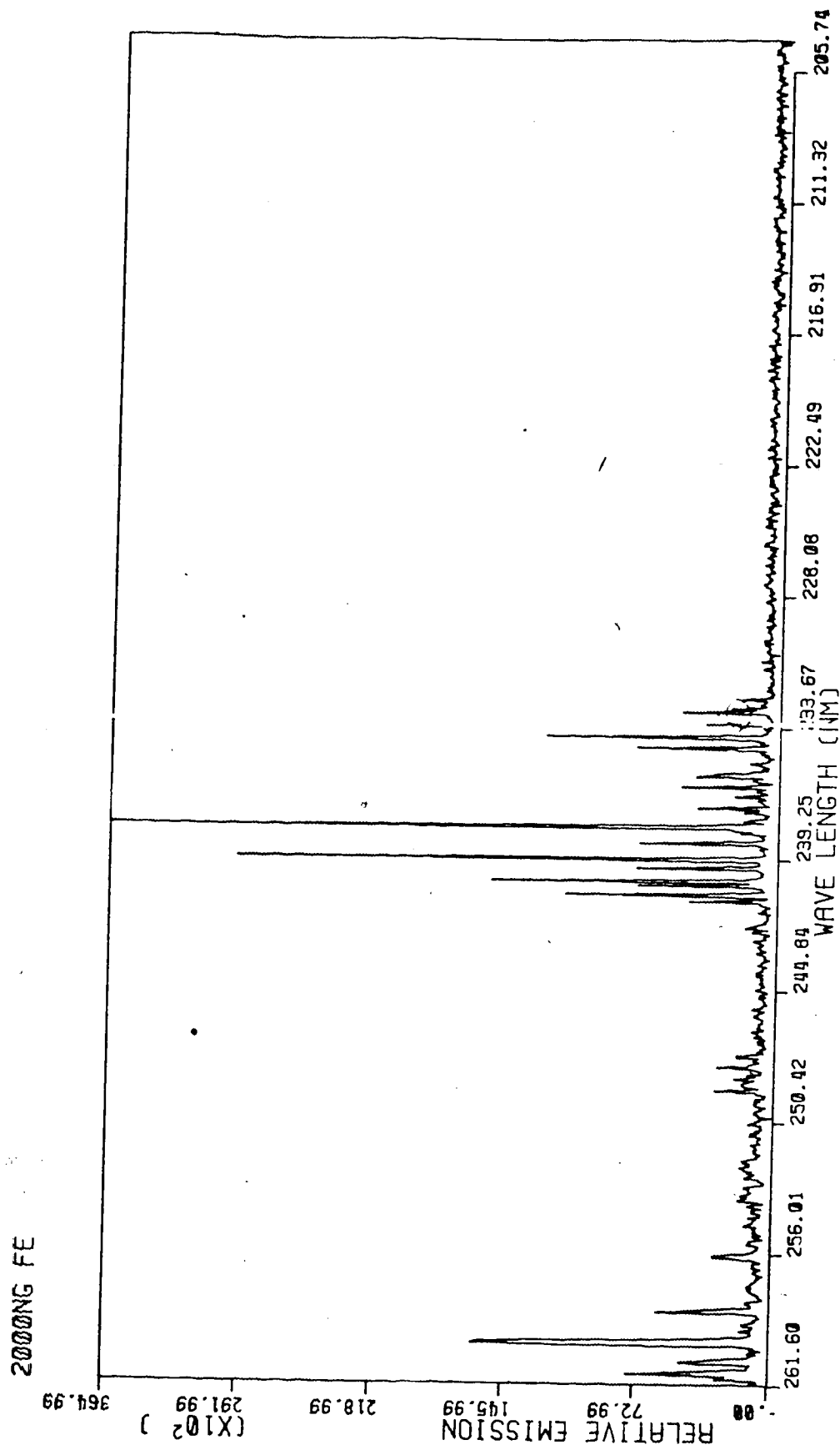


Figure 58. Spectrum from 2000 ng of Fe.

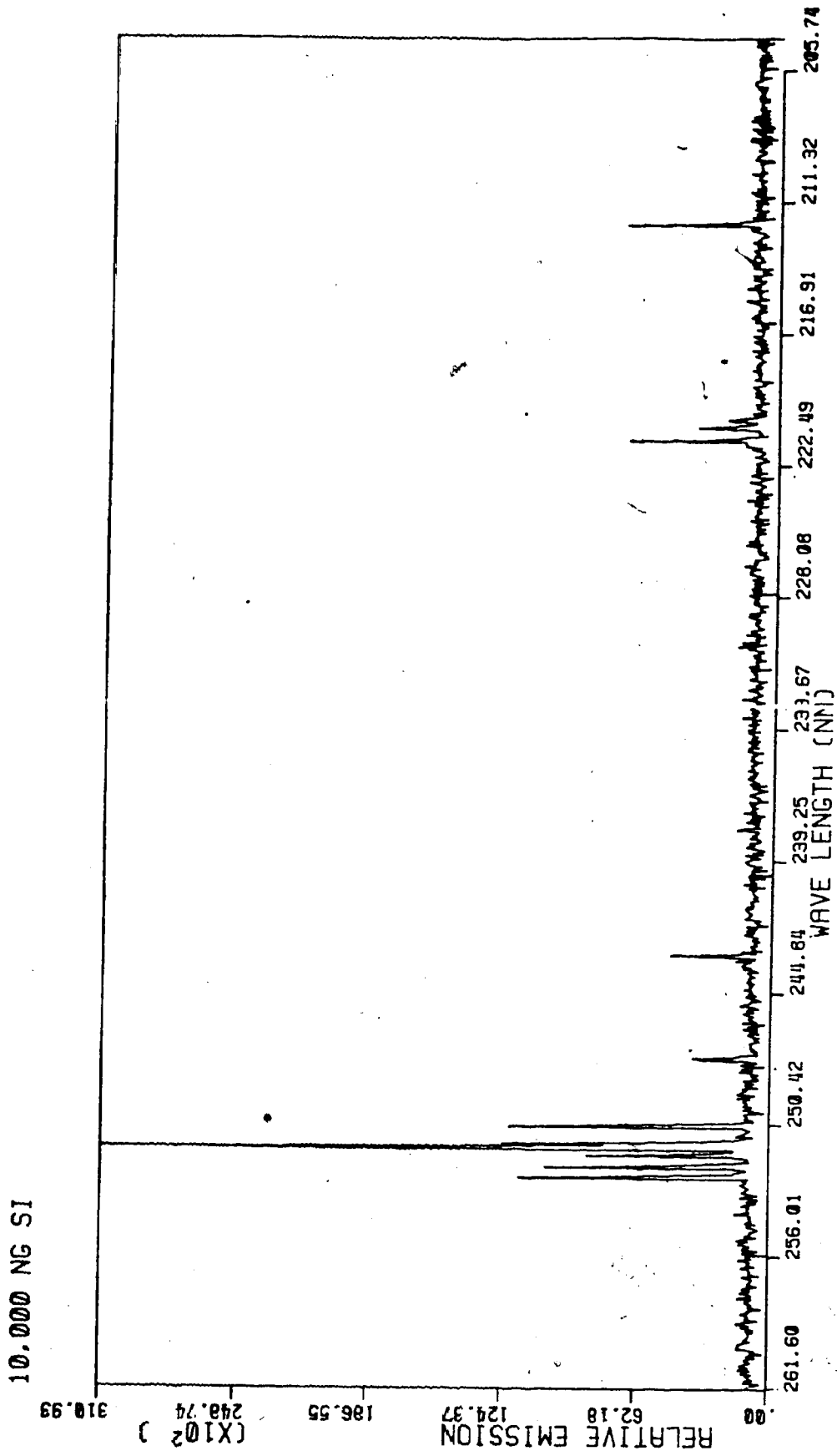


Figure 59. Spectrum from 10,000 ng of Si.

very high concentration in several of the NBS-SRM's. An example of spectral overlap interference can be seen in the Fe spectrum where several small lines overlap the 260.569 nm and 259.373 nm Mn(II) emission lines.

Figures 60 through 66 are the spectra recorded for the seven NBS-SRM's used. The plots have been scaled to keep the Mn(II), In(I), and Zn(I) emission lines on scale. With the exception of the Pine Needle spectrum the spectra are quite complex and it is easy to see why spectral interferences are common and why the choice of an analytical line can be very important.

The sample vaporization time was 3 seconds but to insure that all sample emission was recorded the PDA was clocked at 15 KHz and 75 scans of 0.137 seconds each were time-averaged together for a total integration time of 10.24 seconds. Plasma background and PDA fixed pattern clocking noise were also integrated and subtracted from the emission signals. Emission values were obtained by summing up the values recorded at the 5 diodes representing the peak of the emission line and subtracting the sum of 5 diodes reading background near the emission peak. The Mn(II) emission line at 257.610 nm appears to be clear of spectral interference however the Zn(I) line at 213.856 nm and the Zn(II) line at 206.191 nm both show spectral interference.

Table XXI lists the Mn and Zn concentrations in the

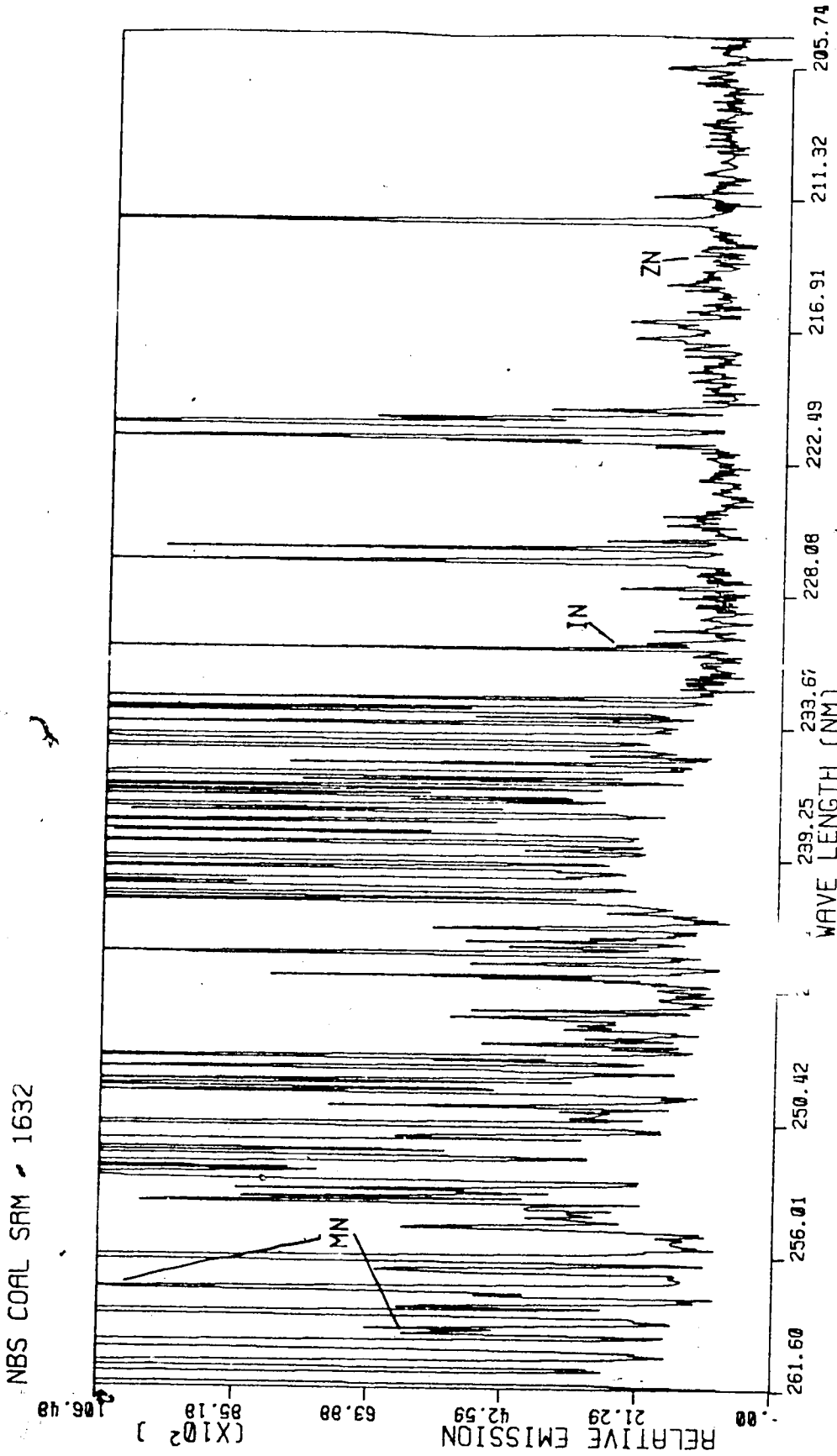


Figure 60. Spectrum from 2.6 mg of 50:50 mixture of NBS-SRM Coal #1632 and graphite (0.28 In).

NBS COAL SRM - 1635

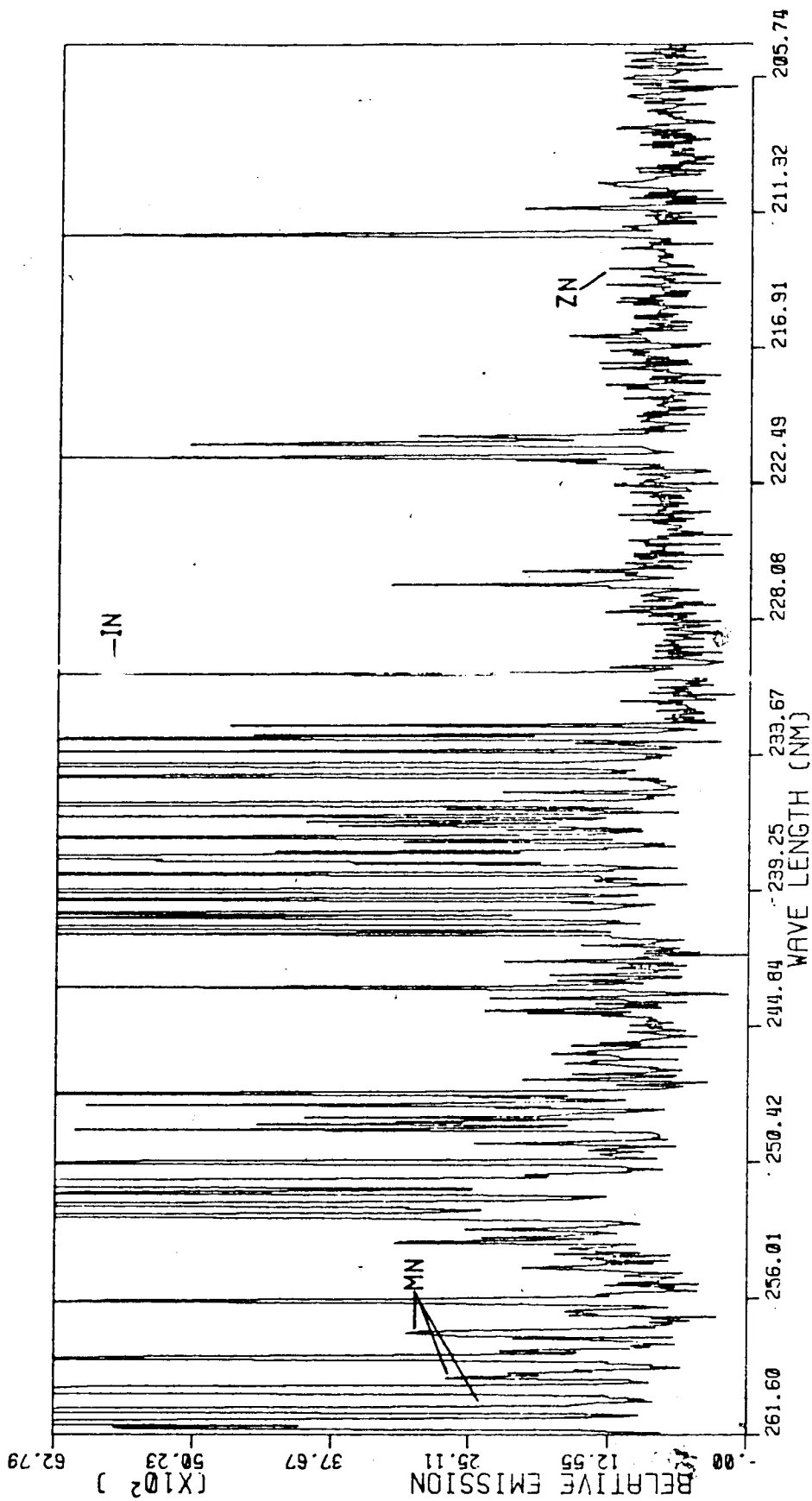


Figure 61. Spectrum from 2.6 mg of 50:50 mixture of NBS-SRM Coal #1635 and graphite (0.28 In).

Figure 62. Spectrum from 2.5 mg of 50:50 mixture of NBS-SRM Coal Fly Ash #1633 and graphite (0.2% In).

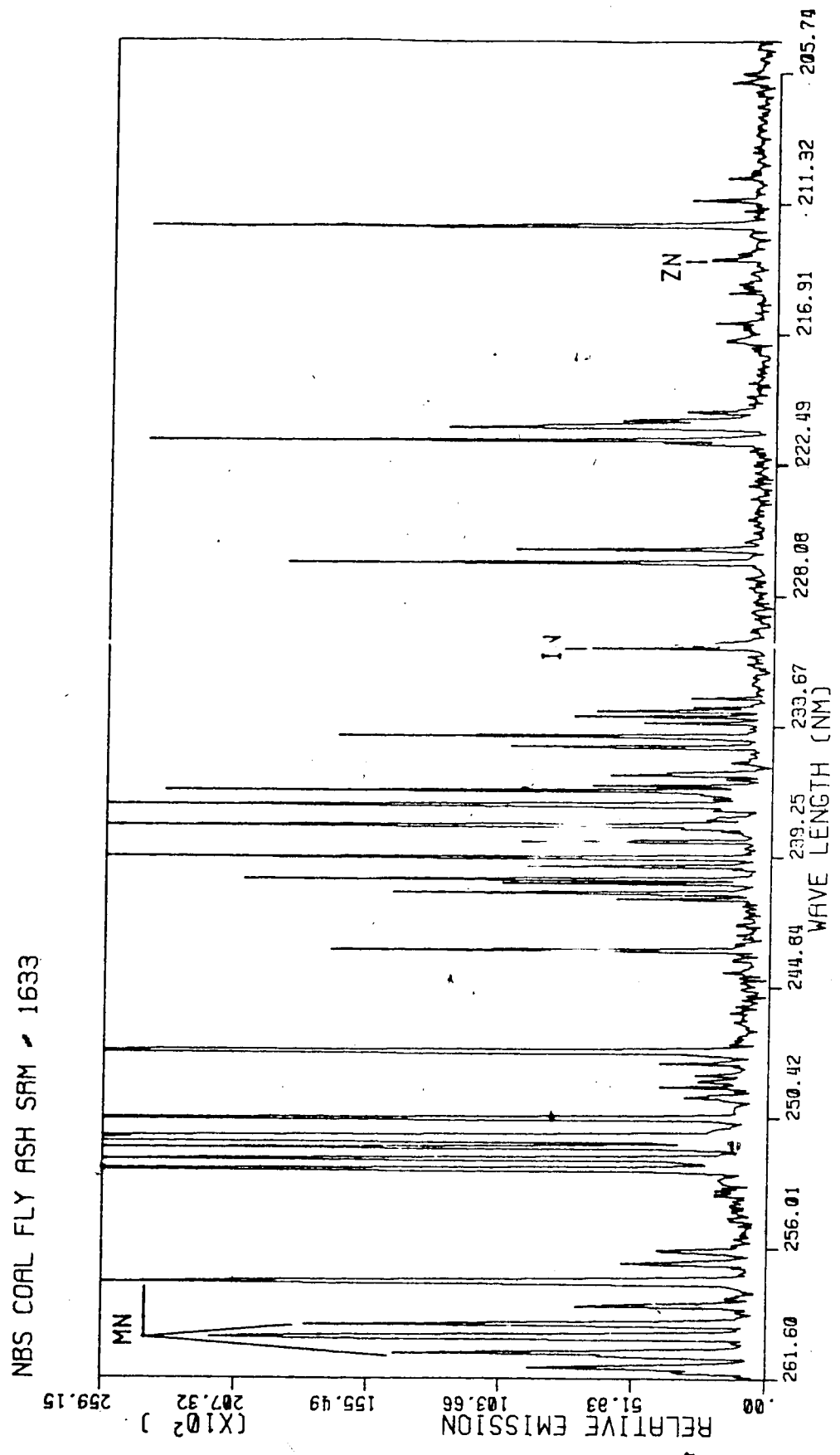


Figure 63. Spectrum from 2.8 mg of 50:50 mixture of NBS-SRM Spinach #1570 and graphite (0.2% In).

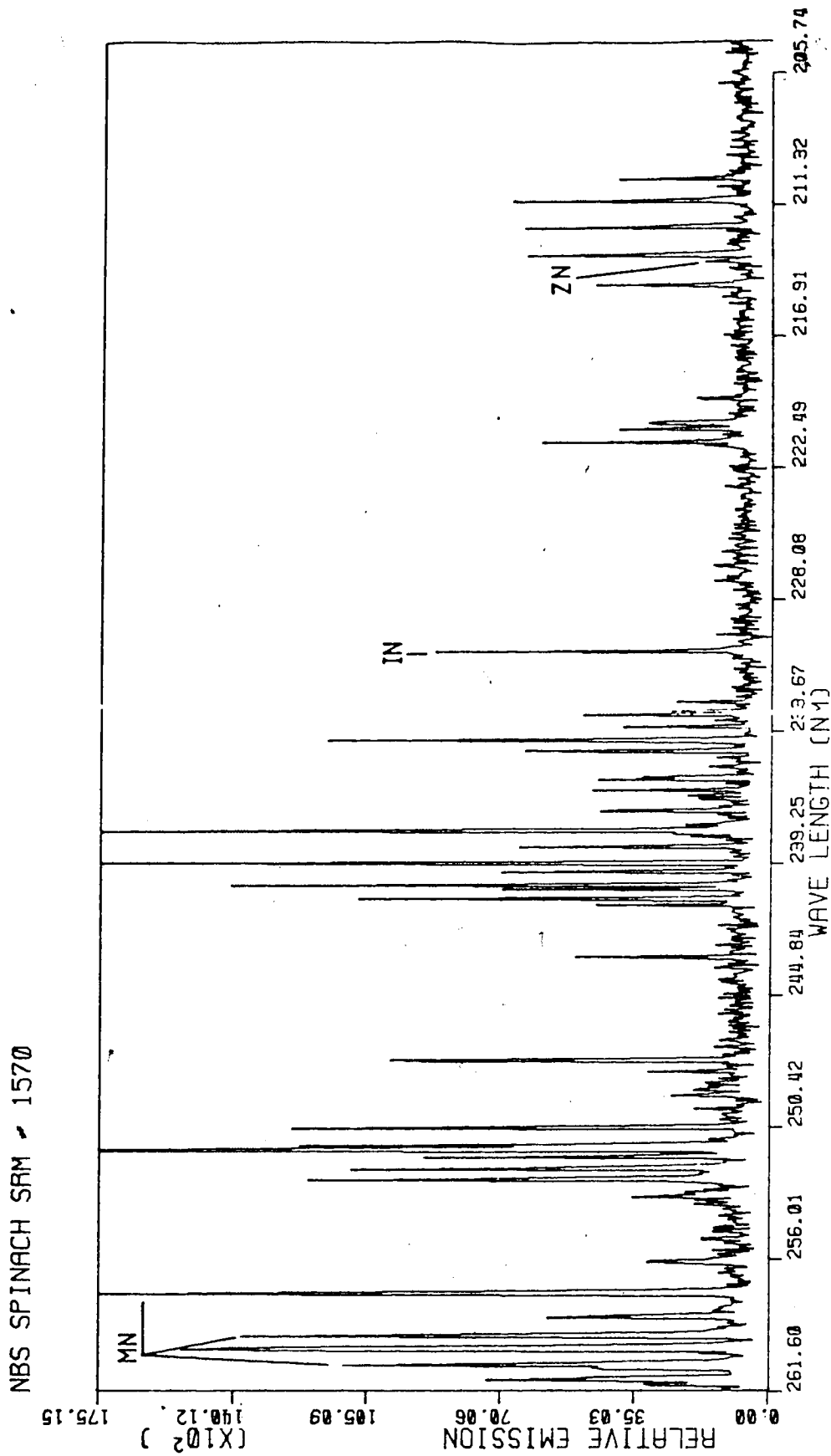


Figure 64. Spectrum from 2.1 mg of 50:50 mixture of NBS-SRM Orchard Leaves #1571 and graphite (0.2% In).

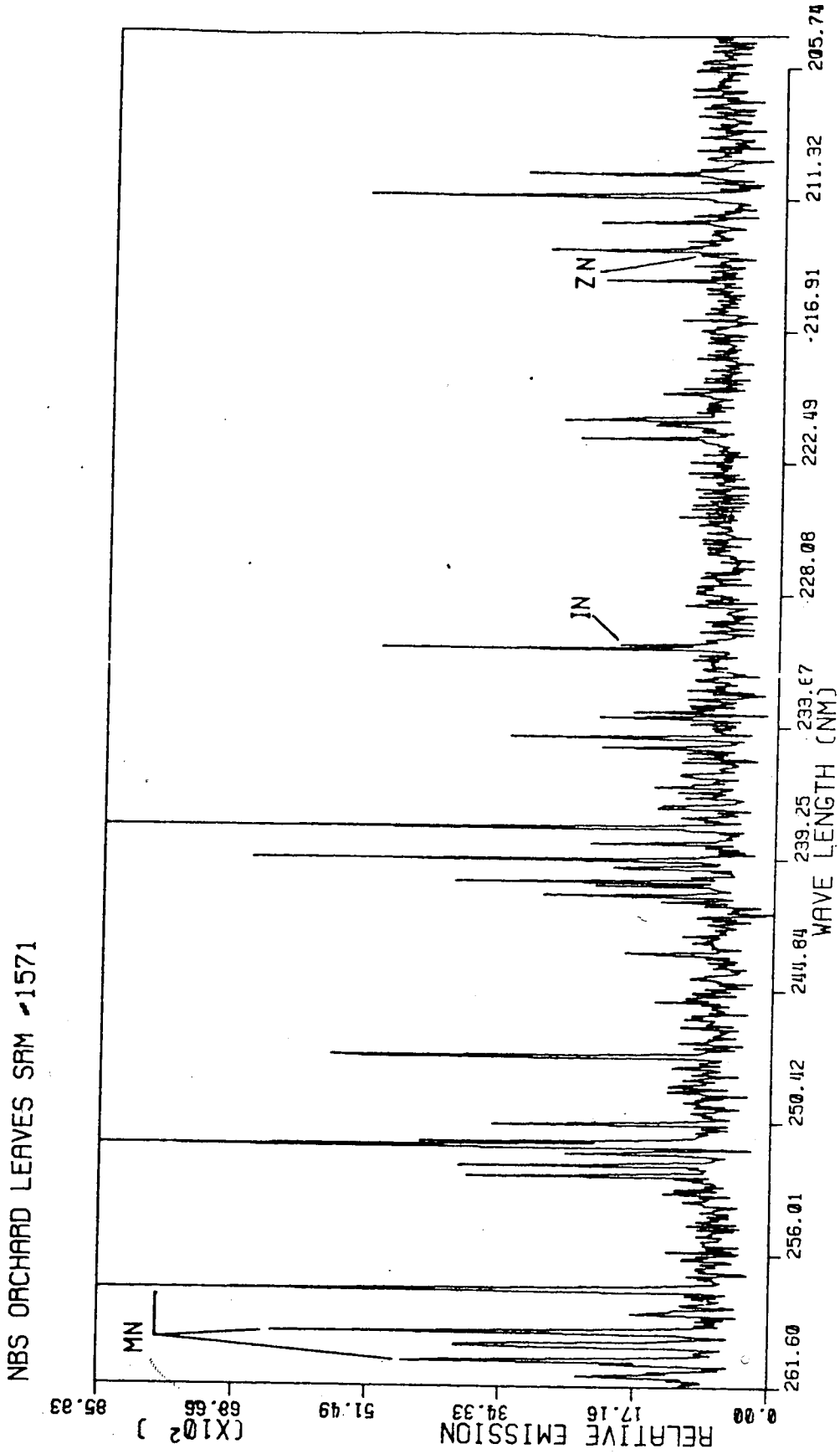


Figure 65. Spectrum from 2.3 mg of 50:50 mixture of NBS-SRM Tomato Leaves #1573 and graphite (0.2% In).

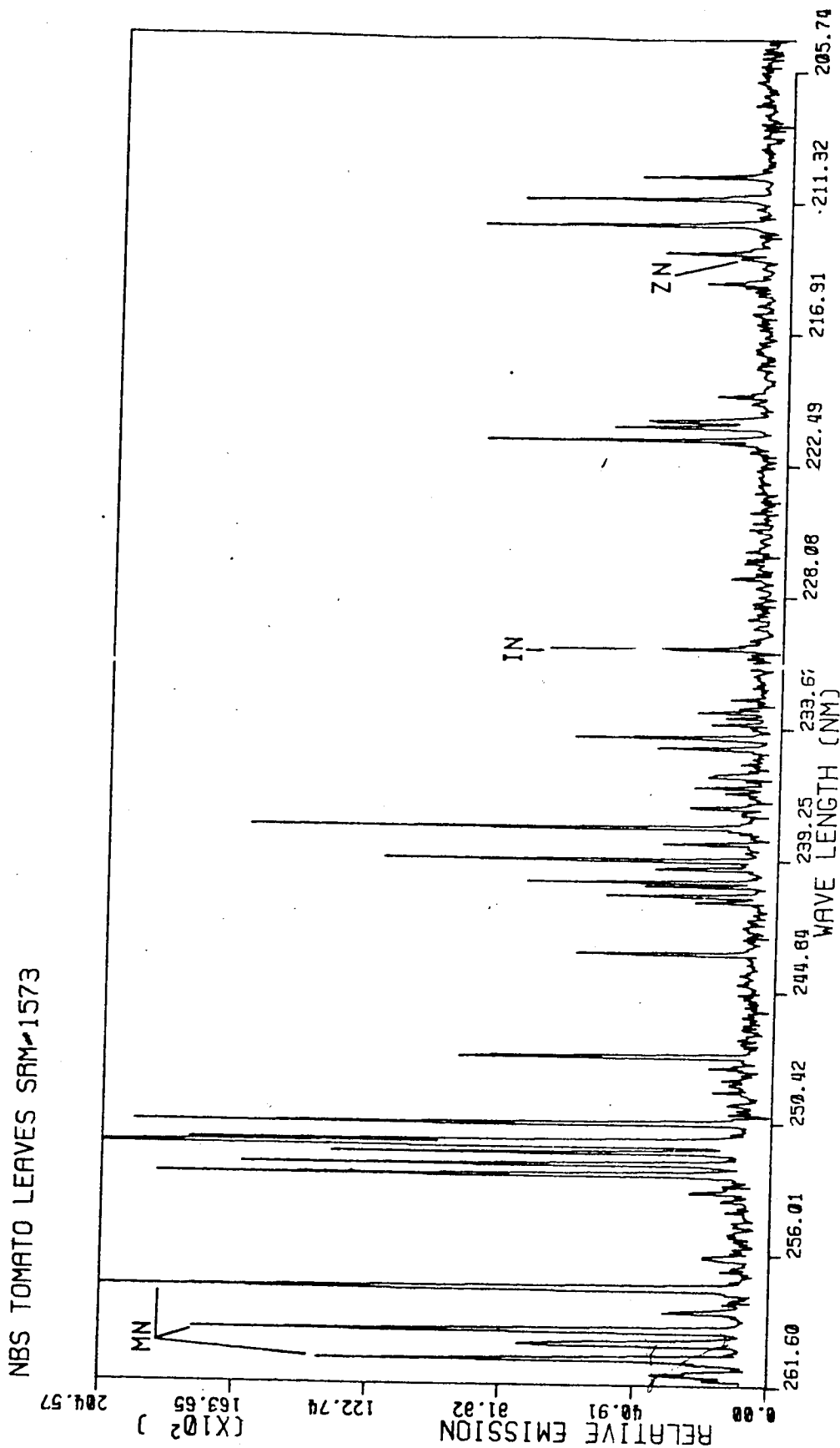


Figure 66. Spectrum from 2.4 mg of 50:50 mixture of NBS-SRM Pine Needles #1575 and graphite (0.2% In).

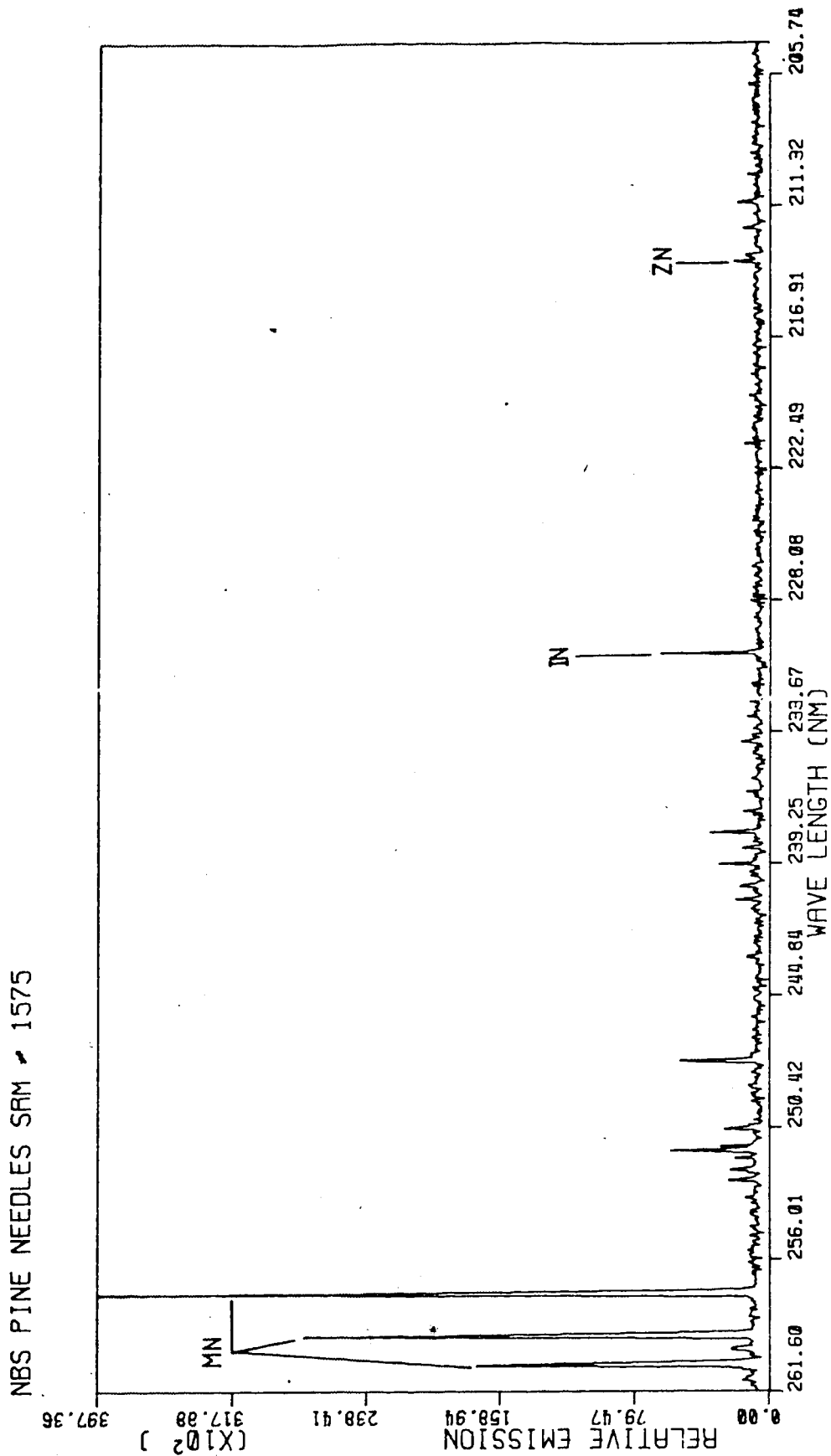


Table XXI
 Concentrations of Mn and Zn in NBS-SRM

<u>Material</u>	<u>SRM #</u>	<u>Concentration Mn</u>	<u>Concentration Zn</u>
Coal	1632	40 ± 3	37 ± 4 ppm
Coal	1635	21.4±1.5	4.7±0.5 ppm
Coal Fly Ash	1633	493 ± 7	210 ± 20 ppm
Spinach	1570	165 ± 6	50 ± 2 ppm
Orchard Leaves	1571	91 ± 4	25 ± 3 ppm
Tomato Leaves	1573	238 ± 7	62 ± 6 ppm
Pine Needles	1575	675 ± 15	--

SRM's used and the analytical results are given in Table XXII and Table XXIII for Mn(II) emission at 257.610 nm and Zn(I) emission at 213.856 nm. The Zn(II) emission line at 206.191 nm is too weak to be recorded under these operating conditions.

Log-log calibration curves are shown in Figures 67 through 70 for the Mn(II) and Zn(I) emission lines. The plots are for the ratio of analyte emission to weight of sample and for the ratio of analyte emission to internal standard emission. In these cases the slopes of the log-log plots show that matrix effects are present, however neither type of plot is clearly preferable. The RSD values of the emission vs sample weight or internal standard emission are also similar, with neither being clearly better. These results indicate that the major problem in these analyses was sampling error, which may be impossible to overcome.

Table XXII

Calibration Data for Mn(II) - 257.610 nm Emission in NBS-SRM's

SRM #	Mn (ppm)	$\bar{I}_{E_t dt(Mn)}/\text{Spl. wt.}$	RSD %	$\bar{I}_{E_t dt(Mn)}/\bar{I}_{E_t dt(In)}$	RSD %
1635	21.4	2,459.2	15.6	0.761	23.0
1632	40.0	9,490.8	17.4	2.773	23.9
1571	91.0	8,515.9	35.6	2.209	30.0
1570	165.0	15,998.2	34.9	3.278	38.0
1573	238.0	15,649.9	27.3	4.823	23.9
1633	493.0	25,364.6	34.5	6.41	30.0
1575	675.0	50,962.0	19.4	12.149	38.0

$\bar{I}_{E_t dt(Mn)}/\text{Spl. wt.}:$

Slope = 0.7

R = 0.9

$\bar{I}_{E_t dt(Mn)}/\bar{I}_{E_t dt(In)}:$

Slope = 0.7

R = 0.9

Table XXIII

Calibration Data for Zn(I) - 213.856 nm Emission in NBS-SRM's

SRM #	Zn (ppm)	$\bar{I}_{E_t dt(Zn)} / \text{Sp1.Wt.}$	RSD %	$\bar{I}_{E_t dt(Zn)} / \bar{I}_{E_t dt(In)}$	RSD %
1635	4.7	322.0	50.6	0.098	53.0
1571	25.0	396.0	21.7	0.077	57.0
1632	37.0	421.3	59.2	0.105	83.0
1570	50.0	825.2	52.3	0.167	42.2
1573	62.0	1,247.6	17.8	0.392	22.7
1633	210.0	2,017.8	11.7	0.626	22.5

 $\bar{I}_{E_t dt(Zn)} / \text{Sp1.Wt.} :$

Slope = 0.5

R = 0.9

 $\bar{I}_{E_t dt(Zn)} / \bar{I}_{E_t dt(In)} :$

Slope = 0.5

R = 0.8

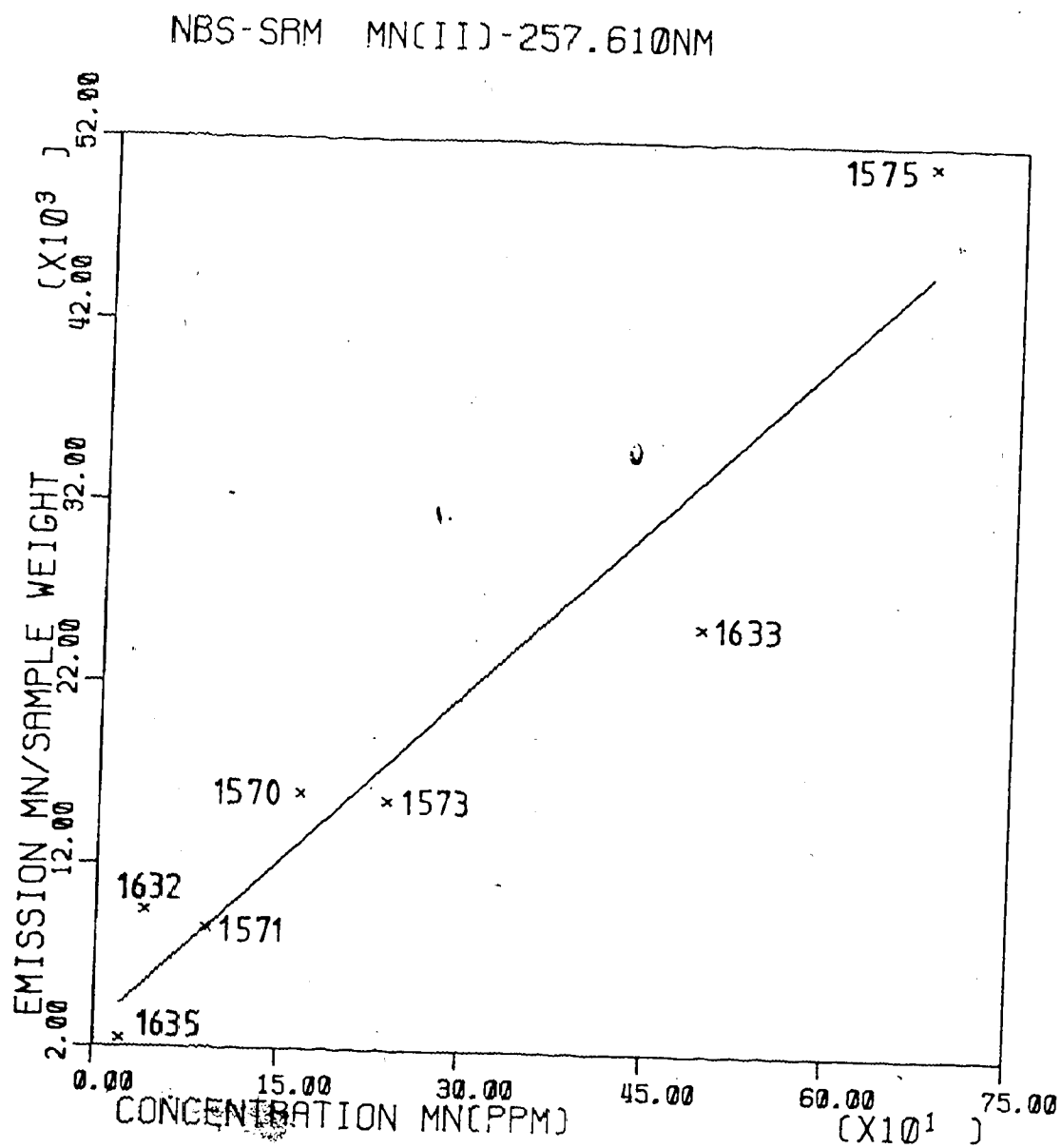


Figure 67. Calibration plot - Mn(II) emission/sample weight vs concentration of Mn in NBS-SRM.

NBS-SRM MN(II)-257.610NM

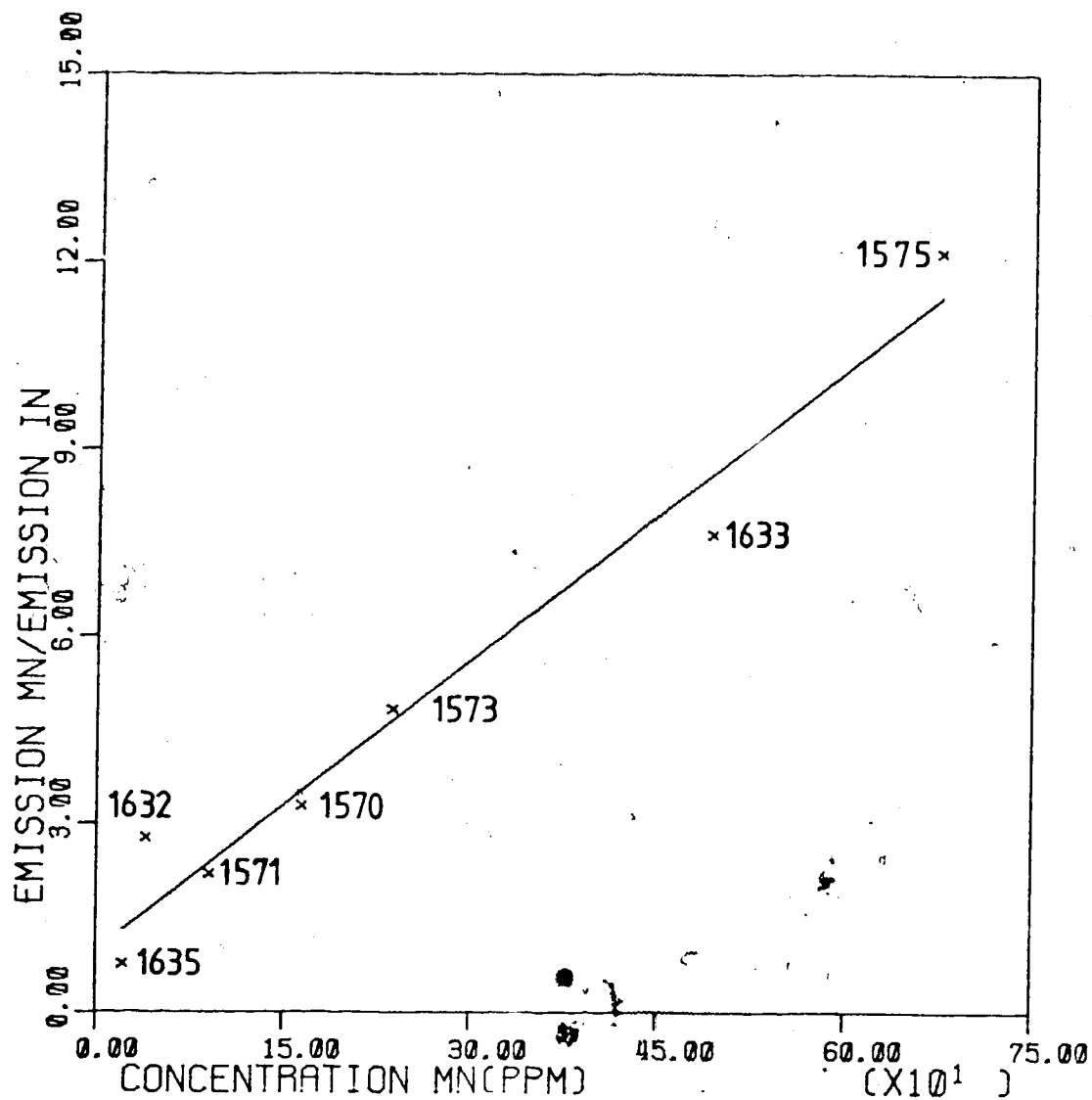


Figure 68. Calibration plot - Mn(II) emission/In(I) emission vs concentration of Mn in NBS-SRM.

NBS-SRM ZN(I)-213.856NM

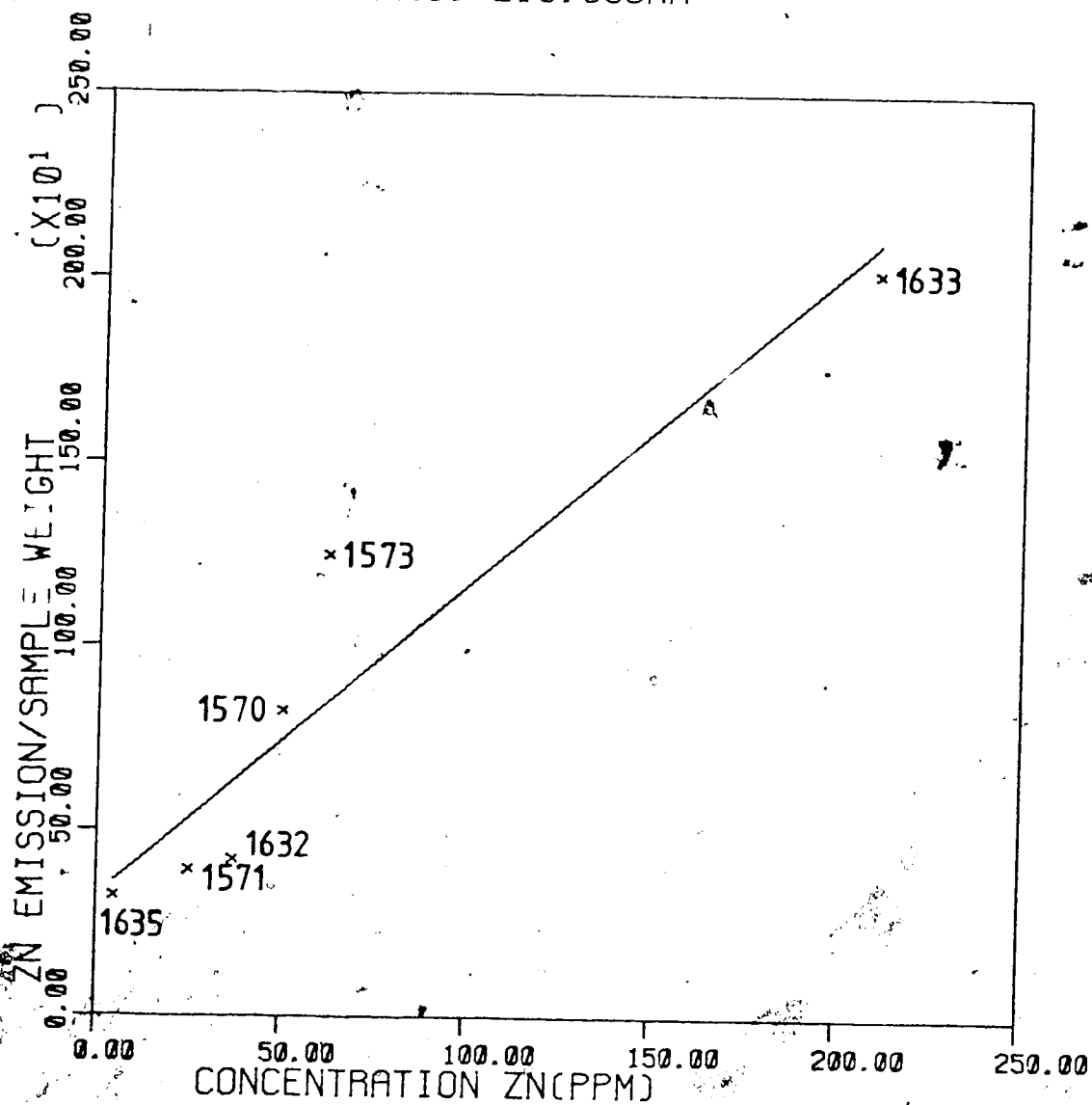


Figure 69. Calibration plot - Zn(I) emission/sample weight vs concentration of Zn in NBS-SRM.

NBS-SRM Zn(I)-213.856NM

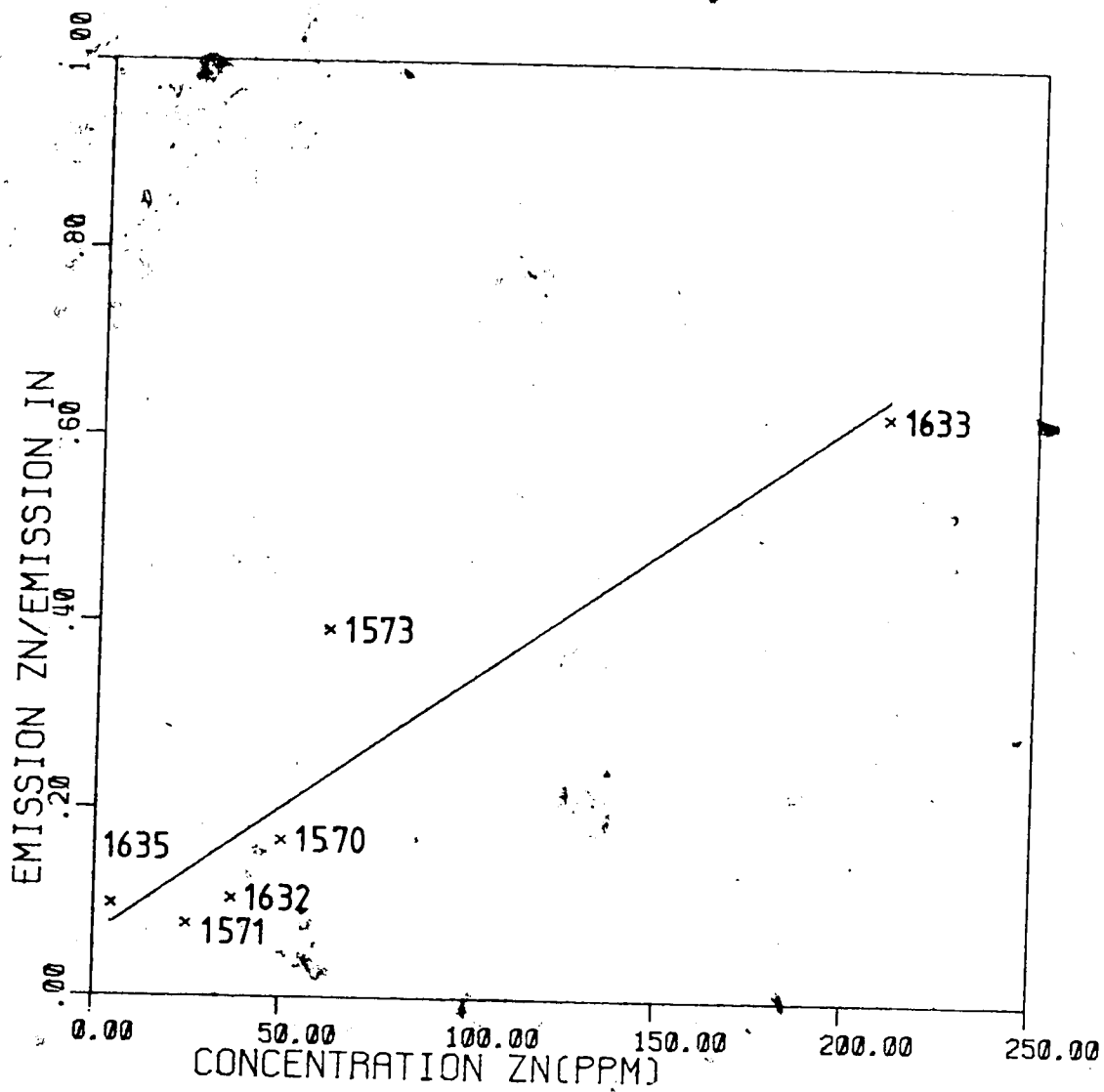


Figure 70. Calibration plot - Zn(I) emission/In(I) emission vs concentration of Zn in NBS-SRM.

The inductively coupled argon plasma was first introduced commercially as a source for optical emission spectroscopy in 1974 and its use has been growing rapidly ever since. The dominant sample introduction technique for plasma emission spectroscopy has been the nebulizer, requiring that samples be in solution and that several mL of solution be available. In our laboratory sample introduction techniques to allow the analysis of small volume (μL) samples in solution and the direct analysis of solid samples by ICAP-OES have been under investigation. In this work, the analytical aspects of the use of a graphite cup electrothermal atomizer in combination with the inductively coupled argon plasma for the analysis of small volume samples in solution and the direct analysis of solids has been studied.

The graphite cup electrothermal atomization device used for this work was constructed from a Varian Model 63 Carbon Rod Atomizer used for atomic absorption spectroscopy. The graphite carbon cup used was enclosed in a small quartz cell. Argon gas flowed through the cell to carry the vaporized sample material into the plasma.

Preliminary investigations of the temporal behavior and analytical capabilities of the EA-ICAP-OES technique were carried out with single element solutions and a single

channel monochromator-PMT detector system coupled to a computer-based data acquisition system. The plasma emission background was found to vary during the atomization, probably due to pressure/flow changes caused by the heating of the argon inside the vaporization cell. The background emission profile was found to vary in detail from atomization to atomization, possibly due to small changes in the heating during atomization, but the integrated emission during the atomization was fairly constant.

Temporal studies of analyte emission during atomization showed the emission profile to be peak shaped with a rise time of about 0.1 second and a fall time of 1 to 3 seconds. The emission rise and fall times were found to increase as sample weight increased. Emission peak height measurements had greater relative standard deviations (RSD) than background subtracted peak area measurements therefore peak areas were used for analytical measurements. The analytical results show that a linear dynamic range of three to four orders of magnitude are possible with a RSD of 5 to 10% at about 100 times the detection limit.

The analysis of lead is widely performed by carbon furnace AAS but suffers from severe matrix interference affects. A study of this effect of a NaCl matrix on EA-ICAP-OES analysis of Pb showed that even at a NaCl concentration greater than in sea water only a small change in

emission peak area was found. This peak area change was mainly due to a change in the plasma background emission and compensation was possible by using a blank of similar NaCl concentration. A study of the vertical emission profile of Pb showed that the emission maximum shifted lower in the plasma with a high NaCl concentration. This finding meant that the choice of slit height and position was very important.

The study of direct solids analysis was carried out with the use of Spex G-standards and National Bureau of Standards-Standard Reference Materials. The use of a computer coupled photodiode array direct reading spectrometer allowed multichannel analysis so that the internal standard analysis technique and background subtraction were possible. Four botanical materials, two coal samples, and a sample of coal fly ash were used to provide a variety of sample matrices. These SRM's were mixed 50:50 with graphite containing indium as an internal standard and a sample size of about 3 mg was used. The results show that while there are matrix effects it was possible to construct reasonable calibration curves for Cd and Zn in the Spex G-Standards and for Mn and Zn in the NBS-SRM's.

Future work can be envisioned in all areas investigated in this experimental work. A recent article by Price, Dymott, and Whiteside (61) on the use of graphite cups for

introducing solid samples into a graphite furnace for AAS shows one possible method for improving the atomization step. Ramp atomization was rejected for this work because it did not provide a long enough heating time for complete vaporization, but the background emission changes were much less than with step atomization. Modification of the power supply so that ramp heating to a plateau several seconds long and feedback control of the heating are certain to improve the technique.

The use of a computer based system was found to be excellent for the temporal studies but the systems limited dynamic range required the use of variable signal amplification which resulted in varying background levels, thus complicating the analytical work. The use of a data acquisition system with significantly larger dynamic range so that the variable amplifier could be eliminated should have a high priority. An excellent candidate would be the use of an integrating digital voltameter system similar to the Laboratory Data Acquisition System (52) developed by M. Blades of our laboratory.

The present work has shown that combining a carbon furnace for sample atomization with ICAP-OES analysis shows good potential, but it has also shown that much work still needs to be done.

BIBLIOGRAPHY

1. W.K. Yuen, Dissertation 1978, University of Alberta, Edmonton, Alberta.
2. S. Greenfield, J.L. Jones, C.T. Berry, Analyst, 89, 713-720 (1964).
3. R.H. Wendt, V.A. Fassel, Anal. Chem., 37, 920-922 (1965).
4. V.A. Fassel, R.N. Kniseley, Anal. Chem., 46, 1110A-1115A (1974).
5. P.W.J.M. Boumans, Optica Pura Y Aplicada., 11, 143-171 (1978).
6. T.B. Reed, J. Appl. Phys., 32, 2534-2535 (1961).
7. H.C. Hoare, R.A. Moystyn, Anal. Chem., 39, 1153-1155 (1967).
8. G.W. Dickinson, Dissertation 1969, Iowa State University, Ames, Iowa.
9. R.M. Dagnall, D.J. Smith, T.S. West, Anal. Chim. Acta, 54, 397-406 (1971).
10. D. Chapman, W.A. Gordon, 1st FACSS, Atlantic City Program, p. 22 (abstract).
11. R.L. Dahlquist, ICP Information Newsletter, 1, 148-153 (1975).
12. V.A. Fassel, G.W. Dickinson, Anal. Chem., 40, 247-249 (1968).
13. R.L. Dahlquist, J.W. Knoll, R.E. Hoyt, Pittsburgh Conference, Cleveland, Ohio, 1975, paper No. 341 (abstract).

14. H.G.C. Human, R.H. Scott, A.R. Oakes, C.D. West,
Analyst, 101, 265-271 (1976).
15. J. Norris, R.L. Watters, Jr., FACSS V, Boston Program,
1978.
16. F. Brech, Trace Metals Symposium, St. Louis, Mo.,
1979; abstract reprinted ICP Information Newsletter, 4,
559 (1979).
17. J.S. Beaty, R.L. Crawford, C.C. Wohlers, Pittsburgh
Conference, Cleveland, Ohio, 1979, paper No. 112 (ab-
stract).
18. F.N. Abercrombie, Pittsburgh Conference, Cleveland,
Ohio, 1977, paper No. 406 (abstract).
19. E.D. Salin, J. Carr, G. Horlick, Pittsburgh Conference,
Cleveland, Ohio, 1979, paper No. 563 (abstract).
20. J. Carr, G. Horlick, Pittsburgh Conference, Atlantic
City, N.J., 1980, paper No. 56 (abstract).
21. J. Carr, Dissertation 1980, University of Alberta,
Edmonton, Alberta.
22. C.B. Baddiel, N.A. Skerten, Pittsburgh Conference,
Cleveland, Ohio, 1979, paper No. 716 (abstract).
23. S. Greenfield, P.B. Smith, Anal. Chim. Acta, 59,
341-348 (1972).
24. R.N. Kniseley, V.A. Fassel, C.C. Butler, Clin. Chem.,
19, 807-812 (1978).
25. D.E. Nixon, V.A. Fassel, R.N. Kniseley, Anal. Chem.,
47, 210-213 (1974).

26. A.M. Gunn, D.L. Millard, G.F. Kirkbright, Analyst, 103 1006-1073 (1978).
27. G.F. Kirkbright, R.D. Snook, Anal. Chem., 51, 1938-1941 (1979).
28. D.L. Millard, H.C. Shan, G.F. Kirkbright, Analyst, 502-508 (1980).
29. E.D. Salin, G. Horlick, Pittsburgh Conference, Cleveland, Ohio, 1979, paper No. 564 (abstract).
30. E.D. Salin, G. Horlick, Anal. Chem., 51, 2284-2286 (1979).
31. Varian-Tectron Model 63-Carbon Rod Atomizer Instruction Manual, Varian, Tectron 1975.
32. F.A. Cotton, G. Wilkinson, F.R.S., "Advanced Inorganic Chemistry", Third Edition, 1972, p. 288.
33. R.E. Sturgen, C.L. Chakrabarti, Prog., Analyt. Atom. Spectrosc., 1, 5-199 (1978).
34. Pyro-Tech PT-101, Ultra Carbon Corp., Technical Bulletin, Ultra Carbon Corp., Bay City, Michigan, 1970, p. 2.
35. J.H. Runnek, R. Merryfield, H.B. Fisher, Anal. Chem., 47, 1258-1263 (1975).
36. V.A. Zatka, Anal. Chem., 50, 538-541 (1978).
37. Heath Monochromator Manual, EU-700 Series, Instrumentation for Spectroscopy, 1967, Heath Co., Benton Harbor, Michigan.
38. M. Margoshes, Spectrochim. Acta, 25B, 113-122 (1970).

39. K.W. Johnson, Spectrosc. Lett., 6, 315-321 (1973).
40. G. Horlick, E.G. Coddington, Anal. Chem., 45, 1490-1494 (1973).
41. G. Horlick, E.G. Coddington, Anal. Chem., 45, 1749-1750 (1973).
42. G. Horlick, E.G. Coddington, Appl. Spectrosc., 27, 366-370 (1973).
43. E.G. Coddington, G. Horlick, Spectrosc. Lett., 7, 33-41 (1974).
44. G. Horlick, E.G. Coddington, S.T. Leung, Appl. Spec., 29, 48-52 (1975).
45. LPS11-S Laboratory Peripheral System Users Guide, DEC Manual #DEC-11-HLPGA-C-D.
46. LPS11-S Laboratory Peripheral System Maintenance Manual, DEC Manual #DEC-11-HLPMA-B-D.
47. Incremental Plotter 100/1200 Series Instruction Manual, Zeta Research, Lafayette, California.
48. G. Horlick, Appl. Spec., 30, 113-123 (1976).
49. G. Horlick, E. Coddington, "Contemporary Topics in Analytical and Clinical Chemistry", Vol. 1, 1977, pp. 195-247.
50. J.E. Edmonds, G. Horlick, Appl. Spec., 31, 536-541 (1977).
51. G. Horlick, M.W. Blades, Appl. Spec., 34, 229-233 (1980).
52. M. Blades, G. Horlick, Talanta, submitted for publication, 1980.
53. W. Frech, A. Adergren, Anal. Chimica Acta, 88, 57-67 (1977).

54. E.J. Czobik, J.P. Matousek, Anal. Chem., 50, 2-9 (1978).
55. D.C. Manning, W. Slavin, Anal. Chem., 50, 1234-1238 (1978).
56. D.C. Manning, W. Slavin, A.A. Newsletter, 17, 43-46 (1978).
57. A. Andersson, A.A. Newsletter, 15, 71-72 (1976).
58. K.C. Thompson, K. Wagstaff, K.C. Wheatstone, Analyst, 310-313 (1977).
59. L.R. Hageman, J.A. Nichols, P. Viswanadham, R. Woodriff, Anal. Chem., 51, 1406-1412 (1979).
60. F.J. Langmyhr, Analyst, 104, 993-1016 (1979).
61. W.J. Price, T.C. Dymott, P.J. Whiteside, Spectrochim. Acta, 35B, 3-10 (1980).

APPENDIX A

Software Developed for the Monochromator-Photomultiplier Readout System

A. Introduction

The software programs developed to interface the photomultiplier detector system with the minicomputer and to allow manipulation, readout, and storage of this data are described in this section. Programming was done in Fortran 01C and Macro 01C languages under the RT11 02C operating system on a DEC PDP 11/10 16 bit minicomputer.

The programming philosophy in this program, and in the following ones, was to break each task into a separate module and to then select the desired task module from a menu. This type of programming has proven to be very efficient since modules can be easily used in several different programs with only small modifications if necessary.

Since Fortran programs are fairly easy to understand only descriptive headings are given at the start of each module. The data acquisition subroutines are written in Macro assembly language which is more difficult to understand therefore each line of the program is fully described. Refer to the appropriate DEC manuals for further information.

B. ADCPMT - Main Program for Monochromator Photomultiplier Readout System

1. Purpose: This program provides an interface between the system user and the data acquisition subroutine and provides the means for obtaining readout or storing data on the disk under user defined names.
2. Operation: This program consists of 9 task modules which are menu selectable. This program is entered via menu selection #4, RESTART(START), where the operator enters the number of data points to be acquired, the data acquisition rate (master clock rate \div number of master clock pulses between samples), a delay after the start pulse until the start of data acquisition, and the sample name. The date and time are automatically read from the operating system. After these entries data acquisition takes place via subroutine GDPMT and then the menu is entered.

From the menu task modules are selected to allow:

1. PLOT: Plot data acquired on the VT-55 screen.
2. LIST: List data acquired on the VT-55 screen.
3. STASTICS: Perform statistical analysis of the data, i.e. calculate the mean value of a set of data, the standard deviation within that set, and calculate the signal to noise within that set.

4. RESTART: Restart data acquisition.
5. WRITE DISK: Write the data acquired on disk under a user selected name.
6. EXIT: Exit from the program.
7. TOTALS: Allows calculations of the totals for selected portions of the data thus providing a means of calculating the integrated signal intensity.
8. READ DISK: Allows a named data file to be read from disk.
9. SMOOTH: Allows a simplified least squares smoothing of the data based on the procedure of Savitzky and Golay.


```

WRITE(7,101)
101  FORMAT(' ', 'NORMALIZED PLOT? YES=1, NO=0')
    READ(5,59,END=120,ERR=100)XNORM
    IF(XNORM .EQ. 1.0)SCFAC=FLOAT(A(NP+7))
    IF(XNORM .EQ. 1.0)GO TO 102
    WRITE(7,103)
103  FORMAT(' ', 'ENTER SCALING FACTOR, F10.0')
    READ(5,59,END=120,ERR=100)SCFAC
102  CONTINUE
    CALL PLOT55(ESCCMD,HOME,0)
    CALL PLOT55(ESCCMD,ESCRN,0)
    CALL PLOT55(CURPOS,0,0)
    WRITE(7,170)TITLE,DAT,TIM,A(NP+1),A(NP+2)
    WRITE(7,56)(A(NP+I),I=3,7)
    D2=FLOAT(A(NP+5))
    DO 150 I=1,NP
    D1=FLOAT(A(I))
    D=((D1-D2)*100)/SCFAC
150  B(I)=IFIX(D)
    CALL PLOT55(STATUS,547,476)
    CALL PLOT55(SELGR,0,0)
    CALL PLOT55(CURPOS,0,0)
    CALL PLOT55(HGRD,1,0,0)
    IF(NPLOT .LE. 512)GO TO 151
    CALL PLOT55(STATUS,551,472)
    CALL PLOT55(SELGR,1,0)
    CALL PLOT55(HGRD,1,101)
151  IF(NP .GT. 512)NPLOT=512
    CALL PLOT55(SELGR,0,0)
    CALL PLOT55(ORIGIN,0,0)
    CALL PLOT55(N,-NPLOT,B)
    IF(NP .LE. 512)GO TO 153
    NPLOT=NP-512
    CALL PLOT55(SELGR,1,0)
    DO 156 I=1,NPLOT
156  C(I)=C(I)+101
    CALL PLOT55(N,-NPLOT,C)
153  CALL PLOT55(DISPLY,0,BELL)
    READ(5,58,END=120,ERR=120)NSTOP
120  CALL PLOT55(ESCCMD,HOME,0)
    CALL PLOT55(ESCCMD,ESCRN,0)
    CALL PLOT55(STATUS,0,1023)
    GO TO 6
C
C
C
    THIS SECTION LISTS THE DATA ON THE VT-55 COPIER.
200  CALL PLOT55(ESCCMD,HOME,0)
    CALL PLOT55(ESCCMD,ESCRN,0)
    CALL PLOT55(DISPLY,0,BELL)
170  WRITE(7,170)TITLE,DAT,TIM,A(NP+1),A(NP+2)
    FORMAT(' ',3A4,3X,3A4,' ',3A4,3X,' NP=',I6,3X,' SPL. FREQ.=',I6,/)
    DO 250 I=1,NP+7,200
    DO 251 J=I,I+190,10
    WRITE(7,63)J,(A(K),K=J,J+9)
63  FORMAT(' ',I4,2X,'>',10(I5,1X))
    IF(K .GT. (NP+7))GO TO 252
251  CONTINUE
    READ(5,58,ERR=120,END=120)NSTOP
253  CALL PLOT55(ESCCMD,HOME,0)
    CALL PLOT55(ESCCMD,ESCRN,0)
250  CONTINUE
252  CALL PLOT55(ESCCMD,HOME,0)
    CALL PLOT55(DISPLY,0,BELL)
    READ(5,58,ERR=120,END=120)NSTOP
    GO TO 120
C

```

```

C
C
C
C
C
300 CALL PLOT55(ESCCMD,HOME,0)
CALL PLOT55(ESCCMD,ESCRN,0)
WRITE(7,301)
301 FORMAT(' ', 'ENTER STARTING DATA POINT, THE STOPPING DATA POINT,
1,/,', ' ', 'AND THE NUMBER OF DATA POINTS PER SET OF DATA. 3F10.0')
READ(5,302,END=120,ERR=120)START,STOP,SET
302 FORMAT(3F10.0)
ISTART=IFIX(START)
ISTOP=IFIX(STOP)
ISET=IFIX(SET)
WRITE(7,170)TITLE,DAT,TIM,A(NP+1),A(NP+2)
WRITE(7,56)(A(NP+I),I=3,7)
WRITE(7,66)
66 FORMAT(' ', ' POINT NOS.          MEAN
1 STD. DEV.          S/N')
DO 310 I=ISTART,ISTOP,ISET
SUM=0.
SQUARE=0.
DO 309 J=I,(I+ISET-1)
SUM=SUM+FLOAT(A(J))
SQUARE=SQUARE+((FLOAT(A(J)))**2)
IF(J.LT. ISTOP)GO TO 308
J=J+1
SET=FLOAT(J-1)
GO TO 303
308 CONTINUE
309 CONTINUE
303 XMEAN=SUM/(SET)
STDEV=SQRT((SQUARE-((SUM**2)/(SET)))/(SET-1))
IF(STDEV.GT. 0)GO TO 304
WRITE(7,305)I,(J-1),XMEAN,STDEV
305 FORMAT(I4,' TO ',I4,1X,2(4X,F10.4),10X,'XXXX')
GO TO 310
304 SNR=XMEAN/STDEV
WRITE(7,67),(J-1),XMEAN,STDEV, SNR
67 FORMAT(I4,' TO-',I4,1X,3(4X,F10.4))
310 CONTINUE
CALL PLOT55(ESCCMD,HOME,0)
CALL PLOT55(DISPLY,0,BELL)
READ(5,58,END=120,ERR=120)NSTOP
GO TO 120

C
C
C
500 THIS SECTION WRITES THE PROGRAM ON DISK WITH THE CHOOSEN NAME.
REWIND 1
WRITE(7,170)TITLE,DAT,TIM,A(NP+1),A(NP+2)
WRITE(7,56)(A(NP+I),I=3,7)
ANP(1)=FLOAT(NP)
CALL ASSIGN(1,'DK:FTN1.DAT',-1,'NEW','NC',1)
WRITE(1)(ANP(1))
WRITE(1)(TITLE(I),I=1,3)
WRITE(1)(DAT(I),I=1,3)
WRITE(1)(TIM(I),I=1,3)
WRITE(1)(A(I),I=1,NP+7)
ENDFILE 1
CALL CLOSE(1)
GO TO 120

C
C
C
THIS SECTION CALCULATES THE TOTALS FOR SELECTED
PORTIONS OF THE DATA.

```



```

700   DO 705 J=1,30
      A1(J)=0
      NDIOD(J)=0
      NDIODN(J)=0
705   CONTINUE
      CALL PLOT55(ESCCMD,HOME,0)
      CALL PLOT55(ESCCMD,ESCRN,0)
      WRITE(7,170)TITLE,DAT,TIM,A(NP+1),A(NP+2)
      WRITE(7,56)(A(NP+I),I=3,7)
      JR=0
      WRITE(7,782)
782   FORMAT(' ','ENTER THE STARTING POINT # AND # OF POINTS.','','
1     ' ENTER EXTRA CARRAGE RETURN TO COMMENCE PROCESSING.')
701   READ(5,781,END=120,ERR=701)DIODE,DIODEN
781   FORMAT(2F10.0)
      IF(DIODE .EQ. 0)GO TO 710
      JR=JR+1
      NDIOD(JR)=IFIX(DIODE)
      NDIODN(JR)=IFIX(DIODEN)
      IF(JR .GE. 30)GO TO 710
      GO TO 701
710   CALL PLOT55(ESCCMD,HOME,0)
      CALL PLOT55(ESCCMD,ESCRN,0)
      WRITE(7,170)TITLE,DAT,TIM,A(NP+1),A(NP+2)
      WRITE(7,740)
740   FORMAT(' ','START      NP      TOTAL')
      DO 716 K=1,JR
716   DO 718 L=NDIOD(K),(NDIOD(K)+NDIODN(K)-1)
      A1(K)=A1(K)+A(L)
      WRITE(7,755)NDIOD(K),NDIODN(K),A1(K)
755   FORMAT(3X,I4,3X,I4,F12.0)
716   CONTINUE
      READ(5,58,END=120,ERR=120)MSTOP
      GO TO 120

C
C   THIS SECTION READS A FILE FROM THE DISK
C
800   WRITE(7,810)
810   FORMAT(' ','ENTER DATA FILE NAME AS *-----,DAT.','',')
      CALL ASSIGN(1,'DK:FTN1.DAT',-1,'OLD','NC',1)
      READ(1)(ANP(1))
      NP=IFIX(ANP(1))
      READ(1)(TITLE(I),I=1,3)
      READ(1)(DAT(I),I=1,3)
      READ(1)(TIM(I),I=1,3)
      READ(1)(A(I),I=1,NP+7)
      ENDFILE 1
      CALL CLOSE(1)
      GO TO 120

C
C   THIS SECTION DOES SMOOTHING OF DATA BY SIMPLIFIED LEAST
C   SQUARES PROCEDURE FROM SAVITZKY AND GOLAY,
C   ANAL. CHEM., 36(8), P1627(1964)
900   WRITE(7,999)
999   FORMAT(' ','INPUT FILTER SIZE:','','', ' 1=5 POINT FILTER',
1     ' /, ' 2=7 POINT FILTER', /, ' 3=9 POINT FILTER',
2     ' /, ' 4=11 POINT FILTER',
3     ' /, ' 5=13 POINT FILTER', /, ' 6=15 POINT FILTER',
4     ' /, ' 7=17 POINT FILTER', /, ' 8=19 POINT FILTER', /,
5     ' 9=21 POINT FILTER')
      READ(5,58,ERR=900,END=120)NGO
      GO TO (910,920,930,940,950,960,970,980,990),NGO
910   DO 915 I=3,(NP-2)
915   B(I)=IFIX(((F10AT(A(I-2))+A(I+2)))*3+(F10AT(A(I-1))+A(I+1)))*12
1     +(F10AT(A(I)))*17)/35)

```

```

DO 916 I=3,(NP-2)
916 A(I)=B(I)
A(1)=A(3)
A(2)=A(3)
A(NP-1)=A(NP-2)
A(NP)=A(NP-2)
GO TO 91
920 DO 925 I=4,(NP-3)
925 B(I)=IFIX((( -FLOAT(A(I-3)+A(I+3))) *2+(FLOAT(A(I-2)+A(I+2))) *3
1 +(FLOAT(A(I-1)+A(I+1))) *6+(FLOAT(A(I))) *7)/21)
DO 926 I=4,(NP-3)
926 A(I)=B(I)
A(1)=A(4)
A(2)=A(4)
A(3)=A(4)
A(NP-2)=A(NP-3)
A(NP-1)=A(NP-3)
A(NP)=A(NP-3)
GO TO 91
930 DO 935 I=5,(NP-4)
935 B(I)=IFIX((( -FLOAT(A(I-4)+A(I+4))) *21
1 +(FLOAT(A(I-3)+A(I+3))) *14
2 +(FLOAT(A(I-2)+A(I+2))) *39+(FLOAT(A(I-1)+A(I+1))) *54
3 +(FLOAT(A(I))) *59)/7)
DO 936 I=5,(NP-4)
936 A(I)=B(I)
DO 937 I=1,4
A(I)=A(5)
937 A(NP-I+1)=A(NP-4)
GO TO 91
940 DO 945 I=6,(NP-5)
945 B(I)=IFIX((( -FLOAT(A(I-5)+A(I+5))) *36
1 +(FLOAT(A(I-4)+A(I+4))) *9+(FLOAT(A(I-3)+A(I+3))) *44
2 +(FLOAT(A(I-2)+A(I+2))) *69
2 +(FLOAT(A(I-1)+A(I+1))) *84+(FLOAT(A(I))) *89)/429)
DO 946 I=6,(NP-5)
946 A(I)=B(I)
DO 947 I=1,5
A(I)=A(6)
947 A(NP-I+1)=A(NP-5)
GO TO 91
950 DO 955 I=7,(NP-6)
955 B(I)=IFIX((( -FLOAT(A(I-6)+A(I+6))) *11
1 +(FLOAT(A(I-4)+A(I+4))) *9+(FLOAT(A(I-3)+A(I+3))) *16
2 +(FLOAT(A(I-2)+A(I+2))) *21+(FLOAT(A(I-1)+A(I+1))) *24
3 +(FLOAT(A(I))) *25)/143)
DO 956 I=7,(NP-6)
956 A(I)=B(I)
DO 957 I=1,6
A(I)=A(7)
957 A(NP-I+1)=A(NP-6)
GO TO 91
960 DO 965 I=8,(NP-7)
965 B(I)=IFIX((( -FLOAT(A(I-7)+A(I+7))) *78-(FLOAT(A(I-6)+A(I+6))) *13
1 +(FLOAT(A(I-5)+A(I+5))) *42+(FLOAT(A(I-4)+A(I+4))) *87
2 +(FLOAT(A(I-3)+A(I+3))) *122+(FLOAT(A(I-2)+A(I+2))) *147
3 +(FLOAT(A(I-1)+A(I+1))) *162+(FLOAT(A(I))) *167)/1105)
DO 966 I=8,(NP-7)
966 A(I)=B(I)
DO 967 I=1,7
A(I)=A(8)
967 A(NP-I+1)=A(NP-7)
GO TO 91
970 DO 975 I=9,(NP-8)
975 B(I)=IFIX((( -FLOAT(A(I-8)+A(I+8))) *21+(-FLOAT(A(I-7)+A(I+7))) *6
1 +(FLOAT(A(I-6)+A(I+6))) *7+(FLOAT(A(I-5)+A(I+5))) *18

```

```

2 +(FLOAT(A(I-4)+A(I+4)))*27+(FLOAT(A(I-3)+A(I+3)))*34
3 +(FLOAT(A(I-2)+A(I+2)))*39+(FLOAT(A(I-1)+A(I+1)))*42
4 +(FLOAT(A(I)))*43/323)
DO 976 I=9,(NP-8)
976 A(I)=B(I)
DO 977 I=1,8
A(I)=A(9)
977 A(NP-I+1)=A(NP-8)
GO TO 91
984 DO 985 I=10,(NP-9)
985 B(I)=IFIX((((FLOAT(A(I-9)+A(I+9)))*136-(FLOAT(A(I-8)+A(I+8)))*51
1 +(FLOAT(A(I-7)+A(I+7)))*24+(FLOAT(A(I-6)+A(I+6)))*89
2 +(FLOAT(A(I-5)+A(I+5)))*144+(FLOAT(A(I-4)+A(I+4)))*189
3 +(FLOAT(A(I-3)+A(I+3)))*224+(FLOAT(A(I-2)+A(I+2)))*249
4 +(FLOAT(A(I-1)+A(I+1)))*264+(FLOAT(A(I)))*269)/2261)
DO 986 I=10,(NP-9)
986 A(I)=B(I)
DO 987 I=1,9
A(I)=A(10)
A(NP-I+1)=A(NP-9)
GO TO 91
DO 995 I=11,(NP-10)
995 B(I)=IFIX((((FLOAT(A(I-10)+A(I+10)))*171
1 -(FLOAT(A(I-9)+A(I+9)))*76
2 +(FLOAT(A(I-8)+A(I+8)))*9+(FLOAT(A(I-7)+A(I+7)))*84
3 +(FLOAT(A(I-6)+A(I+6)))*149+(FLOAT(A(I-5)+A(I+5)))*204
4 +(FLOAT(A(I-4)+A(I+4)))*249+(FLOAT(A(I-3)+A(I+3)))*284
5 +(FLOAT(A(I-2)+A(I+2)))*309+(FLOAT(A(I-1)+A(I+1)))*324
6 +(FLOAT(A(I)))*329)/3059)
DO 996 I=11,(NP-10)
996 A(I)=B(I)
DO 997 I=1,10
A(I)=A(11)
997 A(NP-I+1)=A(NP-10)
GO TO 91
C
C
C
600 STOP
* END

```

THIS SECTION CAUSES AN EXIT FROM THE PROGRAM.

STOP
END

C. GDPMT - Data Acquisition Subroutine

1. This subroutine acquires the data from the Photomultiplier Readout System via A/D conversion by the LPS 11 unit and transfers the acquired data to the main program ADCPMT. Data acquisition is started by a signal from the carbon furnace power supply and clocked by the LPS 11 internal clock.

```
PROGRAM GDPMT.MAC(4-JAN-78)
```

PURPOSE:

```
TO ACQUIRE DATA FROM A PMT WITH THE
DEC LPS UNIT, AND TO TRANSFER
THE DATA TO THE MAIN PROGRAM.
```

```
*****
*
*WRITTEN BY:*
*
*DONALD HULL*
*
*WITH HELP *
*
*FROM:      *
*
*ROBERT HALL*
*
*****
```

```
.TITLE GET DATA FROM A PMT WITH THE LPS UNIT
.MCALL ..V2,..REGDEF,.FETCH,.CLOSE,.PRINT
.MCALL .EXIT,.WRITW,.SRESET,.ENTER,.TTYOUT,.TTYIN
..V2..
.REGDEF
.GLOBL GDPMT
```

```
STR=170400      ;SET ADDRESS A/D STATUS REGISTER
ADB=170402      ;SET ADDRESS A/D BUFFER
DIBUF=170412    ;SET ADDRESS DIGITAL INPUT BUFFER
CLK=170404      ;SET ADDRESS CLOCK STATUS REGISTER
BUFF=170406     ;SET ADDRESS LPSKW BUFFER/PRESET
KBRD=177562     ;SET ADDRESS KEY BOARD
```

```
.CSECT
```

```
GDPMT:  NEG    ISPLF      ;NEGATE # MCR PULSES BETWEEN SFLS
        NEG    NDELAY    ;NEGATE DELAY TIME

KIRST:  MOV     #1040,R1   ;SET POINT COUNTER
        MOV     #A,R3     ;SET ADDRESS OF ARRAY(A)
LPO:    MOV     #0,(R3)+   ;CLEAR ARRAY(A)
        DEC     R1        ;DECREMENT POINT COUNTER
        BNE    LPO       ;RETURN IF POINT COUNTER NOT ZERO
        MOV     #0,CLK
```

```
SET UP FOR DATA ACQUISITION
```

```
.PRINT #WAIT
STRT1:  MOV     NP,R1     ;SET POINT COUNTER
        MOV     #A,R3     ;SET ADDRESS ARRAY(A)
        MOV     DIBUF,R4  ;CLEAR DIGITAL BUFFER
```

```

LP2:   MOV     R4,DIRUF
      MOV     DIBUF,R4
      BIT     #2,R4
      BEQ     LP2,
      MOV     #0,BUFP
      MOV     NDELAY,BUFP
      MOV     #11,CLK
LP3:   TSTB   CLK
      BPL     LP3
DATA:  MOV     #0,BUFP
      MOV     #0,CLK
      MOV     ISPLF,BUFP
      MOV     #40,STR
      MOV     MCR,CLK

```

#CHECK DIGITAL BUFFER FOR
 #START PULSE ON BIT 1
 #RETURN IF NO START PULSE
 #CLEAR BUFFER/PRESET
 #MOVE IN DELAY TO BUFFER/PRESET
 #SET CLOCK FREQUENCY AT 1KHZ, NON-REPEAT
 #TEST FOR END OF COUNT FLAG

#CLEAR BUFFER/PRESET
 #CLEAR CLOCK PRIOR TO LOADING.BUFP
 #SET UP BUFFER/PRESET FOR SPL FREQUENCY
 #SET UP TRIGGER ON A/D STATUS REGISTER
 #SET UP MASTER CLOCK RATE

BEGIN DATA ACQUISITION

```

SPL:   TSTB   STR
      BPL     SPL
      MOV     ADR,(R3)+
      DEC     R1
      BNE     SPL

```

#TEST FOR A/D END OF CONVERSION
 #ON BIT 7 OF A/D STATUS REGISTER
 #STORE SAMPLE DATA
 #DECREMENT POINT COUNTER
 #RETURN FOR ANOTHER POINT IF NOT FINISHED

FINISHED. EXIT FROM SUBROUTINE.

RTS PC

```

      .EVEN
.CSECT DRH
A:     .BLKW  1040.
NP:    .WORD  0
MCR:   .WORD  0
ISPLF: .WORD  0
NDELAY: .WORD  0
      .CSECT
      .EVEN
WAIT:  .ASCIZ /WAITING FOR START PULSE/
END:   .END   GDPMT

```

APPENDIX B

Software Developed to Plot the Monochromator- Photomultiplier Readout System Data on a Zeta Incremental Plotter

A. This program consists of 5 menu-selectable task modules and allow the data acquired with the Photomultiplier Readout System to be plotted. The sections are:

1. READ DISK: Reads data from a named file on disk.
2. AXIS: Draws the plot axis using operator defined axis names, sizes, and dimensions.
3. PLOT: Plots the data within the axis drawn by Module 2.
4. RESTART: Restarts program to allow a new data file to be read for plotting.
5. EXIT: Exits from program.

```

C
C
C      PROGRAM PMTPLT.FOR(22-OCT-79)
C
C      PURPOSE:
C          TO PLOT, WITH THE XY-PLOTTER, DATA STORED ON DISK.
C
C      SUBROUTINES NEEDED:
C          XYLIB
C          SYSLIB
C          /F
C
C      *****
C      *WRITTEN      *
C      *BY:          *
C      *DONALD HULL*
C      *****
C
C      DIMENSION      ANP(1),TITLE(3),DAT(3),TIM(3),X(1040),Y(1040)
C      DIMENSION      XAXIS(5),YAXIS(5),TITPLT(5)
C      INTEGER*2      DBLK(4),A(1040),B(1040)
C      DATA          DAT,TITLE,TIM/3*0.,3*0.,3*0./
C      DATA          DBLK/3RDKO,3RDAT,3RA ,3RDAT/
C
C      THIS SECTION RESTARTS PROGRAM BY CLEARING X & Y ARRAYS.
C
C      700 WRITE(7,110)
C      110 FORMAT(' ', ' ENTER THE NUMBER OF PAGES TO ADVANCE THE PEN. ')
C      READ (5,111)PAGES
C      111 FORMAT(F10.0)
C          ADV=PAGES*8.5
C          CALL PLOTST(0.005,'IN')
C          CALL PLOT(ADV,0.0,-3)
C          CALL PLOTND
C          DO 701 I=1,1040
C              X(I)=FLOAT(I)
C              Y(I)=0.0
C      701
C
C      THIS SECTION SELECTS THE PART OF THE PROGRAM TO BE EXECUTED.
C
C      1 WRITE(7,50)
C      50 FORMAT(' ', 'READ DISK=1, AXIS=2, PLOT=3, RESTART=4, SMOOTH=5
C      1 ,EXIT=6')
C      READ(5,51)NTEMP
C      51 FORMAT(I2)
C          IF(NTEMP .LT. 1 .OR. NTEMP .GT. 8)GO TO 1
C          GO TO(100,500,600,700,900,800),NTEMP
C
C      THIS SECTION READS DATA FILE FROM DISK.
C
C      100 WRITE(7,120)
C      120 FORMAT(' ', ' ENTER DATA FILE NAME AS *----- .DAT. ',/)
C          CALL ASSIGN(1,'DK:FTN1.DAT',-1,'OLD','NC',1)
C          READ(1)(ANP(1))
C          NP=IFIX(ANP(1))
C          READ(1)(TITLE(I),I=1,3)
C          READ(1)(DAT(I),I=1,3)
C          READ(1)(TIM(I),I=1,3)
C          READ(1)(A(I),I=1,NP+7)
C          ENDFILE 1

```



```

CALL CLOSE(1)

C
C
C THIS SECTION DOES BOOK KEEPING ON THE DATA ARRAY.
470 DO 480 I=1,NP+7
480 Y(I)=FLOAT(A(I))
490 DO 491 I=7,1,-1
491 Y(NP+2+I)=Y(NP+I)

C
C THIS SECTION SETS THE MINIMUM VALUE TO 0.0 AND
C THE MAXIMUM VALUE TO BE EQUAL TO THE RANGE FOR
C PLOTTING PURPOSES

C
C CALCULATION OF MAXIMUM, MINIMUM, AND RANGE OF VALUES.
Y(NP+5)=Y(5)
Y(NP+6)=FLOAT(5)
Y(NP+7)=Y(5)
Y(NP+8)=FLOAT(5)

C
C MAXIMUM AND SUBSCRIPT DETERMINATION.
DO 1000 I=6,NP
IF(Y(NP+5) .LT. Y(I))Y(NP+5)=Y(I)
IF(Y(NP+5) .EQ. Y(I))Y(NP+6)=FLOAT(I)

C
C MINIMUM AND SUBSCRIPT DETERMINATION.
IF(Y(NP+7) .GT. Y(I))Y(NP+7)=Y(I)
IF(Y(NP+7) .EQ. Y(I))Y(NP+8)=FLOAT(I)
1000

C
C RANGE DETERMINATION.
Y(NP+9)=Y(NP+5)-Y(NP+7)
DO 492 I=1,NP
492 Y(I)=Y(I)-Y(NP+7)
Y(NP+5)=Y(NP+5)-Y(NP+7)
Y(NP+7)=0.0
WRITE(7,493)TITLE,DAT,TIM,Y(NP+3),Y(NP+4)
493 FORMAT(' ',3A4,3A4,' ',3A4,3X,'NP=',F4.0,3X,'FREQ=',F4.0)
WRITE(7,494)(Y(NP+I),I=5,9)
494 FORMAT(' ',9F10.0,' ',F4.0,' ',F4.0,' MIN=',F10.0,
1 '0',F4.0,' RANGE=',F10.0)
GO TO 1

C
C THIS SECTION DRAWS THE AXIS OF THE PLOT.
500 WRITE(7,501)
501 FORMAT(' ', 'NEW X&Y TITLES AND AXIS LENGTHS? YES=1,NO=0')
READ(5,111,ERR=500,END=500)XNEW
IF(XNEW .EQ.0)GO TO 521
502 FORMAT(5A4)
WRITE(7,510)
510 FORMAT(' ', 'ENTER THE TITLE FOR THE X AXIS, 20 CHARACTERS MAX.')
READ(5,502)XAXIS
WRITE(7,503)
503 FORMAT(' ', 'ENTER THE TITLE FOR THE Y AXIS, 20 CHARACTERS MAX.')
READ(5,502)YAXIS
WRITE(7,520)
520 FORMAT(' ', 'ENTER X AND Y AXIS LENGTHS, 2F10.0.')
READ(5,525)XLONG,YLONG
WRITE(7,504)
521 FORMAT(' ', 'ENTER THE TITLE FOR THE PLOT, 20 CHARACTERS MAX.')
504 READ(5,502)TITPLT

```

```

XMIN=0.0
XMAX=Y(NP+3)
YMIN=0.0
YMAX=Y(NP+5)
525  FORMAT(2F10.0)
      WRITE(7,494)(Y(NP+I),I=5,9)
      WRITE(7,620)
620  FORMAT(' ', ' NORMALIZED PLOT=1, SCALED PLOT=0.')
      READ(5,51)NTEMP
      IF(NTEMP .EQ. 1)GO TO 550
      WRITE(7,625)
625  FORMAT(' ', ' ENTER NEW VALUE FOR Y RANGE, F10.0.')
      READ(5,111)YMAX
550  X(NP+1)=XMIN
      X(NP+2)=(XMAX-XMIN)/XLONG
      X(NP+3)=X(NP+2)/Y(NP+4)
      Y(NP+1)=YMIN
      Y(NP+2)=(YMAX-YMIN)/YLONG
      CALL PLOTST(0.005, 'IN')
      CALL PLOT(1.5,1.0,-3)
      CALL AXIS(0.0,0.0,XAXIS,-20,XLONG,0.0,X(NP+1),X(NP+9))
      CALL AXIS(0.0,0.0,YAXIS,+20,YLONG,90.0,Y(NP+1),Y(NP+2))
      TITLNG=(XLONG-2.8)/2
      CALL PLOT(TITLNG,(YLONG+0.5),3)
      CALL SYMBOL(TITLNG,(YLONG+0.5),0.14,TITPLT,0,20)
      CALL PLOT(0.0,YLONG,+3)
      CALL PLOT(XLONG,YLONG,+2)
      CALL PLOT(XLONG,0.0,+2)
      CALL PLOT(0.0,0.0,+3)
      CALL PLOT(-1.5,-1.0,-3)
      CALL PLOTND
      GO TO 1

C
C
C
600  THIS SECTION PLOTS THE DATA.
      X(NP+1)=XMIN
      X(NP+2)=(XMAX-XMIN)/XLONG
      Y(NP+1)=YMIN
      Y(NP+2)=(YMAX-YMIN)/YLONG
      CALL PLOTST(0.005, 'IN')
      CALL PLOT(1.5,1.0,-3)
      CALL LINE(X,NP,1,0,0)
      CALL PLOT(0.0,0.0,+3)
      CALL PLOT(-1.5,-1.0,-3)
      CALL PLOTND
      GO TO 1

C
C
C
C
900  THIS SECTION DOES SMOOTHING OF DATA BY SIMPLIFIED LEAST
999  SQUARES PROCEDURE FROM SAVITZKY AND GOLAY,
      ANAL. CHEM.,36(8),P1627(1964)
      WRITE(7,999)
      FORMAT(' ', ' INPUT FILTER SIZE: ',//, ' 1=5 POINT FILTER',
1 /, ' 2=7 POINT FILTER',//, ' 3=9 POINT FILTER',
2 /, ' 4=11 POINT FILTER',
3 /, ' 5=13 POINT FILTER',//, ' 6=15 POINT FILTER',
4 /, ' 7=17 POINT FILTER',//, ' 8=19 POINT FILTER',//,
5 /, ' 9=21 POINT FILTER')
      READ(5,51,ERR=900,END=1)NGO
      GO TO 910,920,930,940,950,960,970,980,990,NGO
910  DO 915 I=3,(NP-2)
915  B(I)=IF8((((-FLOAT(A(I-2))+A(I+2)))*3+(FLOAT(A(I-1))+A(I+1)))*12
1 + (FLOAT(A(I)))*17)/35)
      DO 916 I=3,(NP-2)
916  A(I)=B(I)
      A(1)=A(3)

```

```

      A(2)=A(3)
      A(NP-1)=A(NP-2)
      A(NP)=A(NP-2)
      GO TO 470
920   DO 925 I=4,(NP-3)
925   B(I)=IFIX((( -FLOAT(A(I-3)+A(I+3))) *2+(FLOAT(A(I-2)+A(I+2))) *3
1   +(FLOAT(A(I-1)+A(I+1))) *6+(FLOAT(A(I))) *7)/21)
      DO 926 I=4,(NP-3)
926   A(I)=B(I)
      A(1)=A(4)
      A(2)=A(4)
      A(3)=A(4)
      A(NP-2)=A(NP-3)
      A(NP-1)=A(NP-3)
      A(NP)=A(NP-3)
      GO TO 470
930   DO 935 I=5,(NP-4)
935   B(I)=IFIX((( -FLOAT(A(I-4)+A(I+4))) *21
1   +(FLOAT(A(I-3)+A(I+3))) *14
2   +(FLOAT(A(I-2)+A(I+2))) *39+(FLOAT(A(I-1)+A(I+1))) *54
3   +(FLOAT(A(I))) *59)/231)
      DO 936 I=5,(NP-4)
936   A(I)=B(I)
      DO 937 I=1,4
      A(I)=A(5)
937   A(NP-I+1)=A(NP-4)
      GO TO 470
940   DO 945 I=6,(NP-5)
945   B(I)=IFIX((( -FLOAT(A(I-5)+A(I+5))) *36
1   +(FLOAT(A(I-4)+A(I+4))) *9+(FLOAT(A(I-3)+A(I+3))) *44
2   +(FLOAT(A(I-2)+A(I+2))) *69
2   +(FLOAT(A(I-1)+A(I+1))) *84+(FLOAT(A(I))) *89)/429)
      DO 946 I=6,(NP-5)
946   A(I)=B(I)
      DO 947 I=1,5
      A(I)=A(6)
947   A(NP-I+1)=A(NP-5)
      GO TO 470
950   DO 955 I=7,(NP-6)
955   B(I)=IFIX((( -FLOAT(A(I-6)+A(I+6))) *11
1   +(FLOAT(A(I-4)+A(I+4))) *9+(FLOAT(A(I-3)+A(I+3))) *16
2   +(FLOAT(A(I-2)+A(I+2))) *21+(FLOAT(A(I-1)+A(I+1))) *24
3   +(FLOAT(A(I))) *25)/143)
      DO 956 I=7,(NP-6)
956   A(I)=B(I)
      DO 957 I=1,6
      A(I)=A(7)
957   A(NP-I+1)=A(NP-6)
      GO TO 470
960   DO 965 I=8,(NP-7)
965   B(I)=IFIX((( -FLOAT(A(I-7)+A(I+7))) *78-(FLOAT(A(I-6)+A(I+6))) *13
1   +(FLOAT(A(I-5)+A(I+5))) *42+(FLOAT(A(I-4)+A(I+4))) *87
2   +(FLOAT(A(I-3)+A(I+3))) *122+(FLOAT(A(I-2)+A(I+2))) *147
3   +(FLOAT(A(I-1)+A(I+1))) *162+(FLOAT(A(I))) *167)/1105)
      DO 966 I=8,(NP-7)
966   A(I)=B(I)
      DO 967 I=1,7
      A(I)=A(8)
967   A(NP-I+1)=A(NP-7)
      GO TO 470
970   DO 975 I=9,(NP-8)
975   B(I)=IFIX((( -FLOAT(A(I-8)+A(I+8))) *21+(-FLOAT(A(I-7)+A(I+7))) *6
1   +(FLOAT(A(I-6)+A(I+6))) *7+(FLOAT(A(I-5)+A(I+5))) *18
2   +(FLOAT(A(I-4)+A(I+4))) *27+(FLOAT(A(I-3)+A(I+3))) *34
3   +(FLOAT(A(I-2)+A(I+2))) *39+(FLOAT(A(I-1)+A(I+1))) *42
4   +(FLOAT(A(I))) *43)/323)

```

```

DO 976 I=9,(NP-8)
976  A(I)=B(I)
      DO 977 I=1,8
          A(I)=A(9)
977  A(NP-I+1)=A(NP-8)
      GO TO 470
980  DO 985 I=10,(NP-9)
985  B(I)=IFIX((( -FLOAT(A(I-9)+A(I+9))) *136 - (FLOAT(A(I-8)+A(I+8))) *51
1  + (FLOAT(A(I-7)+A(I+7))) *24 + (FLOAT(A(I-6)+A(I+6))) *89
2  + (FLOAT(A(I-5)+A(I+5))) *144 + (FLOAT(A(I-4)+A(I+4))) *189
3  + (FLOAT(A(I-3)+A(I+3))) *224 + (FLOAT(A(I-2)+A(I+2))) *249
4  + (FLOAT(A(I-1)+A(I+1))) *264 + (FLOAT(A(I))) *269) /2261)
      DO 986 I=10,(NP-9)
986  A(I)=B(I)
      DO 987 I=1,9
          A(I)=A(10)
987  A(NP-I+1)=A(NP-9)
      GO TO 470
990  DO 995 I=11,(NP-10)
995  B(I)=IFIX((( -FLOAT(A(I-10)+A(I+10))) *171
1  - (FLOAT(A(I-9)+A(I+9))) *76
2  + (FLOAT(A(I-8)+A(I+8))) *9 + (FLOAT(A(I-7)+A(I+7))) *84
3  + (FLOAT(A(I-6)+A(I+6))) *149 + (FLOAT(A(I-5)+A(I+5))) *204
4  + (FLOAT(A(I-4)+A(I+4))) *249 + (FLOAT(A(I-3)+A(I+3))) *284
5  + (FLOAT(A(I-2)+A(I+2))) *309 + (FLOAT(A(I-1)+A(I+1))) *324
6  + (FLOAT(A(I))) *329) /3059)
      DO 996 I=11,(NP-10)
996  A(I)=B(I)
      DO 997 I=1,10
          A(I)=A(11)
997  A(NP-I+1)=A(NP-10)
      GO TO 470
C
C   THIS SECTION CAUSES AN EXIT FROM THE PROGRAM.
C
800  CALL PLOTST(0.005,'IN')
      CALL PLOT(8.5,0.0,-3)
      CALL PLOTND
      STOP
      END

```

*

APPENDIX C

Software Developed for the Computer Coupled Photodiode Array Readout Systems

- A. ADCFUR - This main program is much like that described in Appendix A, Section B and contains several of the same task modules although they may be slightly modified. The task modules are:
1. PLOT
 2. LIST
 3. PEAK LOCATE: Searches for and lists the value and diode number for all peaks.
 4. RESTART
 5. EXIT
 6. WRITE DISK
 7. READ DISK
 8. TOTALS


```

C
C
C      CONVERSION OF DATA FROM INTEGER*4 TO REAL
C
C      DO 90  J=5,NP
90     C(J-4)=AJFLT(A(J))
        NP=NP-4
        C(NP+1)=XNS
        C(NP+2)=XNP
        C(NP+3)=BKD
C
C      CALCULATION OF MAXIMUM, MINIMUM, AND RANGE OF VALUES.
C
C      C(NP+4)=C(1)
        C(NP+5)=1.
        C(NP+6)=C(1)
        C(NP+7)=1.
        DO 1000 I=2,NP
C
C      MAXIMUM AND SUBSCRIPT DETERMINATION.
C
C      IF(C(NP+4) .LT. C(I))C(NP+4)=C(I)
        IF(C(NP+4) .EQ. C(I))C(NP+5)=FLOAT(I)
C
C      MINIMUM AND SUBSCRIPT DETERMINATION.
C
C      IF(C(NP+6) .GT. C(I))C(NP+6)=C(I)
1000    IF(C(NP+6) .EQ. C(I))C(NP+7)=FLOAT(I)
C
C      RANGE DETERMINATION.
C
C      C(NP+8)=C(NP+4)-C(NP+6)
        WRITE(7,56)(C(NP+I),I=4,8)
56     FORMAT(' ', 'MAX=', F10.0, 2X, '0', F5.0, ' MIN=', F10.0,
1      2X, '0', F5.0, ' RANGE=', F10.0)
C
C      PROCESSING REQUEST.
C
C      WRITE(7,57)
57     FORMAT(' ', 'PLOT=1, LIST=2, PEAK LOCATE=3, RESTART=4, ', //,
1      ' EXIT=5, WRITE DISK=6, READ DISK=7, TOTALS=8')
        CALL PLOT55(DISPLY,0,BELL)
        READ(5,58,END=120)NTEMP
58     FORMAT(I2)
        CALL PLOT55(ESCCMD,HOME,0)
        CALL PLOT55(ESCCMD,ESCRN,0)
        GO TO(100,200,300,400,500,600,700,800),NTEMP
        GO TO 6
C
C      DISPLAY A PLOT OF DATA ON THE VT-55 SCREEN.
C
C      NPLOT=NP
        WRITE(7,101)
101    FORMAT(' ', 'NORMALIZED PLOT? YES=1, NO=0')
        READ(5,59,END=120)XNORM
        IF(XNORM .EQ. 1.0)SCFAC=C(NP+8)
        IF(XNORM .EQ. 1.0)GO TO 102
        WRITE(7,103)
103    FORMAT(' ', 'ENTER SCALING FACTOR, F10.0')
        READ(5,59,END=120)SCFAC
102    CONTINUE
        DO 150 I=1,NP
        B(I)=IFIX(((C(I)-C(NP+6))*100.)/SCFAC)
        IF(B(I) .GT. 100)B(I)=100
150    CONTINUE
        CALL PLOT55(ESCCMD,HOME,0)
        CALL PLOT55(ESCCMD,ESCRN,0)

```

```

CALL PLOT55(STATUS,547,476)
CALL PLOT55(SELGR,0,0)
CALL PLOT55(CURPOS,0,0)
WRITE(7,170)TITLE,DAT,C(NP+1),C(NP+2),C(NP+3)
WRITE(7,56)(C(NP+I),I=4,8)
CALL PLOT55(HGRD,1,0,0)
IF(NPLOT .LE. 512)GO TO 151
CALL PLOT55(STATUS,551,472)
CALL PLOT55(SELGR,1,0)
CALL PLOT55(HGRD,1,101)
151 IF(NP .GT. 512)NPLOT=512
CALL PLOT55(SELGR,0,0)
CALL PLOT55(ORIGIN,0,0)
CALL PLOT55(N,-NPLOT,R)
IF(NP .LE. 512)GO TO 153
NPLOT=NP-512
CALL PLOT55(SELGR,1,0)
DO 156 I=1,NPLOT
156 D(I)=D(I)+101
CALL PLOT55(N,-NPLOT,D)
153 CALL PLOT55(DISPLY,0,BELL)
READ(5,58,END=120)NSTOP
120 CALL PLOT55(ESCCMD,HOME,0)
CALL PLOT55(ESCCMD,ESCRN,0)
CALL PLOT55(STATUS,0,1023)
GO TO 6

C
C THIS SECTION LISTS THE DATA ON THE VT-55 COPIER.
C
200 CALL PLOT55(ESCCMD,HOME,0)
CALL PLOT55(ESCCMD,ESCRN,0)
CALL PLOT55(DISPLY,0,BELL)
WRITE(7,170)TITLE,DAT,C(NP+1),C(NP+2),C(NP+3)
WRITE(7,56)(C(NP+I),I=4,8)
170 FORMAT(' ',3A4,3A4,3X,'NS=',F10.0,3X,'NP=',F10.0,
1 3X,'BKGD=',F10.0)
DO 250 I=1,NP+8,100
DO 251 J=I,I+95,5
WRITE(7,63)J,(C(K),K=J,J+4)
IF(K .GT. (NP+8))GO TO 252
251 CONTINUE
READ(5,58,END=120)NSTOP
253 CALL PLOT55(ESCCMD,HOME,0)
CALL PLOT55(ESCCMD,ESCRN,0)
CONTINUE
250 FORMAT(' ',I4,2X,'>',5(F10.0,1X))
85
252 CALL PLOT55(ESCCMD,HOME,0)
CALL PLOT55(DISPLY,0,BELL)
READ(5,58,END=120)NSTOP
GO TO 120

C
C THIS SECTION DETERMINES PEAK LOCATIONS AND DISPLAYS
C THE LOCATION AND PEAK VALUE ON THE VT-55.
C
300 CALL PLOT55(ESCCMD,HOME,0)
CALL PLOT55(ESCCMD,ESCRN,0)
WRITE(7,170)TITLE,DAT,C(NP+1),C(NP+2),C(NP+3)
WRITE(7,56)(C(NP+I),I=4,8)
WRITE(7,64)
64 FORMAT(' ', 'ENTER THE THRESHOLD,F10.0')
READ(5,59,END=120)THRES
66 FORMAT(' ', 'POINT NO. AMPLITUDE')
DO 320 J=1,NP
NCNT=0
WRITE(7,66)
DO 310 I=J,NP

```



```

IF(C(I) .LT. THRES)GO TO 310
IF(C(I+1) .GT. C(I))GO TO 310
IF(C(I) .LE. C(I-1))GO TO 310
WRITE(7,67)I,C(I)
NCNT=NCNT+1
J=I
IF(I .GE. NP)GO TO 320
IF(NCNT .EQ. 20)GO TO 311
310 J=I
IF(I .GE. NP)GO TO 320
311 READ(5,58,END=120)NSTOP
CALL PLOT55(ESCCMD,HOME,0)
CALL PLOT55(ESCCMD,ESCRN,0)
320 CONTINUE
67 FORMAT(5X,I4,6X,F10.0)
CALL PLOT55(ESCCMD,HOME,0)
CALL PLOT55(DISPLY,0,BELL)
READ(5,58,END=120)NSTOP
CALL PLOT55(ESCCMD,ESCRN,0)
GO TO 120

C
C
C
600 THIS SECTION WRITES THE DATA ON DISK AND NAMES THE DATA FILE.
REWIND 1
WRITE(7,170)TITLE,DAT,C(NP+1),C(NP+2),C(NP+3)
WRITE(7,56)(C(NP+I),I=4,8)
WRITE(7,720)
CALL ASSIGN(1,'DK:FTN1.DAT',-1,'NEW','NC',1)
WRITE(1)(DAT(I),I=1,3)
WRITE(1)(TITLE(I),I=1,3)
WRITE(1)(C(I),I=1,NP+8)
ENDFILE 1
CALL CLOSE(1)
GO TO 120

C
C
C
700 THIS SECTION READS DATA FILE FROM DISK.
720 WRITE(7,720)
FORMAT(' ', ' ENTER DATA FILE NAME AS *-----(.DAT).',/)
CALL ASSIGN(1,'DK:FTN1.DAT',-1,'OLD','NC',1)
READ(1)(DAT(I),I=1,3)
READ(1)(TITLE(I),I=1,3)
READ(1)(C(I),I=1,NP+8)
ENDFILE 1
CALL CLOSE(1)
GO TO 120

C
C
C
800 THIS SECTION CALCULATES THE TOTALS FOR SELECTED
PORTIONS OF THE DATA.
DO 805 J=1,30
A1(J)=0
NDIOD(J)=0
NDIOND(J)=0
-805 CONTINUE
CALL PLOT55(ESCCMD,HOME,0)
CALL PLOT55(ESCCMD,ESCRN,0)
WRITE(7,170)TITLE,DAT,C(NP+1),C(NP+2),C(NP+3)
WRITE(7,56)(C(NP+I),I=4,8)
JR=0
WRITE(7,882)
882 FORMAT(' ', ' ENTER THE STARTING POINT # AND # OF POINTS.',/)
1 ' ENTER EXTRA CARRAGE RETURN TO COMMENCE PROCESSING.')
801 READ(5,881,END=120,ERR=801)DIODE,DIODEN
881 FORMAT(2F10.0)
IF(DIODE .EQ. 0)GO TO 810

```

```
JR=JR+1
NDIOD(JR)=IFIX(DIODE)
NDIODN(JR)=IFIX(DIODEN)
IF(JR .GE. 30)GO TO 810
GO TO 801
810 CALL PLOT55(ESCCMD,HOME,0)
CALL PLOT55(ESCCMD,ESCRN,0)
WRITE(7,170)TITLE,DAT,C(NP+1),C(NP+2),C(NP+3)
WRITE(7,56)(C(NP+I),I=4,8)
WRITE(7,840)
840 FORMAT(' ', ' START      NP      . TOTAL ')
DO 816 K=1,JR
DO 818 L=NDIOD(K),(NDIOD(K)+NDIODN(K)-1)
818 A1(K)=A1(K)+C(L)
WRITE(7,855)NDIOD(K),NDIODN(K),A1(K)
855 FORMAT(3X,I4,3X,I4,F12.0)
816 CONTINUE
READ(5,58,END=120,ERR=120)NSTOP
GO TO 120
C
C THIS SECTION CAUSES AN EXIT FROM THE PROGRAM.
C
500 STOP
END
*
```

B. FGDFUR - This subroutine acquires time-averaged data from the Computer Coupled Photodiode Array Readout system via A/D conversion by the LPS 11 unit and transfers the acquired data to the main program ADCFUR. Data may be background subtracted before transfer to ADCFUR if desired. Data acquisition is started by the combination of the start signal from the carbon furnace power supply and the photodiode array start signal. Data acquisition is clocked by the photodiode array clock.

PROGRAM FGDFUR.MAC(1-OCT-79)

PURPOSE:

TO ACQUIRE DATA WITH THE DEC LPS UNIT,
DO AVERAGING OF THE DATA, AND TO TRANSFER
THE DATA TO THE MAIN PROGRAM.

```
*****
*
*WRITTEN BY:*
*
*DONALD HULL*
*
*WITH HELP *
*
*FROM:      *
*
*ROBERT HALL*
*
*****
```

```
.TITLE FAST GET DATA FROM LPS UNIT
.MCALL ..V2,..REGDEF,.FETCH,.CLOSE,.PRINT
.MCALL .EXIT,.WRITW,.SRESET,.ENTER,.TTYOUT,.TTYIN
..V2..
.REGDEF
.GLOBL FGDFUR
```

```
STR=170400          #SET ADDRESS A/D STATUS REGISTER
ADR=170402          #SET ADDRESS A/D BUFFER
DIBUF=170412       #SET ADDRESS DIGITAL INPUT BUFFER
KBRD=177562        #SET ADDRESS KEY BOARD
```

.CSECT

```
FGDFUR: MOV     #1,BKD          #SET UP BACKGROUND FLAG
RESTRT: MOV     #2080.,R1      #SET POINT COUNTER
        MOV     #A,R3          #SET ADDRESS OF ARRAY(A)
LPO:    MOV     #0,(R3)+       #CLEAR ARRAY(A)
        DEC     R1             #DECREMENT POINT COUNTER
        BNE     LPO           #RETURN IF POINT COUNTER NOT ZERO
```

WAIT FOR KEY BOARD FLAG TO BEGIN DATA ACQUISITION

```
LPI:    .PRINT  #DATAQ          #ASK FOR KEY BOARD FLAG
        .TTYIN                    #GET CHARACTER FROM TTY
        BCS     LP1              #WAIT FOR INPUT
        CMPB   RO,#12           #WAS LAST CHARACTER=LF?
        BNE     LP1              #RETURN IF NOT FINISHED
```

SET UP FOR DATA ACQUISITION

```

MOV DIBUF,R4
MOV R4,DIBUF
LP10: MOV DIBUF,R4
      BIT #2,R4
      BEQ LP10
STRT2: MOV NS,R2
STRT1: MOV NP,R1
      MOV #B,R3
      MOV R2,R0

```

ICLEAR DIGITAL INPUT BUFFER
 ITEST FOR ASH CYCLE FINISH FLAG
 ION BIT 1
 IRETURN IF NO FLAG
 ISET SCAN COUNTER
 ISET POINT COUNTER
 ISET ADDRESS ARRAY(B)
 IMOVE VALUE OF NS TO BCD-INPUT

BEGIN DATA ACQUISITION

```

DATA: MOV DIBUF,R4
      MOV R4,DIBUF
LP2:  MOV DIBUF,R4
      BIT #1,R4
      BEQ LP2

```

ICLEAR DIGITAL INPUT BUFFER

ITEST FOR START FLAG ON
IBIT 0
IRETURN IF NO FLAG

```

SPL:  MOV #20,STR
      TSTB STR
      BPL SPL
      MOV ADB,(R3)+
      DEC R1
      BNE SPL

```

ISET UP TRIGGER ON A/D STATUS REGISTER
 ITEST FOR A/D END OF CONVERSION
 ION BIT 7 OF A/D STATUS REGISTER
 ISTORE SAMPLE DATA
 IDECREMENT POINT COUNTER
 IRETURN FOR ANOTHER POINT IF NOT FINISHED

DOUBLE WORD ADD

```

MOV NP,R1
MOV #A,R3
MOV #B,R0
LP3:  ADD (R0)+,(R3)+
      ADC (R3)+
      DEC R1
      BNE LP3
      DEC R2
      BNE STRT1
      TST IBKD
      BEQ FIN

```

ISET UP POINT COUNTER
 ISET ADDRESS ARRAY(A)
 ISET ADDRESS ARRAY(B)
 ILOW-ORDER WORD ADD
 ICARRY BIT ADD
 IDECREMENT POINT COUNTER
 IRETURN FOR ANOTHER POINT IF NOT FINISHED
 IDECREMENT SCAN COUNTER
 IRETURN FOR ANOTHER SCAN IF NOT FINISHED
 ITEST BACKGROUND FLAG AND

WAIT FOR KEY BOARD FLAG TO START BACKGROUND SUBTRACTION

```

BKGD: .PRINT #BKDAQ
LP4:  .TTYIN
      RCS LP4
      CMPB RO,#12
      BNE LP4
      MOV #0,BKD

```

IASK FOR KEY BOARD FLAG
 IGET CHARACTER FROM TTY
 ICHECK FOR INPUT
 IWAS LAST CHARACTER=LF?
 IRETURN IF NOT
 ICLEAR BACKGROUND FLAG

SET UP FOR BACKGROUND SUBTRACTION

```

STRT4: MOV NS,R2
STRT3: MOV NP,R1
      MOV #B,R3
      MOV R2,R0

```

ISET SCAN COUNTER
 ISET POINT COUNTER
 ISET ADDRESS OF ARRAY(B)
 IMOVE VALUE OF NS TO BCD-INPUT

BEGIN BACKGROUND SUBTRACTION

```

BKG:  MOV DIBUF,R4
      MOV R4,DIBUF
LP5:  MOV DIBUF,R4
      BIT #1,R4
      BEQ LP5
      MOV #20,STR
LP6:  TSTB STR
      BPL LP6
      MOV ADB,(R3)+

```

ICLEAR DIGITAL INPUT BUFFER

ITEST FOR START FLAG ON
 IBIT 0
 IRETURN IF NO FLAG
 ISET UP A/D STATUS REGISTER
 ITEST FOR A/D END OF CONVERSION
 IAT BIT 7 A/D STATUS REGISTER
 ISTORE BACKGROUND DATA

```

DEC      R1      ;DECREMENT POINT COUNTER
BNE      LP6     ;RETURN FOR ANOTHER POINT IF NOT FINISHED

DOUBLE WORD SUBTRACTION

      MOV      NP,R1      ;SET UP POINT COUNTER
      MOV      #A,R3     ;SET ADDRESS ARRAY(A)
      MOV      #B,R0     ;SET ADDRESS ARRAY(B)
SUBK:  SUB      (R0)+,(R3)+ ;LOW-ORDER WORD SUBTRACTION
      SBC      (R3)+     ;CARRY SUBTRACTION
      DEC      R1        ;DECREMENT POINT COUNTER
      BNE     SUBK      ;RETURN FOR ANOTHER POINT IF NOT FINISHED
      DEC      R2        ;DECREMENT SCAN COUNTER
      BNE     STRT3     ;RETURN FOR ANOTHER SCAN IF NOT FINISHED

FINISHED. EXIT FROM SUBROUTINE.

FIN:   RTS      PC

      .EVEN
      .CSECT DRH
A:     .BLKW   2080.
NS:    .WORD   0
NP:    .WORD   0
IBKD:  .WORD   0
      .CSECT
      .EVEN
BKD:   .WORD   0
B:     .BLKW   1040.
DATAQ: .ASCIZ  /STRIKE CR TO START DATA ACQUISITION./
BKDAQ: .ASCIZ  /STRIKE CR TO START BACKGROUND ACQUISITION./
END:   .END     FGDFUR

```

APPENDIX D

Software Developed to Plot the Computer-Controlled
Photodiode Array Readout System Data on a
Zeta Incremental Plotter

- A. This program consists of 6 menu selectable task modules and allow plotting of the data acquired with the photodiode array-based systems. The task modules are:
1. READ DISK
 2. AXIS
 3. PLOT
 4. RESTART
 5. SMOOTH: A Smoothing routine based on the simplified least squares smoothing procedure of Savitzky and Golay.
 6. EXIT


```

C
C
C      THIS SECTION DOES BOOK KEEPING ON THE DATA ARRAY.
490      DO 491 I=8,1,-1
491      Y(NP+2+I)=Y(NP+I)
C
C      THIS SECTION SETS THE MINIMUM VALUE TO 0.0 AND
C      THE MAXIMUM VALUE TO BE EQUAL TO THE RANGE FOR
C      PLOTTING PURPOSES
C
C      CALCULATION OF MAXIMUM, MINIMUM, AND RANGE OF VALUES.
91      Y(NP+6)=Y(1)
        Y(NP+7)=FLOAT(1)
        Y(NP+8)=Y(1)
        Y(NP+9)=FLOAT(1)
        DO 1000 I=2,NP
C
C      MAXIMUM AND SUBSCRIPT DETERMINATION.
        IF(Y(NP+6) .LT. Y(I))Y(NP+6)=Y(I)
        IF(Y(NP+6) .EQ. Y(I))Y(NP+7)=FLOAT(I)
C
C      MINIMUM AND SUBSCRIPT DETERMINATION.
        IF(Y(NP+8) .GT. Y(I))Y(NP+8)=Y(I)
        IF(Y(NP+8) .EQ. Y(I))Y(NP+9)=FLOAT(I)
1000
C
C      RANGE DETERMINATION.
        Y(NP+10)=Y(NP+6)-Y(NP+8)
        IF(NTEMP .EQ. 5)GO TO 495
        DO 492 I=1,NP
492      Y(I)=Y(I)-Y(NP+8)
        Y(NP+6)=Y(NP+6)-Y(NP+8)
        Y(NP+8)=0.0
495      WRITE(7,493)TITLE,DAT,Y(NP+3),Y(NP+4),Y(NP+5)
493      FORMAT(' ',3A4,3A4,3X,'NS='F4.0,3X,'NP='F4.0,3X,'BKGD='F4.0)
        WRITE(7,494)(Y(NP+I),I=6,10)
494      FORMAT(' ',MAX='F10.0,'@',F4.0,' MIN='F10.0,
1 '@',F4.0,' RANGE='F10.0)
        GO TO 1
C
C
C      THIS SECTION DRAWS THE AXIS OF THE PLOT.
500      CONTINUE
502      FORMAT(7A4)
        WRITE(7,510)
510      FORMAT(' ', ' ENTER THE TITLE FOR THE X AXIS, 28 CARACTERS MAX. ')
        READ(5,502)XAXIS
        WRITE(7,503)
503      FORMAT(' ', ' ENTER THE TITLE FOR THE Y AXIS, 28 CARACTERS MAX. ')
        READ(5,502)YAXIS
        WRITE(7,504)
504      FORMAT(' ', ' ENTER THE TITLE FOR THE PLOT, 28 CARACTERS MAX. ')
        READ(5,502)TITP
        XMIN=0.0
        XMAX=Y(NP+4)
        WRITE (7,505)
505      FORMAT(' ',XMIN=0 & XMAX=NP,','/,
1 ' ENTER 1 TO CHANGE, CARRAGE RETURN IF NO CHANGE DESIRED. ')
        READ(5,51)NTEMP
        IF (NTEMP .NE. 1)GO TO 506
        WRITE(7,507)
507      FORMAT(' ', ' ENTER NEW VALUES FOR XMIN AND XMAX, 2F10.0. ')

```

```

506 READ(5,525)XMIN,XMAX
    YMIN=0.0
    YMAX=Y(NP+6)
    WRITE(7,520)
520 FORMAT(' ', ' ENTER X AND Y AXIS LENGTHS, 2F10.0,')
    READ(5,525)XLONG,YLONG
525 FORMAT(2F10.0)
621 WRITE(7,494)(Y(NP+I),I=6,10)
    WRITE(7,620)
620 FORMAT(' ', ' NORMALIZED PLOT=1, SCALED PLOT=0,')
    READ(5,51)NTEMP
    IF(NTEMP .EQ. 1)GO TO 550
    WRITE(7,625)
625 FORMAT(' ', ' ENTER NEW VALUE FOR Y RANGE, F10.0,')
    READ(5,111)YMAX
550 X(NP+1)=XMIN
    X(NP+2)=(XMAX-XMIN)/XLONG
    Y(NP+1)=YMIN
    Y(NP+2)=(YMAX-YMIN)/YLONG
    CALL PLOTST(0.005,'IN')
    CALL PLOT(1.5,1.0,-3)
    CALL AXIS(0.0,0.0,XAXIS,-28,XLONG,0.0,X(NP+1),X(NP+2))
    CALL AXIS(0.0,0.0,YAXIS,+28,YLONG,90.0,Y(NP+1),Y(NP+2))
    CALL PLOT(XLONG,0,+3)
    CALL PLOT(XLONG,YLONG,+2)
    CALL PLOT(0,YLONG,+2)
    CALL PLOT(0,(YLONG+0.5),+3)
    CALL SYMBOL(0,(YLONG+0.5),0.14,TITP,0,28)
    CALL PLOT(0.0,0.0,+3)
    CALL PLOT(-1.5,-1.0,-3)
    CALL PLOTND
    GO TO 1
C
C THIS SECTION PLOTS THE DATA.
C
600 WRITE(7,610)
610 FORMAT(' ', ' CHANGE Y-RANGE? YES=1, NO=CARRAGE RETURN')
    READ(5,51)NQ
    IF(NQ .EQ. 0)GO TO 611
    WRITE(7,625)
    READ(5,111)YMAX
611 X(NP+1)=0.0
    X(NP+2)=XNP/XLONG
    Y(NP+1)=YMIN
    Y(NP+2)=(YMAX-YMIN)/YLONG
    CALL PLOTST(0.005,'IN')
    CALL PLOT(1.5,1.0,-3)
    CALL LINE(X,Y,NP,1,0,0)
    CALL PLOT(0.0,0.0,+3)
    CALL PLOT(-1.5,-1.0,-3)
    CALL PLOTND
    GO TO 1
C
C THIS SECTION DOES SMOOTHING OF DATA BY SIMPLIFIED LEAST
C SQUARES PROCEDURE FROM SAVITZKY AND GOLAY,
C ANAL. CHEM.,36(8),P1627(1964)
C
900 WRITE(7,999)
999 FORMAT(' ', 'INPUT FILTER SIZE:','/', '/', ' 1=5 POINT FILTER',
1 /, ' 2=7 POINT FILTER', '/', '/', ' 3=9 POINT FILTER',
2 /, ' 4=11 POINT FILTER',
3 /, ' 5=13 POINT FILTER', '/', '/', ' 6=15 POINT FILTER',
4 /, ' 7=17 POINT FILTER', '/', '/', ' 8=19 POINT FILTER', '/',
5 ' 9=21 POINT FILTER')
    READ(5,58,ERR=900,END=1)NGO
58 FORMAT(I2)

```

```

          GO TO (910,920,930,940,950,960,970,980,990),NGO
910      DO 915 I=3,(NP-2)
915      F(I)=(((-(Y(I-2)+Y(I+2))))*3+((Y(I-1)+Y(I+1))))*12
          1 +((Y(I))) *17)/35)
          DO 916 I=3,(NP-2)
916      Y(I)=F(I)
          Y(1)=Y(3)
          Y(2)=Y(3)
          Y(NP-1)=Y(NP-2)
          Y(NP)=Y(NP-2)
          GO TO 91
920      DO 925 I=4,(NP-3)
925      F(I)=(((-(Y(I-3)+Y(I+3))))*2+((Y(I-2)+Y(I+2))))*3
          1 +((Y(I-1)+Y(I+1))) *6+((Y(I))) *7)/21)
          DO 926 I=4,(NP-3)
926      Y(I)=F(I)
          Y(1)=Y(4)
          Y(2)=Y(4)
          Y(3)=Y(4)
          Y(NP-2)=Y(NP-3)
          Y(NP-1)=Y(NP-3)
          Y(NP)=Y(NP-3)
          GO TO 91
930      DO 935 I=5,(NP-4)
935      F(I)=(((-(Y(I-4)+Y(I+4))))*21
          1 +((Y(I-3)+Y(I+3))) *14
          2 +((Y(I-2)+Y(I+2))) *39+((Y(I-1)+Y(I+1))) *54
          3 +((Y(I))) *59)/231)
          DO 936 I=5,(NP-4)
936      Y(I)=F(I)
          DO 937 I=1,4
          Y(I)=Y(5)
937      Y(NP-I+1)=Y(NP-4)
          GO TO 91
940      DO 945 I=6,(NP-5)
945      F(I)=(((-(Y(I-5)+Y(I+5))))*36
          1 +((Y(I-4)+Y(I+4))) *9+((Y(I-3)+Y(I+3))) *44
          2 +((Y(I-2)+Y(I+2))) *69
          2 +((Y(I-1)+Y(I+1))) *84+((Y(I))) *89)/429)
          DO 946 I=6,(NP-5)
946      Y(I)=F(I)
          DO 947 I=1,5
          Y(I)=Y(6)
947      Y(NP-I+1)=Y(NP-5)
          GO TO 91
950      DO 955 I=7,(NP-6)
955      F(I)=(((-(Y(I-6)+Y(I+6))))*11
          1 +((Y(I-4)+Y(I+4))) *9+((Y(I-3)+Y(I+3))) *16
          2 +((Y(I-2)+Y(I+2))) *21+((Y(I-1)+Y(I+1))) *24
          3 +((Y(I))) *25)/143)
          DO 956 I=7,(NP-6)
956      Y(I)=F(I)
          DO 957 I=1,6
          Y(I)=Y(7)
957      Y(NP-I+1)=Y(NP-6)
          GO TO 91
960      DO 965 I=8,(NP-7)
965      F(I)=(((-(Y(I-7)+Y(I+7))))*78-((Y(I-6)+Y(I+6))) *13
          1 +((Y(I-5)+Y(I+5))) *42+((Y(I-4)+Y(I+4))) *87
          2 +((Y(I-3)+Y(I+3))) *122+((Y(I-2)+Y(I+2))) *147
          3 +((Y(I-1)+Y(I+1))) *162+((Y(I))) *167)/1105)
          DO 966 I=8,(NP-7)
966      Y(I)=F(I)
          DO 967 I=1,7
          Y(I)=Y(8)
967      Y(NP-I+1)=Y(NP-7)

```

```

GO TO 91
970 DO 975 I=9,(NP-8)
975 F(I)=(((-(Y(I-8)+Y(I+8)))*21+(-(Y(I-7)+Y(I+7)))*6
1 +((Y(I-6)+Y(I+6)))*7+((Y(I-5)+Y(I+5)))*18
2 +((Y(I-4)+Y(I+4)))*27+((Y(I-3)+Y(I+3)))*34
3 +((Y(I-2)+Y(I+2)))*39+((Y(I-1)+Y(I+1)))*42
4 +((Y(I)))*43)/323)
DO 976 I=9,(NP-8)
976 Y(I)=F(I)
DO 977 I=1,8
Y(I)=Y(9)
977 Y(NP-I+1)=Y(NP-8)
GO TO 91
980 DO 985 I=10,(NP-9)
985 F(I)=(((-(Y(I-9)+Y(I+9)))*136-((Y(I-8)+Y(I+8)))*51
1 +((Y(I-7)+Y(I+7)))*24+((Y(I-6)+Y(I+6)))*89
2 +((Y(I-5)+Y(I+5)))*144+((Y(I-4)+Y(I+4)))*189
3 +((Y(I-3)+Y(I+3)))*224+((Y(I-2)+Y(I+2)))*249
4 +((Y(I-1)+Y(I+1)))*264+((Y(I)))*269)/2261)
DO 986 I=10,(NP-9)
986 Y(I)=F(I)
DO 987 I=1,9
Y(I)=Y(10)
987 Y(NP-I+1)=Y(NP-9)
GO TO 91
990 DO 995 I=11,(NP-10)
995 F(I)=(((-(Y(I-10)+Y(I+10)))*171
1 -((Y(I-9)+Y(I+9)))*76
2 +((Y(I-8)+Y(I+8)))*9+((Y(I-7)+Y(I+7)))*84
3 +((Y(I-6)+Y(I+6)))*149+((Y(I-5)+Y(I+5)))*204
4 +((Y(I-4)+Y(I+4)))*249+((Y(I-3)+Y(I+3)))*284
5 +((Y(I-2)+Y(I+2)))*309+((Y(I-1)+Y(I+1)))*324
6 +((Y(I)))*329)/3059)
DO 996 I=11,(NP-10)
996 Y(I)=F(I)
DO 997 I=1,10
Y(I)=Y(11)
997 Y(NP-I+1)=Y(NP-10)
GO TO 91
C
C THIS SECTION CAUSES AN EXIT FROM THE PROGRAM.
C
800 CALL PLOTST(0.005,'IN')
CALL PLOT(8.5,0.0,-3)
CALL PLOTND
STOP
END

```

APPENDIX E

Software Developed for Time Studies with the Computer- Coupled Photodiode Array Readout Systems

- A. MULTFR - This main program is much like those described in Appendix A and C except that the individual photodiode array scans are not time averaged but are stored sequentially on disk as individual scans by the subroutine MULFUR and each individual scan may then be read from the disk by menu selection #4, READ DISK. The task modules are:
1. PLOT
 2. LIST
 3. PEAK LOCATE
 4. READ DISK: Reads any selected scan from the sequential file stored on disk by MULFUR.
 5. RESTART
 6. WRITE DISK: Writes the selected file on disk under the operator selected name.
 7. TOTALS
 8. EXIT


```

C
6   WRITE(7,170)TITLE,DAT,XNS,XNP,C(NP+3)
    WRITE(7,56)(C(NP+I),I=4,8)
    WRITE(7,57)
57  FORMAT(' ','PLOT=1, LIST=2, PEAK LOCATE=3, READ DISK=4',/,
1'  ', 'RESTART=5, WRITE DISK=6, TOTALS=7, EXIT=8')
    CALL PLOT55(DISPLY,0,BELL)
    READ(5,58,END=120)NTEMP
58  FORMAT(I2)
    CALL PLOT55(ESCCMD,HOME,0)
    CALL PLOT55(ESCCMD,ESCRN,0)
    GO TO(100,200,300,400,500,600,700,800),NTEMP
    GO TO 6

C
C   READ INDIVIDUAL SCANS FROM DATA.DAT FILE ON DISK.
C
400 WRITE(7,68)NS
68  FORMAT(' ',I2,' SCANS AQUIRED. WHICH SCAN DO YOU WISH? ENTER
    IN I2 FORMAT.')
720 READ (5,58,END=120)NUMSET
    XNUMST=FLOAT(NUMSET)
    NBLK=(5*(NUMSET-1))
    DO 91 I=1,1040
91   C(I)=0.
    B(I)=0
    ICD=LOOKUP(0,DBLK)
    ICODE=IREADW(NPX,B,NBLK,0)
    CALL CLOSEC(0)
    CALL IFREEC(0)

C
C   CONVERSION OF DATA FROM INTEGER*2 TO REAL
C
90  DO 90 J=5,NPX
    C(J-4)=FLOAT(B(J))
    C(NP+1)=XNS
    C(NP+2)=XNP
    C(NP+3)=XNUMST
    IF(NTEMP .EQ. 7)GO TO 715

C
C   CALCULATION OF MAXIMUM, MINIMUM, AND RANGE OF VALUES.
C
    C(NP+4)=C(1)
    C(NP+5)=1.
    C(NP+6)=C(1)
    C(NP+7)=1.
    DO 1000 I=2,NP

C
C   MAXIMUM AND SUBSCRIPT DETERMINATION.
C
    IF(C(NP+4) .LT. C(I))C(NP+4)=C(I)
    IF(C(NP+4) .EQ. C(I))C(NP+5)=FLOAT(I)

C
C   MINIMUM AND SUBSCRIPT DETERMINATION.
C
    IF(C(NP+6) .GT. C(I))C(NP+6)=C(I)
    IF(C(NP+6) .EQ. C(I))C(NP+7)=FLOAT(I)

1000 C
C   RANGE DETERMINATION.
C
    C(NP+8)=C(NP+4)-C(NP+6)
56  FORMAT(' ', 'MAX=' ,F10.0,2X, 'Q' ,F5.0, ' MIN=' ,F10.0,
1 2X, 'Q' ,F5.0, ' RANGE=' ,F10.0,/)
    GO TO 120

C
C   DISPLAY A PLOT OF DATA ON THE VT-55 SCREEN.
C

```

```

100  NPLOT=NP
      WRITE(7,101)
101  FORMAT(' ', 'NORMALIZED PLOT? YES=1, NO=0')
      READ(5,59,END=120)XNORM
      IF(XNORM .EQ. 1.0)SCFAC=C(NP+8)
      IF(XNORM .EQ. 1.0)GO TO 102
      WRITE(7,103)
103  FORMAT(' ', 'ENTER SCALING FACTOR, F10.0')
      READ(5,59,END=120)SCFAC
102  CONTINUE
      DO 150 I=1,NP
150  B(I)=IFIX(((C(I)-C(NP+6))*100.)/SCFAC)
      CALL PLOT55(ESCCMD,HOME,0)
      CALL PLOT55(ESCCMD,ESCRN,0)
      CALL PLOT55(STATUS,547,476)
      CALL PLOT55(SELGR,0,0)
      CALL PLOT55(CURPOS,0,0)
      WRITE(7,170)TITLE,DAT,C(NP+1),C(NP+2),C(NP+3)
      WRITE(7,56)(C(NP+I),I=4,8)
      CALL PLOT55(HGRD,1,0,0)
      IF(NPLOT .LE. 512)GO TO 151
      CALL PLOT55(STATUS,551,472)
      CALL PLOT55(SELGR,1,0)
      CALL PLOT55(HGRD,1,101)
151  IF(NP .GT. 512)NPLOT=512
      CALL PLOT55(SELGR,0,0)
      CALL PLOT55(ORIGIN,0,0)
      CALL PLOT55(N,-NPLOT,B)
      IF(NP .LE. 512)GO TO 153
      NPLOT=NP-512
      CALL PLOT55(SELGR,1,0)
      DO 156 I=1,NPLOT
156  D(I)=D(I)+101
      CALL PLOT55(N,-NPLOT,D)
153  CALL PLOT55(DISPLY,0,BELL)
      READ(5,58,END=120)NSTOP
120  CALL PLOT55(ESCCMD,HOME,0)
      CALL PLOT55(ESCCMD,ESCRN,0)
      CALL PLOT55(STATUS,0,1023)
      GO TO 6
C
C  THIS SECTION LISTS THE DATA ON THE VT-55 COPIER.
C
200  CALL PLOT55(ESCCMD,HOME,0)
      CALL PLOT55(ESCCMD,ESCRN,0)
      CALL PLOT55(DISPLY,0,BELL)
      WRITE(7,170)TITLE,DAT,C(NP+1),C(NP+2),C(NP+3)
      WRITE(7,56)(C(NP+I),I=4,8)
170  FORMAT(' ',3A4,3A4,3X,'NS=',F10.0,3X,'NP=',F10.0,
1  3X,'SCAN #=',F10.0)
      DO 250 I=1,NP+8,100
      DO 251 J=I,I+95,5
      WRITE(7,63)J,(C(K),K=J,J+4)
      IF(K .GT. (NP+8))GO TO 252
251  CONTINUE
      READ(5,58,END=120)NSTOP
253  CALL PLOT55(ESCCMD,HOME,0)
      CALL PLOT55(ESCCMD,ESCRN,0)
      WRITE(7,170)TITLE,DAT,C(NP+1),C(NP+2),C(NP+3)
      WRITE(7,56)(C(NP+I),I=4,8)
250  CONTINUE
63  FORMAT(' ',I4,2X,'>',5(F10.0,1X))
252  CALL PLOT55(DISPLY,0,BELL)
      READ(5,58,END=120)NSTOP
      GO TO 120
C

```



```

C      THIS SECTION DETERMINES PEAK LOCATIONS AND DISPLAYS
C      THE LOCATION AND PEAK VALUE ON THE VT-55.
C
300    CALL PLOT55(ESCCMD,HOME,0)
      CALL PLOT55(ESCCMD,ESCRN,0)
      WRITE(7,170)TITLE,DAT,C(NP+1),C(NP+2),C(NP+3)
      WRITE(7,56)(C(NP+I),I=4,8)
      WRITE(7,64)
64     FORMAT(' ', 'ENTER THE THRESHOLD,F10.0')
      READ(5,59,END=120)THRES
66     FORMAT(' ', 'POINT NO.  AMPLITUDE')
      CALL PLOT55(ESCCMD,HOME,0)
      CALL PLOT55(ESCCMD,ESCRN,0)
      WRITE(7,170)TITLE,DAT,C(NP+1),C(NP+2),C(NP+3)
      WRITE(7,56)(C(NP+I),I=4,8)
      DO 320  J=1,NP
      NCNT=0
      WRITE(7,66)
      DO 310  I=J,NP
      IF(C(I) .LT. THRES)GO TO 310
      IF(C(I+1) .GT. C(I))GO TO 310
      IF(C(I) .LE. C(I-1))GO TO 310
      WRITE(7,67)I,C(I)
      NCNT=NCNT+1
      J=I
      IF(I .GE. NP)GO TO 320
      IF(NCNT .EQ. 20)GO TO 311
      J=I
310    IF(I .GE. NP)GO TO 320
311    READ(5,58,END=120)NSTOP
      CALL PLOT55(ESCCMD,HOME,0)
      CALL PLOT55(ESCCMD,ESCRN,0)
      WRITE(7,170)TITLE,DAT,C(NP+1),C(NP+2),C(NP+3)
      WRITE(7,56)(C(NP+I),I=4,8)
320    CONTINUE
67     FORMAT(5X,I4,6X,F10.0)
      CALL PLOT55(DISPLY,0,BELL)
      READ(5,58,END=120)NSTOP
      GO TO 120

C
C      THIS SECTION WRITES THE DATA ON DISK AND NAMES THE DATA FILE.
C
600    REWIND 1
      WRITE(7,170)TITLE,DAT,C(NP+1),C(NP+2),C(NP+3)
      WRITE(7,56)(C(NP+I),I=4,8)
      CALL ASSIGN(1,'DK:FTN1.DAT',-1,'NEW','NC',1)
      WRITE(1)(DAT(I),I=1,3)
      WRITE(1)(TITLE(I),I=1,3)
      WRITE(1)(C(I),I=1,NP+8)
      ENDFILE 1
      CALL CLOSE(1)
      GO TO 120

C
C      THIS SECTION READS DATA FROM THE DISK, AND CALCULATES THE
C      TOTALS FOR SELECTED PORTIONS OF THAT DATA.
C
700    DO 705  J=1,100
705    A(J)=0
      DO 706  J=1,30
706    A1(J)=0
      CALL PLOT55(EXCCMD,HOME,0)
      CALL PLOT55(EXCCMD,ESCRN,0)
      WRITE(7,170)TITLE,DAT,XNS,XNP
      WRITE(7,780)
780    FORMAT(' ',/, 'WHICH SETS DO YOU WISH TO USE FOR TOTALS
1    CALCULATIONS?')

```

```

1,/,/,',', 'ENTER THE # OF THE STARTING SCAN AND THE # OF SCANS.')
  READ(5,781,END=120)START,XLENTH
781  FORMAT(2F10.0)
      NSTART=IFIX(START)
      NLENTH=IFIX(XLENTH)
      WRITE(7,798)
798  FORMAT(' ',1X,'RAW DATA OUT=1, NOT=ANYTHING ELSE')
      READ(5,58)IOPT
      JR=0
      TDIOD=0
      WRITE(7,782)
782  FORMAT(' ', 'ENTER THE STARTING DIODE # AND # OF DIODES.',/,/,/,
1, ' ', 'ENTER 0,0 TO COMMENCE PROCESSING.')
```

```

701  READ(5,781,END=120)DIODE,DIODEN
      TDIOD=TDIOD+DIODEN
      IF(TDIOD .GT. 100)GO TO 710
      IF(DIODE .EQ. 0)GO TO 710
      JR=JR+1
      NDIOD(JR)=IFIX(DIODE)
      NDIODN(JR)=IFIX(DIODEN)
      GO TO 701
710  CALL PLOT55(ESCCMD,HOME,0)
      CALL PLOT55(ESCCMD,ESCRN,0)
      IF(IOPT .NE. 1)GO TO 711
      NC=0
      WRITE(7,170)TITLE,DAT,C(NP+1),C(NP+2)
      WRITE(7,794)
794  FORMAT(' ',1X,'SCAN',5X,'DIODE',7X,'VALUE')
711  DO 725 NUMSET=NSTART,(NSTART+NLENTH-1)
      GO TO 720
715  N=0
      IF(IOPT .NE. 1)GO TO 797
793  FORMAT(' ',3X,I2,6X,I4,2X,F10.0)
      DO 797 K=1,JR
      DO 796 L=NDIOD(K),(NDIOD(K)+NDIODN(K)-1)
      NC=NC+1
      IF(L .EQ. NDIOD(K))WRITE(7,793)NUMSET,L,C(L)
      IF(L .NE. NDIOD(K))WRITE(7,795)L,C(L)
795  FORMAT(12X,I4,2X,F10.0)
      IF(NC .LT. 20)GO TO 796
      NC=0
      READ(5,58,END=120)NSTOP
      CALL PLOT55(ESCCMD,HOME,0)
      CALL PLOT55(ESCCMD,ESCRN,0)
      WRITE(7,170)TITLE,DAT,C(NP+1),C(NP+2)
      WRITE(7,794)
796  CONTINUE
797  CONTINUE
      DO 716 K=1,JR
      DO 718 L=NDIOD(K),(NDIOD(K)+NDIODN(K)-1)
      N=N+1
      A(N)=A(N)+C(L)
718  A1(K)=A1(K)+C(L)
716  CONTINUE
725  CONTINUE
      READ(5,58,END=120)NSTOP
      CALL PLOT55(ESCCMD,HOME,0)
      CALL PLOT55(ESCCMD,ESCRN,0)
      WRITE(7,756)TITLE,DAT,START,XLENTH
      WRITE(7,740)
740  FORMAT(' ',1X,'DIODE',9X,'TOTAL',4X,'GROUP TOTAL')
      N=0
      NC=0
      DO 760 K=1,JR
      NCOUNT=NDIOD(K)+NDIODN(K)-1
      DO 750 L=NDIOD(K),(NDIOD(K)+NDIODN(K)-1)

```

```

1,/,/,',', 'ENTER THE # OF THE STARTING SCAN AND THE # OF SCANS.')
781  READ(5,781,END=120)START,XLENTH
    FORMAT(2F10.0)
    NSTART=IFIX(START)
    NLENTH=IFIX(XLENTH)
    WRITE(7,798)
798  FORMAT(' ',1X,'RAW DATA OUT=1, NOT=ANYTHING ELSE')
    READ(5,58)IOPT
    JR=0
    TDIOD=0
    WRITE(7,782)
782  FORMAT(' ', 'ENTER THE STARTING DIODE # AND # OF DIODES.',/,/,/,
1' ', 'ENTER 0,0 TO COMMENCE PROCESSING.')
701  READ(5,781,END=120)DIODE,DIODEN
    TDIOD=TDIOD+DIODEN
    IF(TDIOD .GT. 100)GO TO 710
    IF(DIODE .EQ. 0)GO TO 710
    JR=JR+1
    NDIOD(JR)=IFIX(DIODE)
    NDIODN(JR)=IFIX(DIODEN)
    GO TO 701
710  CALL PLOT55(ESCCMD,HOME,0)
    CALL PLOT55(ESCCMD,ESCRN,0)
    IF(IOPT .NE. 1)GO TO 711
    NC=0
    WRITE(7,170)TITLE,DAT,C(NP+1),C(NP+2)
    WRITE(7,794)
794  FORMAT(' ',1X,'SCAN',5X,'DIODE',7X,'VALUE')
711  DO 725 NUMSET=NSTART,(NSTART+NLENTH-1)
    GO TO 720
715  N=0
    IF(IOPT .NE. 1)GO TO 797
793  FORMAT(' ',3X,I2,6X,I4,2X,F10.0)
    DO 797 K=1,JR
    DO 796 L=NDIOD(K),(NDIOD(K)+NDIODN(K)-1)
    NC=NC+1
    IF(L .EQ. NDIOD(K))WRITE(7,793)NUMSET,L,C(L)
    IF(L .NE. NDIOD(K))WRITE(7,795)L,C(L)
795  FORMAT(12X,I4,2X,F10.0)
    IF(NC .LT. 20)GO TO 796
    NC=0
    READ(5,58,END=120)NSTOP
    CALL PLOT55(ESCCMD,HOME,0)
    CALL PLOT55(ESCCMD,ESCRN,0)
    WRITE(7,170)TITLE,DAT,C(NP+1),C(NP+2)
    WRITE(7,794)
796  CONTINUE
797  CONTINUE
    DO 716 K=1,JR
    DO 718 L=NDIOD(K),(NDIOD(K)+NDIODN(K)-1)
    N=N+1
    A(N)=A(N)+C(L)
    A1(K)=A1(K)+C(L)
718  CONTINUE
716  CONTINUE
725  CONTINUE
    READ(5,58,END=120)NSTOP
    CALL PLOT55(ESCCMD,HOME,0)
    CALL PLOT55(ESCCMD,ESCRN,0)
    WRITE(7,756)TITLE,DAT,START,XLENTH
    WRITE(7,740)
740  FORMAT(' ',1X,'DIODE',9X,'TOTAL',4X,'GROUP TOTAL')
    N=0
    NC=0
    DO 760 K=1,JR
    NCOUNT=NDIOD(K)+NDIODN(K)-1
    DO 750 L=NDIOD(K),(NDIOD(K)+NDIODN(K)-1)

```

```
N=N+1
NC=NC+1
IF(L .EQ. MCOUNT)GO TO 755
WRITE(7,751)L,A(N)
GO TO 753
755 WRITE(7,752)L,A(N),A1(K)
753 IF(MC .LT. 20)GO TO 750
NC=0
READ(5,58,END=120)N$TOP
CALL PLOT55(ESCCMD,HOME,0)
CALL PLOT55(ESCCMD,ESCRN,0)
WRITE(7,756)TITLE,DAT,START,XLENTH
WRITE(7,740)
750 CONTINUE
760 CONTINUE
751 FORMAT(' ',1X,I5,2X,F12.0)
752 FORMAT(' ',1X,I5,2X,2(F12.0,3X))
756 FORMAT(' ',3A4,3A4,3X,' STARTING SCANS=',F4.0,3X,' SCANS=',F4.0)
CALL PLOT55(DISPLY,0,BELL)
READ(5,58,END=120)N$TOP
GO TO 120

C
C
C
800
THIS SECTION CAUSES AN EXIT FROM THE PROGRAM.
STOP
END
```

B. MULFUR - This subroutine first acquires a background scan and stores this. The individual scans are then added to a negative background to give individual background subtracted scans which are sequentially written into the file DATA.DAT. Data acquisition is started by the combination of the furnace start signal and the photodiode array start signal. Data acquisition is clocked by the photodiode array clock.

```
PROGRAM MULFUR,MAC(6-NOV-78)
```

PURPOSE:

```
TO ACQUIRE MULTIPLE SCANS WITH THE PHOTO-DIODE
ARRAY AND TO TRANSFER THESE SCANS INDIVIDUALLY
TO THE DISK(IN BLOCKS) FOR TRANSFER TO
THE MAIN FORTRAN PROGRAM FOR FURTHER PROCESSING.
```

```
*****
*
*WRITTEN BY:*
*
*DONALD HULL*
*
*WITH HELP *
*
*FROM:      *
*
*ROBERT HALL*
*
*****
```

```
.TITLE MULTIPLE SCANS OF FURNACE DATA
.MCALL ..V2...REGDEF,.FETCH,.CLOSE,.PRINT
.MCALL .EXIT,.WRITW,.SRESET,.ENTER,.TTYOUT,.TTYIN
..V2..
.REGDEF
.GLOBL MULFUR
```

```
STR=170400          ;SET ADDRESS A/D STATUS REGISTER
ADB=170402          ;SET ADDRESS A/D BUFFER
DIBUF=170412        ;SET ADDRESS DIGITAL INPUT BUFFER
KBRD=177562         ;SET ADDRESS KEY BOARD
```

```
.CSECT
```

```
MULFUR: MOV      (R5)+,R1          ;RECEIVE DATA FROM FORTRAN
        MOV      @ (R5)+,NS
        MOV      @ (R5)+,NP
        MOV      @ (R5)+,NBLK
        MOV      #0,BLK
        .SRESET
        .FETCH  #CORSPC,#FPRT
        BCC     GO1
        JMP     BADFET
GO1:    .ENTER  #AREA,#0,#FPRT,NBLK
        BCC     RESTR
        JMP     BADENT

RESTR:  MOV      #1040.,R1        ;SET POINT COUNTER
        MOV      #B,R3          ;SET ADDRESS OF ARRAY(B)
LPO:    MOV      #0,(R3)+        ;CLEAR ARRAY(A)
        DEC     R1              ;DECREMENT POINT COUNTER
```



```
AREA: .RADSO /DATA DAT/  
      .BLKW 10  
FMSG: .ASCIZ /BAD FETCH/  
EMSG: .ASCIZ /BAD ENTER/  
WMSG: .ASCIZ /BAD WRITE/  
      .EVEN  
CORSPC: .BLKW 400.  
DATAQ: .ASCIZ /STRIKE CR TO START DATA ACQUISITION./  
BKDAQ: .ASCIZ /STRIKE CR TO START BACKGROUND ACQUISITION./  
END: .END MULFUR
```


APPENDIX F

Software Developed to Plot the Time Studies Obtained with the Computer-Coupled Photodiode Array Readout System

- A. PLOT3D - This plotting program allows any of the selected individual scans acquired under MULTFR to be plotted as 3-dimensional plots. The individual plots are separated by operator choosen x and y axis' values and the program is written to prevent lines being drawn through previously drawn lines. The task modules are:
1. READ DISK: Reads the selected individual scan. .
 2. AXIS
 3. PLOT: Plots the individual scans at operator choosen x, y increments..
 4. RESTART
 5. EXIT


```

1 * IN I2 FORMAT. )
58 READ (5,58)NUMSCN
   FORMAT(I2)
   XNUMSC=FLOAT(NUMSCN)
   NP=IFIX(XNP+4.)
   NBLK=IFIX(5*(XNUMSC-1))
   DO 91 I=1,1040
   C(I)=0.
91   A(I)=0
   ICD=LOOKUP(0,DRLK)
   ICODE=IREADW(NP,A,NBLK,0)
   CALL CLOSEC(0)
   CALL IFREEC(0)

C
C
C   CONVERSION OF DATA FROM INTEGER*2 TO REAL

DO 90 J=5,NP
90  C(J-4)=FLOAT(A(J))
   NP=NP-4
   C(NP+1)=XNS
   C(NP+2)=XNP
   C(NP+3)=XNUMSC

C
C
C   CALCULATION OF MAXIMUM, MINIMUM, AND RANGE OF VALUES.

C(NP+4)=C(1)
C(NP+5)=1.
C(NP+6)=C(1)
C(NP+7)=1.
DO 1000 I=2,NP

C
C
C   MAXIMUM AND SUBSCRIPT DETERMINATION.

IF(C(NP+4) .LT. C(I))C(NP+4)=C(I)
IF(C(NP+4) .EQ. C(I))C(NP+5)=FLOAT(I)

C
C
C   MINIMUM AND SUBSCRIPT DETERMINATION.

IF(C(NP+6) .GT. C(I))C(NP+6)=C(I)
IF(C(NP+6) .EQ. C(I))C(NP+7)=FLOAT(I)

1000 C
C
C   RANGE DETERMINATION.

C(NP+8)=C(NP+4)-C(NP+6)

C
C
C   THIS SECTION SETS THE MINIMUM VALUE TO 0.0 AND
C   THE MAXIMUM VALUE TO BE EQUAL TO THE RANGE FOR
C   PLOTTING PURPOSES

DO 492 I=1,NP
492  C(I)=C(I)-C(NP+6)
   C(NP+4)=C(NP+4)-C(NP+6)
   C(NP+6)=0.0
   WRITE(7,493)C(NP+1),C(NP+2),C(NP+3)
493  FORMAT(' ',3X,'NS='F10.0,3X,'NP='F10.0,3X,'SCAN #='F10.0)
   WRITE(7,494)C(NP+I),I=4,8)
494  FORMAT(' ', 'MAX='F10.0, 'Q',F4.0, ' MIN='F10.0,
1 'Q',F4.0, ' RANGE='F10.0)
   GO TO 1

C
C
C   THIS SECTION DRAWS THE AXIS OF THE PLOT.

500 CONTINUE
502 FORMAT(5A4)
   WRITE(7,510)
510  FORMAT(' ', ' ENTER THE TITLE FOR THE XAXIS, 20 CHARACTERS MAX. ')

```

```

      READ(5,502)XAXIS
      WRITE(7,503)
503  FORMAT(' ', 'ENTER THE TITLE FOR THE Y AXIS, 20 CHARACTERS MAX. ')
      READ(5,502)YAXIS
      WRITE(7,504)
504  FORMAT(' ', 'ENTER THE TITLE FOR THE PLOT, 20 CHARACTERS MAX. ')
      READ(5,502)TITPLT
      WRITE(7,601)
601  FORMAT(' ', 'ENTER X AND Y ORIGIN OFF SETS IN INCHES-2F10.0. ')
      READ(5,602)XOFF,YOFF
602  FORMAT(2F10.0)
      OFF=0
      YOFFY=0
      XMIN=0.0
      XMAX=C(NP+2)
      YMIN=0.0
      YMAX=C(NP+4)
      WRITE(7,520)
520  FORMAT(' ', 'ENTER X AND Y AXIS LENGTHS, 2F10.0. ')
      READ(5,525)XLONG,YLONG
525  FORMAT(2F10.0)
      WRITE(7,494)(C(NP+I),I=4,8)
      WRITE(7,620)
620  FORMAT(' ', 'NORMALIZED PLOT=1, SCALED PLOT=0. ')
      READ(5,51)NTEMP
      IF(NTEMP .EQ. 1)GO TO 550
      WRITE(7,625)
625  FORMAT(' ', 'ENTER NEW VALUE FOR Y RANGE, F10.0. ')
      READ(5,111)YMAX
550  X(NP+1)=XMIN
      X(NP+2)=(XMAX-XMIN)/XLONG
      Y(NP+1)=YMIN
      Y(NP+2)=(YMAX-YMIN)/YLONG
      CALL PLOTST(0.005,'IN')
      CALL PLOT(1.5,1.0,-3)
      CALL AXIS(0.0,0.0,XAXIS,-20,XLONG,0.0,X(NP+1),X(NP+2))
      CALL AXIS(0.0,0.0,YAXIS,+20,YLONG,90.0,Y(NP+1),Y(NP+2))
      CALL PLOT(0.5,(YLONG+0.5),3)
      CALL SYMBOL(0.5,(YLONG+0.5),0.14,TITPLT,0,20)
      CALL PLOT(0.0,0.0,+3)
      CALL PLOT(-1.5,-1.0,-3)
      CALL PLOTND
      GO TO 1

C
C   THIS SECTION PLOTS THE DATA.
C
600  NOFFX=IFIX(XOFF*X(NP+2))
      OFFY=YOFFY*Y(NP+2)
      DO 605 I=1,NP
605  C(I)=C(I)+OFFY
      DO 610 I=1,(NP-NOFFX)
610  IF(Y(I+NOFFX) .GT. C(I))C(I)=Y(I+NOFFX)
      CONTINUE
      DO 615 I=1,NP
615  Y(I)=C(I)
      CALL PLOTST(0.005,'IN')
      CALL PLOT((1.5+OFF),1.0,-3)
      CALL LINE(X,Y,NP,1,0,0)
      CALL PLOT(0.0,0.0,+3)
      CALL PLOT(-(1.5+OFF),-1.0,-3)
      CALL PLOTND
      OFF=OFF+XOFF
      YOFFY=YOFFY+YOFF
      GO TO 1

C
C   THIS SECTION CAUSES AN EXIT FROM THE PROGRAM.

```

```
C  
800 CALL PLOTST(0.005,'IN')  
CALL PLOT(8.5,0.0,-3)  
CALL PLOTND  
STOP  
END
```

```
*
```

APPENDIX G

Software Developed to Calculate the Linear Least Squares Best Fit Equation for Emission Data and Plot this Data and Calculated Line

- A. LFIT - After entry of sample concentration and emission intensity values this program will calculate the linear least squares best fit equation for that data. The linear fitting may be performed on the data as entered or after the logarithm has been calculated for the data thereby allowing log-log linear fitting as well as the normal linear-linear fitting. This feature was frequently used in this work since the concentration-emission intensity data normally covered three to four orders of magnitude.

The plotting section of this program allows plotting of the calculated line, average y values (emission intensity values), and 95% confidence limits within axis for which the operator may choose the size, ranges, and titles.


```

      YAVE(I)=0.
      YSS(I)=0.
139     YPE(I)=0.
      YTOT=0.
      NTOT=0
      SYS=0.0
      YT=0.0
      E=0.
      F=0.
      C=0.
      YSD=0.
      NT1=0
      DO 140 I=1,N
      KK=NR(I)
      X(I)=XS(I)
      IF(JG.EQ.1)X(I)=ALOG10(X(I))
      DO 129 J=1,KK
      Y(I,J)=YS(I,J)
      IF(JG.EQ.1)Y(I,J)=ALOG10(Y(I,J))
      YAVE(I)=Y(I,J)+YAVE(I)
      F=F+X(I)*Y(I,J)
      C=C+X(I)
      E=E+X(I)*X(I)
129     YSS(I)=YSS(I)+Y(I,J)*Y(I,J)
      YT=YT+YAVE(I)
      YAVE(I)=YAVE(I)/FLOAT(NR(I))
      NTOT=NR(I)+NTOT
      SYS=SYS+YSS(I)
      IF(NR(I).EQ.1)GO TO 89
      YPE(I)=YSS(I)-(YAVE(I)**2*NR(I))
      YTOT=YPE(I)+YTOT
      YPE(I)=SQRT(YPE(I)/FLOAT(NR(I)-1))
      YSS(I)=(YPE(I))/(YAVE(I))*100.
      NT1=NR(I)-1+NT1
89     CONTINUE
140    CONTINUE
      IF(NT1.EQ.0)NT1=1
      XA=YTOT/FLOAT(NT1)
      IF(XA.EQ.0)XA=1.
B      AN=FLOAT(NTOT)
      G=0.0
      ANX=(AN*E-C*C)
      A=(AN*F-C*YT)/ANX
      B=(E*YT-C*F)/ANX
      WRITE(7,703)
703    FORMAT(' ', N      X(I)',8X,'Y(I)...')
      DO 702 II=1,N
      KK=NR(II)
      DO 2000 NQ=1,KK,5
      WRITE(7,501)II,X(II),(Y(II,JJ),JJ=NQ,(NQ+4))
      IF(JJ .GT. KK)NQ=KK
2000   CONTINUE
501    FORMAT(I4,6(F12.3))
702    CONTINUE
      WRITE(7,800)
800    FORMAT(' ', ' CHANGE X OR Y VALUES  Y=1,N=0')
      READ(5,504,END=702,ERR=702)NJ
      IF(NJ.EQ.0)GO TO 801
      WRITE(7,803)
803    FORMAT(' ', 'SPECIFY X(I),Y(I,K) TO CHANGE 2F10.0')
      READ(5,804,END=702,ERR=702)I,
804    FORMAT(2F10.0)
      WRITE(7,805)
805    FORMAT(' ', 'INPUT X AND Y VALUES  2F110.0')
      READ(5,804,END=702,ERR=702)X(I),Y(I,J)
      XS(I)=X(I)

```



```

      YS(I,J)=Y(I,J)
      GO TO 131
801  WRITE (5,508)
508  FORMAT (' //,3X,'N',11X,'X',8X,'YAVE',5X,'YSTDDEV',2X,'X REL S.D.
1    ',5X,'YCALC',6X,'DIFF.',9X,'S/N')
      NJ=0
      AMVT=-1000000.
      ANVT=100000.
      XMIN=100000.
      XMAX=-100000.
      DO 13 I=1,N
      YP(I)=A*X(I)+B
      Q=YAVE(I)-YP(I)
      NN=NR(I)
      DO 113 J=1,NN
      NJ=NJ+1
      XGT(NJ)=X(I)
      IF(XMAX.LT.X(I))XMAX=X(I)
      IF(XMIN.GT.X(I))XMIN=X(I)
      YGT(NJ)=Y(I,J)
      IF(AMVT.LT.YGT(NJ))AMVT=YGT(NJ)
      IF(ANVT.GT.YGT(NJ))ANVT=YGT(NJ)
      QQ=Y(I,J)-YP(I)
113  G=G+QQ*QQ
      IF(NR(I).EQ.1)YSS(I)=-1.
509  WRITE (5,509) I,X(I),YAVE(I),YPE(I),YSS(I),YP(I),Q,(100./YSS(I))
13  FORMAT (I4,7F12.3)
      CONTINUE
      SO=G/(AN-2.0)
      DO=SQRT(SO)
      SA=SO*AN/ANX
      DA=SQRT(SA)
      SB=SO*E/ANX
      DB=SQRT(SB)
      IF((NTOT-2-NT1).EQ.0)NT1=2
      XC=(G-YTOT)/FLOAT(NTOT-2-NT1)
      R=(AN*F-C*YT)/((SQRT(ANX))*(SQRT(AN*SYS-YT*YT)))
510  WRITE (5,510) A,B
1  FORMAT ('0','THE BEST FIT LINEAR EQUATION IS Y=',F12.3,' X +
      ',F14.6)
511  WRITE (5,511) DA,ABS((DA/A*100.))
      FORMAT (' ','THE STANDARD DEVIATION OF A=',E14.6,3X,'X= ',F8.3)
512  WRITE (5,512) DB,ABS((DB/B*100.))
      FORMAT (' ','THE STANDARD DEVIATION OF B=',E14.6,3X,'X= ',F8.3)
513  WRITE (5,513) DO
      FORMAT (' ','OVERALL STANDARD DEVIATION =',E14.6)
155  WRITE (5,155)XA,XC,XC/XA
      FORMAT(' ','P.E. ',E14.4,' L.OF.FIT ',E14.4,' F TEST <1',F10.5)
514  WRITE (5,514) R
      FORMAT (' ','CORRELATION COEFFICIENT, R=',F10.6)
      CALL INIT(IX,1000)
      CALL SCROL(5,1020,5)
      CALL APNT(1.,1.,-1,5,-1,-1)
      CALL SCAL(XMIN,ANVT,XMAX,AMVT)
      YPN=1.E20
      YPM=-1.E20
      DO 215 JJ=1,N
      IF(YPM.LT.YP(JJ))YPM=YP(JJ)
      IF(YPN.GT.YP(JJ))YPN=YP(JJ)
215  CONTINUE
      DO 115 JJ=1,NTOT
      XX=XGT(JJ)
      YY=YGT(JJ)
      CALL APNT(XX,YY)
115  CONTINUE
      YP1=YPN

```

```

XP1=XMIN
YPN=YPM-YP1
XPN=XMAX-XMIN
CALL APNT(XP1,YP1,-1,3,-1,1)
CALL LVECT(XPN,YPN)
CALL APNT(XMIN,AMUT)
CALL LVECT(0,-(AMUT-ANUT))
CALL LVECT((XMAX-XMIN),0.)
519 WRITE (5,520)
520 FORMAT ('0','DO YOU WISH A PLOT? Y=1,N=0')
READ (7,504,END=519,ERR=519) JS
IF (JS .NE. 1) GO TO 19
65 WRITE (5,600)
600 FORMAT (' ','ENTER TITLE FOR X AXIS, 32 CHARACTERS MAX.')
READ (7,601,END=519,ERR=519) XAXIS
601 FORMAT (8A4)
WRITE (5,602)
602 FORMAT (' ','ENTER TITLE FOR Y AXIS, 32 CHARACTERS MAX.')
READ (7,601,END=519,ERR=519) YAXIS
WRITE(7,711)
711 FORMAT(' ','INPUT TITLE FOR PLOT 32 CHARACTERS MAX.')
READ(5,601,END=519,ERR=519)TITP
WRITE (5,604)
604 FORMAT (' ','ENTER STARTING & FINISHING POINTS FOR X AXIS,2F12.0')
READ (7,605,END=519,ERR=519) XMIN, XMAX
605 FORMAT (2F12.0)
WRITE (5,606)
606 FORMAT (' ','ENTER STARTING & FINISHING POINTS FOR Y AXIS,2F12.0')
READ (7,605,END=519,ERR=519) YMIN, YMAX
WRITE (5,607)
607 FORMAT (' ','ENTER LENGTH OF X&Y AXIS IN INCHES,MAX=7.0, 2F12.0')
READ (7,605,END=519,ERR=519) XLONG, YLONG
X(N+1)=XMIN
YAVE(N+1)=YMIN
X(N+2)=(XMAX-XMIN)/XLONG
YAVE(N+2)=(YMAX-YMIN)/YLONG
WRITE (5,608)
608 FORMAT(' ','ENTER LINE START & FINISH X VALUES.','','
1 ' IF X1=X2 THEN NO LINE WILL BE PLOTTED.')
READ (5,605) XA,XB
IF(XA.EQ. XB)GO TO 675
IF(XA .GE. XMIN .AND. XA .LT. XMAX)GO TO 60
XA=XMIN
60 IF(XB .GT. XMIN .AND. XB .LE. XMAX)GO TO 61
XB=XMAX
61 YA=A*XA + B
YB=A*XB + B
IF(YA .GE. YMIN .AND. YA .LT. YMAX)GO TO 62
YA=YMIN
XA=(YA-B)/A
62 IF (YB .GT. YMIN .AND. YB .LE. YMAX) GO TO 63
YB=YMAX
XB=(YB-B)/A
63 CONTINUE
XGT(1)=XA
XGT(2)=XB
XGT(3)=X(N+1)
XGT(4)=X(N+2)
YGT(1)=YA
YGT(2)=YB
YGT(3)=YAVE(N+1)
YGT(4)=YAVE(N+2)
675 CONTINUE
DO 811 IK=1,N
KK=NR(IK)
IF(KK.EQ.1)GO TO 677

```

```

      NKK=KK-1
      IF(NKK.GT.10) NKK=11
      ST=YPE(IK)*STAT(NKK)/SQRT(FLOAT(KK))
      YSS(IK)=YAVE(IK)+ST
811     YPE(IK)=YAVE(IK)-ST
      WRITE(7,987)
987     FORMAT(' ', ' THE 95 % CONFIDENCE INTERVAL ABOUT THE MEAN', //,
1       '      Y-HIGH           Y-AVE           Y-LOW')
      DO 988 I=1,N
      WRITE(7,989)I,YSS(I),YAVE(I),YPE(I)
988     CONTINUE
989     FORMAT(1X,I3,3(2X,F12.4))
      YSS(N+1)=YMIN
      YSS(N+2)=YAVE(N+2)
      YPE(N+1)=YMIN
      YPE(N+2)=YAVE(N+2)
677     CALL PLOTST (0.005,'IN')
      CALL PLOT (1.0,1.0,-3)
      CALL AXIS (0.0,0.0,XAXIS,-32,XLONG,0.0,X(N+1),X(N+2))
      CALL AXIS (0.0,0.0,YAXIS,+32,YLONG,90.0,YAVE(N+1),YAVE(N+2))
      CALL PLOT (0.0,YLONG,+3)
      CALL PLOT (XLONG,YLONG,+2)
      CALL PLOT (XLONG,0.0,+2)
      CALL PLOT (0.0,0.0,+3)
      IF(XA.EQ.XB) GO TO 678
      CALL LINE (XGT,YGT,2,1,0,0)
678     CALL PLOT (0.0,0.0,+3)
      IF(KK.EQ.1)GO TO 676
      CALL LINE(X,YSS,N,1,-1,17)
      CALL PLOT(0.,0.,3)
      CALL LINE(X,YPE,N,1,-1,18)
      CALL PLOT(0.,0.,3)
676     CALL LINE(X,YAVE,N,1,-1,4)
      TITLNG=(XLONG-4.48)/2.
      CALL PLOT (TITLNG,YLONG+0.5,3)
      CALL SYMBOL(TITLNG,(YLONG+0.5),0.14,TITP,0,32)
      CALL PLOT (7.5,-1.0,-3)
      CALL PLOTND
19     WRITE (5,518)
518     FORMAT (' ', 'TYPE 1 TO REPEAT CALCULATION OR 0 TO EXIT')
      READ (7,504) JK
      CALL SCROL(-1,-1,-1)
      CALL INIT
      CALL FREE
      IF (JK .EQ. 1) GO TO 131
      STOP
      END

```

APPENDIX H

Preparation of Solutions

All solutions used for this work were prepared from ACS Reagent-Grade Chemicals (or equivalent). The water used for dilution was the distilled water provided on tap by the Department of Chemistry. Distilled water blanks were run throughout this work and none of the elements tested analytically (Table VII) were present at detectable levels. Single element stock solutions of 1000 ppm of the elements were prepared from soluble salts and all other solutions were made by serial dilutions as necessary.

Stock Solutions

<u>Element</u>	<u>Compound</u>	<u>Weight (g/L)</u>	<u>Solvent</u>
Pb	$\text{Pb}(\text{NO}_3)_2$	1.5898	Water
Mg	$\text{MgCl}_2 \cdot 6\text{H}_2\text{O}$	8.3625	Water
Ag	AgNO_3	1.5746	Water
Cu	$\text{Cu}(\text{NO}_3)_2 \cdot 3\text{H}_2\text{O}$	3.8023	Water
Cd	$\text{Cd}(\text{NO}_3)_2 \cdot 4\text{H}_2\text{O}$	2.7444	Water
Zn	$\text{Zn}(\text{NO}_3)_2 \cdot 6\text{H}_2\text{O}$	4.5506	Water
Na*	NaCl	2.5421	Water

* Na was prepared as a 20,000 ppm solution.